Research of bifunctional catalysts for C-C bond forming reactions

Karel Aelvoet

Research of

Bifunctional catalysts

For

C-C bond forming reactions

Karel Aelvoet

University of Durham

2008

Declaration

All work presented in this thesis is the authors own work, unless otherwise stated or acknowledged by references. The copyright of this thesis rests with the authors. No quotations from it should be published in any format, including electronic and the internet without being acknowledged appropriately.

Development and application of modular bifunctional catalysts

Karel Aelvoet, Andrew Whiting*

Department of Chemistry, University of Durham, Science site, South Road, Durham DH1 3LE, UK
Fax +44 191 384 4737, e-mail: andy.whiting@durham.ac.uk

Bifunctional catalysis is a well understood phenomenon in nature, with enzymes frequently using two (or more) functional groups to accomplish selective transformations on a suitable substrate. It is becoming clear however, that bifunctional catalysis is not merely of interest to explain or mimic biological efficiency and rate enhancement, but is a viable design principle for the development of new molecular catalysts.[1-4]

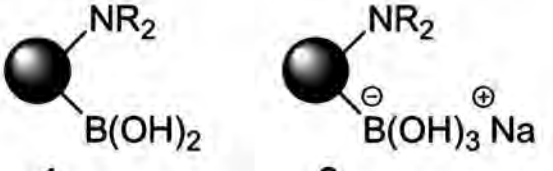

1 **2**

In this thesis we have prepared achiral amino-boronic acid compounds with different scaffold structures based on general structures **1** and **2**.[5] Although these compounds did not show any reactivity towards the MBH and aza-MBH reaction, they were very successful as catalysts for the aldol reaction. For this reaction it was possible to select the wanted product (aldol or chalcone product) using the same bifunctional catalyst only by changing the solvent. Also with hydroxyacetone some excellent results were gained with yields between 49 to 97% for both aromatic and aliphatic aldehydes in very high regioselectivity.[6] (see Equation)

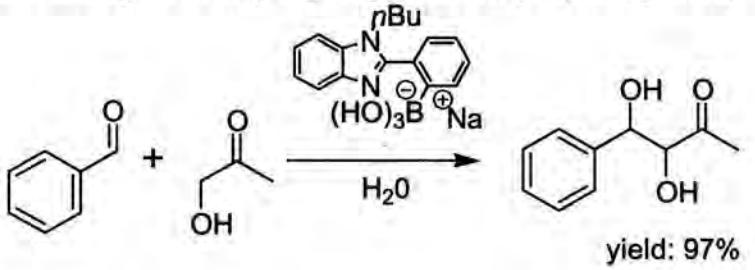

yield: 97%

references

1. Rowlands, G.J. *Tetrahedron* **2001**, *57*, 1865-1882.
2. List, B. *Acc. Chem. Res.* **2004**, *37*, 548-557.
3. Saito, H.; Yamamoto, H. *Acc. Chem. Res.* **2004**, *37*, 570-579.
4. Notz, W.; Tanaka, F.; Barbas III, C.F. *Acc. Chem. Res.* **2004**, *37*, 580-591.
5. Hérault, D.; Aelvoet, K.; Blatch, A.J.; Al-Majid, A.; Smethurst, C.A.; Whiting, A. *J. Org. Chem.* **2007**, *72*, 71-75.
6. Aelvoet, K.; Batsanov, A.S.; Blatch, A.J.; Grosjean, C.; Patrick, L.G.F.; Smethurst, C.A.; Whiting, A. *Angew. Chem. Int. Ed.* **2008**, *47*, 768-770.

Abbreviations

RNA	ribonucleic acid
BINOL	1,1'-Bi-2-naphthol
e.e.	enantiomeric excess
DABCO	1,4-diazabicyclo[2.2.2]octane
MBH	Morita-Baylis-Hillman
Aza-MBH	Aza-Morita-Baylis-Hillman
Ts	tosyl
Ph	phenyl
RLS	rate limiting step
NMR	nuclear magnetic resonance
KIE	kinetic isotope effect
DMF	dimethylformamide
DCM	dichloromethane
DBU	1,8-diazabicyclo[5.4.0]undec-7-ene
pH	$-\log[H^+]$
THF	tetrahydrofuran
IL	ionic liquid
[bmim]	1-*n*-butyl-3-methylimidazolium
Tf	triflate
[bdmim]	1-*n*-butyl-2,3-dimethylimidazolium
3-HQD	3-hydroxyquinuclidine
pK_a	acid dissociation constant
PTA	1,3,5-triaza-7-phospha-adamantane
HMT	hexamethylenetetramine
DMAP	4-dimethylaminopyridine
IR	infrared
TMG	tetramethyl guanidine
ppm	parts per million
TBAA	tetrabutylammonium acetate

d.e.	diastereomeric excess
o,p,m	*ortho, para, meta*
UV	ultraviolet
n,s,t	linear, secondary, tertiary
2D-NOESY	2-dimensional-nuclear Overhauser effect spectroscopy
DMSO	dimethyl sulfoxide
CSA	camphorsulfonic acid
Z, E	*Zusammen, Entgegen*
C_2-symmetry	symmetric after rotation of 180°C
HFIPA	hexafluoroisopropyl acrylate
MVK	methyl vinyl ketone
*t*Boc	tert-butyloxycarbonyl
BINAP	2,2'-bis(diphenylphosphino)-1,1'-binaphthyl
rt	room temperature
Ac	acetyl
TLC	thin layer chromatography
ES(+)	positive electrospray
Rf value	retardation factor
BuLi	butyl lithium
DBTCE	1,2-dibromotetrachloroethane
TMSCl	trimethylsilyl chloride
TBCD	1,5,7-triazabicyclo[4,4,0]dec-5-ene
TBME	tert-butyl methyl ether
^{i}Pr	isopropyl
PPA	polyphosphoric acid
Temp.	temperature
2-HEA	2-hydroxylethyl acrylate
TFAA	trifluoroacetic anhydride
TFA	trifluoroacetic acid
4-NBTs	N-(*p*-nitrobenzylidene)toluene-*p*-sulfonamide
LDA	lithium diisopropylamide

"Z-T" transition state	Zimmerman-Traxler transition state
Bn	benzyl
Conv.	conversion
S.M.	starting material
Equiv.	equivalents
HPLC	high-performance liquid chromatography
GC	gas chromatography
k_{obs}	observed rate constant
K	equilibrium constant
AIBN	azobisisobutyronitrile
TMEDA	tetramethylethylenediamine
HMPA	hexamethylphosphoramide
PMA	phosphomolybdic acid
UV-VIS	ultraviolet-visible spectroscopy
EI(+)	positive electron impact ionization
Mp.	melting point
HRMS(ESI+)	high resolution mass spectrometry (positive electrospray ionization)
Cat.	catalyst
Ar	aryl
J	*J*-coupling, coupling constant
M	molar (concentration)
MALDI	matrix-assisted laser desorption ionization

Acknowledgements

First of all I would like to thank Dr. Andrew Whiting for giving me the opportunity to work in England, more specifically to work in his group and also for the guidance and the inspiration during the PhD. I also thank the rest of the Whiting group for giving me advice and support inside and outside the lab. The advice of Dr. Grayson was also always appreciated. I also mention the analytical services of the University of Durham (NMR, elemental analysis, crystallography and mass) which helped me through my project. Also thanks goes to Dr. C. Grosjean for analyzing the kinetic data. And finally, I would also like to acknowledge the EPSRC for the funding of this project.

During my time in England I met a lot of interesting people, especially at Ustinov college of which some of them became personal friends. A special "*gracias*" goes out to the Spanish armada, better known as Gorge, Paco and Pablo for the happy Mondays, the chorizo and rioja. Unfortunately, my drinking brothers went back to Spain in the middle of my PhD but their places were quickly taken by fresh Finnish blood from Juho, Gorgina and Peter D. (and also a little bit by Cookie). I will also remember Mekenna who showed me that you cannot judge Americans only by stereotypes without having even met one. Also, thanks to my Egyptian friend Amr and his cooking abilities of serving huge amounts of delicious food. Greetings to my flatmates at the Providence House, the Saturday football team, the chess club, Peter B., Ben M.,.... and many more (don't feel insulted if I didn't mention you, I'm just writing this part as fast as possible to submit!).

Natuurlijk kan ik ook het thuisfront niet vergeten: Daarbij speciale dank aan mijn ouders die steeds klaarstonden om mij te helpen tijdens deze 3 jaar en mij door dik en dun steunden, ook de groeten aan Barry, Muylle, Rosier, Larno,... die altijd mijn bezoek aan België aangenaam maakten, een dikke merci aan Davy, een lotgenoot, die mij altijd begeleidde in Londen wanneer ik daar een tussenstop maakte, ook een dankuwel aan Michel en Tinga die mij steeds uitnodigden voor een heerlijk diner en verfrissende cocktails,... allemaal bedankt tijdens deze 3 jaar en jullie zal ik wel nog zien in de toekomst.

Table of contents

1. Introduction 11

1.1. Bifunctional catalysts 11

2. The Morita-Baylis-Hillman reaction 14

2.1. Introduction 14

2.2. Aza-MBH reaction 15

2.3. The mechanism 16

2.4. Rate improvements 19

2.4.1. Substrates 19

2.4.2. External conditions: solvent and salt effects 21

2.5. Catalysts 26

2.5.1. Nucleophilic catalysts 26

2.5.2. Acid based catalysts 33

2.6. Asymmetric MBH reaction 37

2.6.1. Chiral substrates 38

2.6.2. Chiral nucleophilic catalysts 49

2.6.3. Chiral acid based catalysts 57

2.6.4. Chiral ionic liquids. 69

2.7. In summary 70

3. Research work 71

3.1. Synthesis of amino-boronic acid compounds as potential catalysts 71

3.1.1. Synthesis of catalyst **127** 72

3.1.2. An interesting observation of **127** 75

3.1.3. The original synthesis pathway to catalysts **128** and **129** 77

3.1.4. The new synthesis pathway for the catalysts **136** and **129** 79

3.1.5. An overview of the regioselective direct lithiation of **135** 81

3.1.6. Synthesis of catalyst **143** 84

3.1.7. The introduction of new catalyst **150** 87
3.1.8. A summary 89
3.2. The Morita-Baylis-Hillman reaction 89
3.2.1. Standard MBH reactions 89
3.2.2. Screening of catalysts **126, 127** and **136** for MBH 94
3.2.3. The aza-MBH reaction 96
3.2.4. The incorporation of ReactIR 98
3.2.5. Conclusions 99
3.3. The aldol reaction 100
3.3.1. Introduction 100
3.3.2. Bifunctional catalysts for aldol reaction 106
3.3.2.1. Bifunctional organocatalysts for aldol reaction 107
3.3.2.2. Bifunctional metal catalysts for aldol reaction 109
3.3.2.3. In summary 114
3.3.3. The first screenings with amino-boron catalysts for aldol reaction 114
3.3.4. The screening of catalyst **129** with 2-butanone 118
3.3.5. The screening of catalyst **129** with acetone 119
3.3.6. The screening of catalyst **129** with hydroxyacetone 121
3.3.7. The screening of the blank reactions 124
3.3.8. Kinetic analysis on the aldol reaction with **129** 125
3.3.9. A close mechanistic view on the "ate" catalysed aldol reaction 131
3.3.10. A recapitulation 134
3.4. Synthesis of new chiral bifunctional catalyst 134
3.4.1. Retrosynthetic pathway of **257** 135
3.4.2. Pathway A: cyclisation by direct lithiation 137
3.4.3. Pathway A: cyclisation by Heck reaction 139
3.4.4. Pathway A. radical cyclisation 143
3.4.5. Pathway A: Parham cyclisation 144
3.4.6. Pathway A: cyclisation by Grignard reaction 147
3.4.7. Pathway B: C-C coupling 148
3.4.8. Pathway B: Synthesis of scaffold **258** 150
3.4.9. Direct lithiation on scaffold **258** 152
3.4.10 Summary 153

4. Conclusions and future work 154

5. Experimental work 156

5.1. General experimental 156

5.2. Synthesis of catalysts 157

5.3. Synthesis of MBH and aza-MBH products 163

5.4. The aldol reaction 167

5.5. Synthesis of new chiral catalyst 174

6. References 186

7. Appendix 196

7.1. Figure **1**: Crystal of **132** 196

7.2. Figure **9**: Crystal of **164** 206

7.3. Figure **2**: Crystal of **244** 211

7.4. Figure **3**: Crystal of **248** 216

1.Introduction

Throughout history, man has always been amazed by the potential of Nature. Especially in chemistry, where respect for the chemical efficiency of enzymes is considerable. Enzymes are long, linear chains of specific amino acids which can be modified. They can have different functions (e.g. as building blocks and regulation). One of the most important aspects of enzymes is their apparent simplicity and yet they can convert molecules rapidly and efficiently into new products. This reactivity is not only due to their shape, so substrates can easily fit, but also to the presence of different functional groups at the right place. In Nature, there are twenty basic amino acids, of which ten are polar. So the range of different functional groups is relatively limited. In recent years, man has been trying to mimic their activity and function to obtain similar or comparable results. One of these areas is the introduction and development of man-made catalysts which can mimic enzyme activities. In intial explorations in this area, chemists created large molecules which resemble real enzymes, for example, Breslow *et al.*[1] demonstrated bifunctionally-catalysed reactions on RNA models. In addition, Imbriglio *et al.*[2] used oligopeptides for asymmetric Morita-Baylis-Hillman reactions. Nowadays, catalysts are becoming more compact and their development involves modelling to aid design, hence, the functional groups are placed at the right orientation to effect catalytic reactions. There has also been an increase in publications showing the advantages of multifunctional catalysts. In particular, bifunctional compounds, for different asymmetric reactions have been developed, e.g. aldol, cyanosilation, Strecker, allylation and epoxide ring opening.

1.1.Bifunctional catalysts

Bifunctional catalysts are molecules that consist of a scaffold on which two functional groups are attached. This scaffold is normally an organic molecule with the role of positioning the functional groups correctly for catalysis, with the added requirement of providing stereocontrol, for example, by being chiral. In most cases, this scaffold is designed through the assistance of

molecular modelling. The reactive functional groups mediate the reaction being catalysed and are the essential components required for catalytic activity. In Nature, these groups are functions such as OH, COOH, NH_2, SH etc. and their role is to create complex stability between the catalyst and the substrate through hydrogen or electrostatic bonding. This complex stability has to be synchronised with substrate activation to enable reaction to take place, and it should be sufficiently labile to allow release of the product to allow catalytic turnover. In organic chemistry, the range of functional groups which can be used for catalytic applications is particularly wide and we can even employ systems such as Lewis acids.

According to Rowlands,[3] there are two major types of bifunctional catalysts which are classified by the way the functional groups cooperate. In the first group, there are two metals (Lewis acid, alkali or transition metal) that are coordinated to the same ligand and are available to bind to both the substrate and/or reactant during the catalytic process. Those metals can be the same (homobimetallic) or different (heterobimetallic). One of the most investigated catalysts of this type are those reported by Shibasaki.[4] These complexes exhibit both Lewis acid properties at the central metal atom and Brønsted basic properties at the outlying alkali metals centres. The scaffold is based on the BINOL structure, for example, systems such as **1**.

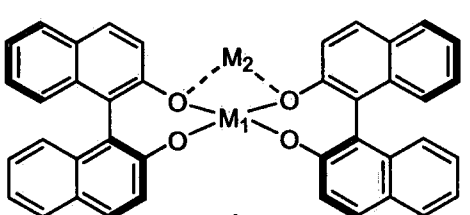

1

M_1: Al
M_2: Li

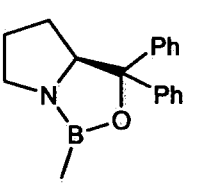

2

The second group contains a Lewis acid centre and a basic site in the same catalyst complex. Typically the substrate binds to the Lewis acid and a stoichiometric amount of a second metal reagent is required to bind to the base and deliver the reagent in a selective manner. One of the most important catalysts in this group is the proline-derived oxazaborolide catalyst for the chiral reduction of ketones, introduced by Corey, Bakshi and Shibata[5] (CBS-reduction) (see **2**), in which the ketone is reduced by a borane source (BH_3.THF or $BH_3.Me_2S$) which is complexed to

catalyst **2** (5 to 10 mol%) and high enantioselectivity can be obtained (e.e. > 95%) of corresponding alcohol. The Lewis base in this molecule is the nitrogen atom which coordinates with the reducing BH_3. This leads to activation of the borane with simultaneous intensification of the Lewis acidity of the endocyclic boron atom and ultimately activation of the ketone. The CBS-catalyst is an excellent example of a bifunctional catalyst. It has a low molecular weight and consists only of the most necessary functions. But more importantly, the two active sites are placed in such a manner that not only do they position the reagent and substrate to give an enantioselective reaction, but they also cooperate to activate both reactants. For our research, it is this type of catalytic system which is interesting, and indeed, our bifunctional catalysts also have a boron and nitrogen atom in the active systems. The only difference is that the function of the nitrogen atom can act as a nucleophile rather than a Lewis base, depending upon the structure. This gives us the advantage that we do not have to add a second metal reagent, however, we must make sure our catalysts are designed in such a way that the nitrogen atom is free to act in this way and neither too sterically hindered nor irreversibly coordinated to boron.

2.The Morita-Baylis-Hillman reaction

2.1.Introduction

The Morita-Baylis-Hillman reaction was first reported by Morita *et al.*[6] in 1968. It originally involved a 3-compound reaction where a C-C bond was formed between the α–position of an acrylate ester or acrylonitrile with an aldehyde under catalytic influence of tricyclohexylphosphine. In 1972, this reaction was patented in Germany by Baylis and Hillman.[7] Instead of phosphines, they used DABCO (diazabicyclo[2,2,2]octane) as catalyst (Equation 1). It was further popularised by the work of Drewes[8] and Hoffmann[9] in the early eighties.

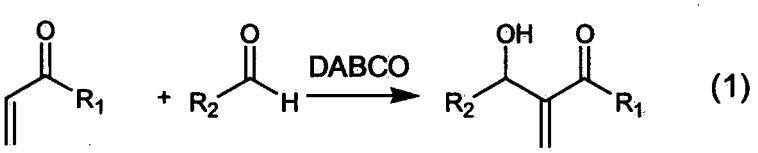

3 4 5 (1)

Nowadays, the three compounds are generally an active alkene **3** (mainly acrylates, acrylonitrile, and to a lesser extent, alkyl vinyl ketones which tend to give side reactions, see Shi *et al.*[10]), an electrophile **4** (mainly an aromatic aldehyde but also α–keto esters, aldimine derivatives, and fluoro ketones) and a catalyst (mostly nucleophilic, tertiary amines or phosphines and sulfines). The product of the reaction is a densely functionalized molecule containing an α-methylene and a β-hydroxyl group, which have been used in the synthesis of many natural products (e.g. integerrinecic, senecivernic and retronecic acids[8]). Not only is the product very appealing for organic chemistry, but also the lack of side products is very beneficial. The major drawbacks for the MBH reaction are the low reaction rates[11] and the limited substrate scope (especially for inducing chirality on the secondary hydroxyl group). In the last few years, the interest in MBH reaction has grown exponentially (more than 80% of the references used in this review were published within the last decade) indicating the importance of this reaction.

2.2.The aza-Morita-Baylis-Hillman reaction

Besides the 'normal' MBH reaction, there is also the aza-MBH reaction.[12] In this case, imines are used instead of aldehydes. To increase the rate of the reaction, several electron withdrawing groups, such as tosylates or mesylates, are generally attached to the nitrogen (Equation 2).

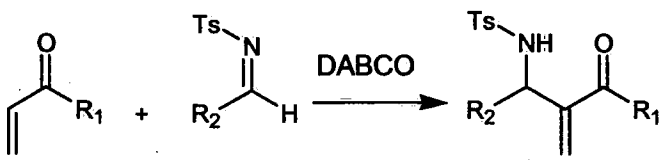

(2)

3 6 7

The reaction mechanism of the aza-MBH reaction is identical to the one of the general MBH reaction and the same catalysts can, in general, be applied for both reactions. In this review, the focus will be on the normal MBH reaction but some examples of the aza-MBH will also be discussed. The high reactivity of electron deficient imines can cause several side reactions, such as susceptibility to hydrolysis to the aldehyde, which then give rise to a mixture of aza-MBH and 'normal' MBH products. In addition, there is also the possibility of overreaction leading to intramolecular cyclisation or aldol product.[13] These side reactions are very substrate dependent (Scheme 1) which make it hard to synthesise a generally applicable catalyst for the aza-MBH reaction. For example, Scheme 1 provides an example that shows the influence of the ring size on the products in the aza-MBH reaction. Because of these issues, the general MBH has tended to be more researched and applied.

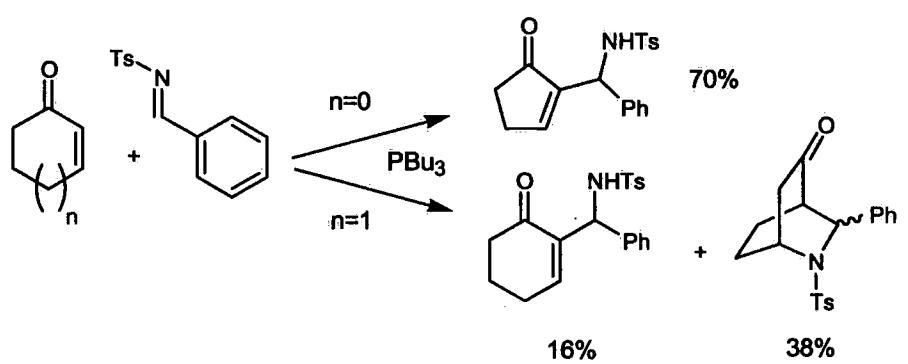

Scheme 1. Influence of ring size on aza-MBH reaction.

2.3.The mechanism

The mechanism of the MBH reaction is generally believed to proceed through a Michael-addition by the catalyst on the activated olefin resulting in a zwitterionic enolate **8** which can undergo nucleophilic attack onto an aldehyde **4** in an aldol fashion, to obtain a new zwitterion **9**. Subsequent proton migration and release from the catalyst gives us the desired molecule **5** (Scheme 2). Beside the MBH product, there is also some formation of dioxane products.

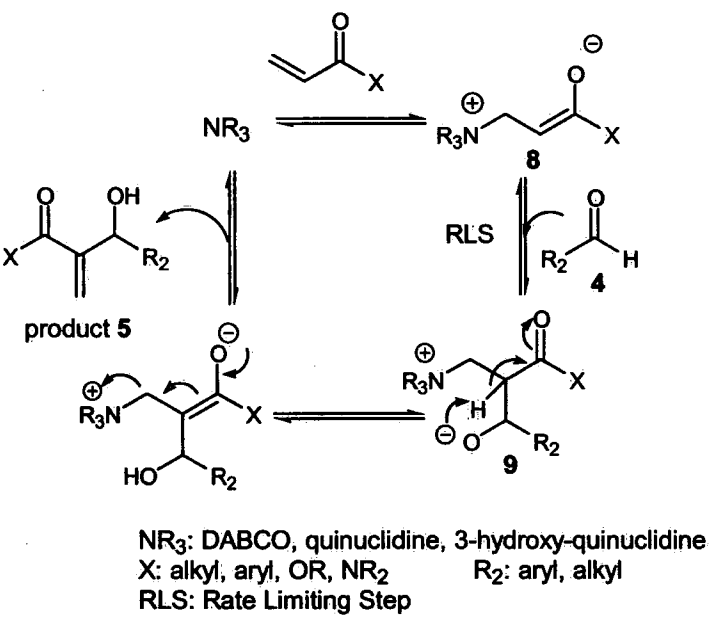

Scheme 2. Proposed mechanism for the MBH reaction.

This reaction mechanism was confirmed through electrospray ionization mass and tandem mass spectrometry by Santos *et al.*,[14] as they achieved the isolation of several intermediates and were able to analyse them. Also, kinetic studies by Bode *et al.*[15] showed evidence for this mechanism. Through these studies, it is known that the formation of the second zwitterion **9** (from the attack on the aldehyde) is the rate limiting step. Overall, the mechanism follows third-order kinetics (or a *pseudo*-second-order if the concentration of the catalyst is considered constant). Originally, it was thought that the reaction was irreversible, but thanks to the work of Fort *et al.*,[16] it became clear that the reaction is under equilibrium.

This mechanism has been accepted for some time, but recently questions were raised regarding this mechanism because most of the data, collected in the eighties, did not explain all the features of the MBH reaction. Aggarwal *et al.*[17] claim that in the initial phase of the reaction, the rate limiting step is not step 2, but step 3 (the proton transfer). Only when about 20% of the product is formed does step 2 become the rate limiting step. The reason for this is autocatalysis by the product which could be observed by the presence of an induction period in the conversion to the product. It is known that polar solvents catalyse the reaction (see below) and since the MBH product is an alcohol, it can catalyse its own formation. This induction period is absent when catalytic quantities of product or polar solvent are present. This hypothesis was also confirmed by Leitner *et al.*[18] by ^{1}H NMR experiments. Although they did not observe any autocatalysis, the rate equation showed a fractional rate order of 0.5 in aldehyde (rate= k_{obs}[catalyst][acrylate][aldehyde]$^{0.5}$). This fractional order indicated that the rate limiting step (RLS) was partly influenced by proton transfer. By adding the Brønsted acid 3,5-bis(CF_3)phenol (1 equiv. per aldehyde) they noticed an 14-fold rate enhancement and a first-order dependence of the aldehyde. This demonstrates that the elimination step was not involved in the RLS anymore. Even more revolutionary is a new interpretation of the MBH mechanism by Price *et al.*[19] (Scheme 3). In their approach, not one, but two aldehydes are consumed during the reaction. The start is identical to the accepted MBH mechanism where the Lewis base attacks on the acrylate and the zwitterion **8** formed undergoes a 1,2-addition to the aldehyde. However, instead of the proton transfer, there is then an addition of a second aldehyde to form the hemiacetal **10**. This hemiacetal undergoes a deprotonation to form an intermediate **12** which breaks down to the MBH product in a series of post-rate limiting steps.

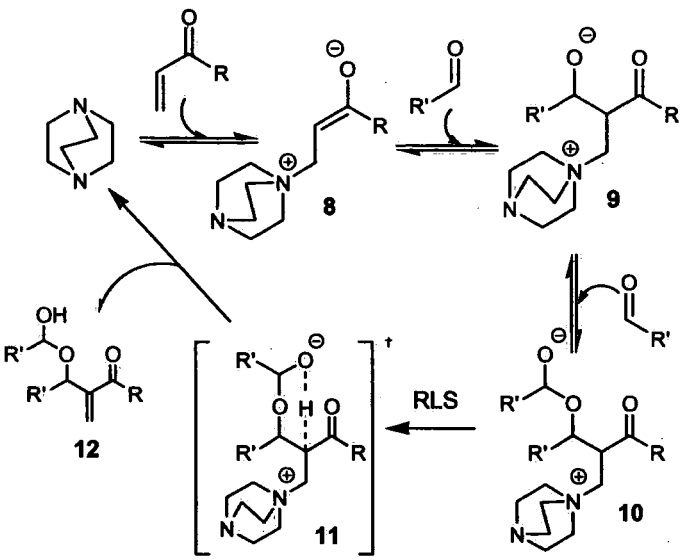

Scheme 3. The new proposed MBH mechanism.

This mechanism has been proposed on the basis of order plots and kinetic isotope effects (KIE) on the α-position. These show that the total reaction is fourth order and second order in aldehyde {rate = k_{obs}[aldehyde]^2[acrylate][DABCO]}. This also means that the RLS must have two equivalents of aldehyde, so it cannot be the 1,2-addition but it must be the deprotonation to the intermediate **11**. It becomes also clear that the second aldehyde is needed to get a good proton transfer, because the alkoxide **9** resulting from the 1,2-addition is geometrically unable to act as an intramolecular base. With this mechanism, Price *et al.*[19] predict that it is possible to explain some of the MBH features which was not possible to explain previously. For example, it is now easy to understand why dioxanes are common side products. This mechanism could also provide the answer as to why the MBH reaction is so slow. Most reactions are run with 1 equivalent of acrylate and 1 equivalent of aldehyde, following the accepted mechanism. However, this new mechanism shows that two equivalents of aldehyde are consumed, so the concentration of aldehyde decreases quickly which slows the overall rate. Perhaps because this publication is relatively recent (June 2005), there have not been any responses published either in support or otherwise.

Because of the level of speculation around the mechanism of the MBH reaction over the years, Zhu *et al.*[20] summarized it as follows: "Indeed, the deprotonation of the α-H of **9** is the RLS but because an intramolecular proton transfer from the α-carbon to the vicinal alkoxide anion (amide

anion in the case of aza-MBH) is geometrically constrained, two alternative transition states must be concluded. One occurs in the presence of protic solvents according to the findings of Aggarwal *et al.*[17] which gives **13**. The other one occurs in the presence of aprotic solvents and follows the mechanism by Price *et al.*[19] giving **14**."

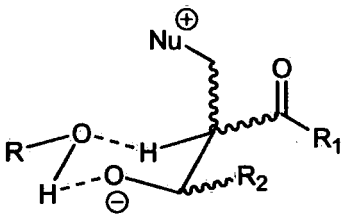

13

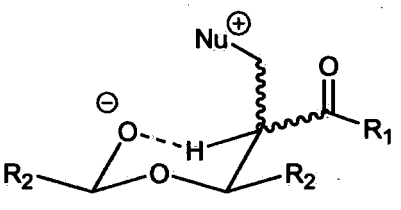

14

The understanding of the mechanism and the defining of the RLS is very important. It is through the RLS that any chirality at the hydroxyl group can be introduced. Hence this knowledge is required for the design and development new chiral catalysts for MBH.

2.4.Rate improvements

2.4.1.Substrates

One of the big disadvantages of the MBH reaction, as alluded to above, is the low rate of these types of reaction. Several articles report reaction times of weeks and even months until there are perceptible amounts of product formed.[11] The reaction rate is of course very dependent upon the substrates used. It is clear that by making the aldehyde more electrophilic (by adding more electron withdrawing groups), the reaction progresses faster. That is why reactions with *p*-nitrobenzaldehyde are particularly fast. On the other hand, it is difficult to predict the influence of the ester part of the acrylate on the rate of the reaction; this topic was researched thoroughly by Y.Fort *et al.*[16] Their findings were that firstly, when they used several benzyl acrylates with different functions on the *para-*, *meta-*, and *ortho*–positions (electron-donating and electron-withdrawing groups), they could investigate the electronic effects since steric effect were minimal (all essentially the same in each case). They concluded that there was not any significant

difference between the influence of electron-donating or electron-withdrawing groups on the rate. This can be explained by the fact that electron-donating groups favour the nucleophilicity of the zwitterion, but disfavour its formation, and the reverse argument can be applied for electron-withdrawing groups. They also showed that the influence of the groups decreases when they are further away from the carbonyl group. In a second experiment, alkyl acrylates were employed to examine the influence of the chain length on the rate. As expected, the rate of reaction decreased by increasing the chain length. This behaviour can only be explained through steric hindrance. Finally, they also used functionalised alkyl acrylates, however, there was no effect to be found since there is a combination of steric and electronic effects that influence the rate.

An interesting discovery was found by Basavaiah *et al.*[21] in the use of terminal hydroxyl acrylates for MBH reactions. They showed that these compounds speed up the reaction in comparison to simple normal alkyl acrylates. For example, under the same conditions the reaction with 10-hydroxydecyl acrylate was complete in 6 days with a yield of 78%; while the reaction with decyl acrylate was still not complete even after 12 days, giving a yield of 60%. This acceleration can be explained by the formation of an intramolecular hydrogen bond between the terminal hydroxyl group and alkoxide. According to these workers, there are two possible intermediates: one with a hydrogen bond to the terminal hydroxyl group in zwitterion **8** (see **15**) or involving zwitterion **9**, where the aldehyde is already attached (see **16**). Alternatively, the intermediate could involve the formation of an intermolecular hydrogen bond that accelerates the reaction, because even long alkyl chains with a terminal hydroxyl show the same effect. A disadvantage of these types of acrylates is that a large amount of side products due to trans-esterification are produced.

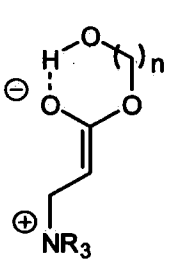

15

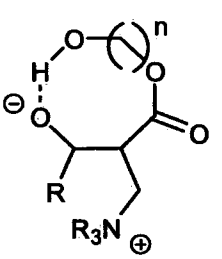

16

Another interesting observation on this matter was found by Chen *et al.*[22] by screening different acrylates. They noticed a significant rate acceleration when α-naphthyl acrylate was employed as unsaturated carbonyl compound. Under normal conditions (using 50 mol% DABCO in acetonitrile), methyl acrylate and benzaldehyde yields 68% of product after 4 days. Under the same conditions but using α-naphthyl acrylate, 88% of product was isolated after only 20 minutes. Different aldehydes were screened and in all cases an increase of rate was observed (between 35-82% yield after 20 minutes). Even more interesting was the ability to use not only aromatic aldehydes but also aliphatic ones. Normally, aliphatic aldehydes are not particularly useful for the MBH reaction because there is the possibility of deprotonation of the α-proton of the aldehyde when the catalyst is too basic. In this way, different side products can be formed which is not normally the case under the reaction conditions used. A possible explanation for the observed acceleration with α-naphthyl acrylate is still under investigation but it is thought that the substituted acrylate may possess stereo- and/or stereoelectronic properties which stabilize the oxy-anion intermediate. Besides the conventional MBH product, it was also found small quantities of dioxane products increased by using more equivalents of aldehyde. This was in accordance with the data published by Price *et al.*[19] (see above).

2.4.2.External conditions: solvent and salt effects

There have been already several attempts reported at accelerating the MBH reaction. One way to do this is by changing the external conditions, for example, by the use of microwave irradiation,[23] sonication,[24] high pressure,[25] lower temperature,[26] mechanochemistry,[27] and supercritical carbon dioxide.[28] One of the most investigated factors is the influence of different solvents on the reaction. Since the mechanism of the MBH reaction proceeds through the formation of zwitterions, a lot of researchers have tried to use polar solvents and more specific protic solvents, such as methanol,[29] formamide,[30] sulfolane,[31] DMF,[32] 1,4-dioxane[33] and even pure water[34] with some success. The big disadvantage with polar solvents is the fact that they do not dissolve all the reagents, hence, sometimes a mixture of solvents is needed. Basavaiah *et al.*[35] used aqueous trimethylamine (30% w/v) since it is readily available and cheap, as both a solvent and catalyst. Under these conditions, methyl acrylate and 4-nitrobenzaldehyde provide 56% MBH product after only 5 h, compared to conventional conditions (50 mol% DABCO in DCM)

which give 47% MBH product after 3 days. Since it was clear that water speeds up the reaction, further research was taken to determine the influence of pH on the rate. Hailes *et al.*[36] applied trimethylamine and DBU in aqueous acidic media at pH 1. It was hoped that the protonation of the acrylate and aldehyde would increase the rate, however, only very minor acceleration was observed in some cases, and most frequently, the reaction was slowed down. This shows clearly that the catalyst is protonated and hence, was unable to act as a nucleophile. This is to be expected since amines are basic. Besides acidic conditions, basic conditions were also applied for MBH reactions. Cheng *et al.*[37] used imidazole as a catalyst in a THF-water mixture. They noticed by bringing the solution to pH 8.6 by adding sodium bicarbonate the reaction improved significantly. They presumed that imidazole in neutral water is automatically protonated. Hence, by increasing the pH, the imidazole becomes more deprotonated, and therefore, active as catalyst. When the pH was pushed higher than 8.6, however, more side reactions occurred. This was probably due to the presence of hydroxy anions which start to react with the different reagents. This also shows that the basic pH influences the MBH reaction depending on the catalyst used.

Originally it was thought that simple hydrogen bonds between solvent and zwitterion **8** (see **17**) would be the reason for acceleration, however, recent work by Aggarwal *et al.*[17] shows that there is actually a proton exchange between the polar solvent and the zwitterion **9** (see **18**).

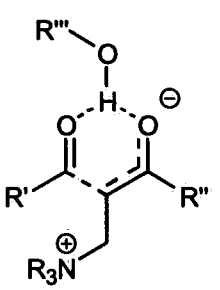

17

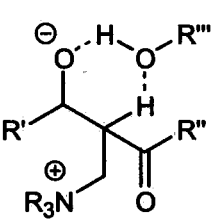

18

They managed to follow the reaction by isotope exchange and kinetic isotope effects (KIE) between the solvent and the intermediate. This work is likely to be important because if this is the case, it would prove that the proton transfer is the RLS, instead of the attack on the aldehyde.

Not only is this ground breaking in terms of the mechanism, but it could also help in the future to explain the origin of asymmetric induction and with the development new catalysts.

A new method to improve the rate of the MBH reaction is the use of ionic liquids (IL). Ionic liquids are inert organic solvents with unique properties such as high polarity and zero vapour pressure. Therefore, they are recyclable and hence, are considered 'green chemicals' by some. It is this high polarity that is appealing to organic chemists. Their high polarity is caused by the presence of organic salts such as imidazolium **19** or pyridinium **20** cations with counter ions such as PF_6 or BF_4. For example **19** [bmim] was one of the first IL which was used for MBH reaction, and therefore, it has been heavily investigated by several groups, such as Santos *et al.*[38], Ko *et al.*[39] and Kumar *et al.*[40]. They noticed a 10 to 30 fold rate increase when DABCO was used in an IL in place of acetonitrile solvent.

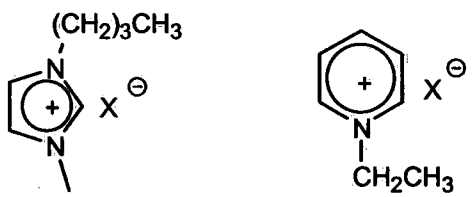

X=BF_4, PF_6

19 **20**

To understand the role of the IL on the acceleration of the MBH, Eberlin *et al.*[41] repeated several reactions in an IL and analysed different intermediates by electrospray ionization mass spectrometry. They managed to identify the different peaks of the supramolecular species and found out that the IL participates in almost every step of the catalytic cycle of the MBH reaction. They concluded the IL firstly activates the aldehyde towards a nucleophilic attack by coordination and then stabilizes the zwitterionic species through supramolecular coordination. To optimize reaction conditions further, Afonso *et al.*[42] and Ko *et al.*[39] screened different counter ions of **19**. They noticed increasing reactivity of [bmim]X with X=OTf>BF_4>PF_6>Cl>NTf_2>CH_3CN. Also, different Lewis acids[38,39] ($La(OTf)_3$ or $Sc(OTf)_3$) were added to the IL, however, only minor or no acceleration by the Lewis acids was observed.

This is surprising because it is known that Lewis acids normally increase the rate of the MBH reaction (see below). A scientific explanation has not been established for this observation as yet, however, it is thought that the Lewis acid interacts with DABCO causing a decrease in the effective DABCO concentration.

Although there are benefits to ionic liquids, it is necessary to consider these organic salts as active molecules, so it is not surprising that one of the big disadvantages of ionic liquids is the presence of side reactions. As reported by Aggarwal *et al.*,[43] the use of imidazolium salts **19** in the presence of a mild base gives a reactive nucleophile **21** which can consume the aldehyde, leading to lower yields (Scheme 4).

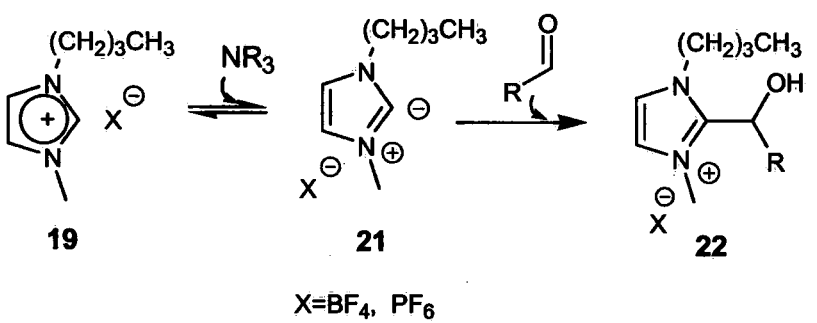

Scheme 4. Side reaction with IL **19**.

This type of side reaction was also noticed by previous researchers. Detailed investigations by Afonso *et al.*[42] showed that the deprotonation was highly dependent of the counterion ($Cl^- > BF_4^- > PF_6^- > Tf_2N^-$) with 16% adduct of **22** with PF_6^- and 44% with Cl^-.

Because of this side reaction, the use of non-imidazolium-based ILs such as **20** has gained more interest.[44,45] This results not only in a rate improvement, but the IL was inert to reagents and water. Another way to tackle this side reaction was to add an extra methyl group on position 2 of **19**. Following this procedure, Chu *et al.*[46] created an IL based on salt **23** [bdmim]. This avoided the possible deprotonation reaction and showed higher yields of the MBH products.

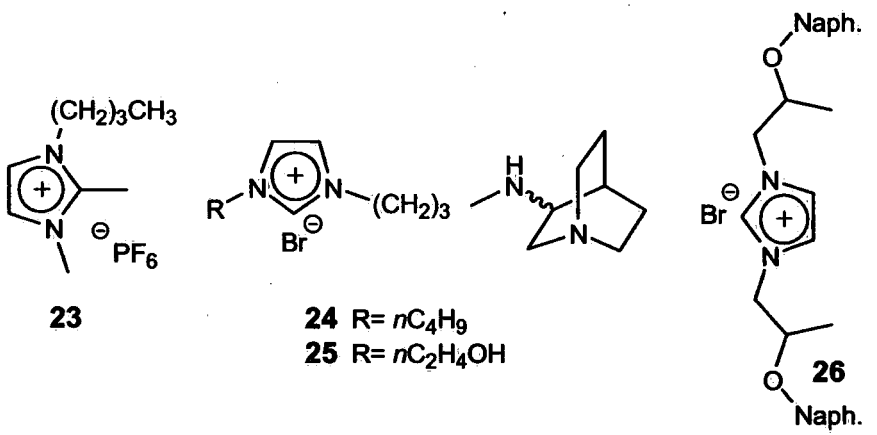

23

24 R= nC_4H_9
25 R= nC_2H_4OH

26

Building on previous knowledge, Cheng *et al.*[47] reported the first IL-supported catalyst **24** where quinuclidine on **19** was attached, giving an entropic advantage to the overall reaction process. Only by adding MeOH to the IL could a significant increase in rate be observed compared to 3-quinuclidinone or DABCO in MeOH. Under these conditions, no side reaction due to the IL was observed. The fact that MeOH was needed to accelerate the reaction indicated the importance of hydrogen bonding, and therefore, derivative **25**[48] was created by adding an extra hydroxyl group on the scaffold. This resulted in clear improvements compared to **24** and no extra solvents were necessary. Also, Tsai *et al.*[49] introduced a variant of **19** by adding 2-naphthol side chains on the imidazole to give **26**, resulting in an increased rate and a decrease in side products.

Besides the use of organic salts, inorganic salts such as $LiClO_4$ and LiCl have also been investigated for the MBH reactions. The first group to apply these salts for the MBH reaction was that of Kobayashi *et al.*[50] In 1999 they screened different salts and noticed a dramatic acceleration when $LiClO_4$ was added under certain reaction conditions. They presumed that the stabilization of the zwitterion **8** was enabled by means of added salt. Further investigations by Kumar *et al.*[51] concluded that it was difficult to find a conventional role for the salt in the reaction. Although the use of salt has a big influence on the reaction, it depends very much on the solvent used and the particular reactants employed. For example, salt promotes the reaction of benzaldehyde with methyl acrylate in water, formamide and *N*-methyl formamide, but this reaction is inhibited in ethylene glycol. This is strange since ethylene glycol is also a polar protic solvent. On the other hand, the reaction of benzaldehyde with acrylonitrile in the presence of LiCl reacts faster in ethylene glycol compared to water and formamide. This complex behaviour

shows us that besides hydrophobic effects and solvent polarity, salting-in and –out phenomena can also influence the rate of the MBH reaction.

2.5.Catalysts

Another way to speed up the MBH reaction is to modify the catalyst or add a co-catalyst. Generally there are two types of catalysts: nucleophilic and acidic.

2.5.1.Nucleophilic catalysts

A nucleophilic catalyst usually contains often a Lewis base which accomplishes the actual Michael addition part of the MBH reaction. This base is most commonly an amine but the amino function can be replaced by phosphorous or sulfur groups. The geometry of this type of catalyst is specified by the position of the binding atom. This means that the nucleophilic atom is pushed out of the molecule so it can react faster. Therefore, most of these catalysts possess a bicyclic or tricyclic structure including all the quinuclidine based-molecules, such as DABCO and quinuclidine itself, which were the first catalysts used by Baylis and Hillman. One of the most used catalysts of this group, besides DABCO, is 3-hydroxyquinuclidine **27** (3-HQD).[52] This catalyst shows a considerable rate enhancement in comparison to DABCO. It was initially believed this was due to an intramolecular hydrogen bond between the hydroxyl group of the catalyst and the enolate **28**.[52,53] However, through modelling studies, it became clear that this type of bond could induce strain in the enolate. Since then, the acceleration has been ascribed to the ability of 3-hydroxyquinuclidine (3-HQD) to protonate the developing zwitterionic intermediate intermolecularly, as shown in **29**.[24]

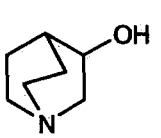

27

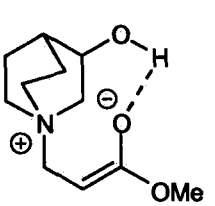

28

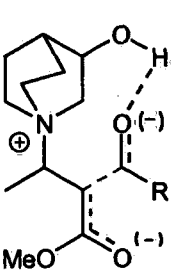

29

In contrast, Aggarwal *et al.*[54] compared 3-hydroxyquinuclidine with DABCO in water. Normally you would suspect that the rate of reaction would be the same since the hydrogen bonds between 3-HQD and enolate are interupted in water. Strangely, 3-HQD was still superior over DABCO and this prompted Aggarwal to conclude that there had to be a correlation between the reactivity and the pK_a of the catalyst. More specifically, it showed that the best nucleophilic catalysts have a high pK_a in organic solvents. This is explained by the fact they can carry the positive charge which is formed during the attack on the alkene.

Besides the use of amines as Lewis bases, phosphorus-based catalysts are also very common. Morita *et al.*[6] was first to use tricyclohexylphosphine as a catalyst in 1968 and since then, new phosphorus catalysts have emerged including Et_3P, Bu_3P, Ph_3P, and Ph_2MeP.[13,55,56] Although tertiary phosphines have better nucleophilicity and weaker basicity than their nitrogen analogues, the major drawback of these catalysts is the possibility of oxidation by air, especially when the phosphorous centre is made more nucleophilic. Hence, triphenylphosphine is stable in air but less reactive than other phosphines because of the delocalisation of the electron pair on phosphorous. On the other hand, tributylphosphine is much more reactive but less stable. One of the first air-stable trialkylphosphines for MBH reactions was introduced by He *et al.*[57,58] 1,3,5-Triaza-7-phosphaadamantane **30** (PTA) is a cage-like phosphine and appears to be more air-stable than Ph_3P. It shows equal reactivity to DABCO and is also useful for the aza-MBH reaction. PTA was compared to its nitrogen counterpart HMT (the same molecule only the phosphorous is replaced by nitrogen), which was also screened for MBH reactions.[59] PTA showed much higher reactivity than HMT, which indicated the crucial role of phosphorous. ^{31}P NMR data and X-ray crystal of the PTA-zwitterion between PTA and methyl acrylate showed unambiguously that the Michael addition of PTA occurs at the phosphorus atom. This X-ray crystal is very important since it also verifies the importance of the Michael addition step in the catalytic cycle.

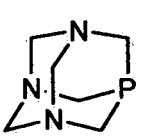

30

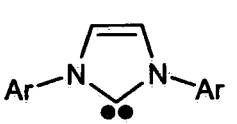

Ar: 2,6-(*i*-Pr)$_2$C$_6$H$_3$

31

Other Lewis bases used as catalysts are the chalcogenides, in the form of sulfides and selenides, however, because of a lack of nucleophilic reactivity the co-addition of a Lewis acid was necessary (see below).

Rather unusual catalysts for the MBH reaction are alkoxide anions. Because these salts are normally more basic than nucleophilic, it is perhaps surprising they are used for this reaction. Frater *et al.*[60] were the first to apply alkoxides for an intramolecular MBH reaction, although with limited success (only 10% yield). More in-depth investigations on these salts were carried out by Cheng *et al.*[37, 61]. They screened DBU with 4,4-dimethylcyclic enones and benzaldehyde in different solvents. In DMF, MeCN, DCM, etc., only traces of the MBH products were observed which they ascribed to steric hindrance. Interestingly, in MeOH and EtOH they isolated more than 90% of the MBH products. Further investigations showed that the catalyst in these cases was not DBU, rather the methoxide and ethoxide anions. This was eventually confirmed when sodium ethoxide and sodium methoxide was used as sole catalyst, giving the same result. Despite the excellent yields for 4,4-dimethylcyclopent-2-enone with different aldehydes, other enones gave mixtures of MBH and aldol products.

Other unusual catalysts for the aza-MBH reaction are *N*-heterocyclic carbenes. The most stable *N*-heterocyclic carbenes are imidazol-2-ylidenes which are prepared by deprotonation of imidazolium salts. Ye *et al.*[62] were the first to report an MBH reaction catalysed by this type of molecule. They used *N*-heterocyclic carbene **31** and screened it for the MBH reaction of cyclopent-2-en-1-one and cyclohex-2-en-1-one with a variety of *N*-tosylarylimines. They managed to gain very good yields (72-99%) under the optimized conditions. Although it was clear by ^{1}H NMR that **31** reacted with the imines itself, this process did not lead to lower yields which indicated that the addition reaction was reversible.

A special catalyst in this general group is Et_2AlI.[63] Although aluminium is a Lewis acid, it still can be considered as a nucleophilic catalyst because the iodide can also carry out the Michael addition process in the reaction mechanism. The efficiency of this catalyst is the result of the combination of the Lewis acid (aluminium) and the nucleophilic iodide ion. The mechanism goes through several steps (Scheme 5), however, it is basically identical to the original mechanism.

One major difference is that during the proton transfer, since this involves the release of ethane it makes the reaction irreversible.

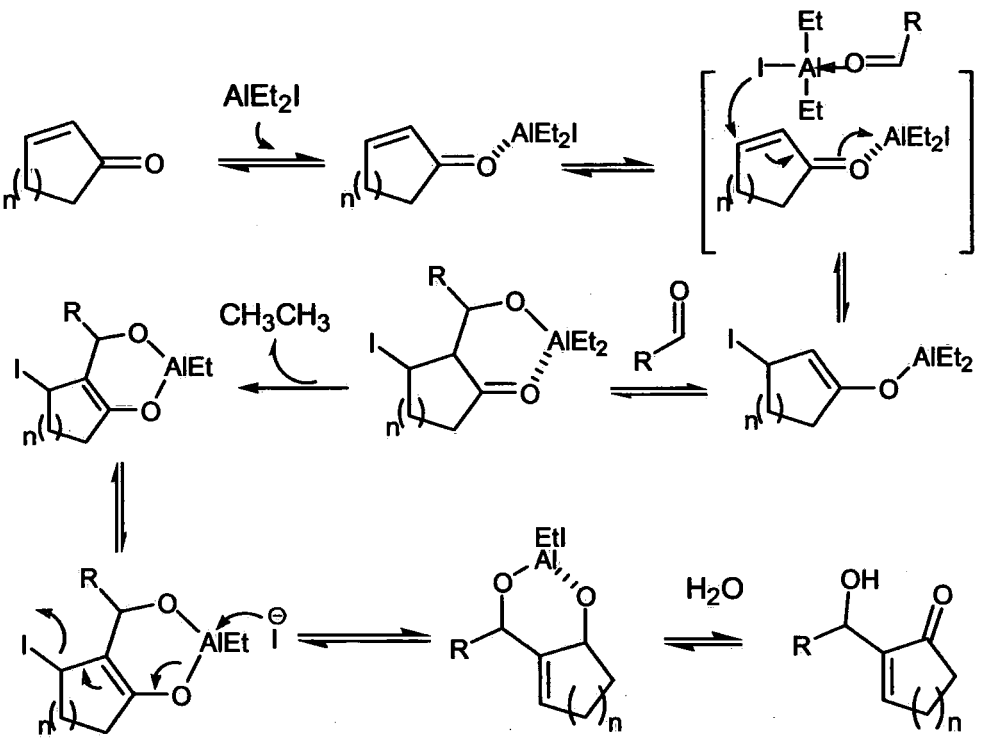

Scheme 5. MBH mechanism with Et_2AlI.

Unfortunately, the reaction needs to be carried out at 0 °C and with 1.2 equivalents of Et_2AlI, otherwise, too many side products are created. This prevents the reaction from reaching completion and only about 60% product is formed after 24 h. These conditions also limit the use of other reagents because when α,β-unsaturated acyl ketones are employed, the reaction stops at the stage of the halo aldols. A good explanation for this behaviour is not known yet. The same conditions and mechanism also applies when $TiCl_4$[64] is used as the catalyst, however, in this case HCl is formed.

Not only is the nucleophilicity of the catalyst important, but the ability to stabilize the intermediate plays also a key factor. This was concluded through experiments with DBU (1,8-diazabicyclo[5,4,0]undecene),[65] tetramethylguanidine[66] and DMAP. These catalysts show very

good reactivity in comparison with geometrically similar molecules although they are not particularly nucleophilic or the most hindered systems employed. The reason for their higher reactivity is their ability to stabilize the positive charge intermediate on the attacking nitrogen atom and delocalise it onto other nitrogen atoms (Scheme 6).

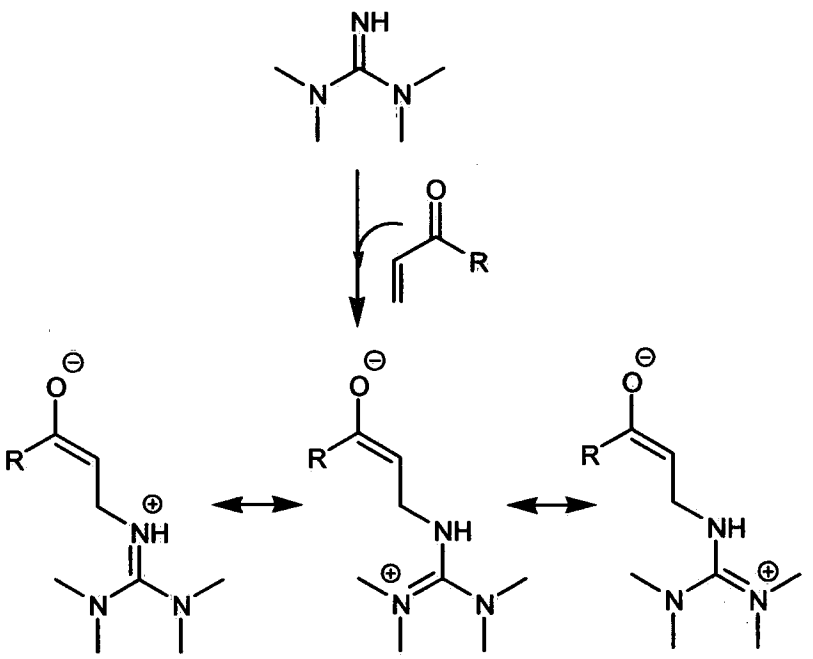

Scheme 6. Stabilization of positive charge during Michael addition.

The ability to carry a positive charge has also a major drawback, especially in protic solvents as water. In these conditions the catalysts will easily be protonated and lose their reactivity. This was studied by Cheng *et al.*[67,37] while working on the MBH reaction with different heterocyclic catalysts in a water-THF mixture. When imidazole was used on its own, *p*-nitrobenzaldehyde and cyclopent-2-enone gave 92% MBH product in 16 h. By adding $NaHCO_3$ the yield increased to 88% in 1.5 h. Also different azoles[68] were tested as catalyst for the MBH. The same behaviour was noticed only in lower yield compared to imidazoles.

The newest development in MBH research is the use of heterogeneous catalysts. Heterogeneous catalysts are normally solid phase polymers which have at surface functional groups which are catalytically active. The advantages of these types of catalysts are their reusability and the ease

of removal from the reaction mixture. In this way, the mixture has just to be washed from the polymer which can be used again. The first group to make use of these types of polymers for the aza-MBH reaction was that of Jung *et al*[69] in 1998. They applied a three component reaction with a methyl acrylate attached to the polymer instead of a catalyst. To this they added an excess of different aldehydes, tosylamides and DABCO. After 20 h at 70 °C, the excess reagents were removed and the aza-MBH product could be easily cleaved from the solid phase in good yields. Today, it is more often the catalyst which is attached to the polymer. The synthesis of these catalysts can be achieved in a number of different ways depending upon the different research group. An important factor for solid phase chemistry is the use of a good solvent, because the solvent is responsible for the polymer swelling, which is necessary for accessibility to the reagents.

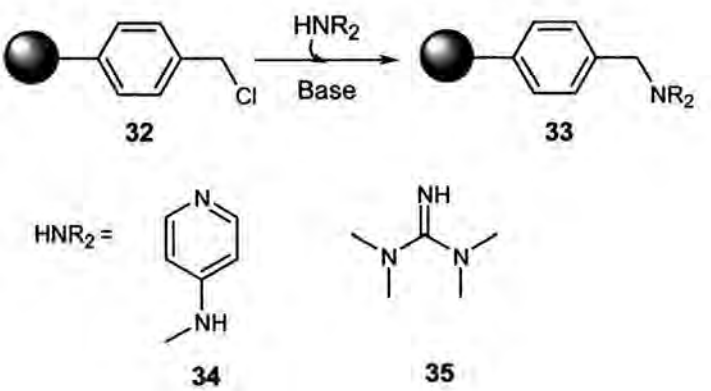

(3)

In the literature, there are two groups who have created polymers by modification of Merrifield resin **32** (polystyrene with chlorobenzyl groups) for use in MBH reactions and substituted with a nitrogen-based nucleophile (Equation 3). One of the groups is that of Corma *et al.*,[70] who used as the nucleophile, 4-methylaminopyridine **34**. They reported moderate yields with several reagents but only when an excess of alkene was used. Also, they noticed a decrease in activity of the catalyst every time it was reused. Through IR spectroscopy they found that several new bands from 1650 to 1750 cm^{-1} appeared in the reused catalysts. This meant that there were several carbonyl groups present in the deactivated polymer. According to Corma, zwitterion derivative **37** was produced by reaction between the catalyst and the alkene on the polymer. Only by washing the solid phase with 2 M NaOH was the normal activity regained (Equation 4).

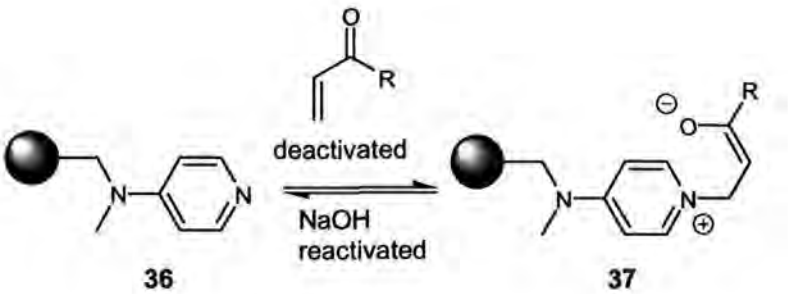

36 37 (4)

The other group, Leadbeater *et al.*,[66] used tetramethyl guanidine (TMG) **35** as the nucleophile. Although TMG is a very good catalyst for the MBH reaction, when connected to a polymer it showed no reactivity. This inactivity may be caused by the steric crowding in the environment of the polymer. To investigate this, they prepared benzyl-TMG. This is a homogeneous catalyst and is less bulky, and so, it is more readily accessed by the reagents. However, this catalyst also showed also no reactivity. Therefore, they suggested that the amine hydrogen on free TMG is the key to its activity towards the MBH reaction and substitution of this hydrogen for the benzyl group renders the complex inactive.

A different type of this kind of polymer system was created by Shi *et al.* In this case, the polymer was formed from 4-diphenylphosphine styrene monomers **38** which were polymerized using suspension conditions. This approach had the advantage of building in different types of building blocks **39** to modify the solid phase. Also it was interesting to see the influence of a phosphorous nucleophile (Equation 5).

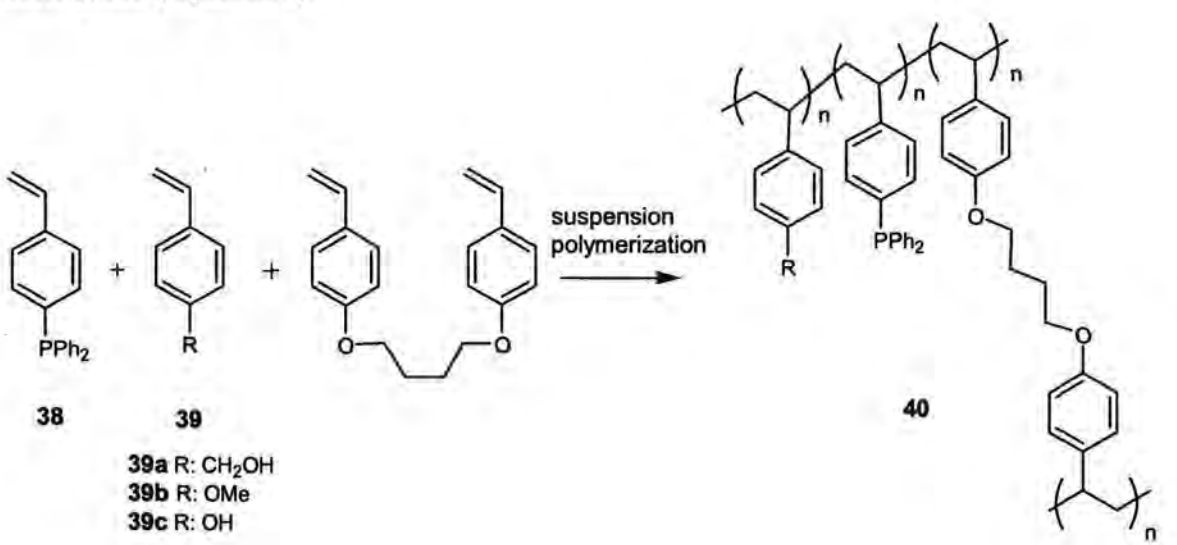

38 **39** **40** (5)

39a R: CH_2OH
39b R: OMe
39c R: OH

In the first series of experiments,[71] Shi only used monomer **38** and **39a** to create the solid phase. They screened sulfonated imines with methyl acrylate for the aza-MBH in different solvents with different catalyst loading. They noticed two important parameters which influenced the yield: The swelling degree of the solid phase and amount of active groups on the polymer. Although both influenced the yield in a positive way, however, there was a negative correlation between these two parameters. This was interpreted to mean that with more active groups on the polymer, there was a lower degree of swelling of the polymer, and *vice versa*. Therefore, there was a limit on the number of active groups required to achieve the highest swelling and highest yield of aza-MBH product. The best results were obtained with a 1.5 mmol PPh_3 gm^{-1} loading in THF. In the second series of experiments,[72] Shi introduced monomer **39b** into the solid phase to make it more polar and hence, to increase the rate. Surprisingly, it appeared that the incorporation of 4-methoxystyrene **39b** was much more beneficial than the corresponding 4-methanolstyrene **39a** for the aza-MBH. This was unexpected because it is known that protic compounds increase the speed of the aza-MBH reaction (see earlier). They tested the same catalyst **40** also for the conventional MBH and it appeared that the phenolstyrene **39c** gave the best results, as expected.[73] The reason as to why the aza-MBH and the regular MBH behave different is not known yet.

2.5.2.Acid based catalysts

The use of acid-based catalysts for the MBH reaction is applied generally today. Their purpose is to complex with the oxygen atoms of the carbonyl groups of the unsaturated carbonyl derivative and hence, make it easier for the nucleophile to attack. It is important to mention that acid-based catalysts are considered, in most cases, as co-catalysts. This means that they are not necessary but they are often helpful. On the other hand, nucleophilic catalysts are necessary for all MBH reactions as without them, even in the presence of an acid catalyst, there can not be any product formed. There are two major groups of this type of assisting co-catalyst: the Brønsted acids and the Lewis acids.

The Brønsted acids normally possess an alcohol or secondary amine so it will complex with the carbonyl groups through hydrogen bonding. This group is mostly applied and includes also the

protic solvents as MeOH, water, etc. The simplest Brønsted acid catalysts are the phenols. These have a pK_a which is not too low to avoid possible protonation of the nucleophile, but is low enough for catalysis. Both Leitner[18] and Liu[56] screened different phenols in the aza-MBH reaction with PPh_3 as nucleophile and both groups came up with almost the same result. Leitner had the best results with 3,5-bis(CF_3)phenol (pK_a~ 8) and Liu with *p*-nitrophenol (pK_a~7.2). They noticed a significant acceleration when the phenols were added and followed the reaction with ^{31}P NMR. They observed an interesting new signal at 29.96 ppm corresponding to the phosphonium enolate which indicated that the Brønsted acid stabilized the enol. This signal was not observed without the addition of the phenol. Besides the phenols, there are also more complicated Brønsted acids. Connon *et al.*[74] created a kind of organocatalyst based on bis-aryl ureas. They tried several structures bearing in mind the need to keep the pK_a as low as possible in order to have the maximum binding affinity. Also, an important aspect was to avoid complexation of the catalyst with Lewis-base or ionic functionalities which could lead to self-quenching. In their research, they found catalyst **41** to be the most reactive. It catalysed the MBH reaction of benzaldehyde and methyl acrylate in the presence of DABCO to yield 88% of product in 20 h. Under the same conditions without their catalyst, only 32% product was obtained. It was interesting to know that they were able to recover 87% of their catalyst and hence, they could reuse it. They postulated that the catalyst enhanced the reaction with hydrogen-bonds operating through a transition state **43** or through a Zimmerman-Traxler-type of transition state **44**. To support this hypothesis, they repeated the reaction and used an equimolar amount of tetrabutylammonium acetate (TBAA). In this case, they noticed no reaction of the catalyst because TBAA was binding with the urea N-H bonds. To improve the reactivity of the catalyst they synthesised **42**. This molecule contained at one side DABCO and at the other side the Brønsted acid, mimicking a bifunctional catalyst. By connecting the two parts they hoped to get more entropic advantage. However, experiments showed that **42** was less reactive then DABCO. This reinforces the findings by Aggarwal *et al.* that good nucleophilic catalysts have to contain a function with a high pK_a.

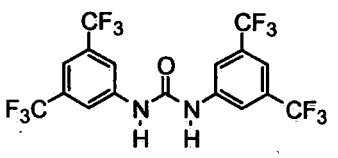

41

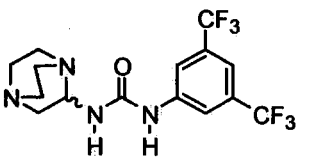

42

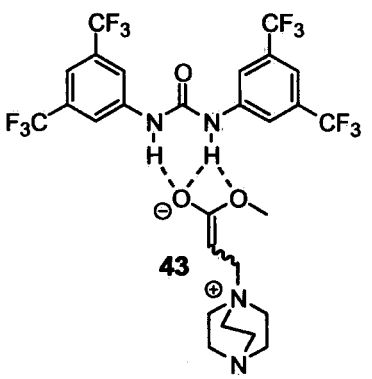

43

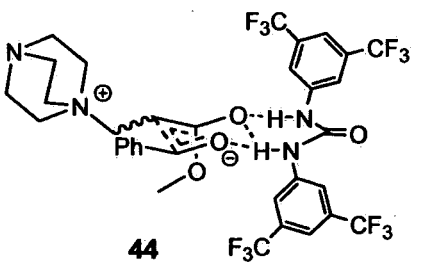

44

The best co-catalysts are the Lewis acid catalysts. They show very high reactivity and are also commonly used. The reason why they are so reactive is because they pull, through complexation, the electrons away from the oxygen of the carbonyl group, which makes the carbonyl carbon more electron deficient. An additional advantage of these catalysts is the possibility to form a complex with two or more carbonyl groups. Hence, they can bring the aldehyde and the alkene close together and this gives an entropic advantage to the reaction. It is important to take a hard Lewis acid (*i.e.* oxo-philic) because otherwise it would complex with the Lewis base. This is why normal Lewis acids, such as $BF_3.OEt_2$ are avoided. The most useful Lewis acids are the transition metals of group 3 such as $La(OTf)_3$ and $Sm(OTf)_3$. Aggarwal *et al.*[75] investigated in detail the use of $La(OTf)_3$ and found that no reaction occurred when less than 10 mol% DABCO was used, probably because it associated with the Lewis acid. Above this concentration, DABCO performed the role of nucleophile and $La(OTf)_y(DABCO)_2$ acted as Lewis acid through transition state **45**. To avoid the complexation between the two catalysts, Aggarwal tested several diol ligands making advantage of the oxo-philic nature of the metal and to displace the bond Lewis base. He found that (+)-BINOL gave good rate enhancements. Not only did the reaction now occur with less than 10 mol% DABCO, but the effect of the Lewis acid was more profound (a stronger Lewis acid was generated). Even more importantly, the consequence was that now it

was possible for an asymmetric function to be introduced into the catalyst which gave the opportunity to do asymmetric synthesis.

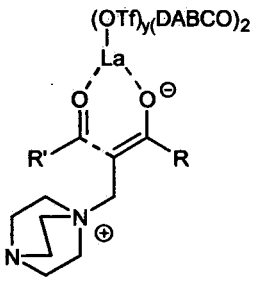

45

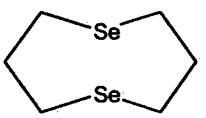

46

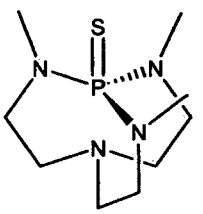

47

A very efficient Lewis base –Lewis acid combination was found in the chalcogenides with $TiCl_4$. This combination takes advantage of the weak interaction between a hard Lewis acid and a soft chalcogenide Lewis base. Kataoka *et al.*[76] were one of the first groups to use this combination for the MBH. They screened several chalcogenides and Lewis acids and found that the combination between bis-selenide **46** and $TiCl_4$ gave the best results. It was important to use the same number of equivalents of $TiCl_4$ as reagent, since it appeared that the Lewis acid bound to the product. A possible explanation for the good results with **46** was because of a transannular interaction between the two selenides which made the **46** more nucleophilic. An improved version was achieved by Verkade *et al.*[77] They created the proazaphosphatrane sulfide **47** which appeared to have a very nucleophilic sulfur atom. This nucleophility resulted not only from the nitrogens next to the phosphorous, but also from the bridgehead nitrogen axial to the phosphorous, all of which donate their electrons to the sulfur. When 2-cyclohexenone and *p*-nitrobenzaldehyde were used for the MBH reaction with $TiCl_4$ (1 eq) and **46** (0.1 eq), 85% product was isolated after 1 h. When **47** (0.05 equiv.) was used under the same conditions, already 94% was isolated after only 10 minutes. This indicated that **47** is probably the fastest nucleophile currently known for MBH. There has been controversy about the possible mechanism of this reaction. One possibility suggested was that the chalcogenide attacked the $TiCl_4$ and hence, liberating chloride anion which could then act as the nucleophile for the Michael addition. Another possibility could be that the chalcogenide itself directly achieves the Michael addition. This last possibility was confirmed by Goodman *et al.*[78] when they managed to isolate the Michael addition adduct with the sulfide cation at the β-carbon using tetrahydrothiophene and $BF_3.OEt_2$. Also, Verkade *et al.*[77]

came to the same conclusion, when they used **47** without any Lewis acid and only obtained 5% product. When $BF_3.OEt_2$ was added, the yield increased to 50%. Because it is very unlikely that a halide ion can be released from $BF_3.OEt_2$, the increase in yield is most likely to be due to coordination between BF_3 and carbonyl oxygen, and **47** is the only molecule which does the addition. When $BF_3.OEt_2$ alone was used, no product was formed.

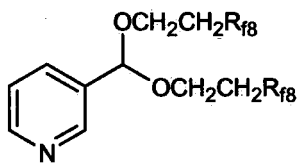

48

Another recent development in the MBH reaction is the use of fluorous biphasic systems. These systems exist of an organic layer (upper layer) with the reagents, and a fluorous phase (lower layer) with different fluorinated catalysts. These systems have the advantage of easy isolation of the product by removing the upper phase from the lower phase; the latter can be recycled and reused. This system was first applied for the MBH reaction by Yi *et al.*[79] The idea behind this system was to bring the different reagents into the lower phase by coordination with fluorinated Lewis acid and then, to react with the fluorinated nucleophilic catalyst. After reaction, the products formed can then move back into the organic layer. It was clear that in this case, the Lewis acid has two roles: not only to enhance the MBH reaction, but also to act as phase transfer catalyst. Yi *et al.* found the best results with $Yb(SO_3R_{f8})_3$ (R_{f8}= $(CF_2)_7CF_3$)) and catalyst **48**. It was important to fluorinate both catalysts (Lewis acid and base) sufficiently so they would not dissolve into the organic phase.

2.6.Asymmetric MBH reaction

For organic chemists, there is an even more important aspect to the MBH reaction product than the simple connection of two reagents, namely the formation of a chiral secondary alcohol, derived from the addition to the aldehyde. The possibility to control this chiral centre could be very useful for the synthesis of natural products. There are a number of papers focussing on this part of the MBH reaction, and yet there is still no general catalyst which is not substrate limited and which gives very good e.e.s (over 99%). According to Zhu *et al.*,[20] there are two major reasons for this:

1) A misunderstanding of the mechanism could be the major factor for lacking a general asymmetric MBH catalyst. Only recently it became clear that the RLS is not the addition of the aldehyde but the proton transfer. In the past, researchers thought that the same rules used for the aldol reaction could also be applied for the MBH reaction because of the manner of the addition involving an enolate to form 2 stereogenic centres. However, it is now clear that this is an oversimplified mechanistic view. A good MBH catalyst is not a catalyst which induces any chirality in the addition of the aldehyde, but which promotes the subsequent proton-shift of only one of the 4 diastereomers since the second step (the addition) is reversible.
2) The racemization of the final product by the presence of catalysts occurs, which is due to to the fact that the last step is reversible. The presence of nucleophilic catalysts causes this effect, which is because they are also basic in character. This was observed by Leitner *et al.*[18] when they added a phosphorous catalyst to an enantiomerically pure aza-MBH product.

To create this chiral centre in an enantiocontrolled manner, different approaches have been applied which can be divided into 4 basic groups: 1) by chiral substrates; 2) by chiral nucleophilic catalysts; 3) by chiral acidic catalysts; 4) or by chiral liquid. In some cases, there is rather fine line between these groups, especially in the most recent papers, where researchers have combined different approaches to improve the levels of asymmetric induction. Bearing in mind that most researchers have not necessarily followed recent developments in the MBH reaction mechanism, they have, therefore, tended to follow the old mechanistic view of the reaction. As a consequence fairly moderate results are sometimes obtained.

2.6.1.Chiral substrates

One way to obtain asymmetric induction is by attaching a chiral auxiliary to the substrates (to the aldehyde or the alkene). These modifications give, in some cases, very good diastereomeric excess (d.e.) of the product. The only drawback is the fact that extra reactions are needed to attach and remove these auxiliaries.

One of the first attempts to induce chirality on the aza-MBH reaction was achieved by Kündig *et al.* They initially wanted to increase the rate of the aza-MBH reaction by complexation of aromatic imines with an electrophilic $Cr(CO)_3$ group, and hence, making the imine more reactive.[80] Not only did they manage to speed up the reaction but they also unexpectedly created diasterocontrol.[81] They observed this diastereocontrol when they screened different *o*-substituted planar chiral benzaldehyde complexes reacted with methyl acrylate. The best d.e. (>95%) was obtained when a pure *(R)*-(-)-*o*-anisaldehyde(tosylimine)$Cr(CO)_3$ complex **49** was used giving the *(R,R)*-complex **50** in 93% yield (Scheme 7).

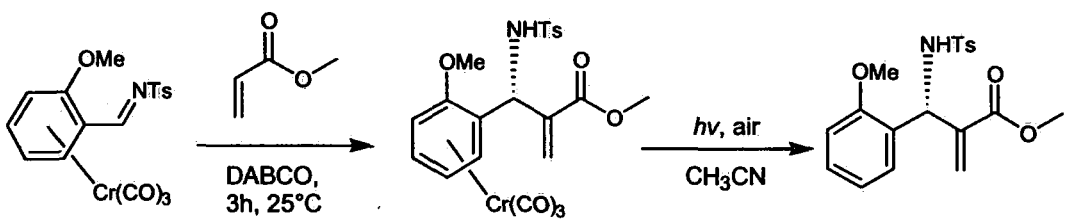

49 **50** **51**

yield 93% yield 92%

d.e. >95% e.e.: 96%

Scheme 7. Aza-MBH reaction with chiral Cr-complex **49.**

The cleavage of the directing $Cr(CO)_3$ group was easily achieved under UV irradiation. The final product **51** was obtained in very good yield and e.e. A mechanistic explanation as to why the *(S)*-configuration was the major enantiomer was not given in their paper, however, it is thought that electronic repulsion between the methoxy group on the benzyl ring and the formed enolate could be decisive. This is why only electron rich substituents as methoxy, Cl, etc. on the ring system give good d.e. It is already clear that, although there is good yield and e.e., this method is very substrate limited. Not only is the procedure limited to aromatic aldehydes, but it is also limited by the presence of an *o*-directing group on the aromatic group. This procedure was further expanded to the general MBH reaction and to the use of acrylonitrile instead of the methyl acrylate.

An often used chiral auxiliary is the (-)-menthyl system **52**. Isaacs *et al.*[82] used this to make a chiral acrylate and tested it with several aldehydes. They found the best results when sterically

large aldehydes were used, such as benzaldehyde and *p*-tolualdehyde. Although the yields in those cases were quite low, it was possible to obtain a d.e. of almost 100% (Equation 6). Through molecular models, it was possible to conclude that the most favourable attack had to occur at the *Si*-face of the carbanion leading to the (*R*)-configuration at the new chiral centre.

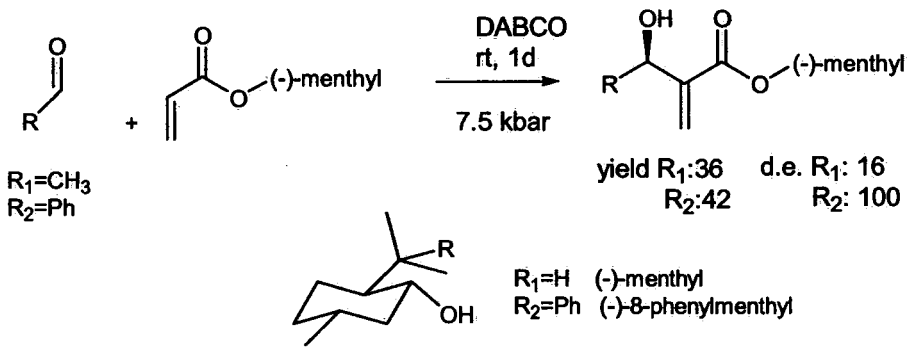

(6)

It is also important to do the reaction under high pressure because at atmospheric pressure using the same conditions, a d.e. of only 22% was obtained. The consequence of this is that an excess of aldehyde (4:1) had to be used to dilute the acrylate, otherwise polymerisation would occur. Basavaiah *et al.*[83] repeated these reactions at atmospheric pressure and to increase the reaction rate 1 equiv. of DABCO was added. Under these conditions, the same results as Isaacs were obtained, with d.e.s between 7 (*iso*-butanal) to 20% (furfural).

In addition, Bauer *et al.*[84] used a (-)-menthyl derivative **52**, a (-)-8-phenylmenthyl chiral auxiliary, which was attached to the aldehyde rather than the acrylate, forming a chiral glyoxylate system **53**. The result was a good yield of 78% and an even better d.e. of > 95% (Equation 7).

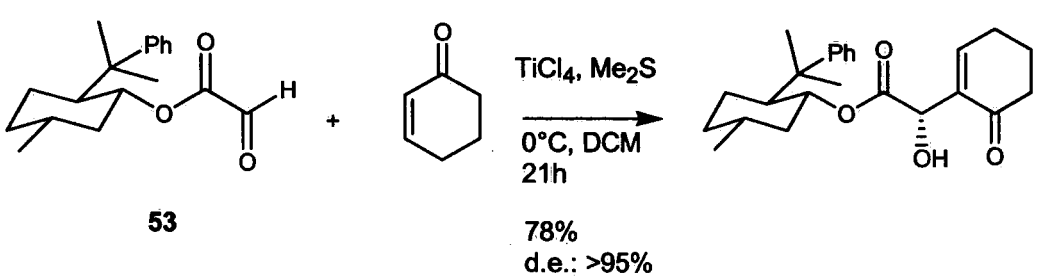

(7)

The absolute stereochemistry of the new stereogenic centre was established by X-ray as *S*. The proposed model **54** has both carbonyl groups in an s-*cis* conformation, chelating with the Lewis acidic Ti(IV) centre. In this way the phenyl ring shields one of the diastereotopic faces of the reacting formyl group. Simultaneously, the oxygen of cyclohexanone complexes the Lewis acid and is so brought close to the active aldehyde. They tried also several acyclic alkenes but they did not obtain any MBH product. The reason, as mentioned earlier, is the use of titanium(IV) chloride, which reacts with acyclic alkenes to form the halo aldol products.

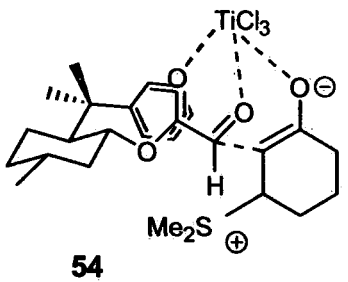

54

Since it became clear that the aza-MBH reaction could be accelerated by adding a strongly electron withdrawing tosyl group on the nitrogen, it seemed interesting if the corresponding *N*-sulfinimines could be used to induce chirality. By placing a chiral controller on the nitrogen of the imine, both aromatic and aliphatic imines could be employed. Also, the synthesis of chiral sulfinimines is straightforward and there is the possibility of tuning the sulfinyl substituent which is an advantage. The only problem is the lower reactivity of these sulfinimines since they are less electron withdrawing than sulfonyl derivatives. Both Aggarwal *et al.* and Shi *et al.* have investigated sulfinimines. Aggarwal *et al.*[85] used as a standard reaction, *N*-*p*-toluenesulfinimines **55** with methyl acrylate catalysed by 3-hydroxyquinuclidine (3-HQD). The reaction appeared to be sluggish (only 23% yield over 7 days and d.e. 76%), but by adding $In(OTf)_3$ as Lewis acid catalyst the yield was increased to 89% with a d.e. of 64% (Equation 8).

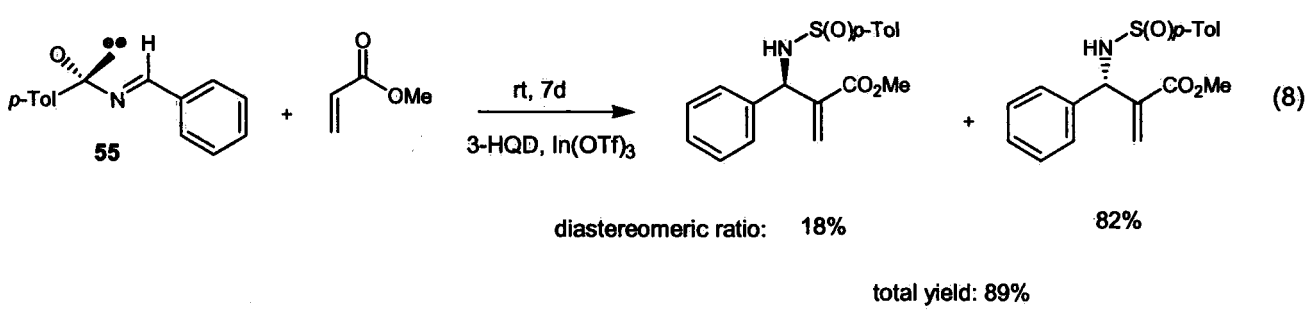

(8)

Because these workers employed racemic 3-HQD, it was feared there would be matched and mismatched stereochemical effects resulting from diastereoisomeric transition states. Therefore, the reaction was repeated with each of the enantiomers (*S*)-3-HQD and (*R*)-3-HQD. In both

cases, the same yield was obtained and only a small variation in the d.e. was observed. This indicated that the stereochemistry of the sulfinimine dominated the control in the stereoselectivity of the process. It is also interesting that in both cases, with or without Lewis acid, the same (*S*)-configuration (verified by X-ray crystallography) was observed at the nitrogen centre. Therefore, two different transition states had to be involved (see Scheme 8).

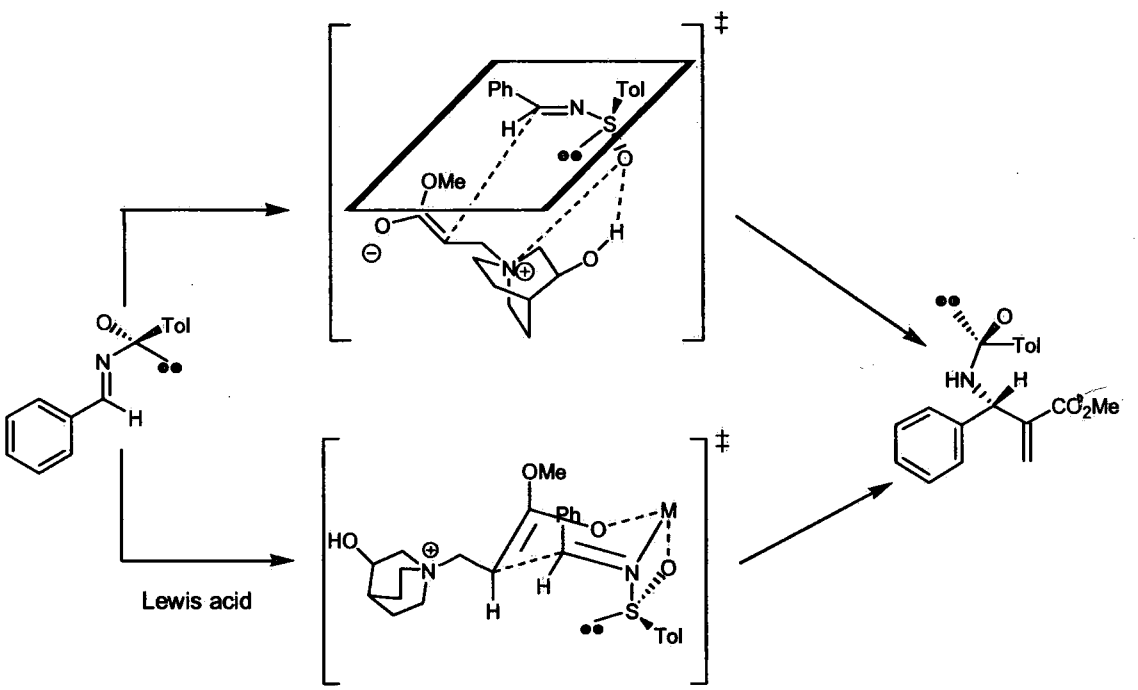

Scheme 8. Proposed transition states without and with Lewis acid.

When no Lewis acid is used, the preferred conformation is the one with the bulky substituent on the sulfur out of the plane of the double bound (in this case the *p*-tolyl substituent). Then, the nucleophile will approach *anti* to this large *p*-tolyl group. This conformation is also favoured by Coulombic attraction between the sulfinyl oxygen and the quaternary ammonium and perhaps by hydrogen bonding as well. When a Lewis acid is added, the conformation takes on a chair-like transition state and the metal coordinates the two oxygens and the nitrogen. The phenyl group and the sulfur will be *anti* to each other according to the model proposed by Davis[86] to explain the attack of ester enolates on sulfinimines. Those two transition states both predict the (*S*)-configuration product will result. *N-tert*-Butanylsulfinimine was also tested with methyl acrylate,

resulting in higher diastereoselectivity but with lower yields. This was expected since a *tert*-butyl group is sterically larger than a *p*-tolyl.

Shi *et al.*[87] also used *N*-*p*-toluenesulfinimines as chiral directing group, reacting with cyclopent-2-en-1-one as the alkene. Instead of 3-HQD as catalyst, $PhPMe_2$ was used as the catalyst which although rather slow compared to more reactive nucleophiles like PBu_3, these were considered too unstable to run over several days. Under these conditions it was possible to optimise the reaction in toluene to 72% yield and 82% d.e. (Equation 9).

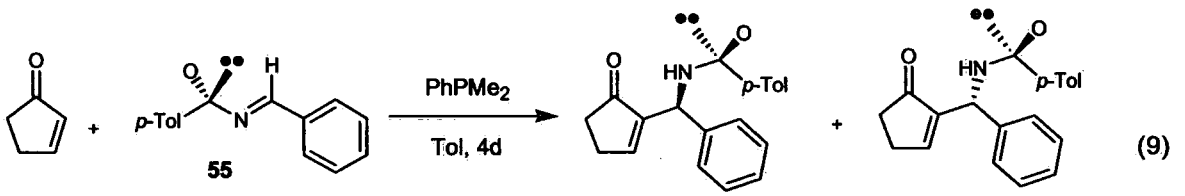

(9)

diastereomeric ratio: 91 9

total yield: 72%

The major compound was the (*S*)-configuration (verified by X-ray analysis) just like Aggarwal's observation. A possible transition state **56** was given with the *p*-tolyl group in the same plane as the double bond. The enolate will approach the imine *anti* to the oxygen at the sulfur group due to electronic repulsion at the *Si*-face. Also the phenyl group at the imine and the 5-membered ring will be placed *anti* to each other to minimize the steric interaction. This conformation results in the (*S*)-conformation. They also screened different aromatic imines resulting in good yields and d.e.s; the best result being with *p*-bromophenylsulfinimines with an 83% yield and 86% d.e. An attempt to extend the scope of this process by using cyclohex-2-en-1-one resulted in no reaction.

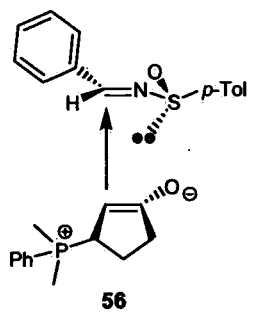

56

Besides the (-)-menthyl being employed as an auxiliary for the MBH reaction, other systems have been examined, including sugars. Krishna *et al.* in particular carried out a considerable amount of research with these compounds. They investigated the induced chirality by adding the sugar function both to the electrophile (aldehyde) and to the acrylate. In both cases, the yield was moderate and the d.e. was rather low. Again, the results depended upon the reagents chosen.

Firstly, the sugars **57** were connected to the aldehydes,[88] the diastereomers were separated by column chromatography and 2D-NOESY was used to analyse the results. From this, it was determined that the major compound was the (*S*)-configuration (Equation 10).

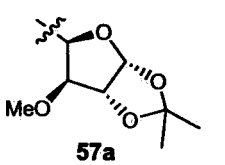

57a

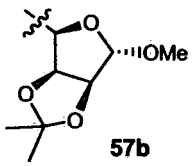

57b

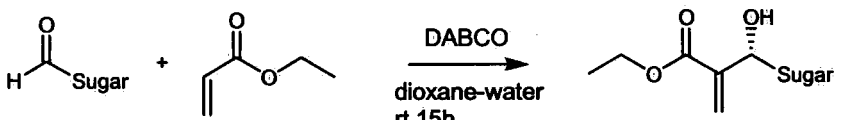

(10)

Yield **58a**:73% d.e. **58a**:36
58b:56% **58b**:56

The induced chirality could be explaind by following a Felkin-Ahn-type model with a non-chelating protocol, since the reaction was proposed to proceed with a direct addition onto the aldehyde. However, the application of this method is not straightforward since it is sometimes difficult to determine which group is sterically determining.[89] However, it was clear that the alcohol created was always *anti* to the oxygen of sugar. This could indicate that the process was reversible and was governed by the thermodynamic drive to the most stable product.

Secondly, they added sugars **59** to the acrylate[90] by esterification and used DABCO as nucleophile, because DBU gave hydrolysis of the acrylate (other nucleophiles gave no reaction). Because the modified acrylates were less reactive, the reaction took some days and the major compound was determined by ^{1}H NMR to be mainly the (*R*)-product (Equation 11).

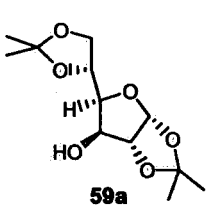

59a

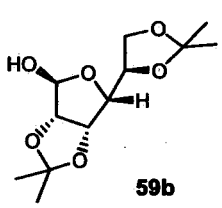

59b

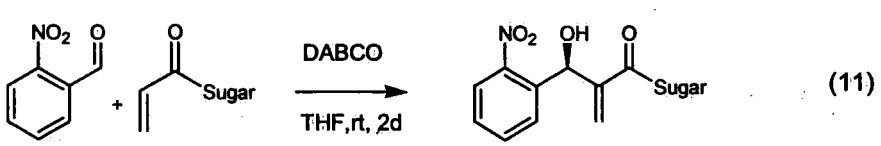

(11)

yield **60a**:91% d.e. **60a**:40 (*R*)
60b:88% **60b**:40 (*R*)

Again, it was difficult to give a general explanation for the induced chirality, since the outcome depends heavily on the attached sugar. It was thought that the greater distance between the sugar and the enolate could have been responsible for the lower d.e. Attempts were made to reconstruct a possible transition state, however, because there was free rotation of the sugar it was hard to say what was defining the final reactive conformation and hence, the resulting product stereocemistry.

Finally, these workers also used both a modified acrylate and a modified aldehyde to study the effect of "double asymmetric induction".[91] Although the yield was low (40%) due to too much steric hindrance, a good d.e. (> 95%) was obtained (Equation 12). It is, therefore, important to employ chiral auxiliaries which induce the same sense of absolute stereocontrol, *i.e.* they "match", which results in improved selectivity. Again, the (*R*)-configuration was the major product obtained, as shown by ^{1}H NMR analysis.

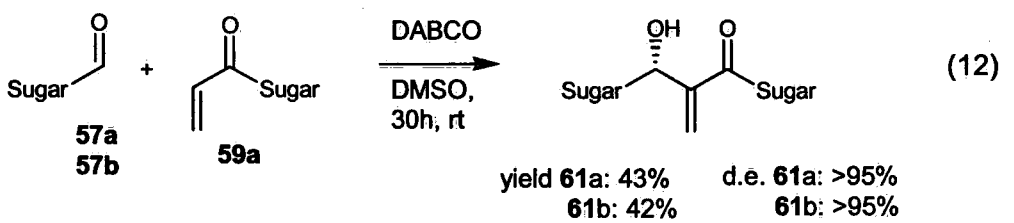

yield **61a**: 43% d.e. **61a**: >95%
61b: 42% **61b**: >95%

(12)

Another chiral auxiliary that is often used, is the camphor-derived system, for example, as often used by Oppolzer *et al.*, *i.e.* sultam **62**. This auxiliary showed good results for stereoselective control, for example with the aldol reaction. Leahy *et al.*[92] used it to make the alkene chiral for the MBH reaction, with a variety of aldehydes. Good yields were obtained and even better e.e.s (>99%). The reaction worked best for aldehydes that were unbranched at the α-position. They managed to change the reaction conditions in such a way that the sultam could be removed in the same step. Unfortunately, by this method only 1, 3-dioxane-4-ones **64** was obtained, and hence, an extra step to obtain the corresponding MBH product **65** was required (Scheme 9).

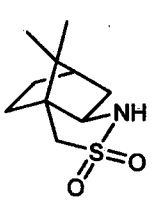

62

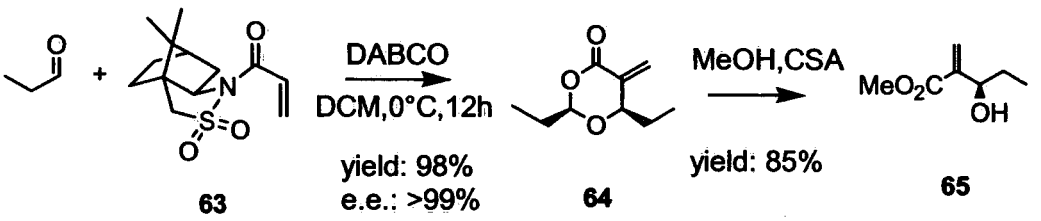

Scheme 9. MBH with chiral sultam.

One of the most interesting advantages of Oppolzer's sultam is the possibility to generate the two enantiomeric products. The only difference to obtain these enantiomers is the presence of a Lewis acid during the reaction. It is accepted that the addition of the catalyst (Scheme 10) to the alkene will result in the formation of a (*Z*)-enolate because of electronic interactions. This enolate could exist in either of the two possible rotameric forms, *i.e.* **66** or **67**. With rotamer **66** the carbonyl sulfonyl groups align and is favoured when a Lewis acid is present and coordinated to both. In all other circumstances, rotamer **67** is formed preferentially because in this *anti*-orientation, dipole interactions between the carbonyl and sulfonyl groups are minimized. Therefore, the *anti*-configuration should be present in the illustrated MBH reaction since no Lewis acid was added. In all MBH reactions with different aldehydes, using the same conditions, the (*R*)-configuration product was obtained in all cases. This means that the aldehyde approaches the alkene from the *Re*-face, presumably avoiding the axial oxygen of the sulfonyl group during addition to the bottom due to steric interactions. Through Newman-projection **68**, it can be seen that the proton approaches over the bulky quaternary ammonium group generating **69**, which eventually gives the MBH (*R*)-product (see Scheme 10).[93]

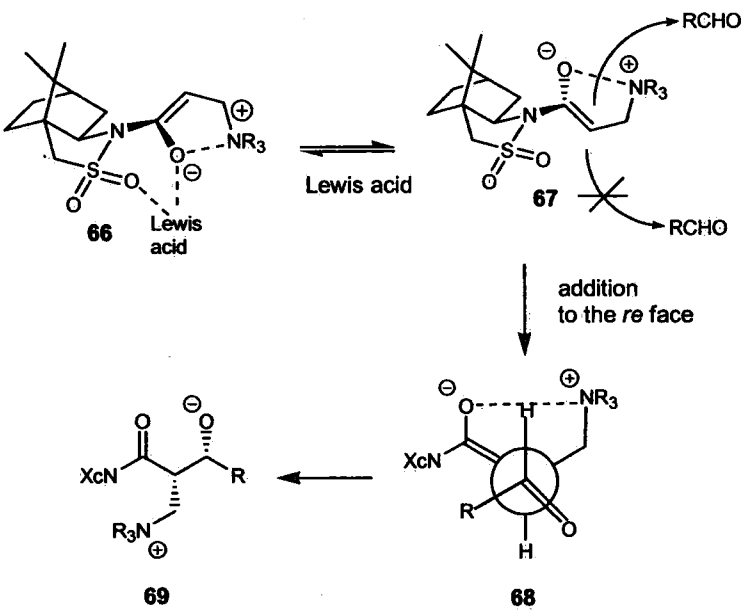

Scheme 10. Proposed trantition states with chiral sultam.

Also, Basavaiah *et al.*[83] used Oppolzer's chiral auxiliaries to induce diastereocontrol in the MBH reaction. Like Leahy, this group attached the auxiliary to the alkene forming a derivatized acrylate. The two auxiliaries were screened intensely with different aldehydes **70** and **71** and the reactions were slow, even with 1 equivalent of DABCO. The fact that these reactions were slow (several days) could well have been because of steric influences of the substituents on the nitrogen (Equaton 13). The best d.e. (70%) was obtained with propionaldehyde using **71**, although the yield was rather low (45%). It is clear that these auxiliaries, **70** and **71**, have profound differences, compared to the normal Oppolzer's sultam **62**, namely they are not bicyclic systems being acrylates. Therefore, there is a possibility of rotation of the sulfonamide function which would probably lead to lower diastereocontrol. However, the d.e. could be increased by fractional crystallisation of the diastereoisomeric mixture giving the corresponding product in almost 100% d.e.

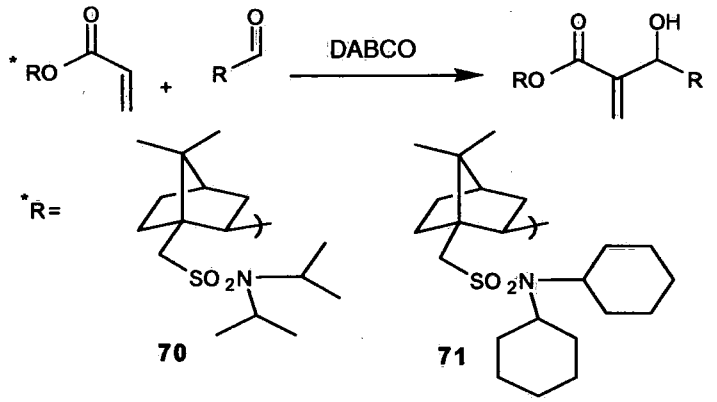

(13)

A more recent paper making use of a Oppolzer camphor derivative was published by Chen *et al.*[94] In their approach, the sultam **62** was modified by removing the sulfur and replacing it by a nitrogen. An extra carbonyl group was also added next to this new nitrogen giving a new camphor-based chiral auxiliary **72**. As with in previous reports, the camphor derivative was connected to the alkene giving **73**. By these adaptations it was possible to isolate the MBH derivatives directly and not the lactone products. Compound **73** was screened with different aldehydes and different solvent systems, with the reactions involving sterically less hindered aldehydes (acetaldehyde, propionaldehyde, etc.) running several days to obtain good yields of products. With more sterically hindered aldehydes, no product at all was isolated.

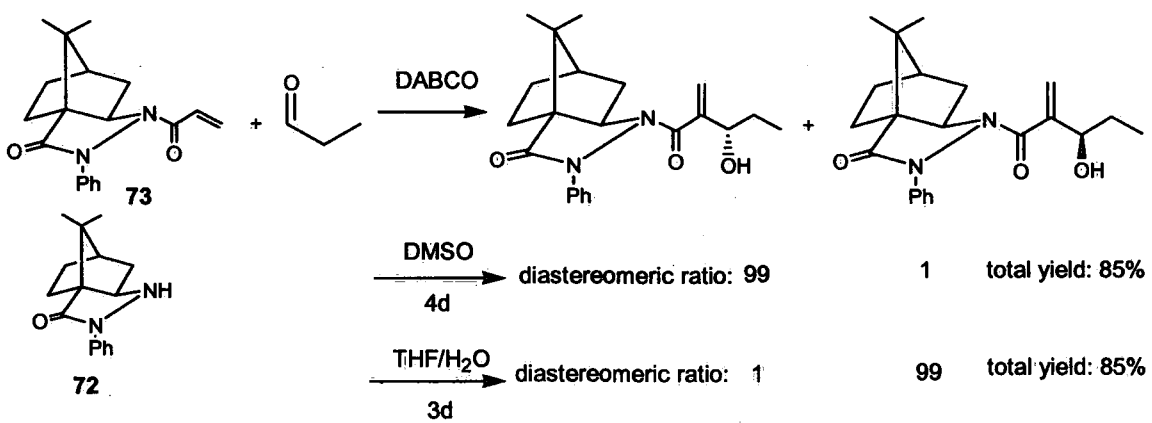

(14)

(15)

When the reaction was run in DMSO, the (*S*)-product (analysed by X-ray) was obtained as the major compound, in good yield and good d.e. (Equation 14). Surprisingly, when THF/water was used, a mixture was obtained, with the (*R*)-product as major, and in exactly the same yield and d.e. (Equation 15). This was interesting since both enantiomers could be made simply by changing the solvent system used. This also showed that the stabilization of the zwitterionic

intermediate by intermolecular hydrogen bonding with solvent molecules and/or disruption of the intramolecular ionic bond by DMSO might play a crucial role in the transition state to define the predominant stereochemistry induced. It is also important to try and mimize steric interactions with the camphor skeleton into account with the approaching aldehyde. To date, an exact mechanistic explanation for the induced chirality has not been proposed.

2.6.2.Chiral nucleophilic catalysts

More interesting is the use of chiral catalysts for the MBH reaction because no extra reactions are needed in order to obtain the MBH product. Originally only chiral nucleophilic catalysts were used, with the first reactive catalysts of this type being a chiral (*S,S*)-2,3-disubstituted DABCO **74**, which has C_2-symmetry (introduced by Hirama *et al.*[95]). In this case, the reactions were slow, and therefore, it was necessary to work under high pressure (5 Kbar). This did not only improve the yield but had also an impact upon the e.e. Despite the extreme conditions, a yield of 45% was obtained with a low e.e. of 47% for the (*S*)-configuration product. In addition, because of the high pressure, an excess of the aldehyde was required. Marko *et al.*[96] also used pressure to increase the e.e. This group screened quinidine **75** with methyl vinyl ketone and different aldehydes. It was difficult to assess the influence of pressure since the e.e. depended on the bulkiness of the aldehyde: steric large aldehydes gave lower e.e. when the pressure was increased. However, sterically small aldehydes produced an increased e.e. up to a certain pressure, yet the e.e. decreased with further increases in pressure. The e.e.s were limited to a maximum of 45%.

Improved results were obtained when quinuclidine-derived chiral amines were used. After testing several derivatives, Hatakeyama *et al.*,[97] found that quinuclidine **76** showed the best results, due to the free hydroxyl group situated in the right position to assist with the protonation step. The best results were obtained using hexafluoro-isopropyl acrylate (HFIPA) resulting in the (*R*)-product with *p*-nitrobenzaldehyde in 91% e.e. and 58% yield (Equation 16). Several aldehydes were examined giving very good e.e.s (91 to 99%) and moderate yields (31 to 58%).

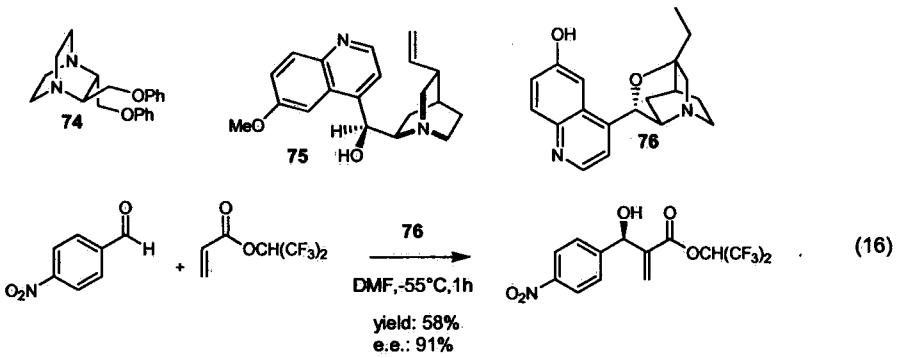

Besides the MBH product, these workers also obtained a small amount of dioxanone (11% yield 4% e.e.) as the side product. It was also noted that low temperature was necessary to maintain the high e.e. The mechanistic explanation for the formation of the *R*-configuration product was proposed as follows: when catalyst **76** is added to the acrylate, enolate **77** is formed with the (*Z*)-configuration. The aldehyde then approaches from below in order to minimize steric hindrance and allowing the formation of a hydrogen bond with the hydroxyl group. In this way, two betaine intermediates are possible, *i.e.* **78** and **79**. Looking at the Newman projection before the elimination step (see **80** and **81**) and with the proton axial on the ammonium group, it is clear that the (*R*)-configuration should be preferred because there is less steric hindrance between COOR and R' groups (Scheme 11).

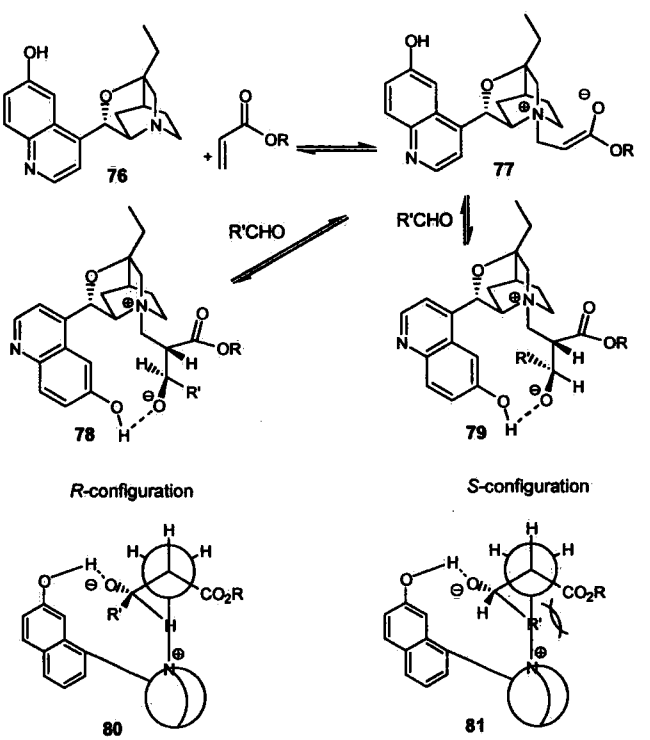

Scheme 11. Proposed transition state with **76**.

To increase the yield, Hatakeyama *et al.*[98] modified **76** on different positions. This resulted in the finding that cage-like tricyclic structures and the phenolic OH groups of **76** were essential for both high chirality and rate acceleration. Also, the branched structure of HFIPA played a key role and it was also important to keep **76** dry, since X-ray analysis showed that coordination of water with **76** led to partial hydrolysis of HFIPA. The use of azeotropically dried **76** improved the yield of Scheme 24 from 58% to 75%. Hatakeyama *et al.*[99] also synthesised the enantio-complementary catalyst of **76**, giving the same yields and e.e.s but with (*S*)-configuration.

Although the e.e.s for the MBH products resulting from the use of **76** and HFIPA were good, the yields were still moderate. One way to increase these yields was by adding different co-catalysts, such as proline. Shi *et al.*[100] also used catalyst **76** for the MBH reaction of methyl vinyl ketone. However, instead of increasing the yield, it was found that by adding *D*-proline, it was possible, in some cases, to invert the absolute configuration of the product. In other cases, the (*R*)-configuration product was present in even higher e.e. For example, using *p*-nitrobenzaldehyde with *D*-proline gave a greater amount of the (*R*)-product, which was because of chelation between the nitro-group and the *D*-proline, making it more bulky and hence, the (*R*)-configuration product was preferred. On the other hand, using *p*-bromobenzaldehyde gave the (*S*)-product. This catalyst action could be explained by the fact that *D*-proline was chelating with the hydroxyl group of the catalyst **76**, and hence, the hydrogen bond between betaine intermediate and aldehyde was destroyed (Scheme 11).

Shi *et al.*[101] were also the first group to test **76** for the aza-MBH reaction. Compound **76** was screened with methyl vinyl ketone and methyl acrylate using different tosylate-imines. The reactions with methyl vinyl ketone were carried out at -30 °C in a DMF/MeCN mixture for 24 h, giving moderate to good yields (54-80%) and e.e.s (46 to 99%). Because acrylates are less reactive, the temperature and reaction time had to be increased to 0 °C in DCM and 72 h. In this case, yields were between 58-87% and e.e.s between 71-83%. In all cases, the major product was the (*R*)-configuration (verified by X-ray), which they explained in the same way as Hatakeyama *et al.* (see above). Ironically, Hatakeyama *et al.*[102] also screened **76** for the aza-MBH reaction with HFIPA and obtained as the major product, the (*S*)-configuration (analysed by X-ray). These reactions were run at -55 °C with *N*-diphenylphosphinyl imines due to their higher reactivity and

selectivity compared to the normal tosylate-imines. Good yields (42-97%) were obtained, with good e.e.s (54-73%), although lower than the normal MBH reaction. It was observed that the e.e. was dependent upon the bulkiness of the imine: the larger the imine, the higher the e.e. Therefore, it was concluded that this was a significant factor in the transition state. According to Hatakeyama *et al*, although the aza-MBH follows the same steps as the general MBH, there are two possible steric interactions, not only between R' and COOR (see **83**), but also between R' and R'' (the group attached to the imine, see **82**) Since the latter was more severe, the predominant aza-MBH product had the (*S*)-configuration. This could also explain the higher e.e. with more bulky imines (Scheme 12).

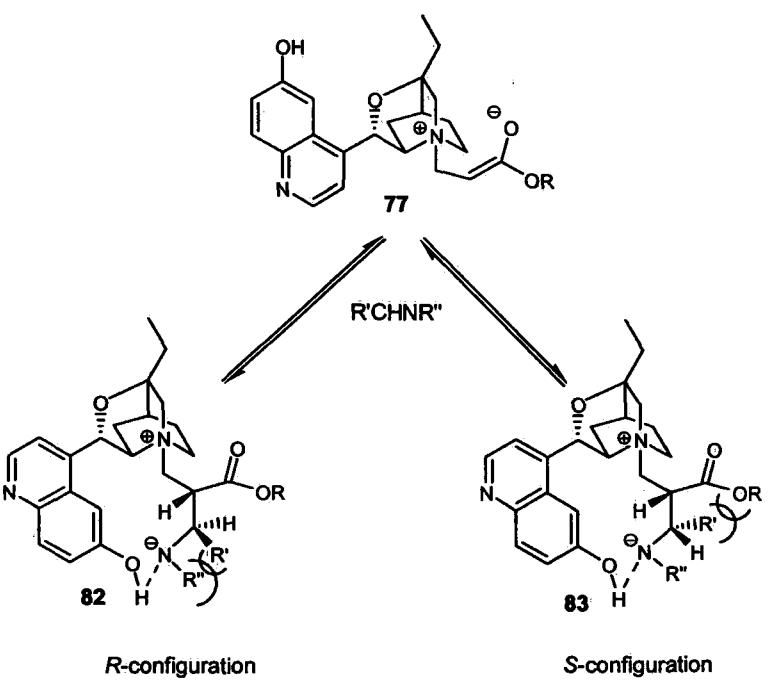

Scheme 12. Proposed transition state with **76** for aza-MBH.

The use of **76** was further extended to the three-component aza-MBH reaction in one pot by Adolfsson *et al.*[103] In this case the tosylimine, aldehyde and methyl acrylate were mixed together with **76** and dry molecular sieves. Because the reaction was initially too slow, $Ti(O^iPr)_4$ was added as Lewis acid. The result very much depended on the aldehydes used, giving good yields (75-95%) and moderate e.e.s (49-74%). Interestingly, their major product had also the (*R*)-configuration, similar to the results of Shi *et al.*

Since the introduction of small organocatalysts for the aldol and Mannich reactions earlier this decade, these catalysts have also gained interest for the MBH reaction. The use of proline as co-catalyst has been mentioned earlier with **76**, however, more common is the addition of a small nucleophile like imidazole instead of **76**. In an earlier publication, Shi *et al.*[104] reported the symbiotic activity between L-proline and imidazole for the MBH reaction of methyl vinyl ketone (MVK). Proline on its own did not catalyse the reaction and imidazole gave only 40% conversion, however, together they gave high yields (80 to 90%) for several aldehydes after 1 day at room temperature. Unfortunately, the products were all racemic mixtures. It was thought the L-proline attacks the alkene to form an enamine which is more reactive towards the imidazole, however, there is no real evidence for this mechanism. Imbriglio *et al.*[2,105] also used this combination, however, because of the lack of enantiomeric selectivity, these workers modified the imidazole by adding L-amino acids. Libraries of different combinations of amino acids were linked to the imidazole and screened for reactivity on the MBH reaction. It was found that an oligopeptide catalyst of ten L-amino acids linked to the imidazole was the best catalytic system. The combination of L-proline with this oligopeptide gave, for several aldehydes reacting with MVK, good yields (52-96%) and good e.e.s (63-81%) for the (*R*)-product. Interestingly, changing L-proline for D-proline also changed the configuration of the product to (*S*), but the e.e. dropped to 39%. This indicated that the stereochemistry of proline not only potentially dominates the RLS, but also demonstrates "match-mismatching"; the mechanism is still under investigation. Not only have artificial oligopeptides been employed for the MBH reaction, but enzymes such as serum albumin and others have also been screened. Unfortunately, they have yet prove useful, showing only low yields and low e.e.[106]

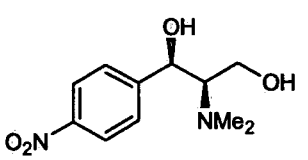

84

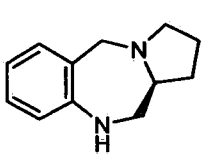

85

Besides the use of imidazole, some rather uncommon nucleophiles as **84** and **85** have also been showing good reactivity for MBH reactions with proline as co-catalyst. Compound **84** is a precursor of the antibiotic chloramphenicol, however, strangely together with proline it managed

to catalyse the reaction of MVK with different aldehydes giving the MBH product in good yield (46-91%) and good e.e. (30-82%) although after some days of reaction.[107] Zhao *et al.*[108] also made some interesting nucleophiles which did not catalyse MBH reaction on their own, and were active only in the presence of proline. The best nucleophile was **85**, leading to a maximum yield of 80% and 83% e.e. with MVK. Since **84** and **85** were both chiral, there was also a possibility of "match-mismatch" in the stereochemical outcome of the reaction. Further research showed that the proline stereochemistry was the determining factor in the configuration of the MBH product. The exact mechanistic explanation for both nucleophiles was still under investigation.

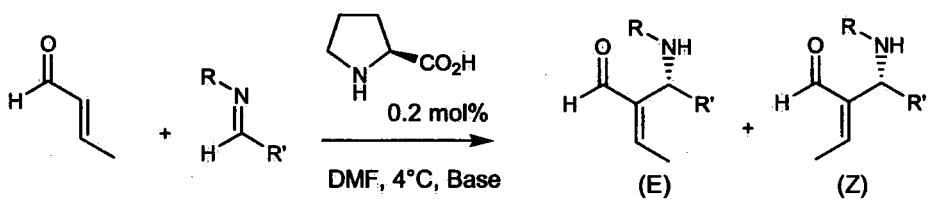

Barbas:	R: *p*-methoxyphenyl R': CO_2Et	Base: imidazole	17	:	1	70%, e.e.: 98%	(17)
Cordova:	R: Boc R': Aryl	Base: DABCO	4	:	1	45%, e.e.: 99%	(18)

Since it became clear that proline showed some enantioselective influence as co-catalyst for the MBH reaction, it did not take long to investigate its effect on the aza-MBH reaction. Barbas *et al.*[109] used crotonaldehyde and a *p*-methoxyphenyl protected α-imino ester with proline (Equation 17). Only a low yield (35%) of product was isolated, however, with better e.e. (96%) than the normal MBH. By adding imidazole to the proline-catalyzed reaction, the yield increased to 70% with the same e.e. Despite the products being aza-MBH-type products, it is still believed that the reaction proceeds through a Mannich-type of mechanism instead of an MBH mechanism. It was interesting to observe the reaction working on β-substituted-α,β-unsaturated carbonyl compounds which are normally rather sluggish due to steric hindrance. Since the (*E*)/(*Z*)-conformation was reversible, it was not surprising that the major product was the (*E*)-isomer due to its higher thermodynamic stability. In addition, Cordova *et al.*[110] worked on this topic using *N*-Boc-protected aryl imines and DABCO as nucleophile (Equation 18), producing good yields and excellent e.e.s (>97%).

Due to effectiveness of proline, many related derivatives were created in order to improve its catalytic activity in the MBH reaction so that it could be used as a catalyst rather than a co-catalyst. One of the first was Barrett *et al.* who transformed L-proline into the corresponding chiral pyrrolizidine base **86**.[111] A more bulky catalyst was prepared to assist the stereoselectivity while retaining the nucleophilicity. A hydroxyl group was also introduced to assist with forming a hydrogen bond with the substrate. The first results gave moderate yields (21-93%) but with rather low e.e.s (21-47%) with ethyl vinyl ketone after 3 days. However, by adding $NaBF_4$, the yield improved dramatically (58-93%) as did the e.e.s (37-72%) after only 18 h. It was clear that the sodium played an important role in the transition state, which resulted in the *(R)*-configuration product. A possible mechanism is given as **87**, where the metal activates the carbonyl group.

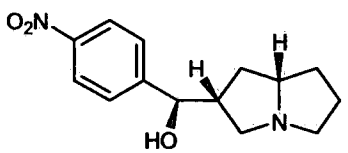

86

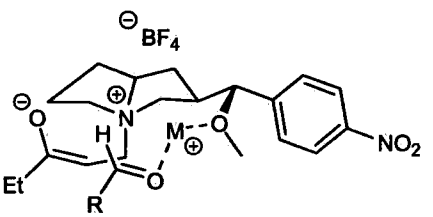

87

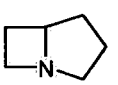

88

Another proline derivative prepared by Barrett *et al.* was **88**,[112] which was considered to be more reactive than the pyrrolizidine systems since the nitrogen lone pair was more accessible due to its increased pyramidalization. This catalyst was screened with ethyl vinyl ketone, showing that it was more reactive consuming the ketone after only 2 hours giving a yield of 70%, although only at lower 26% e.e. This lack of good asymmetric control could be reasoned due to the absence of a hydroxyl group.

A catalyst which more closely resembles proline is system **89**, created by Krishna *et al.*[113] Compound **89** was readily synthesised from proline by reduction and methylation. Just like proline, **89** is a bifunctional catalyst with a Brønsted acid and Lewis base, which provides good yields (64-94%) and moderate e.e.s (20-78%) with both MVK and methyl acrylate. It appeared the hydroxyl group was vital in the reaction since the methoxy derivative gave no MBH product. A possible transition state is proposed as **90**, which clarifies the *(R)*-configuration of the major

product involving a hydrogen bond between the hydroxyl group and the oxy anion in intermediate **90** which is favourable since both functions are positioned close to each other.

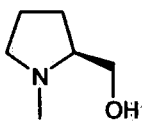

89

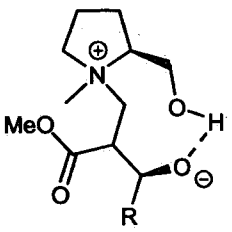

90

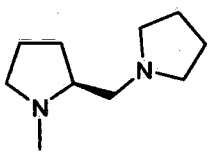

91

A very similar catalyst **91** was introduced by Hayashi *et al.*[114] Although **91** had the same scaffold as proline, it lacked an acidic group, being replaced by another basic amine. It had been observed that both the substituent on the nitrogen of the proline pyrrolidine and the amine moiety not derived of the proline, played a crucial role in the yield and e.e. of the MBH product. Compound **91** appeared to be the best catalyst for MBH reaction with yields between 40 and 96% and e.e.s between 44 and 75% with MVK. By comparison of the optical rotations with the literature, it was possible to determine the absolute configuration of the products as *(S)*. This was surprising since **91** had the same *S*-configuration as that derived from proline and its derivatives, however, these MBH products were all *(R)*. A possible mechanistic explanation for this outcome has not been found yet.

Besides the proline derivatives, there are also some chiral imidazolines known which also catalyse the MBH reaction. Two of them (**92** and **93**) were synthesised by Tan *et al.*[115] with **92** being the first one to be screened with methyl acrylate and using different aldehydes. Although the yields were good (63-90%) and the e.e.s were moderate (31-54%), the reactions seemed to be slow (4 to 14 days), even with one equivalent of **92**. To increase the speed of the reaction and to improve the e.e., **92** was modified by introducing bulkier groups. In this way, **93** was prepared carrying a chiral methylnaphthyl group which increased the e.e. to 60%. Screening **93** with MVK, yields between 59 and 96% were obtained with e.e.s between 47-69% after 3 to 4 days with 50 mol% catalyst. No mention has been made about a possible mechanism and even the stereochemical outcome was not reported.

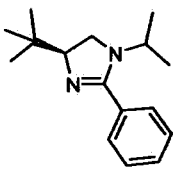

92

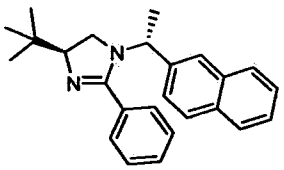

93

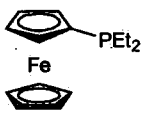

94

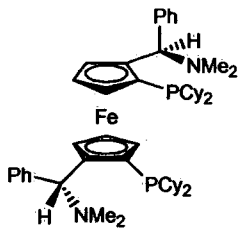

95

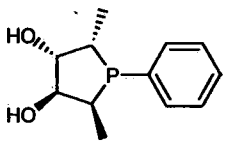

96

Not only are chiral amines used as nucleophiles for the MBH reaction, but some chiral phosphines have also been prepared for this reaction. As mentioned earlier, their high sensitivity to air oxidation limits their application, so only a few have been made to date. One of them is based on ferrocenyldialkylphosphines since these have shown high reactivity due to the electron-rich ferrocene moiety.[116] Hence, diethylphosphine **94** can complete the MBH reaction between methyl acrylate and different aldehydes within 1 hour with good yields (76-98%). By making **94** chiral it was hoped to induce some asymmetric induction into the MBH products. Several chiral ferrocenyldialkylphosphines were screened and **95** came out as the best (yield 78%; e.e. 65%).

In addition, chiral hydroxyl phospholanes such as **96** have also been used.[117] It was clear that **96** accelerated the MBH reaction due to the interactions between the hydroxyl groups and the enolate intermediate. Some good yields were observed (to 83%), however, the e.e.s were low (only 19% maximum).

2.6.3.Chiral acid based catalysts

As soon as it became clear that acid catalysts speed up the MBH reaction, it did not take long for the first chiral acid catalysts to be introduced. Especially, a lot of progress has been made using chiral Brønsted acids. These chiral Brønsted acids can be divided into two major groups based on their scaffold; the chiral bis-aryl ureas and the BINOL catalysts.

When Connon *et al.*[74] first reported the acceleration of bis-aryl ureas (like **41**) in the MBH reaction in 2004, it provided considerable new potential for this reaction. It became possible to use bis-aryl ureas as a catalytic core which could be surrounded with a chiral functionality to

induce e.e. It is important to see these bis-aryl ureas as chiral co-catalysts since they do not react without a Lewis base. The first group to apply these chiral ureas was Nagasawa *et al.*[118] who created thiourea catalyst **97** by placing two thiourea groups onto a cyclohexane. The oxygen of the carbonyl group was replaced with a sulfur forming a thiourea, because this increased the Brønsted acidity of the protons on the nitrogens. The idea to use two thiourea centres was rationalized by the possible transition state **98**, since it was assumed that one of the thioureas could be used to stabilize the enolate intermediate and the other could be used to introduce the aldehyde by activating the carbonyl group. Important in this case was the angle between the two thioureas since this would determine the chirality of the MBH product. The importance of the two thiourea centres was supported by a test using only one thiourea centre connected to a cyclohexane which only gave traces of the product. Compound **97** was then screend with several Lewis bases, benzaldehyde and cyclohexenone. It was found that DMAP gave the highest yield (90%) with 22% e.e. Imidazole gave the highest e.e. 61%, though only 10% yield. Because the reactivity with imidazole was low, improved conditions were required. This was achived with DMAP and by lowering the temperature to -5 °C to increase the e.e. Under these conditions good yield (38-99%) were obtained and good e.e.s (33-90%) with several aldehydes. The major product had the (*R*)-configuration which was explained by the possible transition state **98**.

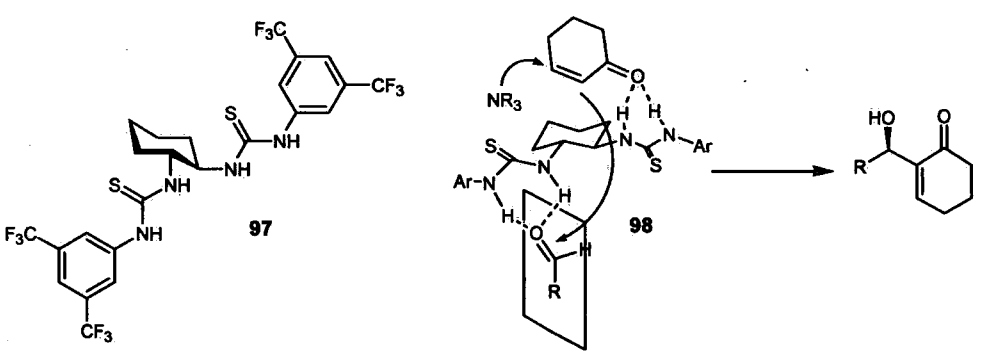

Berkessel *et al.*[119] used the same concept as Nagasawa *et al.*, however, modifications were made to the cyclohexane to improve the e.e. Catalyst **99** was synthesized which looked similar to **97** but had some differences which led to significant improvements. One of the modifications was to increase the distance between the two thiourea centres. This gave the enolate and the aldehyde more space and hence, decreased steric hindrance but were both still close enough to react.

Several methyl groups were also placed on the cyclohexane to shield the rest of the catalyst. In this way improved e.e.s were obtained. In addition, **99** was screened with several bases and in their case DABCO was the most promising. It was important not to use protic solvents because these solvents could break the hydrogen bonds between the catalyst and the reagents, therefore, the reactions were carried out in toluene or neat. By optimizing the reaction conditions at 10 °C, good yields (29-75%) and good e.e.s (52-96%) were obtained with cyclohexenone and different aldehydes. The configuration of the major compound was (*R*), as expected.

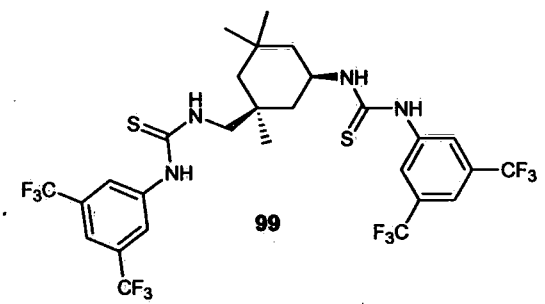

99

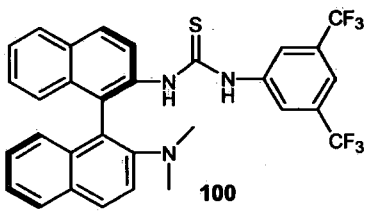

100

A slightly different approach in the use of these thioureas was followed by Wang *et al.*[120] Their catalyst **100** was composed of only one thiourea group and a (*R*)-binaphthyl amine group with the idea of using the amine as nucleophile to create the enolate which could be stabilized by hydrogen bonding with the thiourea. The chiral binaphthyl group would then be responsible for which side the aldehyde could enter. This bifunctional catalyst had the advantage that no other base had to be added and could make use of the high selectivity of the binaphthyl scaffold. After finding the best reaction conditions (in CH_3CN at 0 °C), cyclohexenone was screened with different aldehydes, resulting in good yields (63-84%) and good e.e.s (80-94%). These high e.e.s showed how efficient the binaphthyl scaffold was for the MBH reaction and inspired other research groups (see below).

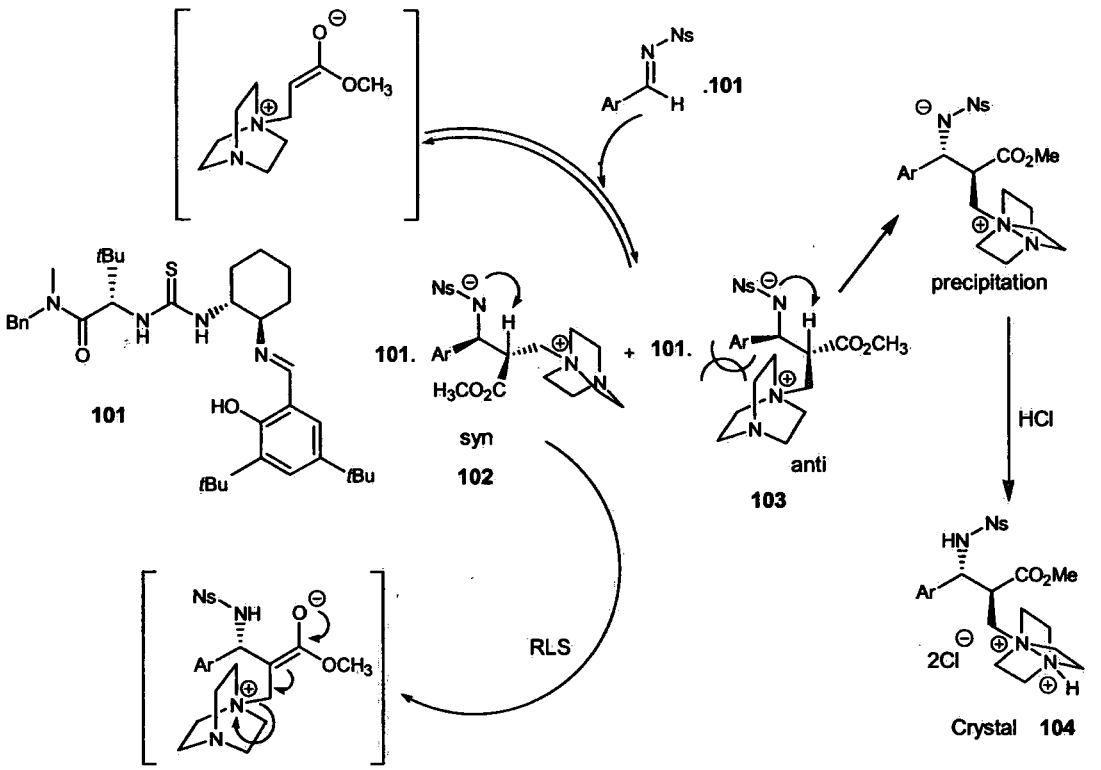

Scheme 13. Proposed mechanism for **101**.

The good results with these chiral thiourea derivatives also attracted the attention of Jacobsen *et al.*[121] who examined the application of chiral transition metals coordinated to these kinds of thiourea molecules for the aza-MBH reaction. Through this screening, **101** was found (normally an excellent Mannich catalyst) to be the most successful, applied to the reaction of methyl acrylate and DABCO with several nosyl imines to obtain some impressive e.e.s (91 to 99%) but rather disappointing low yields (30-50%). An interesting fact was the pronounced inverse relationship between the e.e. and the conversion. This indicated that a deeper mechanistic investigation was needed (Scheme 13). A closer look at the reaction showed that the system was not homogeneous, rather it was biphasic since there was some precipitation. By adding HCl to the precipitation it was possible to isolate the crystalline salt **104** which was the *anti*-intermediate formed just before the elimination step. This X-ray structure was a key factor in the investigation, not only because it was the pure the *anti*-compound, but also, because it was the first time this intermediate had been isolated from any MBH reaction, supporting the general MBH mechanism (see above). By extra kinetic studies on their reaction, it was found that the deprotonation step was the RLS. Hence, a possible explanation according to Jacobsen *et al.* was

that the reaction follows the general MBH mechanism with DABCO doing a Michael addition onto the alkene. This is then followed by the attack onto the imine. Important is the complexation between the imine and the thiourea catalyst **101**, forcing the attack to only one side. Therefore, there were only two isomers possible instead of four: **102** with the nitrogen group and DABCO *syn*; and **103** with the nitrogen group and DABCO *anti*. Since the intramolecular proton transfer for **102** was relatively easy, it decomposed quickly to the aza-MBH product, in contrast to **103**, where the elimination went slowly due to steric hindrance in the requisite eclipsed conformation. This led to a build-up of **103** which eventually precipitated out and could be analysed. This mechanism was in accordance with all the data obtained and justified the inverse relationship between e.e. and yield. Even more striking is the fact that this mechanism actually supports the statement by Zhu *et al.*[20].

Since Noyori introduced the BINAP system to achieve hydrogenation with high e.e.s, a lot of reactions have made use of this chiral binaphthyl compound and one of them is the MBH reaction. The first attempt was made by Soai *et al.*[122] in 1998 where BINAP was used as the nucleophilic catalyst with methyl acrylate and different aldehydes, however, only low yields (12-26%) and low e.e.s (25-44%) were obtained. Since it was known that polar solvents accelerate the MBH reaction, Ikegami *et al.*[123] replaced BINAP with (±)-BINOL **105** as co-catalyst. This was not only to induce some e.e., but also to make the reaction faster. A quantitative yield was obtained after only 1 hour at room temperature using PBu_3, however, no asymmetric induction of note was obtained (e.e. < 10%). When the proton of the hydroxyl group was replaced by a methyl function, catalytic activity was lost altogether. Interestingly, the corresponding calcium catalyst **106** was useful and induced an e.e. of 56%, although in a lower yield (64%). With this knowledge, Schaus *et al.*[124] tried different metals to coordinate with the BINOL. In their approach with cyclohexenone and different aldehydes, an yttrium-BINOL complex gave the highest e.e. (78%) albeit in moderate yield (45%). During the course of their investigation, it was found out that the metals were actually not needed and that BINOL was capable of catalyzing the MBH reaction by itself in 74% yield and 32% e.e. Two structural features on the BINOL were found to be important for achieving high e.e.: 1) saturation of the BINOL derivative; and 2) substitution at the 3,3'-positions.[125] By understanding this , it was possible to create a catalyst **107** which proved to be promising with yields of 80% and e.e.s of 95%. The reaction was carried

out at -10 °C with PEt_3 as nucleophile over 48 h. Catalyst **107b** showed higher reactivity with aliphatic aldehydes, while **107a** afforded the best results with more hindered aldehydes. An explanation for this behaviour is not known but presumably it is due to electronic effects by making the naphthol more acidic. It is important to stress that these results were only noted when cyclohexenone was used. In the case of other alkenes, lower or almost no e.e.s were observed.

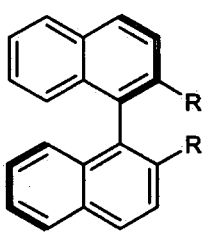

105

BINAP: R=P(Ph)$_2$
BINOL: R=OH

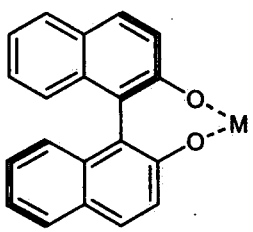

106

M= Ca
M= Y(O^{i}Pr)

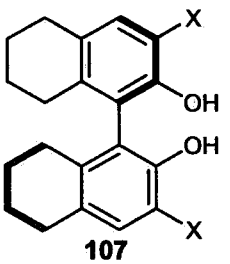

107

107a X= 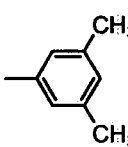

107b X= 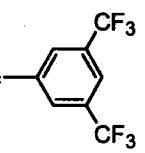

The BINOL scaffold has not only been used for the general MBH reaction but also for the aza-MBH reaction with good results. One of the major differences between the MBH and aza-MBH concerning BINOL is its function: in the MBH, BINOL is used as co-catalyst where they add an extra nuclophile such as PBu_3. But in the aza-MBH reaction the BINOL is modified to a bifunctional catalyst where the nucleophilic part is attached to the scaffold. This is possible due to the higher reactivity of imines. This has a major advantage because now nothing extra has to be added. There are two key players on this aza-MBH topic which have both their own bifunctional BINOL catalyst: Shi and Sasai.

Shi *et al.* were the first one to publish their catalyst **108** which was a mixture of (*R*)-BINOL and (*R*)-BINAP.[126] It was assumed that the cooperative effect of the nucleophilic phosphorous as Lewis base and the hydroxyl group as Brønsted acid would improve the reaction and that the chiral binaphthyl group would induce any e.e. In their first tests, MVK was screened with different *N*-sulfonated imines. Good yields (82-96%) and e.e.s (81-92%) were obtained with the *S*-configuration as major in all reactions. It was important to add molecular sieves to avoid possible hydrolysis. These reactions were repeated with ethyl vinyl ketone and phenyl acrylate.

With ethyl vinyl ketone the reaction was much slower so lower yields (50-78%) were obtained but with fairly the same e.e. (78-92%). With phenyl acrylate the yields (84-97%) were practically the same but this time the e.e.s were rather moderate (52-77%). Also in these cases (*S*)-product was the major. Strangely, when cyclopentenone and cyclohexenone were used with **108** no product was formed at all.[127] Only by making the catalyst more reactive through replacing the $P(Ph)_2$ by PMe_2, any product was formed. Although cyclopentanone gave now good yields (80-93%), the e.e.s were rather poor (32-55%) and with cyclohexenone the e.e.s were even worse (14-23%). A possible explanation for the lower reactivity is the steric hindrance because both are β-substituted alkenes and this could also explain the lower e.e.s.

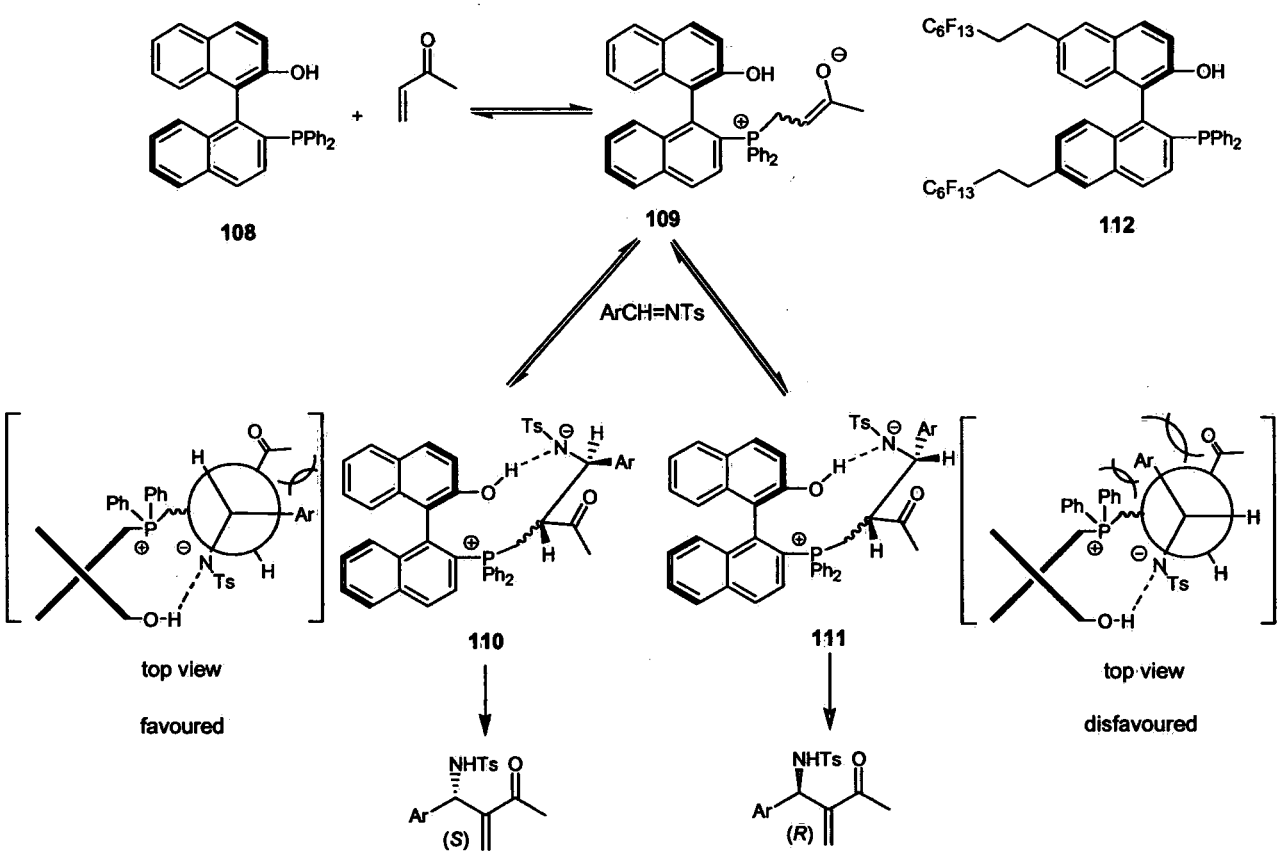

Scheme 14. Proposed mechanism with **108**.

Through the different experiments it was possible to construct a possible mechanism (Scheme 14).[128] In the first step, the phosphorous attacks the alkene and the newly formed enolate intermediate is stabilized by the hydrogen bond of the hydroxyl. Then, the binaphthyl scaffold lets the imine approach one side which leads to two possible configurations. In configuration

110, the aryl group of the imine interacts only with the carbonyl group, while in the other configuration **111**, the aryl group has steric hindrance with both the carbonyl and the phenyl group on the phosphorous. Since the first configuration is kinetically more favoured, it will predominate leading to the major (*S*)-product. This mechanism was supported by several experiments. The importance of the hydroxyl group was shown by removing it which gave almost no product. The presence of the enolate **109** was confirmed by ^{31}P NMR which showed a new peak at 25.3 ppm and in the ^{1}H NMR spectrum, the proton of the hydroxyl group was shifted to lower field. The influence of steric interactions was deduced through the different imines which showed a direct connection between bulkiness and e.e. In an attempt to improve the e.e., Shi *et al.* introduced "pony tails" at the 6,6'-positions of their catalyst (see **112**).[129] These "pony tails" are long perfluoroalkane chains which are known to improve enantioselectivity. In this case, unfortunately, no significant improvements were noticed.

Sasai *et al.* also created a bifunctional BINOL catalyst for the aza-MBH reaction, however, in their case the scaffold was effectively (*R*)-BINOL and the nucleophile was attached to the 3-position. The reason for maintaining the two hydroxyl groups of the BINOL was to preserve its high Brønsted acidity which would be able to stabilize the enolate more effectively than only one hydroxyl group. In the first attempts, a (diphenylphosphino)phenyl group was connected to the 3-position.[130] The three possible isomers (*o*, *m* and *p*) were screened and the *ortho*-(diphenylphosphino)phenyl **113** appeared to be most reactive. Compound **113** was then further screened with different imines and MVK, resulting in good yields (90-97%) and e.e.s (87-95%). Even with ethyl vinyl ketone, good yields (87%) and e.e.s (85-89%) were observed and all products had the (*S*)-configuration.

In a second attempt, the phosphine group was replaced by a DMAP moiety.[131] Again, different derivatives were tested and **114** came out as best. In this catalyst, it was not only important to adjust the spacer between the DMAP (Lewis base) and BINOL correctly, but also the *N*-substituent played a key role. By making the substituent more bulky, higher e.e.s could be obtained, therefore, *iso*-propyl gave the best results. By different experiments it was found that both hydroxyl groups of the BINOL played a crucial role in the catalytic mechanism.[132] Also, it was proven that the nucleophilic nitrogen was the tertiary nitrogen and not the pyridine nitrogen.

Again, **114** was screened with MVK with different imines and this time, even better results were obtained (yields 93-100% and e.e.s 88-95%) with the (*R*)-product as the major because of the use of (*S*)-BINOL. Although no mechanism was given, it is thought the reaction goes through the conventional route where the Lewis base adds to the alkene and the enolate is stabilised by both hydroxyl groups.

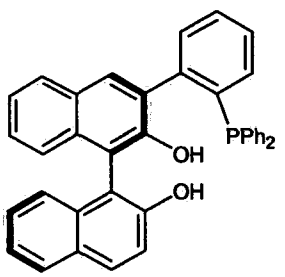

113

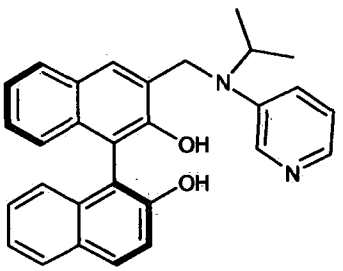

114

Intrigued by the good results of Sasai *et al.*, Shi *et al.* started also to modify catalyst **108**. Since it was now clear that the presence of different hydroxyl groups on the BINOL had a major impact on the yield and e.e., an extra BINOL was introduced onto scaffold **108** on the 3-position.[133] In that way, not only would the reaction be faster but the extra BINOL would increase the e.e. An important aspect was not only to have the right distance between the two BINOL groups, but also to make sure that both groups were "matched" stereochemically. The best results were obtained from the (*R,R*)-catalyst **115** which with MVK and several *N*-tosylimines at -20 °C gave good yields (85-97%) and excellent e.e.s (90-96%). The scope was further extended to ethyl vinyl ketone (yields 83-86%, e.e.s 90-93%) and acrolein (yields 74-90%, e.e.s 86-99%). All products had the (*S*)-configuration except the aromatic imines with an *ortho*-substituent which gave (*R*), however, still in good e.e. (90-92%). This was attributed to some steric interaction with the BINOL. To see the influence of each functional group on the catalyst **115** a number of small experiments were carried out. In a first test, the two hydroxyl groups were methylated on the newly attached BINOL and compared with **115**. The yield was dramatically reduced to 55%, however, the e.e. was only changed to a small extent to 88%. This indicated that the two hydroxyl groups on the BINOL were mainly responsible for the stabilization of the enolate and less for chirality. The entropic importance of both the binaphthalene groups attached were also investigated by screening and comparing reactions of **115**, with **108** and (*R,R*)-BINOL. In the latter, a lower yield (89%) and lower e.e. (84%) was obtained. This showed that both naphthol groups took part in the activation of the carbonyl group, however, the asymmetry was mainly

induced by the chirality of the phosphinonaphthol, hence, it was not necessary to add a complete BINOL group. Therefore, Ito *et al.*[134] proposed catalyst **116** to be at least as reactive, or even more reactive, than **115**. An extra phenol group was added to **108** instead of a BINOL, also at the 3-position. It was claimed that two hydroxyl groups would already be sufficient to stabilize the enol and by making it possible for sterically hindered substrates to approach more easily. It was assumed that a longer spacer and a smaller group would increase the molecule's flexibility which would enhance the positioning of the secondary hydroxyl group for stabilization. Again, **116** was screened with MVK and different imines to gain some excellent yields (97-100%) and e.e.s (94-97%). As expected, all products had the (*S*)-configuration. At the moment, **116** may be considered as the best catalyst for aza-MBH reaction.

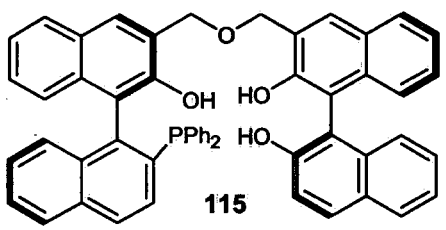

115

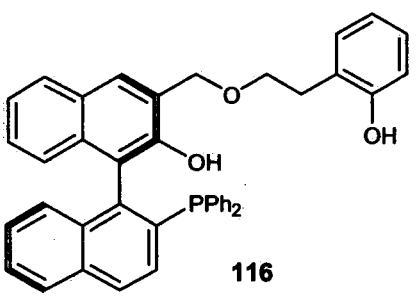

116

A rather special chiral Brønsted acid was reported by Warriner *et al.*[135] who created **117** which was based on a dimer of quinidine **75**. By adding just 0.5 equivalents of acid, it was envisaged that the quinidine section would be protonated which then could be used as a Brønsted acid and the other quinidine would then act as Lewis base. In this way, they tried to make this kind of system into a bifunctional catalyst based on an ammonium salt. In the first set of screenings with **117** and methyl acrylate, moderate e.e.s (60-77%) were obtained, however, in low yields (4-11%). When the more reactive HFIPA was used as alkene, the reaction was selective for these types of catalysts (see above), the yields however, were only 11%. A possible explanation for the low yields and moderate e.e.s was the loss of the hydroxyl group on the quinidine **75** which was now used to anchor both quinidines to the scaffold.

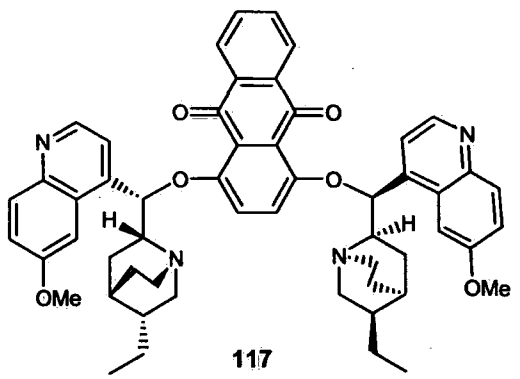

117

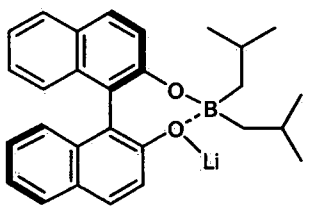

118

Besides the chiral Brønsted acids, there are also some chiral Lewis acids which have been used to assist the MBH reaction. An obvious way to make Lewis acids chiral is to coordinate with different chiral ligands. As mentioned before, Aggarwal *et al.*[75,136] introduced the (±)-BINOL to lanthanide metals to improve the reaction rate. Unfortunately, only racemic mixtures were obtained when a single enantiomer of binol was employed. Other oxygen rich chiral ligands were also examined, however, only a maximum e.e. of 5% was obtained. Better results were obtained by Sasai *et al.*[137] who used BINOL attached to different Lewis acids and modified them to heterobimetallic complexes. These types of salts appeared to be more reactive than normal Lewis acid complexes and a library of different catalysts using Al, B, La, etc. as Lewis acid was combined them with a different number of BINOL moieties. Out of this came catalyst **118** which seemed to be the most efficient. It was important to add a nucleophilic catalyst to start off the reaction. Out of a range of different nucleophiles, P^nBu_3 appeared the best. When **118** was screened with cyclohexenone and different aldehydes, some good yields and e.e.s were obtained. Surprisingly, with aliphatic branched aldehydes, which with BINOL catalysts were totally unreactive, some impressive results were noticed (yields 45-97%, e.e.s 97-99%). On the other hand, aromatic aldehydes, which are commonly used, gave lower yields (32-93%) and lower e.e. (15-19%).

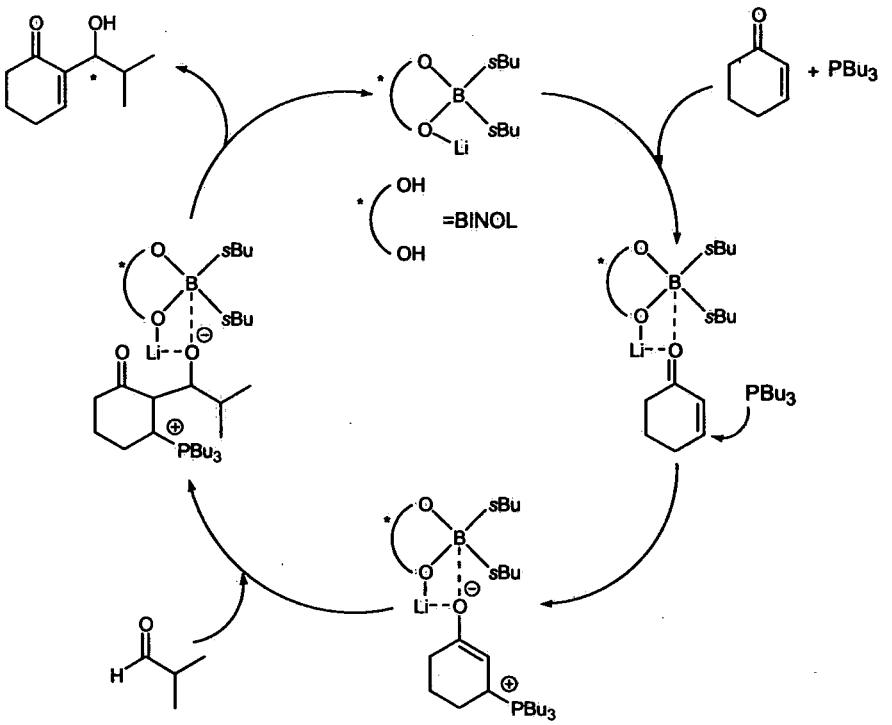

Scheme 15. Proposed mechanism with **118**.

This striking difference to conventional MBH catalysts towards aldehydes showed that a deeper mechanistic study was needed. By ^{31}P NMR, it was clear the enolate was formed through the phosphorous catalyst. The role of the lithium was not really known, but it was thought it helped to stabilize the enolate and also increased the Lewis acidity of the boron by coordinating with the phenoxide. It could also be responsible for positioning the alkene at the right place towards the BINOL. The two *s*-butyl chains on the boron were probably shielding one side so that the aldehydes could only approach from the binol side. This could probably explain why branched aliphatic aldehydes resulted in high e.e.s. Taking these speculations into account, a possible mechanism was proposed (Scheme 15).

Not only is BINOL used as chiral ligand, but some interesting new ligands were designed by modelling to improve catalytic systems. Yang *et al.*[138] created new chiral ligands that incorporated a donor group functionality into the ligand, which would moderate the Lewis acidity of the metal. This would subsequently affect the Lewis acid capability towards the activation of the unsaturated carbonyl compound. According to their results, the best donor group for these metals was a carboxylic acid. To induce the enantioselectivity, camphor-

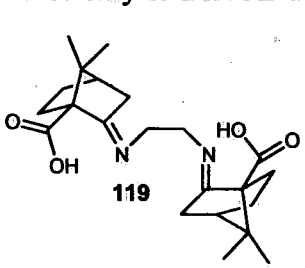

119

derived dimers with C_2-symmetry were employed. The best results were obtained with ligand **119** and $La(OTf)_3$ using a trial and error method to optimise the reaction conditions to avoid amine-Lewis acid complexation. It was found that it was necessary to use only a tenth of the metal compared to the nucleophile. For several combinations of aldehyde and acrylate, good yields (about 80%) and good e.e. (about 75%) were obtained after 10 hours at room temperature. Even more remarkable was the discovery that with the α-naphthyl acrylate and several aldehydes, the corresponding MBH products were already formed after only 20 minutes with yields of 75 to 80% and an e.e.s of 71 to 95%.

2.6.4.Chiral ionic liquids

The use and advantages of ionic liquids (ILs) for the MBH reaction have been mentioned earlier, herefore, it is not surprising this area of research has been developed further by making chiral derivatives of the ILs. Two papers have reported on this topic. One, Vo-Thanh *et al.*[139] created the ephedrine based ionic liquid **120** which could be prepared from (-)-*N*-methylephedrine in two steps. Together with DABCO, **120** catalyses the reaction of methyl acrylate and benzaldehyde in good yield (78%) but low e.e. (20%). By increasing the amount of **120** to three equivalents, the e.e. increased to 44% but the yield dropped to 60%. When more equivalents of **120** was used the yield dropped further, however, the e.e. stabilised. A possible explanation for the lower yield is probably due to side reactions in which the deprotonated hydroxyl group of **120** reacted with the aldehyde. Further research showed that the alkyl group on the nitrogen and the counter ion almost had no effect on the reaction. On the other hand, the hydroxyl group on **120** was crucial to induce chirality on the MBH product. This could be explained by hydrogen bonding between the hydroxyl and carbonyl groups creating a fixing point for templating the reaction outcome. To be sure it was the IL **120** which was responsible for the yield and e.e., the reaction was repeated with (-)-*N*-methylephrinidine and DABCO, however, in this case only 9% e.e. was noticed. To ascertain the generality of the system, methyl acrylate was further screened with different aldehydes to give good yield (60-82%) but rather poor e.e.s (16-44%). An interesting observation was made;when *p*-nitrobenzaldehyde was used, a good yield (78%) of product was observed,

however, with no asymmetric induction. This was probably due to the hydrogen bond interaction between the hydroxyl group of **120** and the nitro group.

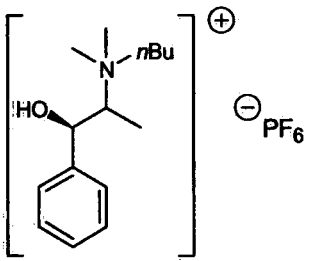

120

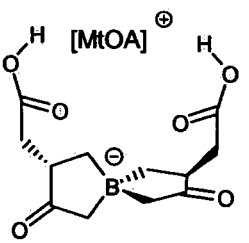

121

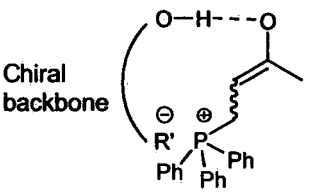

122

The other research group which has reported on this topic is that of Leitner *et al.*[140] who created borate anion **121** based on *L*-(-)-malic acid for the aza-MBH reaction. With triphenylphosphine applied as nucleophilic catalyst, different tosylimines were screened with MVK and some good e.e.s (71-84%) were observed, however, with low yields (34-37%). The e.e. also decreased to 10% when the corresponding tosylimine of *p*-nitrobenzaldehyde was employed which was as resulting from interference between OH group on **121** and NO_2 group. Although all products had the (*R*)-configuration, it was not known how the mechanism worked exactly. It was thought that the possible intermediate **122** was formed whereby the enolate was stabilized by hydrogen bonds to the boron anion. By X-ray crystallography, the two carboxylic arms of the malic acid were shown to be able to form a cavity where the imine might fit.

2.7.In summary

Today, the Morita-Baylis-Hillman reaction is highly topical because the products are potentially useful for further synthesis. Not only is the reaction useful for connecting two molecules, but it is also useful for the formation of a chiral centre, which is particularly appealing for organic chemists. It has been shown that there has already been a lot of improvement to increase the reaction rate and the e.e. in the MBH reaction, however, there is still a lack of good general catalytic systems. All the catalysts reported to date which are reactive, are usually reactive for only one or a small series of substrates. In addition, it is clear that there are catalysts that increase the rate but give poor e.e., and *vice versa*, hence, there is much scope for further developments

3.Research Work

The subject of this thesis is research into the development and application of bifunctional catalysts for C-C bond formation. It was proposed that bifunctional catalysts developed within the Whiting group may possess potential in this area because they contain a nitrogen atom and a boron atom on the same scaffold. This gives the possibility of combining nucleophilic and Lewis acidic groups into one catalyst. This combination may lead to active catalyst systems which could also be developed into asymmetric variants. This would be the first time that bifunctional catalysts of this type would have been used for C-C bond formation reactions, and in particular for the MBH and aldol reactions.

The discussion of the research work in this thesis is divided into four major parts: In the first, the synthesis of several amino-boronic acid compounds will be discussed together with some interesting observations; in the second, this section is focused on the MBH reaction, including an overview of standard MBH reactions and aza-MBH reactions and screenings; in the third, the aldol reaction is discussed, with corresponding results of screening reaction of the bifunctional catalysts; and in the fourth, approaches to the synthesis of new chiral bifunctional catalyst systems is discussed, together with side products obtained.

3.1.Synthesis of amino-boronic acid compounds as potential catalysts.

The general basis for this type of catalyst is exemplified by model **123**, consisting of a boronic acid and an amino functional group situated on a molecular scaffold. This scaffold can be either chiral or achiral, depending on the reaction to be examined. The most important aspect of this type of catalyst is the correct placement of the Lewis acidic and Lewis basic groups relative to each other. Both groups must work cooperatively and can, therefore, not be placed too closely in order to avoid de-activation due to intramolecular chelation.[141] The use of bifunctional amino boronate catalysts is not new. The

123

first reported catalysts of this type were developed by Letsinger *et al.*[142] which involved systems **124** and **125**. These catalysts appeared to be successful for hydrolysing the chloroalcohols.

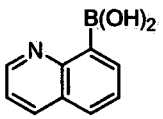

124

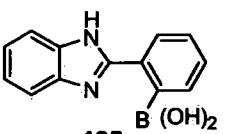

125

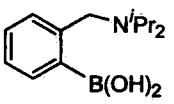

126

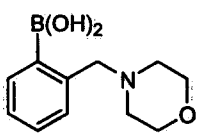

127

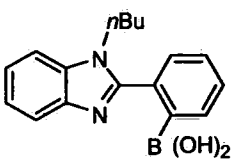

128

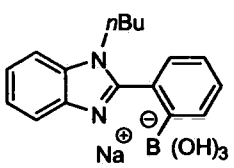

129

Also, in the Whiting group, some interesting and potentially effective bifunctional amino boronate catalysts were created, such as **126**, **127**, **128** and **129**. Compounds **126** and **127** were optimised by Giles and showed good reactivity towards catalysing the direct amide formation between amines and carboxylic acids.[143,144] Compounds **128** and **129** were developed as potential catalysts for the aza-Baeyer-Villiger reaction and were synthetically improved by Blatch.[145] For this project, the first task was to repeat the synthesis of catalysts **127**, **128** and **129**, and then to make modifications to develop a robust, facile preparation and fully study the application of these systems.

3.1.1.The synthesis of catalyst 127

Since catalyst **127** has some structural resemblance to DABCO, it seemed reasonable to use it as potential catalyst for the MBH reaction. Hence, attempts were made to reproduce its synthesis according to the method of Giles.[143] This catalyst was prepared by reductive amination[146] of 2-formylbenzeneboronic acid **130** with morpholine **131** (Equation 19).

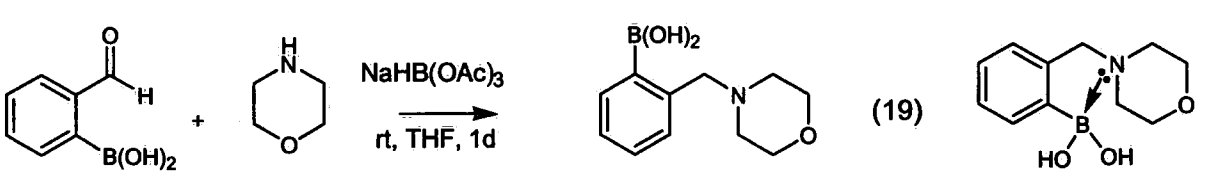

130 + **131** → **127a** (40%) (19) **127b**

In the first attempt, **130** was dissolved in dry THF with 3Å molecular sieve pellets added to remove the water. To this solution, 1 equivalent of morpholine was added and stirred for 20 minutes followed by treatment with 4 equivalents of sodium triacetoxyborohydride and stirring for 22 hours. The reaction was quenched by the addition of water and filtered to remove the sieves. The mixture was then washed with water to remove the excess of reducing agent. The ^{1}H NMR spectrum of the crude product showed that there was a mixture of three major compounds, including the product, which could be detected by the singlet of the benzylic protons. There was also starting material **130** which had a singlet for the aldehyde and the resonance for alcohol hydroxyl group at 2.67 ppm. Further purification was achieved by solid phase extraction with silica bonded C18-*p*-benzenesulphonic acid. Unfortunately, this was time consuming and only a low yield of product (17%) was recovered.

Therefore, some modifications were required to push the reaction to completion. The first modification was the use of an excess (1.1 equivalent) of morpholine since there was unreacted starting material present in the crude product, and therefore, not all aldehyde was converted into the imine. Also the reaction time was increased to 2 days and the reducing agent was added after 1 day instead of 20 minutes, to make sure all aldehyde was converted to the corresponding imine. Also, the quenching of the reaction was expanded to 2 hours. The reaction was easily followed by TLC and full conversion was observed without any side products. The pure product could be obtained in yield 51% simply by washing with water and drying. The loss of product was probably caused by washing, since the product is relatively polar due to the boronic acid. Both CHN analysis and accurate mass analysis proved that the product was isolated. Interestingly, ^{1}H, ^{13}C and ^{11}B NMR spectra in $CDCl_3$ gave the impression that there was a mixture of several products. Spectrum 1 shows the ^{1}H NMR spectrum of the pure product in $CDCl_3$. It is clear from the spectrum that it contains a lot of peaks which are not expected for this product **127**. Only by adding a drop of D_2O was Spectrum 2 obtained which appears to be a clean spectrum, with all the peaks assignable to the hydrogens of the product **127**. Similar effects were observed in the ^{13}C NMR spectrum in $CDCl_3$ which contained seven extra peaks at 140.7, 132.0, 127.0, 125.6, 64.1, 59.4 and 51.2 ppm compared to the spectrum after the addition of a drop of D_2O. Also, the ^{11}B NMR spectrum in $CDCl_3$ had one extra peak at 16.0 ppm compared to that which contained a drop of D_2O which had a single peak at 29.2 ppm corresponding to the boronic acid **127a**. These

different NMR peaks could be assigned to intra- or inter-molecular hydrogen bonding resulting in different shifts. The shift of the boron peak to 16.0 ppm is most likely due to B-N chelation coming from **127b**. This is reinforced by ^{13}C NMR shifts of the alpha-*N* carbons which show a low field shift due to this chelation. This could also explain why the addition of D_2O normalizes the observed complexity. Another interesting aspect of the ^{1}H NMR spectrum was that there were missing triplets at 3.65 ($(CH_2)_2O$) and at 2.45 ($(CH_2)_2N$). On Spectrum 2, only broad peaks could be observed. This is due to slow conformational interchange of the morpholine to the different chair conformations. Only by dissolving the product in DMSO with a drop of D_2O and heating it to 70 °C did the triplets become clear. All this evidence showed the pure product **127** had been obtained.

Spectrum 1. ^{1}H NMR of **127** in $CDCl_3$.

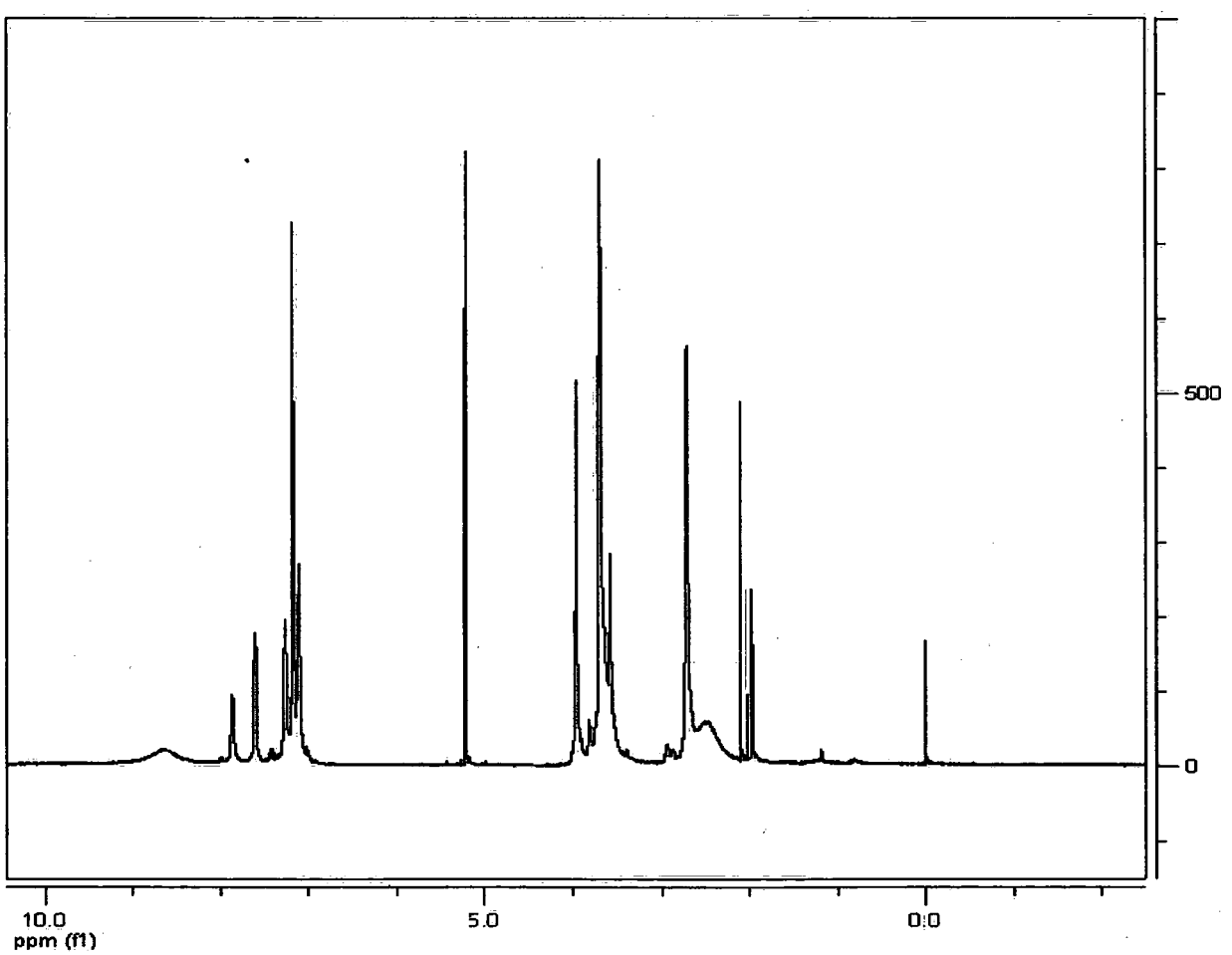

Spectrum 2. ^{1}H NMR of **127** in $CDCl_3$ and D_2O.

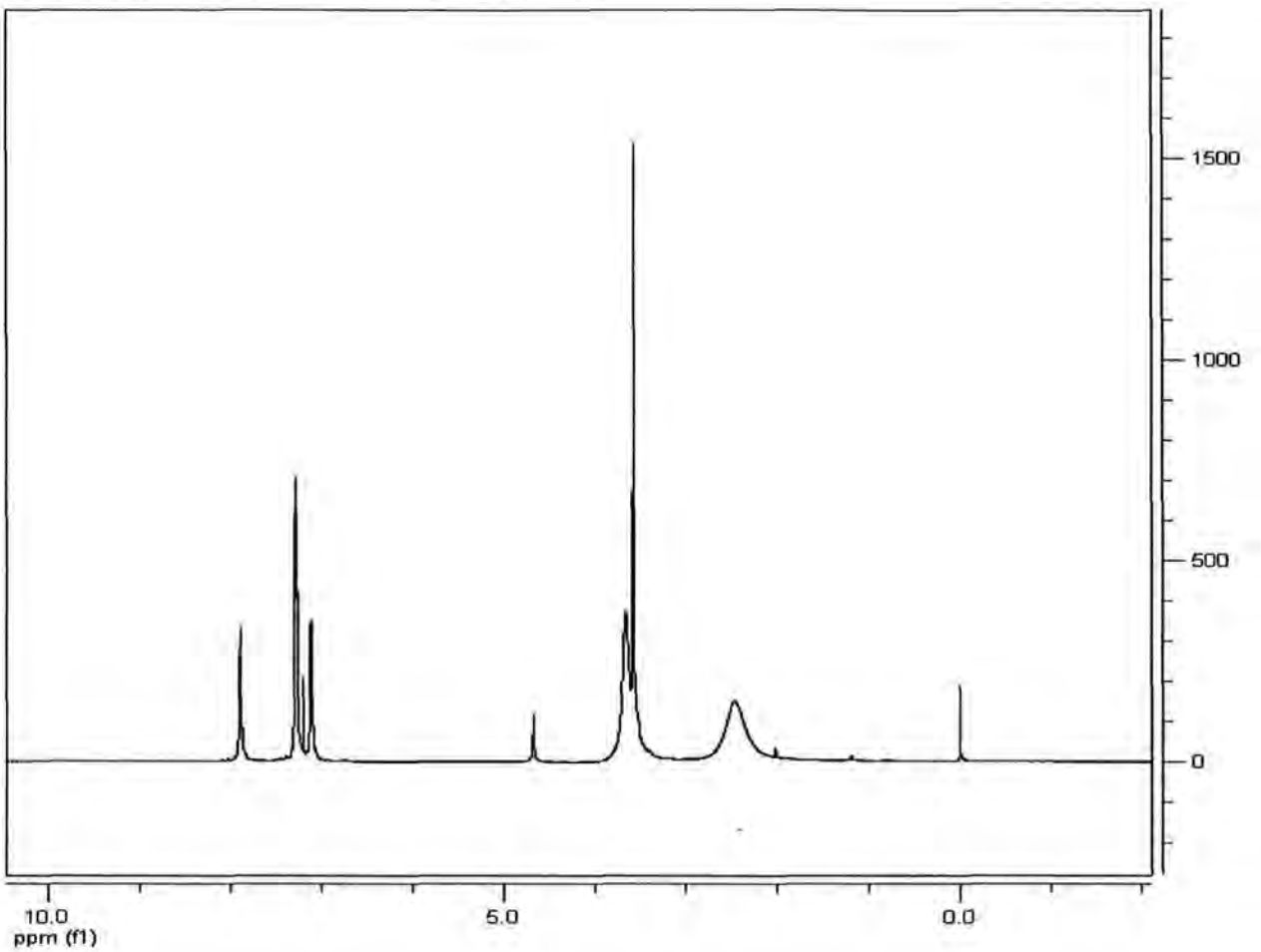

3.1.2. An interesting observation derived from **127**

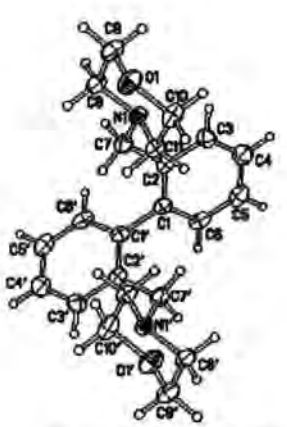

Figure 1. crystal of **132**.

Because it would have been useful to obtain the corresponding single crystal X-ray structure of compound **127**, attempts were made to grow crystals suitable for X-ray analysis. Hence, **127** was dissolved in water and left for almost a year in the open air. At which point, crystals were isolated and analysed by X-ray crystallography. Strangely, the crystals did not correspond to **127**, surprisingly, they corresponded to the dimer **132** (Figure 1, see appendix for crystallography data, Equation 20). To be sure that this result was not caused by traces of any transition metal residues, the procedure was repeated and the same

result was obtained. Even more surprising was the fact that the crystals were chiral. This could also be detected by the ^{1}H NMR which gave two doublets associated to the two benzylic protons and was further investigated by variable temperature ^{1}H NMR spectroscopy. It was expected that the two doublets amalgamate into each other at higher temperatures, however, even at 120 °C they were still separated. This potentially shows the enantiomers of **132** are atropisomerically stable and that the energy barrier to rotation may be quite high.[147]

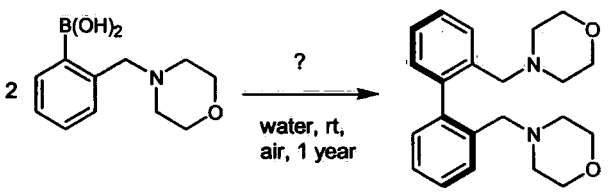

127 **132** (20)

Several articles[147,148] have reported this type of coupling reaction under similar conditions, *i.e.* between boronic acid compounds using palladium catalysis. Therefore, it was considered that it might be possible to repeat the reaction again but with a significant increase in rate due to the palladium catalysis (Equation 21).

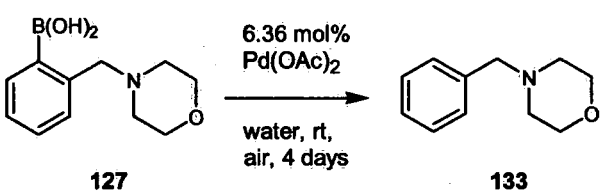

127 **133** (21)

80%

After 4 days the reaction (Equation 21) was complete, however, by TLC it was clear that the product did not correspond with **132**. After purification, ^{1}H NMR and mass spectrometry showed the product obtained was the deboronated product **133**. The reaction was repeated with NaOAc added as base and only **133** was obtained in the same yield. When Pd/C was used only starting material **127** was recovered. To date the exact mechanism of the coupling is unclear. Although the reaction with palladium did not deliver **132**, it can not be ruled out as catalyst. Also traces of other transition metals could be responsible for this result. Due to the presence of oxygen, the mechanism is perhaps most likely to proceed through the formation of borate peroxides which

eventually lead to radical biaryl coupling. It is also interesting that this behaviour was only noticed with **127**, and similar attempts on boronic acids **126** and **128** did not gave any coupling. This could indicate the necessarity of the morpholine group in the mechanism of the coupling.

3.1.3.The original synthesis pathway to catalysts **128** and **129**

The next catalysts for which attempts at synthesis were made were **128** and **129**. These catalysts have a 2-phenylbenzimidazole group as backbone with an *n*-butyl group and boronic acid attached. These catalysts looked interesting as potential catalysts for the MBH reaction because they might also have the ability to stabilize the intermediate (Scheme 6). Even more encouraging was the publication of Cheng *et al.*[67] who reported the use of a 2-phenylimidazole as catalyst for the MBH reaction in presence of Na_2CO_3. It was also suggested that the sodium carbonate was inactive in the reaction, and acted simply as a base to make the 2-phenylbenzimidazole more nucleophilic.

The pathway to **128** initially followed is represented in Scheme 16 and was developed by Blatch.[145] In the first step, an *n*-butyl group was attached onto the 2-phenylbenzimidazole backbone by an S_N2 alkylation reaction to give **135**. The second step was a direct lithiation with *t*-BuLi and tri*iso*propylborate as electrophile to give **128**.

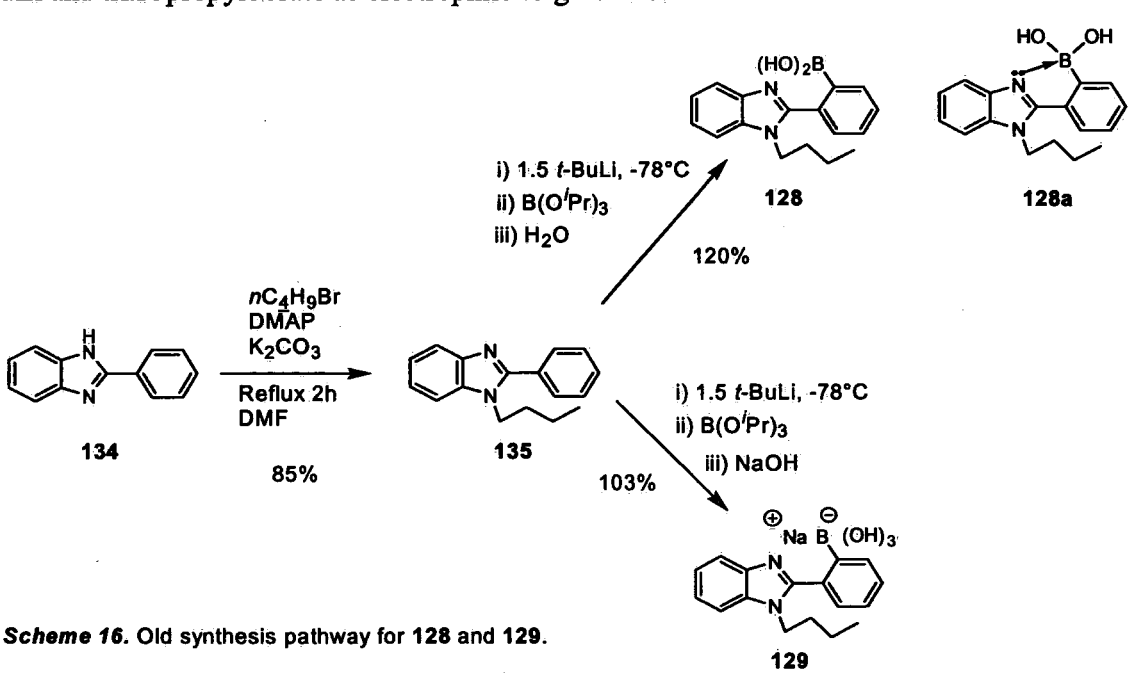

Scheme 16. Old synthesis pathway for **128** and **129**.

Following the same procedure as Blatch, the 2-phenylbenzimidazole and *n*-bromobutane were dissolved in DMF. To this, potassium carbonate and DMAP were added. The mixture was refluxed for 2 hours and stirred for 8 hours at room temperature. The ^{1}H NMR spectrum of the crude product showed only two compounds; the 2-phenylbenzimidazole **134** and the product **135**. Further purification by silica gel column chromatography gave a yield of 41% of **135**. Analytical data were identical to that reported by Blatch.[145] The moderate yield was due to losses upon separation on silica gel.

The second step of the synthesis was the direct lithiation of product **135**. In this case the same procedure used by Blatch was employed.[145] After drying **135** over phosphorous pentoxide, it was dissolved in dry ether and cooled to -78 °C. The *t*-BuLi was added slowely to the product **135** and the mixture stirred for 2 hours at -78 °C. Then, triisopropylboronate was added and the mixture was allowed to warm to room temperature over 12 hours. Afterwards, the reaction was quenched with water and the product precipitated and was isolated by filtration without any further purification. The pH of the water layer was important in this process since this determined which catalyst was isolated. When the reaction was quenched with neutral water, catalyst **128** would precipitate. On the other hand, when a base was used, catalyst **129** was produced and the only way to distinguish the two catalysts **128** and **129** was by their ^{11}B NMR spectra. Since **128** was the boronic acid, the ^{11}B NMR peak was around 30 ppm, and the corresponding salt **129** was much lower at around 5 ppm. For the synthesis of catalyst **128**, a precipitate was formed and it was clear that a reaction had occurred by the shift of several aromatic peaks to lower field in the ^{1}H NMR spectrum and the loss of one proton in the integration of the aromatic peaks. The major problem in this case was that the precipitated material contained a mixture of derivatives of **128**. Not only was this clear from the ^{1}H NMR spectrum, but also the ^{11}B NMR spectrum showed two peaks at 20 and 10 ppm, corresponding to the boroxine **136** and the intramolecular B-N chelated **128a** forms. The expected boronic acid peak at 30 ppm was not present and the ES(+) mass spectrum did not show any peak at 295.2 corresponding to the product **128**. The only observable ion for the product was 277.3 (37 %) corresponding to M-OH. Other peaks of the ES(+) mass spectrum could not be explained. Although no further purification was carried out, the ^{1}H NMR spectrum in $CDCl_3$ still showed some starting material. Also the ES(+) mass spectrum showed a peak at 251.3 (17 %)

corresponding to **135**, which could explain why Blatch obtained a yield higher than 100%. The synthesis of catalyst **129** was also repeated following the procedure of Blatch, however, the yield was too low (< 1%) to obtain accurate data for the product.

3.1.4.The new synthesis pathway for the catalysts 136 and 129

Because the original pathway to prepare the active catalysts **128** and **129** (Scheme 16) gave low yields and had purification problems, a new pathway was required, as outlined in Scheme 17.

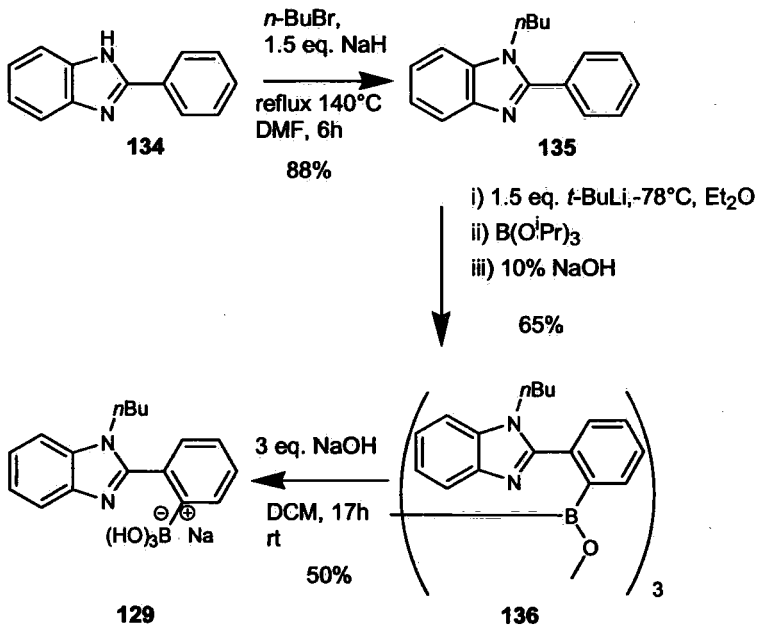

Scheme 17. New synthesis pathway for **136** and **129**.

In the first step, an *n*butyl group was attached on the 2-phenylbenzimidazole backbone by an S_N2 alkylation reaction following the same procedure as Blatch, using potassium carbonate and DMAP, however, only 41% yield of **135** could be obtained. Therefore, two modifications were carried out: Firstly, changing the method of purification. Because the starting material and product had had the same Rf value on silica gel, separation was difficult. Better separation was achieved on aluminium oxide and hence, the yield increased to 61%. Secondly, changes were made in the reaction conditions. Because a significant fraction of starting material was present in the crude ^{1}H NMR spectrum, it was necessary to push the reaction to completion by using a

stronger base, such as NaH and increasing the reaction time.[149] Both these changes led to full conversion of the reaction and no further purification was required to give other than the basic work up and the product **135** was isolated in 88%.

The second step (Scheme 17) was the direct lithiation of **135**. This was the most important and most difficult step in the synthesis with the first attempts using the same procedure proposed by Blatch.[145] Only in the case where water was used for quenching the reaction to pH 7, was a significant amount of product isolated. By ^{1}H and ^{11}B NMR spectroscopy the isolated product appeared to be a mixture of boroxine **136**, the intramolecular chelate form **128a** and starting material **135**. This was concluded on the basis of two peaks at around 20 and 10 ppm on the ^{11}B NMR spectrum corresponding to the boroxine **136** and the intramolecular chelated form **128a**. The presence of starting material was determined by ^{1}H NMR spectroscopy. Therefore, further purification by column chromatography using aluminium oxide gave the boroxine **136**, which was isolated as a pure compound in 65% yield. Isolation as the boroxine **136** made it much easier to analyse the product and to calculate the yield, and the structure was confirmed by ^{11}B NMR spectroscopy which had a single peak at 18 ppm with further evidence of structure and purity being obtained from accurate mass and CHN analysis.

Using the boroxine **136**, several attempts were made to obtain the corresponding boronic acid **128** by recrystallising **136** in a mixture of acetonitrile and water. Unfortunately, only a mixture of compounds was obtained. However, since it had been proposed, but not proved, that **129** was an active catalyst for aldol reactions, a new way to create and isolate this compound was considered. Because it was important to be sure that the "ate"-complex could be formed from the corresponding boroxine, an NMR experiment was suggested. The boroxine **136** was dissolved in $CDCl_3$ and an excess of NaOD was added, which produced immediate precipitation. This precipitate was filtered and analysed by NMR in a D_2O/CD_3CN mixture. The ^{1}H NMR spectrum showed the "ate"-complex was present, which was supported by the ^{11}B NMR spectrum which had a single peak at 4 ppm. Although the CHN analysis was too low in C and N (presumably due to the presence of NaOH and water), this experiment gave interesting information. Not only could the "ate"-complex be formed out of the boroxine, but it could also be isolated by precipitation. Therefore, the reaction was repeated in DCM on larger scale using exactly 3

equivalents of NaOH.[150] The reaction was left for 3 hours at room temperature. Again, the precipitate was isolated by filtration and isolated in only 38% yield. This time the CHN analysis confirmed that pure **129** had been isolated. The low yield of the product **129** was due to the low solubility of NaOH in DCM. Therefore, by dissolving the NaOH in water (40% NaOH solution) and leaving the reaction overnight gave an improved yield of 50%.

One of the major problems with borate complex **129** was its low solubility in organic solvents, due to the combination of its polar "ate"-complex centre and the aromatic backbone. This complicated obtaining a good ^{13}C NMR spectrum which was achieved by using a mixture of THF, acetonitrile and water whereupon the product could be completely dissolved. Unfortunately, this combination of solvents gives unclear ^{1}H and ^{13}C NMR spectra because of the non-deuterated solvent peaks interfering with the peaks of the product. Therefore, all spectra were analysed in an acetonitrile/water mixture.

3.1.5.An overview of the regioselective direct lithiation of 2-phenylbenzimidazole **135**

As mentioned before, the direct lithiation of 2-phenylbenzimidazole **135** with $B(O^iPr)_3$ as electrophile appeared to be regioselective, giving only the corresponding *ortho*-boroxine **136** as product. This high regioselectivity is presumably controlled by the chelation of the lithium with the electron pair of the sp^2 nitrogen, bringing the base to this *ortho*-position (Scheme 18).

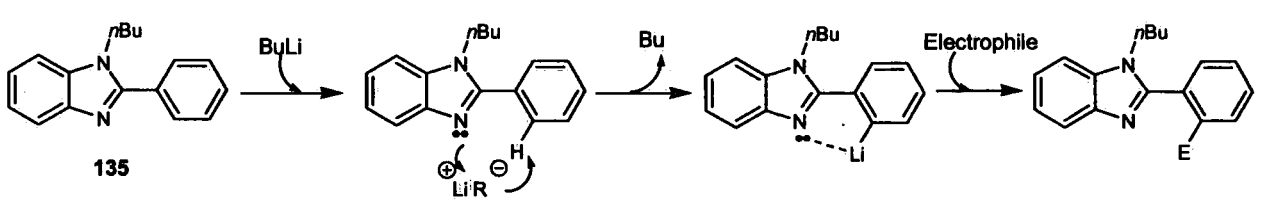

Scheme 18. Regioselective direct lithiation of **135**.

Therefore, it seemed interesting to investigate if the same behaviour would be observed by using different electrophiles (Equation 22, Table 1).[151]

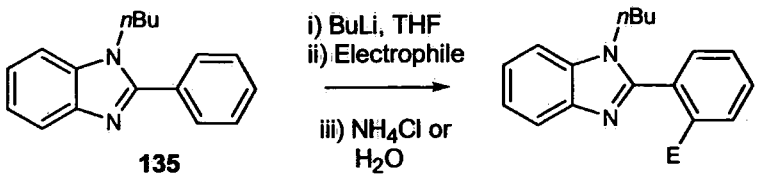

(22)

136 E= BO_2
137 E= CHO
138 E= Br
139 E= TMS

Table 1: The different conditions for each electrophile with the obtained yield.

ntry.	Electrophile	Equivalents of electrophile	Type of BuLi	Equivalents of BuLi	Temp. (°C)	*Ortho*-product[a] (%)	Recovered S.M.[a] (%)	Side products[a] (%)
1	DMF	8	*n*-BuLi	1.5	-78	/	100	/
2	DMF	8	*n*-BuLi	1.5	-42	31	48	21
3	DMF	8	*n*-BuLi	2	-25	87	3	10
4	$(BrCCl_2)_2$	2	*n*-BuLi	1.5	-78	/	100	/
5	$(BrCCl_2)_2$	2	*n*-BuLi	1.5	-42	42*	19	39
6	$(BrCCl_2)_2$	2	*n*-BuLi	2	-25	5+70*	6	19
7	Br_2	2	*n*-BuLi	2	-25	9	N.A.	N.A.
8	TMSCl	2	*n*-BuLi	2	-25	62*	7	31
9	TMSCl	2	*n*-BuLi	2	-42	87	3	10
10	$B(O^iPr)_3$	2	*t*-BuLi	1.5	-78	66	N.A	N.A
11	$B(O^iPr)_3$	3	*n*-BuLi	2	-25	N.A.	N.A.	69

* Traces of side product or S.M. were present on ^1H NMR.
[a] Based on isolated yield.

First, the DMF quenched reaction (Table 1, entries 1-3) was carried out at -78 °C using 1.5 equiv. of *n*-BuLi (entry 1). However, only starting material **135** was observed; hence, the reaction temperature was increased to -42 °C to promote the lithiation and subsequent reaction with DMF (entry 2). In this case, 31% of the benzaldehyde derivative **137** was isolated. Raising the temperature again to -25 °C gave a further increase in yield to 87% (entry 3) of the corresponding aldehyde **137**. It is also interesting to note that the percentage of side products observed in the crude NMR spectra also decreased with the increasing temperature.

For the bromination of **135** to give **138** (Table 1, entries 4-7), the initial reaction was carried out at -78 °C using 1.5 equiv. of *n*-BuLi; however, only starting material **135** was recovered (entry 4). When the temperature was increased to -42 °C (entry 5), almost complete conversion of **135** was achieved, however, separation of the starting material and product **138** was difficult due to

their similar retention times. With the use of 2 equiv. of *n*-BuLi at -25 °C (entry 6), the conversion of **135** was improved, however, again due to separation problems, only 5% of **138** was isolated after silica gel column chromatography. A marginal improvement in yield to 9% was possible using Br_2 as electrophile (entry 7). Attempts to separate **135** and **137** by Kugelrohr also failed.

In contrast, the lithiation of benzimidazole **135** and the reaction with TMSCl gave the corresponding trimethylsilyl compound **139** in a much more straightforward manner (Table 1, entries 8 and 9). Carrying out the reaction at -25 °C using 2 equiv. of *n*-BuLi (entry 8), followed by quenching with TMSCl, gave a crude product which by ^{1}H NMR spectroscopy also showed the presence of a major side product. The direct metalation was substantially improved to give regioselective trimethylsilylation when the reaction was carried out at lower temperature (-42 °C), resulting in 87% yield of **139** (entry 9).

In interest of our research with bifunctional catalysts, $B(O^iPr)_3$ was originally taken as electrophile. The standard conditions at -78 °C with 1.5 equiv. of *t*-BuLi in ether were formulated by Blatch and gave after precipitation (at pH 7) and column chromatography the pure *ortho*-boroxine **136** (Scheme 17). This reaction was repeated in THF and in this case, no precipitation at pH 7 was observed. After extraction and purification by column chromatography, the same yield as that gained in ether was obtained (entry 10). In an attempt to increase the yield, the reaction was rerun at -25 °C using 2 equiv. of *n*-BuLi (entry 11). In this case, a mixture of side products was isolated after separation on column chromatography. Because the standard conditions at -78 °C give selectively the boroxine product **136**, it was considered to follow these conditions in the future.

An interesting aspect of this overview is the influence of the electrophile on the lithiation position of **135**. Normally, it is expected that only temperature would define how high the regioselectivity of deprotonation would be, but in this overview it is clear that the electrophile also plays a role. E.g.: at –25 °C with TMSCl and $(BrCCl_2)_2$ there are side products present where the lithiation did not only happen at the *ortho*-position, but also on other positions, hence, the by-product fractions. However, in the case of DMF almost all the deprotonation happened

solely at the *ortho*-position. This shows that the electrophile can interfere in the proton exchange making the lithiation reaction less selective.

3.1.6.The synthesis of catalyst **143**

Besides the synthesis and optimisation of the already made catalysts, it was thought that it would be useful to introduce a new catalyst based on a bicyclic guanidine structure. This structure was chosen since Leadbeater *et al.* reported that this type of molecule showed good reactivity towards the MBH reaction.[66] The considered synthesis pathway comprised of two steps and was based on the commercially available 1,5,7-triazabicyclo[4.4.0]dec-5ene **140** and 2-bromobenzyl bromide **141** (Scheme 19).

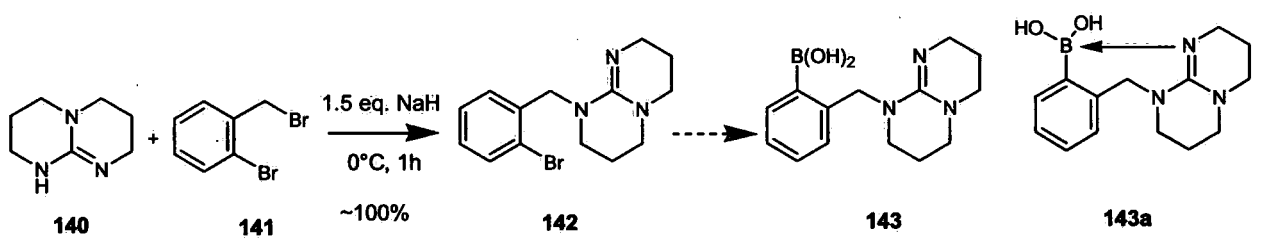

Scheme 19. Synthesis pathway of catalyst **143**.

The first step was an S_N2 reaction of the bicyclic guanidine **140** onto **141**[152]. In the first attempt, the guanidine **140** was dissolved in dry THF at room temperature with an excess of NaH. An equimolar amount of **141** was added to the mixture and kept on stirring overnight. After quenching and work-up, the crude proton NMR spectrum showed all starting material was consumed and two new peaks had emerged corresponding to the product **142** and the salt **144**.

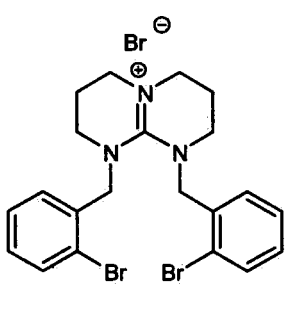

144

This was supported by the ES(+) mass. The formation of the salt **144** showed that the reaction was too fast, therefore, some adaptations were added to the procedure: The reaction was slowed down by lowering the temperature to 0 °C and the reaction time was reduced to one hour. Also, a small excess (1.3 equiv.) of guanidine **140** was used, which could be easely removed by washing, and the 2-bromobenzyl bromide **141** was added dropwise to avoid the salt formation of **144**.[153] By

removing the oil of the NaH, the reaction could be pushed to completion and the product could be isolated only by washing the crude with water, giving a yield of almost 100%. Although the exact mass spectrum showed only one peak corresponding with **142** and the ^{1}H and ^{13}C NMR spectra were clean, the CHN analysis was not in accordance with the proposed structure. This indicated there were side products present. Due to the high polarity of the guanidine group, column chromatography could not be used. Therefore, **142** was submitted to an acid wash. This implied that **142** was dissolved in water at pH 1 and washed with ether, hoping the ether fraction would extract the side products, and then neutralisation to pH 14 and re-extraction with DCM would result in isolation of pure **142**. Unfortunately, no difference in CHN analysis was noticed, and the ^{1}H NMR spectrum still showed a clean product. Because of the low CHN analysis, the assumption grew that the isolated product was not **142** but rather the corresponding salt **145**. This was theoretically possible since it is known the guanidine derivatives are very basic with a *p*Ka of the guanidinium compound at 14 or higher. This could explain also the low solubility in organic solvents and the high yield of the reaction.

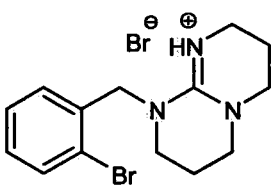

145

The following step was a lithium-halogen exchange with bromide and boron added as electrophile to replace the lithium. This standard reaction[154,155] is normally run at low temperature with a small excess of BuLi in a dry, inert solvent. The first attempts were done using only 1.0 to 1.5 equiv. of BuLi giving almost only starting material **142**. Since more evidence indicated the formation of the salt **145**, it was considered that an increase in the amount of BuLi to 2.5 equiv. was required. In this way, the BuLi would first neutralize the salt **145** to **142** and the excess BuLi could then be used to do the actual lithiation exchange reaction. The reaction was carried out at -78 °C in THF with 2.5 equiv. of *t*-BuLi syringed in dropwise. After adding 2 equiv. of $B(O^{i}Pr)_3$, the reaction was left running overnight. The reaction mixture was quenched and dissolved in water (pH 14), and washed with ether to remove any side products. By neutralizing the water phase to pH 9, the crude could be isolated through extraction with ethyl acetate. Unfortunately, less than one fourth of the starting mass was recovered crude. This was just enough to obtain spectroscopic data but not enough to purify further. The ^{1}H NMR spectrum of the crude product showed a mixture of several products including the starting material. Also the ^{11}B NMR spectrum gave interesting peaks at 33 and 13 ppm. This could be

assigned to the corresponding boronic acid **143** and the chelating form **143a**. Because the recovery of product was so low (< 20%), the reaction was repeated but now on larger scale (400 mg). The same procedure was followed as before, only the reaction time was increased. After the reaction was quenched with NaOH (20%, pH 14) and washed with ether, the water phase was saturated with brine and washed at every pH from 14 to 7 with ethyl acetate. In this way, it was possible to investigate at which pH the boron compound **143** was neutral. Unfortunately, very small amounts of product were recovered (< 75 mg) and still 130 mg of crude mass was missing in the water phase. For further purification an ion-exchange resin was used with sulfonic acid on the surface. The water phase was brought to pH 1 and ran over the resin. The resin was washed with water which was gradually increased in pH from 1 to 14 using ammonia. The fractions between pH 7 and 14 were collected and analysed. The collected fractions were only a disappointing 50 mg and the ^{1}H NMR spectra of the different fractions showed a mixture. Also the ^{11}B NMR spectra continuously showed two peaks at 33 and 13 ppm.

Through the experimental data it became clear that the synthesis of **143** was problematic. There were actually three major problems:

1) The uncertainty about the S.M. Although almost all data (^{1}H and ^{13}C NMR spectra and exact mass spectrum) indicated that it was **142**, there was still a possibility that the S.M. was rather **145** (see elemental analysis). This plays a crucial role in the next step because without knowing the exact compound, the lithiation is hard to control. E.g.: when not enough equivalents of BuLi were used, the reaction would not complete and only S.M. was recovered. On the other hand, when too much BuLi was used, too many side products were formed.
2) The insolubility of the S.M.: Because of the use of BuLi only dry, non reactive solvents could be used such as ether. Unfortunately, several different ethers were tried, including THF, diethyl ether, TBME, di-isopropyl ether, etc., however, none of them dissolved the S.M. Also in dry acetals, such as dimethoxymethane and dimethoxyethane the same behaviour was noticed. Different attempts to dissolve **142** by increasing the temperature to 0 °C were in vain. This insolubility could also play a key role in the low conversion.

3) Difficult isolation: The presence of a guanidine group together with a boronic acid makes **143** very polar and can lead to the formation of corresponding zwitterion. This high polarity makes **143** very hydrophilic, leaving it in the water phase and this could be the reason for the low recovery.

Other types of reactions were also tried besides the lithiation to generate the product. One way was by the use of palladium chemistry.[156,157] In that case, **142** was dissolved in dioxane and $Pd(OAc)_2$ was added together with pinacol borolane to form corresponding pinacol product. In this way it was hoped the product would be less water soluble and a greater conversion would be achieved. Unfortunately, only S.M. was recovered. Also the reversed synthetic pathway was tried, with first the attachment of the boron and afterwards the guanidine group. In this step, 2-bromobenzyl bromide **141** was submitted to a lithiation[158] with $B(O^iPr)_3$, however, the reaction was not successful due to the large amount of side products.

3.1.7.The introduction of a new catalyst **150**

Because compound **125** was introduced by Letsinger *et al.* and showed earlier some reactivity for hydrolysing chloroalcohols, it was thought to be useful to make a molecule with the same structure but with a chiral centre in the active place. In that way, it might be possible to induce some chirality in the products. Therefore, it was considered to make this indole derivative **150**. Previous work, done by Dr. T. Schütz, involved the first steps of the pathway, including the Fischer synthesis[159] and the tin reduction.[160] Because the following step included a halogen-lithium exchange, it was considered more beneficial to protect the amine so its proton would not neutralise the BuLi. After screening several protecting groups it was found by Dr. T. Schütz that the benzyl group[161] gave the best results. Unfortunately, after several attempts, it was not possible to create the final product (Scheme 20).

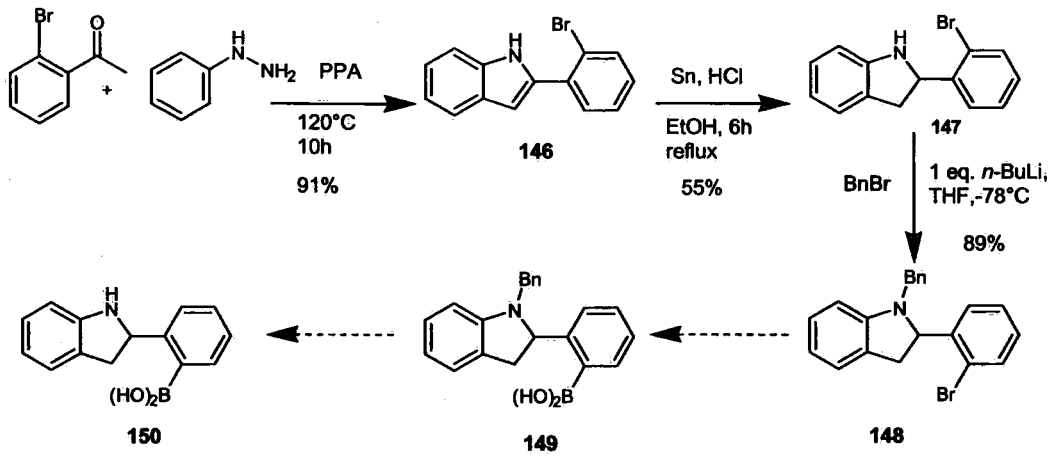

Scheme 20. Synthesis of indole catalyst **150**.

In the different attempts by Dr. T. Schütz to create **149**, the BuLi was always dissolved in THF at -78 °C and **148** was added slowly. Although the ^{11}B NMR spectrum gave a single peak at 32 ppm corresponding to boronic acid **149**, it was by ^{1}H NMR spectroscopy and TLC clear that different products were formed. After purification by column chromatography, none of fractions appeared to contain the corresponding product.

This time the reverse way was chosen and product **148** was dissolved in THF at -78 °C with the BuLi added dropwise. In this way, it was hoped to have less side products. In the first attempt 1.5 equiv. *t*-BuLi was used. Again, one boron peak was present on the NMR at 32 ppm, but the ^{1}H NMR and TLC gave the same result as in Dr.T. Schütz's case and after purification no product **149** was present. Also when the less reactive *n*BuLi was use, several side products appeared. A problematic side effect was the instability of the indoline compounds. After one day it started to change colour from yellow to dark green and on the NMR spectrum a small amount of decomposed product was noticed.

It appeared that the lithium-halogen exchange was not selective enough, presumably because of the presence of an extra phenyl group. In future a different protecting group might be used or a different pathway. One of the options is the introduction of the boron group by palladium.[156] In that case, the amine does not have to be protected.

3.1.8.Summary

Because the synthesis of different catalysts like **127**, **136** and **129** was now reliable and optimized, it was possible to make them on large scale (15 g) and use them for screening for different reactions, together with **126**. In the next two chapters an overview will be given of the different screenings for the MBH reaction and the aldol reaction.

3.2.The Morita-Baylis-Hillman reaction

In this part the research on the MBH reaction will be discussed. This will start off with the search for an ideal standard MBH reaction to which our catalysts can be compared, followed by the actual screenings. It also covers the aza-MBH reaction with its screenings. At the end some final notes are included about the incorporation of the ReactIR in our research.

3.2.1.Standard Morita-Baylis-Hillman reactions

In order to learn more about the Morita-Baylis-Hillman reaction and the product, it was decided to do some standard reactions. By this method, it would be possible to find one good, general standard reaction which could be used every time to compare with the new bifunctional catalysts. This standard reaction had to fulfill some demands:

1) One of the most important aspects is the reactivity. It is needed that the reaction goes fast enough so a sufficient amount of product is formed. This would make it easier to isolate the product and to calculate the yield for comparison. Also, it allows more screening reactions to be done in shorter time. Knowing the slow rate of the MBH reaction, this could be the most difficult demand. Therefore, several modifications were made on basis of solvent, and substrate, etc. during the screening in order to speed up the reaction.

2) Another important point is the lack of side products. A good standard reaction should form little or even no side products. Not only does this simplify the isolation of the product, but it also makes it easier to draw conclusions when the different catalysts are being compared.

3) Finally, the conditions in which the standard reaction is run is a key factor. The standard reaction should run preferentially under general mild conditions, not under extreme conditions. This means at room temperature where possible and under atmospheric pressure, etc. This is important since the bifunctional catalysts would be studied under identical conditions.

In the search for this one good standard reaction and the right conditions, there were 6 parameters that were changed:

1) The solvent: the solvent plays a very important role in the MBH reaction, not only for the solubility, but also to speed up the reaction. In some cases DCM was used to make sure everything dissolves, in other cases a polar solvent[29] was used to increase the speed. Sometimes no solvent was used at all.
2) Substrates: besides the use of the most common substrates for the MBH reaction, namely benzaldehyde and methyl acrylate, also more reactive substrates were used, such as *p*-nitrobenzaldehyde and methyl vinyl ketone. Although these more reactive substrates increase the speed, they tend also to form more side products.
3) Type of catalyst: two catalysts were used, DABCO and DBU.[65] DABCO is considered as the most general catalyst for MBH reaction. DBU is very reactive due to stabilisation of the intermediate.
4) Amount of catalyst: preferentially a small amount of catalyst was used. Although, in some cases the amount was increased to examine the behaviour.
5) Reaction time: since the MBH reaction is so slow, it took for most of the reactions several days to induce some product.
6) Temperature: most MBH reactions were done at room temperature. Only once the reaction was done at 0 °C.[26]

Generally, the MBH reactions were carried out with 1 equivalent of aldehyde and 1.1 equivalent of alkene and were easy to follow by TLC. When *p*-nitrobenzaldehyde or benzaldehyde was used, the products could be detected under UV, in the other cases potassium permanganate was used to visualise the products on TLC. Also on the proton NMR spectrum the product could very easily been detected since a hydroxyl group emerged around 2.98 ppm. Since almost no side products were formed, the isolation of the MBH product could be done with column chromatography on silica gel. The reported yields are the one of the isolated product.

The general Equation 23 is given below and all the test reactions are represented in following Table 2.

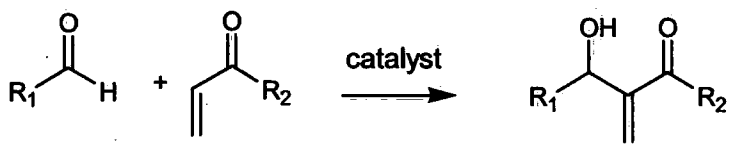

(23)

151 **152** **153**

***Table 2*: Screenings of standard MBH reactions.**

Entry	Aldehyde (R_1)	Alkene (R_2)	Solvent	Catalyst	Mol% Cat.	Time	Temp (°C)	Yield[a]
1	C_6H_5	OCH_3	neat	DABCO	10	8d	25	75%
2	C_6H_5	O-*n*-C_4H_9	neat	DABCO	10	5d	25	32%
3	*n*-C_2H_5	OCH_3	neat	DABCO	10	11d	25	7%
4	CH_3	O*t*C_4H_9	neat	DABCO	10	9d	25	S.M.
5	C_6H_5	OCH_3	H_2O/diox.	DABCO	10	4d	25	S.M.
6	C_6H_5	OCH_3	H_2O/diox.	DABCO	100	42h	25	3%
7	C_6H_5	OCH_3	H_2O/diox.	DABCO	300	42h	25	17%
8	C_6H_5	OCH_3	sulfolane	DABCO	50	48h	25	24%
9	C_6H_5	OCH_3	sulfolane	DABCO	100	48h	25	24%
10	C_6H_5	OCH_3	neat	DBU	100	6h	25	44%
11	C_6H_5	OCH_3	neat	DABCO	100	6h	25	15%
12	C_6H_5	OCH_3	THF	DABCO	0.1	6h	0	S.M.
13	C_6H_5	OCH_3	dioxane	DABCO	0.1	6h	0	S.M.
14	*p*-$NO_2C_6H_5$	CH_3	sulfolane	DABCO	50	24h	25	14%
15	*p*-$NO_2C_6H_5$	OCH_3	DCM	DABCO	50	3d	25	47%
16	*p*-$NO_2C_6H_5$	OCH_2CH_2OH	DCM	DABCO	50	3d	25	60%

[a] Based on isolated yield.

The first reactions (Table 2, entries 1-4) were general reactions to obtain some standards which could be used in the future. These reactions were done neat and ran for several days at room temperature giving the corresponding MBH products **154** (entry 1), **155** (entry 2)[16] and **156** (entry 3).[93] In the original literature[9] the MBH reaction of *t*-butyl acrylate (entry 4) was reported to proceed in a yield of 89% after 7 days, however, in our hands, only starting material was obtained. Other reports[16] also used *t*-butyl acrylate and reported that the reaction was extremely slow due to steric hindrance. The result was a yield of 65% after 28 days under the same conditions. Since these reactions (entries 1 to 4) were so slow, it was needed to find a way to improve the speed.

The first attempt on this reaction to increase the speed involved changing solvents, since it has been reported[29] that polar solvents are accelerating for the MBH reaction. Initially, a combination of 1,4-dioxane and water, which is mono-phasic, was employed (Table 2, entries 5-7). These were carried out with benzaldehyde and methyl acrylate at room temperature in open air and the concentration of DABCO was changed to see how this influenced the reaction outcome. Strangely, the literature[33] reports yields of more than 80% with 100 mol% DABCO. It is interesting that the amount of catalyst does change the yield of the reaction, however, although this behaviour was also not reported in the literature, it is the expected result. However, most striking was our inability to reproduce the literature reactivity and large amounts of catalyst were required in order to obtain any discernible reaction.

As second solvent, sulfolane was used (Table 2, entries 8 and 9) because there was a literature report[31] claiming that this solvent may be considered as the best general solvent for MBH giving good yields. However, sulfolane, which is similar to DMSO, has a high boiling point (285 °C). Hence, it was difficult to remove it by rotary evaporation. It was also necessary to allow the sulfolane to absorb some water because it is a solid at room temperature. Again, the MBH reactions were carried out at ambient temperature under argon with DABCO as catalyst. Also, the concentration of the catalyst was changed to see its influence. In this case the concentration of DABCO does not seem to make any difference. This behaviour was unexpected and could not be explained.

Besides changing the solvent, also the catalyst was replaced (Table 2, entries 10 and 11). Aggarwal[65] reported good results with neat DBU in neat conditions on the same substrates, benzaldehyde and methyl acrylate, and obtained a yield of 89% after 6 hours. However, when this reaction was repeated, yields were much lower than those reported. This reaction was done twice, once in open air and once under argon, but there was no significant difference in yield. It was surprising to see such high reactivity of DBU compared to DABCO.

Rafel *et al.*[26] had reported that lowering the temperature to 0 °C also increased the reaction efficiency. This was very strange because normally you would expect the reverse. The reason for this increase is not known yet. The same experiment was repeated (Table 2, entries 12 and 13) but only starting material was obtained. Also different solvents were tried, but again, no change was noticed. The same results were reported by Leadbeater *et al.*,[66] i.e. that they obtained no reaction. This was also the only article which reported the lowering of temperature for the MBH reaction. No other articles referred to this behaviour.

Another way to accelerate the reaction was to use more reactive compounds (Table 2, entries 14 to 16). The most reactive compounds for the MBH reaction are thought to be 4-nitrobenzaldehyde and methyl vinyl ketone (MVK). However, our attempt (entry 14) gave poor yields. This was due to the high reactivity of MVK, leading to several side products. This was verified by TLC and the ^{1}H NMR spectrum. Only after several columns it was possible to isolate the product **157**.[58] The same result was also reported by Aggarwal *et al.*[30] and Shi *et al.*[10] The reaction was repeated (entry 15) with the more stable methyl acrylate. Also the solvent was changed from sulfolane to a more general solvent as DCM. Although the reaction was slower (47% yield of **158**[35] after 3 days), it appeared to be cleaner since no side products were formed.

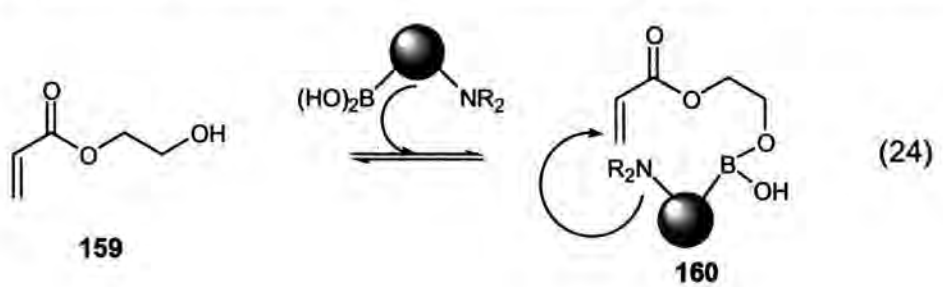

159 **160** (24)

Besides the reactive MVK, another acrylate which has a hydroxyl group on the end of the aliphatic chain, i.e. 2-hydroxyethyl acrylate **159** (2-HEA), was used for a test reaction (entry 16). Basavaiah *et al.*[21] had already reported that there was an increase in product formation with DABCO when 2-HEA was used. The explanation for this increase, as mentioned earlier, was due to the possibility of an intramolecular hydrogen bond between the hydroxyl group and the formed enolate-ion, when the DABCO attacked (see **15** and **16**). Not only was this increase of reaction speed promising, but also the fact that the boron of our bifunctional catalyst could complex with the free hydroxyl group (see **160**) seemed very interesting (Equation 24). In this way, an entropic advantage could be obtained because our bifunctional catalyst could be brought to the active place and react faster. Unfortunately, beside the MBH product **161**, a lot of side products were obtained due to esterification. The product and these side products could be analysed after isolation.

When summarising all our attempts to increase the rate of the MBH reaction, together with an increase in yield, it can only be concluded that the use of 4-nitrobenzaldehyde and methyl acrylate gave the best results because these substrates are the most reactive and almost no side products were formed. As catalyst, DBU was ideal, since it was stable and soluble in almost all solvents and it gave an even higher reactivity than DABCO. Therefore, in the future, the reaction with 4-nitrobenzaldehyde and methyl acrylate in neat at room temperature with DBU as catalyst could be considered as standard reaction.

3.2.2.Screening of amino-boronate catalysts for MBH reaction

The potential of the bifunctional catalysts to promote the MBH reaction was investigated by screening them over a series of reactions. These reactions were run at the same time as with the corresponding DABCO reactions and under the same conditions. Since catalyst **126**, **127** and **136** were fully characterised and isolated in a pure form, it was possible to use these catalysts for the screening reactions. Catalyst **129** was not used since the presence of the hydroxy anion could cause side reactions with the methyl acrylate. The reactions were followed in a similar way as the corresponding DABCO reactions. The general equation is identical to Equation 23. All the test reactions are represented in following Table 3.

Table 3: Screening of **126**, **127** and **136** for MBH.

Entry	Aldehyde (R_1)	Alkene (R_2)	Solvent	Catalyst	Mol% Cat.	Time	Temp (°C)	Yield[a]
1	C_6H_5	OCH_3	H_2O/Diox	**126**	10%	4d	25	S.M.
2	C_6H_5	OCH_3	H_2O/Diox	**126**	100%	2d	25	S.M.
3	C_6H_5	OCH_3	H_2O/Diox	**126**	300%	2d	25	S.M.
4	C_6H_5	OCH_3	neat	**126**	100%	6h	25	S.M.
5	*p*-$NO_2C_6H_5$	OCH_3	sulfolane	**126**	50%	30d	25	S.M.
6	*p*-$NO_2C_6H_5$	OCH_3	DCM	**126**	50%	4d	25	S.M.
7	*p*-$NO_2C_6H_5$	OCH_3	DCM	**127**	50%	5d	25	S.M
8	*p*-$NO_2C_6H_5$	OCH_3	DCM	**136**	50%	7d	25	S.M.
9	*p*-$NO_2C_6H_5$	OCH_2CH_2OH	DCM	**126**	50%	5d	25	S.M.
10	*p*-$NO_2C_6H_5$	OCH_2CH_2OH	DCM	**127**	50%	6d	25	S.M.
11	*p*-$NO_2C_6H_5$	OCH_2CH_2OH	DCM	**136**	50%	7d	25	S.M.

[a] Based on isolated yield.

As the corresponding DABCO reactions, the bifunctional catalyst **126** was screened in the polar mono-phasic solvent of water and dioxane using benzaldehyde and methyl acrylate (Table 3, entries 1 to 3). Unfortunately, no product was detected by TLC or ^{1}H NMR spectroscopy, even when 300% catalyst **126** was used. The explanation for this result is probably insolubility since the white powder of the catalyst **126** was observed at the bottom of the flask. Therefore, the reaction was repeated without any solvent (Table 3, entry 4), hoping that the catalyst **126** would dissolve in the liquid of methyl acrylate as indeed, did DABCO. Again, the solid powdery catalyst **126** was lying on the bottom of the flask, and no product was formed.

In the following reaction (Table 3, entry 5), the benzaldehyde was changed to the more reactive *p*-nitrobenzaldehyde. Also, a solvent was used again, namely sulfolane, as mentioned before, which was considered to be the best general solvent for MBH reaction.[31] The reaction was kept on for almost one month just to see if still any product could be arise. But again, no product was detected. Also in this case, the catalyst **126** did not dissolve very well. Therefore, it was chosen to do the further reactions in DCM since it was known our catalysts dissolve very well in this solvent.

At that time catalysts **127** and **136** were prepared and fully characterised, so it was now possible to use the three catalysts for screening. In entries 6, 7 and 8 the general procedure was followed with *p*-nitrobenzaldehyde and methyl acrylate as substrates in DCM to dissolve the bifunctional catalysts. The reactions ran for several days but only starting material was observed in the ^{1}H NMR spectrum.

In the last test reactions (Table 3, entries 9, 10 and 11), the methyl acrylate was replaced by 2-hydroxyethyl acrylate **159**. In this way, it was hoped, as mentioned before, that the boron of our bifunctional catalyst **126**, **127** and **136** would complex with the free hydroxyl group (see **160**) and so induce some speed. Unfortunately, no product was formed in these reactions, also no side products were detected.

It is clear none of the bifunctional catalysts **126**, **127** and **136** are suitable for the MBH reaction. This inactivity is partly due to insolubility of the bifunctional catalysts in most appropriate solvents for MBH. This result was not too unexpected since catalysts **126** and **127** were the first catalysts which were tested. Moreover, catalyst **126** was not really developed for the MBH reaction; it was created for the amide condensation of carbon acids by Giles.[143] Although Cheng *et al.*[37] reported successfully the use of 2-phenylimidazole as a catalyst for this reaction, **136** failed to give any product at all. This could probably be explained by the presence of the *n*-butyl tail on the basic nitrogen, making it more bulky and less nucleophilic.

3.2.3.The aza-Morita-Baylis-Hillman reaction

Besides the normal MBH reaction, it was also interesting to investigate if the bifunctional catalysts were useful for the more reactive aza-Morita-Baylis-Hillman reaction. Therefore, some *N*-tosylimines were synthesised to use in the test reactions. To get the best results, it was necessary to make the most reactive example, i.e. based on 4-nitrobenzaldehyde **162** reacted with *p*-toluenesulfonamide **163** (Equation 25).

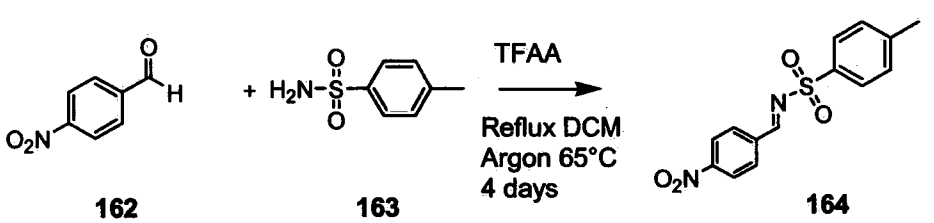

162 **163** **164** (25)

The normal way to make these tosylimines is by Dean Stark methods,[162] where water is removed by azeotropic removal such as in toluene. This manner was tried, however, only traces of product

were detected by ^{1}H NMR spectroscopy. Hence, a new approach[163] was followed using TFAA which acts as a dehydrating agent and becomes hydrolysed to TFA by the water which is formed (Scheme 21).

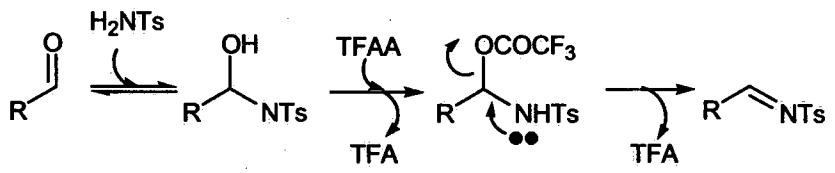

Scheme 21. Mechanism to form imines with TFAA.

After 12 hours a large amount of product **164** was formed,[164] as indicated by ^{1}H NMR spectroscopy where the aldehyde proton shifted from 10.08 ppm to 9.06 ppm, corresponding to the imine. Because the product was so reactive, it was not possible to isolate it by chromatography on silica gel or alumina due to degradation. The only way to isolate the product was to let the reaction go to completion after several days and then to crystallise the product **164** with ethyl acetate. Interestingly, the experiment showed that increasing the temperature slowed down the reaction rather than accelerating it. This could be explained by the fact that the boiling point of TFA and TFAA respectively is 70 and 39 °C, so over 70 °C all the TFAA evaporates without catalysing the reaction.

After the synthesis and isolation of imine **164**, it was used to test our catalysts for the aza-Morita-Baylis-Hillman reaction. Again, methyl acrylate **165** was used as the unsaturated carbonyl compound together with **164** (4-NBTs) in DCM (Equation 26, Table 4).

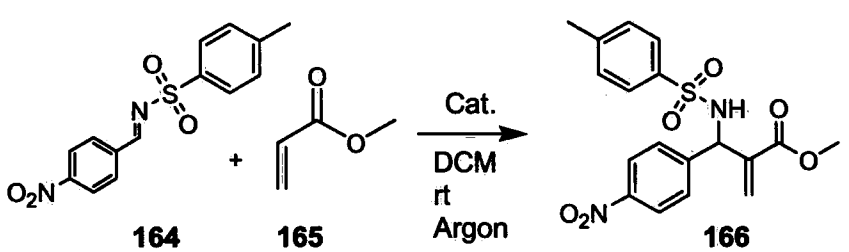

(26)

Table 4: Screening for the aza-MBH reaction.

Entry	Imine	Ketone	Catalyst (50 mol %)	Time	Yield[a]
1	4-NBTs	methyl acrylate.	DABCO	3 days	57%*
2	4-NBTs	methyl acrylate.	**126**	3 days	S.M.
3	4-NBTs	methyl acrylate	**127**	3 days	S.M.
4	4-NBTs	methyl acrylate	**136**	3 days	S.M.

*Isolated yield + traces of MBH product.
[a] Based on isolated yield.

The first reaction (Table 4, entry 1) was considered to be the standard reaction with DABCO as catalyst in DCM. By examination of the alkenic and benzylic protons in the crude ^{1}H NMR spectrum, it was obvious that the aza-MBH product **166** was formed.[12] Since imine **164** is highly reactive, it was easily hydrolysed to nitro-benzaldehyde, which can then form the normal MBH product **154** which was also clear from the crude ^{1}H NMR spectrum. Because both products **166** and **154** had the same Rf value as also reported[12], these products were isolated in the same fraction. Separation of both products on different chromatographic columns with silica gel and alumina was tried, but total separation was not achieved. Also, several attempts to crystallise the aza-MBH product **166** using different solvents were made, but no significant results were obtained.

The screening of our catalysts (Table 4, entries 2-4) was carried out in sufficient DCM to be sure the bifunctional catalysts would dissolve. The reactions were run at the same time as the DABCO catalysed reaction. Unfortunately, in all cases, no aza-MBH product was observed, only some aldehyde due to hydrolysis of the imine was obtained.

3.2.4.ReactIR studies

In our research for the Morita-Baylis-Hillman reaction, ReactIR was also employed. This could be very useful to see if a certain catalyst is reactive or not by watching specific peaks appearing/disappearing. Firstly, some test reactions had to be run using standard substrates benzaldehyde **167** and methyl acrylate **165** (Equation 27).

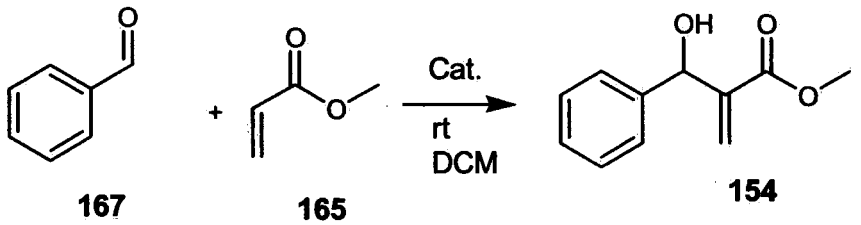

167 165 154 (27)

As catalyst, DABCO was examined intially. Unfortunately, this reaction was too slow and only after several days were any very minor peak changes noticed. An additional problem was polymerisation occurred after several days. This was observed due to the white solid which precipitated from the reaction mixture. Hence, a more reactive catalyst had to be used, namely DBU and in this case it was clear which peaks emerged and which disappeared. Firstly, the methyl acrylate was added to the DBU to see if any intermediate **8** could be detected. This was not possible, probably because the exchange reaction was too fast. Only when benzaldehyde was added, did the reaction proceed. This was demonstrated by the decrease of the carbonyl absorption of benzaldehyde (1724 cm^{-1}) and of methyl acrylate (1693 cm^{-1}) and there was an increase in the broad absorption between 3000-3150 cm^{-1} which correspond to the formation of the hydroxyl group. Because none of our bifunctional catalysts were reactive in the MBH reaction, this method was not used further.

3.2.5.Conclusion

It is clear that there is still a long way to go to achieve the objective of making suitable bifunctional catalysts for the MBH reaction. It was disappointing that none of our catalysts showed any reactivity towards the MBH reaction or aza-MBH reaction, even with the most reactive substrates. On the other hand, some of the catalysts tested were not specifically prepared for this reaction, so their inactivity is perhaps not a surprise. The next step was to investigate if our catalysts were suitable for new reactions, such as the aldol reaction.

3.3.The aldol reaction

Since it became clear our catalysts were ineffective for the MBH reaction, it was decided to turn to other possible reactions such as the aldol reaction. Previous researchers in the Whiting group, i.e. Blatch and Patrick, also worked on this topic of bifunctional catalysis and noticed some reactivity of our catalysts towards this reaction. Unfortunately, it was not possible to provide any conclusive evidence about how and which catalyst structure was actually responsible for an observed reaction and many further questions needed to be answered. Therefore, it was considered useful to repeat some of the original results, determine what the exact catalytic system was and to expand the applications and determine the mechanism of the reaction.

3.3.1.Introduction

The aldol reaction is one of the most applied reactions in organic chemistry, especially on an industrial level. The reaction was discovered independently by Wurtz[165] and Borodin in 1872. It normally involves the nucleophilic addition of a ketone enolate **168** to an aldehyde to form a β-hydroxy ketone **171**, or "**aldol**" (**ald**ehyde + alco**hol**). The reason why this reaction is so interesting is not only because of the C-C bond formation and the highly functionalised centre (a carbonyl group and alcohol), but rather for the formation of two chiral centres (on the α- and the β-carbon). It is known the reaction can proceed both under basic and acid conditions. Under basic conditions an enolate ion **169** is formed by deprotonation, under acid conditions tautomerization leads to an enol intermediate **170**. A common side product in the aldol reaction is the condensation product where water is eliminated from the aldol product to form product **172** (Scheme 22).

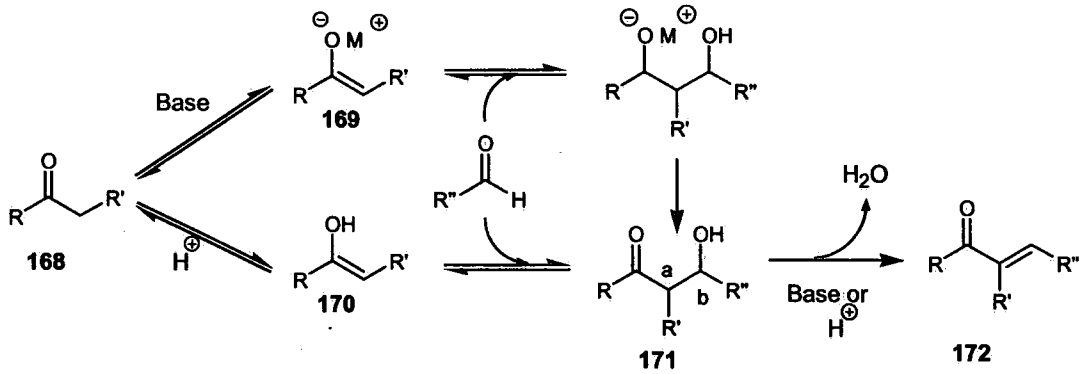

Scheme 22. Standard aldol mechanism.

Although the aldol reaction is useful, it is considered one of the hardest reactions to control due to its versatility. The first major problem is to define the nucleophile and the electrophile, i.e. if acetophenone and propiophenone are mixed together with a base, then potentially four products can be formed (the two products by self reaction and two products by cross reaction). The reason for the different products is because both reagents can react as nucleophile and electrophile. Even in the worst case, there will be overreaction where the aldol product will react with another electrophile, or formation of condensation product occurs. A possible way to tackle this problem is to use only combinations of ketones and aldehydes in a correct order of addition. The ketone is first added to the base to form the enolate and afterwards the aldehyde is included. Because aldehydes are much more electrophilic than ketones, the ketone will selectively attack the aldehyde and there will be no self-reaction. A second problem is the selectivity for deprotonation of the nucleophile. In the case of acetophenone, there is only one site which can be deprotonated. However, if an asymmetric ketone is used, such as 2-butanone, there are two possible positions for deprotonation; a kinetic and thermodynamic position. Under kinetic conditions (using low temperatures, an equivalent of a strong hindered base such as LDA and non-protic solvents) fast deprotonation will occur and 2-butanone will form enolate **173** which will then react with the aldehyde. On the other hand, under thermodynamic conditions (room temperature, slight sub-stoichiometric amount of small, weak base and protic solvents) the deprotonation occurs at the ethyl side (sterically most hindered side) giving **175** (Scheme 23).

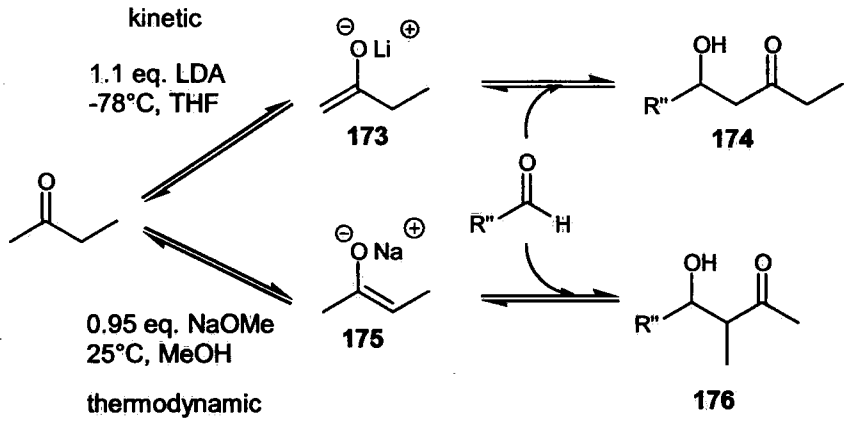

Scheme 23. Regioselectivity in aldol reaction.

The third problem is the control of the two new stereogenic centres. Due to those two new centres, there are four different isomers possible. For organic chemists, it is important to create only one of those four isomers. An extra difficulty is the reversibility of the aldol reaction which implies that the selectivity must happen in an irreversible way so no racemisation can occur. To induce and control these centres a certain transition state model must be applied. The most encountered transition state model for the aldol reaction is the 'Zimmerman-Traxler' transition state model[166] from 1957 which counts for lithium, boron, magnesium, etc. metal enolates. In this model, the aldehyde complexes to the metal enolate through a chair conformation. This model also explains why *E*-enolates give the *anti*-aldol product and *Z*-enolates the *syn*-aldol product. In this model, the chiral auxiliary, normally attached to the enolate plays an important role. Not only does it control the *E/Z*-conformation, but it also defines which side the aldehyde can approach. The first step in this model is the *E/Z*-enolate formation which is almost solely dependent upon steric hindrance. When the steric repulsion between R and the auxiliary is greater than the repulsion between R and the metal-oxygen (OM), the *Z*-conformation is adopted (see **178** and **179**). This plays a key role in defining the *syn*- and *anti*-aldol control. The next step is the addition of the aldehyde through a chair conformation. In this conformation, the aldehyde can approach from above or below the enolate depending on the chirality of the auxiliary, but the R'' of the aldehyde will always be equatorial in the chair because of higher stability in that orientation. The position of the R group is dependent on the *Z/E*-conformation; in the *Z*-conformation the R group will have the same direction as the OM and will be axial and in the *E*-

conformation it has the same orientation as the auxiliary and is equatorial. These different conformations (Scheme 24) will eventually result in the four different isomers possible.

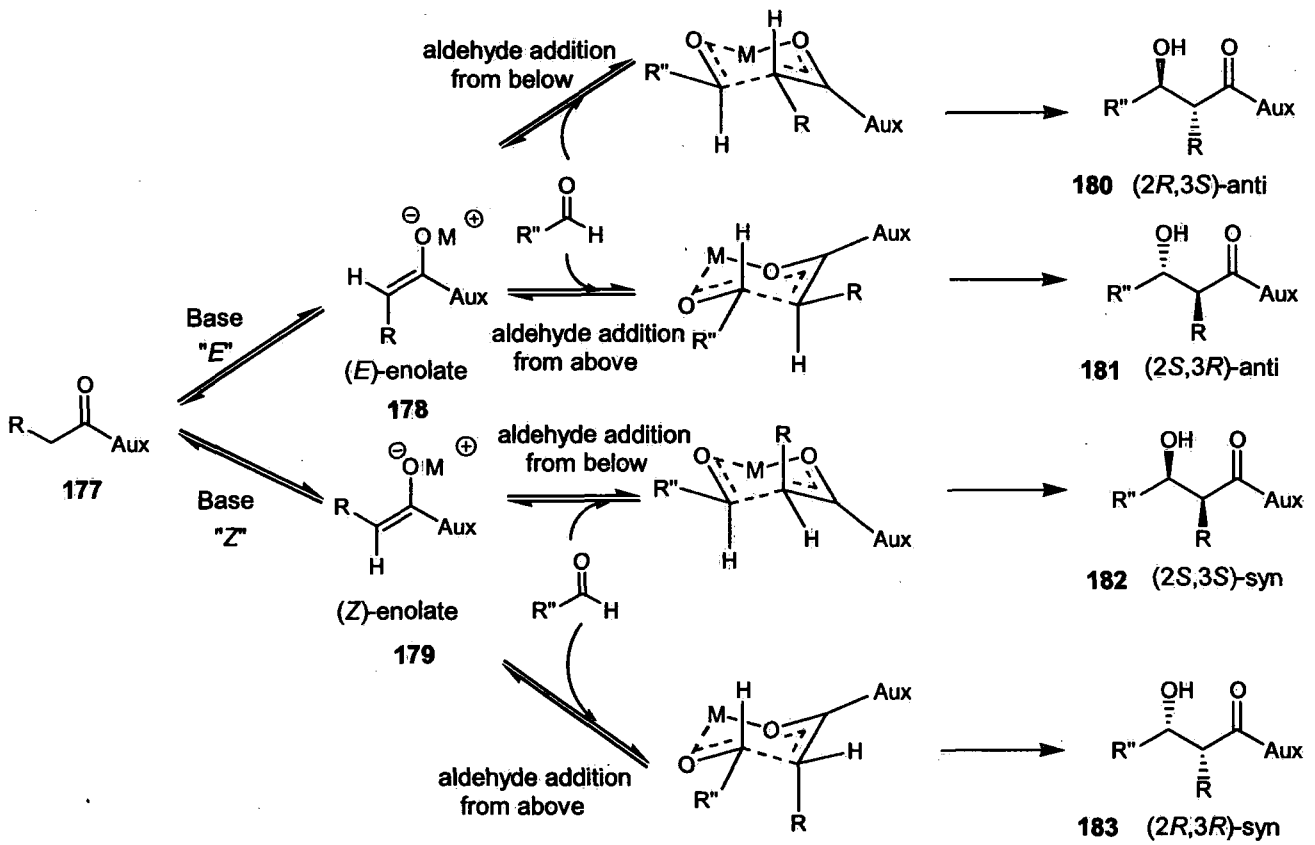

Scheme 24. Zimmerman-Traxler transition states on aldol reaction.

This theoretical model can be applied to some more practical examples.

The first example uses a mandelic acid derivative as chiral auxiliary and Hünig's base.[167] Also dialkyl boron triflate is added to form the corresponding boron enolate. This Lewis acid plays an important role because it will easily complex with the aldehyde and form the corresponding chair. In the first step boron enolate **185** is produced in the *Z*-conformation. Then, the aldehyde reacts, giving chair conformation **186**. Due to dipole-dipole repulsion between the two oxygens, an antiperiplanar conformation is adopted. In this conformation, the cyclohexyl group blocks the

'upper' face forcing the aldehyde to approach from below (see **186**). This results in aldol product **187** with both groups *syn* and *R,S* stereo-centres.

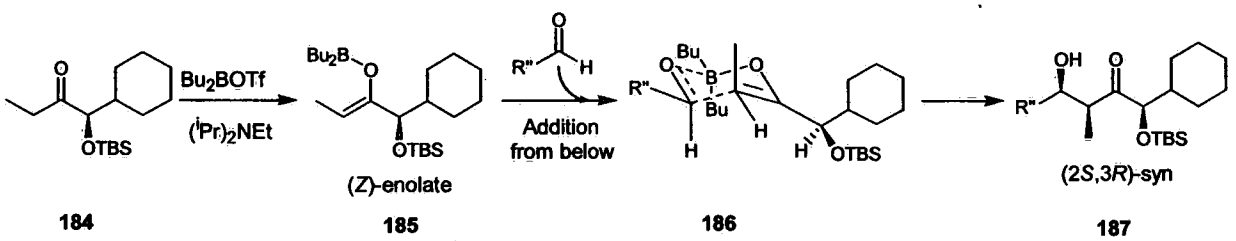

184 **185** **186** **187**

Scheme 25. Zimmerman-Traxler model controlled by mandelic acid.

In the next example oxazolidinones **188** and **189** are used as chiral auxiliaries, and are known as the Evans' oxazolidinones because Evans introduced them for the first time in the late seventies.[168] Not only are they cheap and easy to recover, but they also show high levels of stereochemical control, even at relatively long distance. These auxiliaries were first used to control enolate alkylation but later their application was further extended to the aldol reaction. Looking at the reaction in Scheme 26, the same step is followed as in the previous example with the same reagents. Although this time, the boron complexes both with the enolate and the oxygen of the auxiliary. When the aldehyde reacts an interesting change happens; because the boron only can bear maximum four bonds, the B-O bond with the auxiliary becomes broken and a new chelation takes place between the aldehyde and the boron. This leads to a 180° rotation of the auxiliary because of lower dipole-dipole repulsion and results in a conformation where the benzyloxy group covers the 'upper' face. Therefore, it is clear in the six-membered ring **194** that the aldehyde again approaches from below resulting in aldol product **195**. This example shows that the boron not only is responsible for the chair conformation but also defines which enantiomer is formed by chelation.

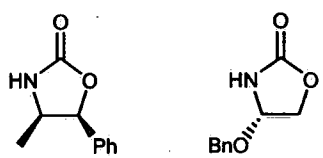

188 **189**

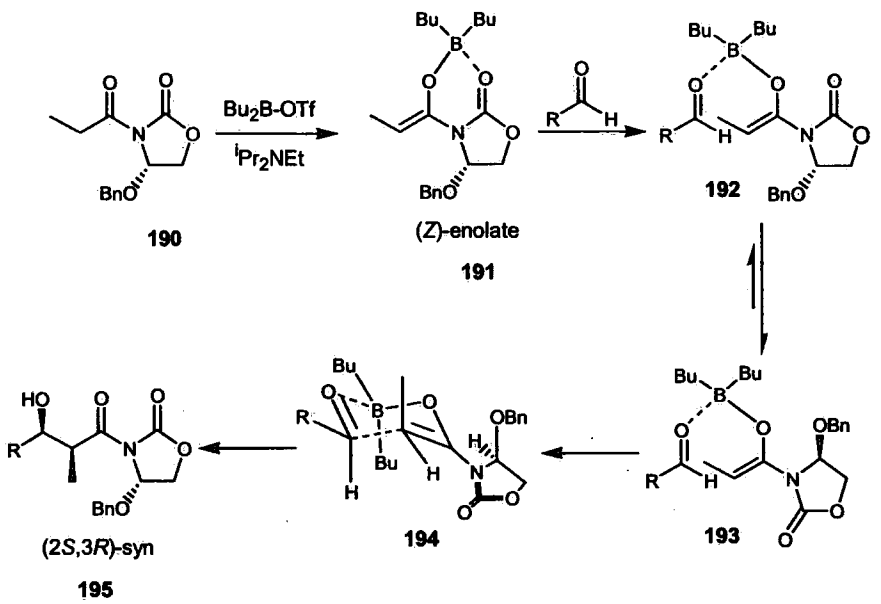

Scheme 26. Zimmerman-Traxler model controlled by Evans' oxazolidines.

Not all the aldol reactions follow the "Z-T" transition state, and a third example is included which goes through an open transition state. In this case, the chiral auxiliary is also an Evans' oxazolidinone and the same procedure is followed as in previous examples. The difference this time is the addition of an aldehyde which is already forming a complex with aluminium. Due to this complexation, the aldehyde is not free anymore to chelate with the boron. This results in an open transition state **198** which does not go through a chair conformation. In the open transition state **198** the boron will keep on chelating with the auxiliary which covers with its isopropyl group the back face.[169] This forces the aldehyde to come on the top face. Through the Newman projection it is also clear that the R group of the aldehyde will avoid steric hindrance with the bulky auxiliary by positioning itself between the smaller methyl group and the oxygen. This transition state **198** delivers the *anti*-aldol product **199** with *R,R* stereo-centres (Scheme 27).

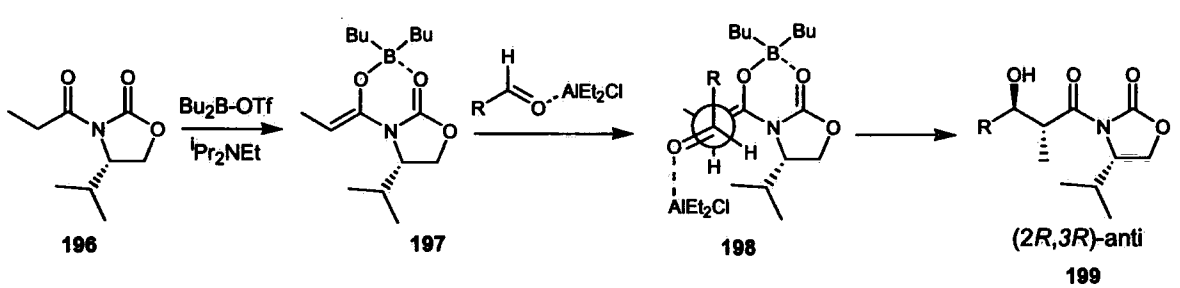

Scheme 27. Open transition state model.

It is clear that this methodology, by using a chiral auxiliary and the Lewis acid, is very successful for the aldol reaction. It is possible to have full control of the *syn/anti* ratio and to produce selectively one specific enantiomer just by choosing the right conditions. Although all this effort has resulted in good results, there are still some drawbacks. A small drawback is the use of these chiral auxiliaries. Because these auxiliaries have to be attached to the molecule, an extra step is needed in the synthesis to remove them. A more important drawback is the limitation of this approach. Through experiment, it has been shown that ketones which do not carry an α–substituent do not follow this Z-T transition state, and therefore, give a mixture of aldol products (Scheme 28).[170]

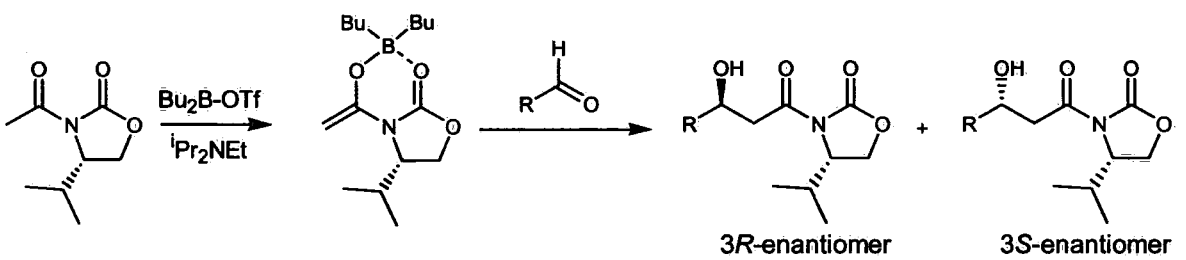

Scheme 28. Exception on Zimmerman-Traxler model.

In order to deal with these types of problems, modern solutions may be the creation of chiral catalysts which can be used for any reagent and only have to be added in catalytic amounts. In this short review there is a focus on the use of bifunctional catalysts, since this is also our major interest.

3.3.2.Bifunctional catalysts for the aldol reaction

As mentioned before, this short review only handles the use of chiral bifunctional catalysts, which in turn can be divided into two major groups: the bifunctional organocatalysts (which is dominated by proline and its derivatives); and the bifunctional transition metal catalysts (which are mainly BINOL-scaffold based metal catalysts). Other techniques such as the use of optimized chiral auxiliaries (like Crimmins' thiazolidinethione) or the use of silyl enol ethers (like the Mukaiyama aldol reaction) which are commonly used to obtain pure enantiomer aldol products will be neglected.

3.3.2.1.Bifunctional organocatalysts for the aldol reaction

In the late nineties, a research group at the Scripps Research Institute in La Jolla, California was working on class I aldolase mimics. Their objective was to find the active centre of this enzyme with the purpose to reproduce its activity only by applying a small molecule which mimicked this centre. To their surprise, it was noticed that the activity of this class I aldolase could be reproduced by only one single amino acid, namely proline. This discovery was a milestone in organocatalysis because it was shown that simple amino acids could catalyse reactions with high yield and e.e. This research group consisted of Barbas, List and others. Another important player in this field was MacMillan, who actually introduced this term 'organocatalysis'.

One of the first publications which introduced this new concept was published by B. List, R.A. Lerner and C.F. Barbas 3rd in 2000.[171] It reported the aldol reaction with acetone and different aldehydes in DMSO under catalytic amount of proline (Equation 28). It was possible to obtain yields between 54-97% with good e.e.s (60-96%). In attempts to improve both the yield and e.e., also several proline derivatives were screened but proline still gave the best result.

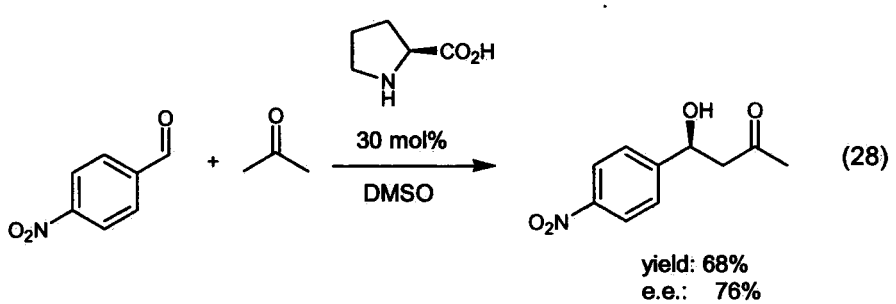

(28)

yield: 68%
e.e.: 76%

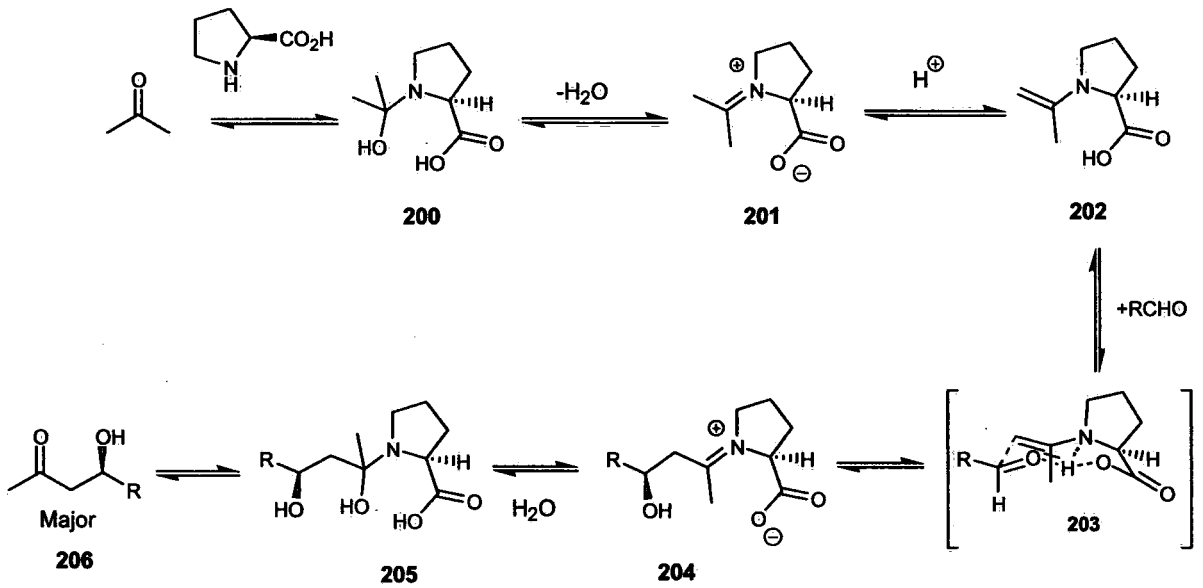

Scheme 29. Proposed aldol mechanism with proline.

The mechanism shown in Scheme 29, shows an enamine type of reaction postulated where the nitrogen acts as a nucleophile to form enamine **202**. The aldehyde then approaches the enamine from the front directed by the hydrogen bonding of the carboxylic acid creating a kind of metal-free Zimmerman-Traxler type transition state **203** with the R group of the aldehyde equatorial. This gives eventually the corresponding imine **204** which through hydrolysis results in the aldol product **206** and releases the proline. This mechanism shows clearly the bifunctional aspect of proline where the nitrogen acts as a Lewis base and the carboxylic acid as a Brønsted acid. It is this symbiosis which makes proline such a highly active and precise catalyst.

List *et al.* published a follow up paper[172] where again proline was the catalyst for the aldol reaction, but this time with hydroxyacetone as ketone. The use of hydroxyacetone for the aldol reaction is much more challenging because not only is there the possibility of two new chiral centres but there is also a regiocontrol difference (thermodynamic *vs.* kinetic). During their screenings it was clear that the deprotonation occurred almost selectively next to the hydroxyl site (regioselectivity >20:1) giving the *anti*-diol **207** as the major product (Equation 29). Depending on the different aldehydes used, good yields (38-95%) and diastereoselectivity (*anti:syn*, >20:1 to 1.5:1) were gained with some excellent e.e.s (97-99%). The same mechanism as previously proposed (Scheme 29) was applied to explain the outcome, but this time the

hydroxyl group of the ketone had to be included. The hydroxyl group was placed equatorial in the transition state **208** to induce the highest stability which resulted in the (2*S*,3*S*)-*anti*-product. The use of hydroxyacetone is of interest for our research because under similar conditions, our best results were obtained (see below).

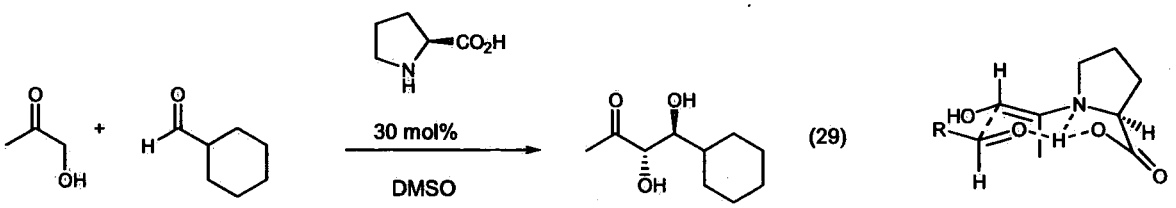

regioselectivity: >20:1
diastereoselectivity: >20:1
enantioselectivity: >100:1

As mentioned before, MacMillan *et al.* were also working on this topic. Their research showed that enantioselective aldol cross coupling of nonequivalent aldehydes was possible with 10 mol% proline.[173] The problem with this reaction was not only the possible polymerisation but also the control of the nucleophile to avoid self-reaction. By using a syringe pump addition, it was possible to obtain solely cross-aldol products with very good yields (75-88%) and excellent e.e.s (91-99%). Again, the *anti*-aldol product was the major compound, as explained by the same mechanism as before.

3.3.2.2.Bifunctional metal catalysts for the aldol reaction

The reason why enzymes and other bioorganic catalysts (such as proline) are so efficient is due to the synergistic cooperation of the active centres. Besides these bioorganic catalysts, there are also some artificial made catalysts that use the same concept of functional groups on an asymmetric scaffold. The advantage of these artificial catalysts is the possibility to modify them and to make them efficient for a broad spectrum of reagents (in contrast with enzymes which are normally efficient for a small group of reagents and so are very reagent selective). Also, these new artificial catalysts can be specially created for reactions which are not very common in Nature and so for which there is not any bioorganic catalyst available. In our research, the focus will be on the artificial catalysts which catalyse the aldol reaction. A good aldol catalyst is a

catalyst which promotes a *direct* asymmetric aldol reaction. This means that when the catalyst is added to the reagents the chiral aldol product is gained immediately, so there is no need to create latent enolates prior to the reaction (like Mukaiyama aldol reaction where enol silyl ethers or methyl ethers are formed beforehand). Another advantage of using *direct* aldol catalysts is the lack of a stoichiometric amount of base which is normally needed to form the corresponding enol. These conditions show that these catalysts must be multifunctional, i.e. not only must they activate the aldehyde in order to get a high e.e., but they also have to abstract an α-hydrogen of the ketone to generate an enolate. This explains why this type of aldol catalysts normally consists of a Lewis acid and a Brønsted base. The Lewis acid is normally a transition metal which will complex with the aldehyde and the Brønsted base is needed for the proton abstraction of the ketone. Both groups will be placed on a chiral scaffold to induce any e.e. In this short review the most significant breakthrough results will be discussed.

One of the first bifunctional metal based aldol catalysts was published in 1986 by Hayashi *et al.*[174] by creating the chiral ferrocenylphosphine molecule **209** which formed an active gold(I) complex. This complex was able to catalyse the asymmetric aldol reaction of isocyanoacetate **210** with different aldehydes giving the corresponding *anti*-aldol product **211** in good yield (83-99%) and e.e. (72-97%) (Equation 30). The presence of the α-cyano group in the ketone was crucial; not only did it enhance the deprotonation to the enol, but more importantly, it complexed with the gold(I) to form a rigid structure leading to the chiral aldol product **211**.

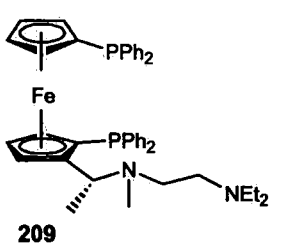

209

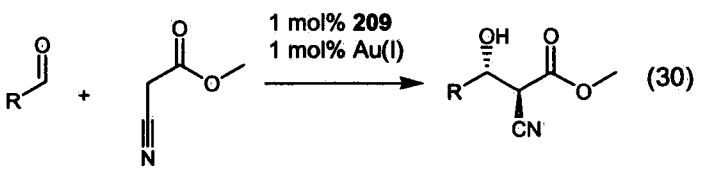

210 (4*S*,5*R*)-aldol **211**

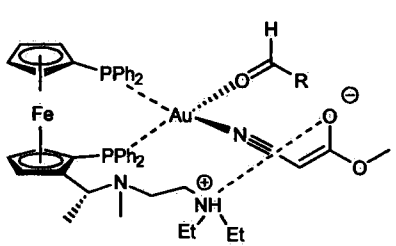

212

According to these findings, transition state **212** was given as possible explanation. From this transition state **212** it is clear that the phosphorous atoms complex with the gold(I) and that the amino side chain is responsible for the chirality and the deprotonation. The formed enol will be stabilised by a

hydrogen and the cyano-gold(I) bond. In the next step, the aldehyde enters the least hindered side and also complexes with the gold(I). Due to steric hindrance, the bulky R-group of the aldehyde will be at the same position as the hydrogen of the enol. All this will finally result in the *anti*-aldol product. This catalytic complex can be considered as one of the first artificial bifuntional catalysts for the aldol reaction with gold(I) as Lewis acid and the nitrogen group in this case as Brønsted base.

A well known name in the research of multifunctional asymmetric catalysis is also Shibasaki, especially for the synthesis of BINOL-based catalysts which are connected by different transition metals to one identity. These complexes are then being screened for different chiral reactions such as the Michael addition, epoxidation, Mannich reaction, etc. Along this line, these catalysts were also screened for the *direct* aldol reaction for which some showed good reactivity. The first published heteropolymetalic catalyst which showed reactivity for the aldol reaction was complex **214**.[175] This catalyst was synthesised by creating first the $LaLi_3$tris(binaphthoxide) complex **213** to which KOH and water was added (Equation 31). The best results were obtained when 2-hydroxyacetophenone **215** was used with primary aldehydes. In that case, the *anti*-product **216** was isolated as major compound in a moderate 3:1 diastereomeric ratio, but in good yield (78-92%) and excellent e.e.s (90-95%) (Equation 32). Although the exact mechanism is still unclear, it is widely accepted that the lanthanide complexes with the oxygens of the different reagents and that the KOH is responsible for the enolate formation. This could also explain why the use of 2-hydroxyacetophenone is so efficient since there is an extra oxygen present for chelation.

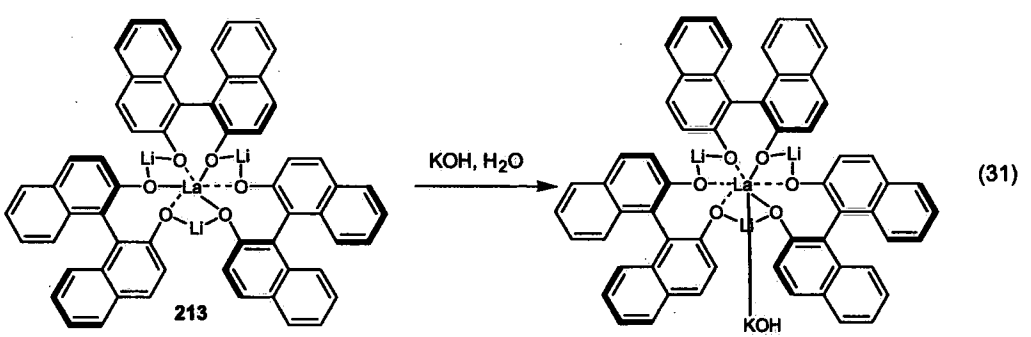

(31)

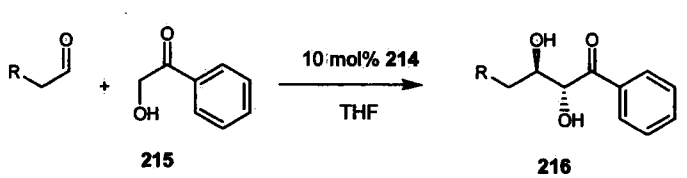

215 216

(32)

Because complex **214** was very substrate limited, and to avoid the extra addition of KOH, a new catalyst was created on the same principle. This time the skeleton **217** existed out of two BINOL scaffolds, which were connected by an oxygen linker, and two additional hydroxyl groups to simulate the KOH. The actual catalyst **218** was formed by adding the lanthanide as Lewis acid and exactly 3 equiv. of *n*BuLi (Equation 33).[176] In that way, the hydroxyl groups were converted to anions which made them more nucleophilic. In the first screenings, the bulky aldehyde **219** was used to obtain the best e.e. with different ketones (Equation 34). Both aromatic and aliphatic ketones gave moderate results (yield: 62-70% and e.e.s of 40-67%) but in all cases the kinetic aldol product **220** was formed. No reactions with other aldehydes were mentioned.

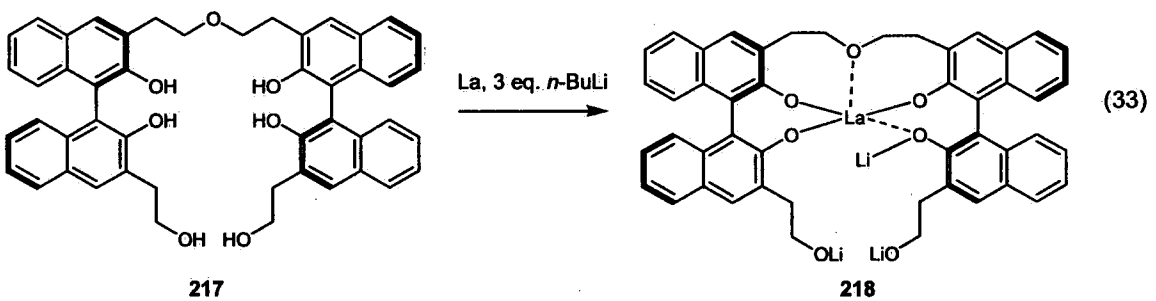

217 **218**

(33)

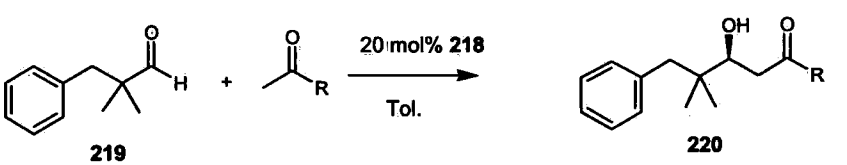

219 **220**

(34)

To extend this work, Shibasaki *et al.* used a similar scaffold **221**, but this time without the hydroxyl tails, but combined together with zinc.[177] Also, in this case, an active complex for the *direct* aldol reaction was created. Through ethane gas emission measurements and X-ray crystal structure analysis, the active catalyst was verified as compound **222**. An extra 0.5 equiv. of $ZnEt_2$ was present in the solution to accelerate the reaction (Equation 35). The best results were gained when hydroxyketone **223** was used with different aldehydes giving good yields (81-95%) and e.e.s (87-99%) (Equation 36). Surprisingly, the major diastereomer **224** was the *syn*-adduct (*syn*:*anti* ratio, 4:1) which was explained by the *Z*-configuration of the enol. An even more interesting observation was the lack of any base. This meant that the enol was rather formed by acid catalysis (probably by Brønsted or Lewis acid) than by Brønsted base. This double acid catalysis is rare in bifunctional catalysts, especially for the *direct* aldol reaction.

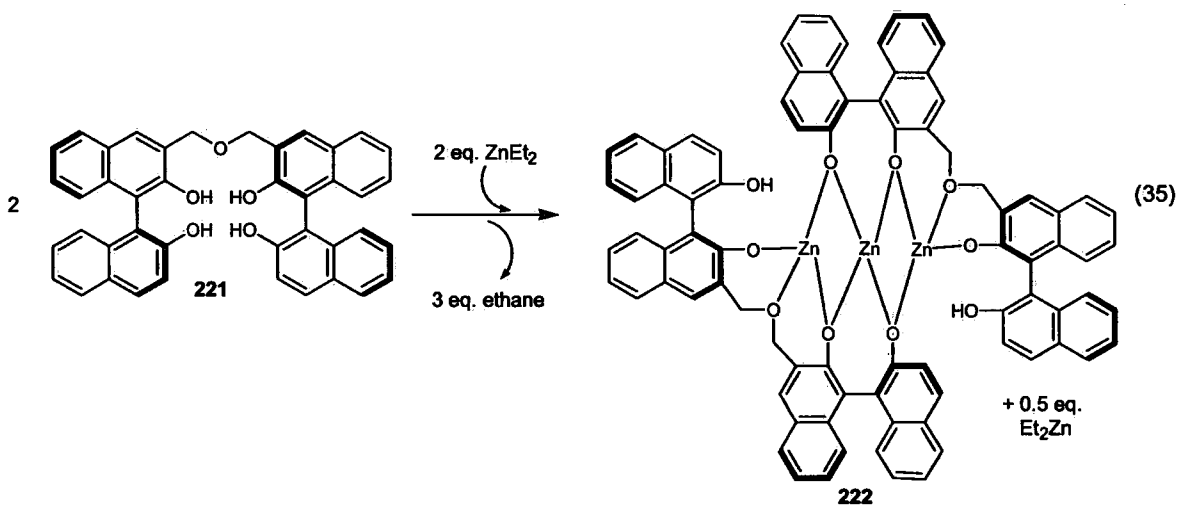

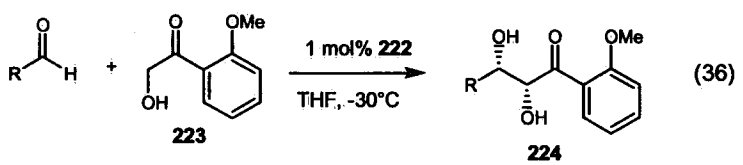

The use of zinc as Lewis acid for the *direct* aldol reaction was further explored by other researchers. The idea emerged to create this type of pocket where the zinc molecule could fit in. This crown compound could then be modified by adding an extra Brønsted base or by adding any chirality. One of the first attempts in this type of catalysis was reported by Calter *et al.*[178] who created this kind of triaza molecule **225** as pocket and added an amino tail as Brønsted base to form the enolate. Although the catalyst was non chiral, together with one equiv. of zinc, a yield of 66% of the aldol product was isolated from acetone and benzaldehyde.

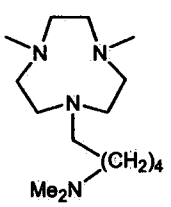

225

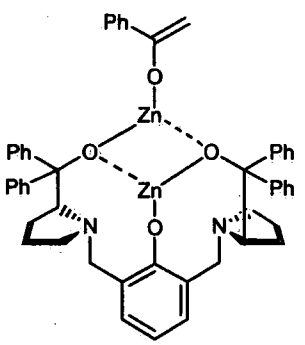

226

Trost *et al.* improved this method by synthesizing this new chiral crown compound **226**.[179] This time, the Brønsted base was already present in the form of a phenoxide which stabilized the zinc

molecules together with two other hydroxyl groups. The chirality was induced by two saturated pyrrole rings which were made bulkier by adding several phenyl groups. By examining the evolution of ethane gas, it was found that in reality not one, but two zinc molecules were complexing with the pocket molecule. The efficiency of this catalyst was investigated by screening acetophenone with different aliphatic aldehydes. Although the yields were rather moderate (33-79%), the e.e.s were impressive (93-99%). From a mechanistic point of view, it was thought that the phenoxide was too deep in the pocket to function as base for the enolate. So it was more likely it complexed with the zinc molecules which formed the enolate through Lewis acid catalysis.

3.3.2.3.In summary

It is clear that the aldol reaction is one of the most investigated reactions in the world. Nowadays it is almost possible to create any aldol product with any desired stereo-centres. Though the way to create this product will in some cases take several steps, therefore, there is still an opportunity to improve the reaction and develop new catalytic systems. For example, proline gives good yields and excellent e.e.s, but only *anti*-products are formed under relatively high catalyst loadings. Also, Shibasaki's metal catalysts show some drawbacks concerning high substrate selectivity, without even mentioning the environmental impact. These are the types of problems we wanted to address and solve in our research by using bifunctional catalysts based on nitrogen and boron.

3.3.3.The first screenings

The first screenings for the aldol reaction were all done on small scale and only a work up was used to purify the reaction mixture. In that way, it was possible to see easily which catalysts were active and what the outcome was. The different products were analysed by crude ^{1}H NMR spectroscopy; completion of the reaction could be determined by the disappearance of the benzylic proton peak of the aldehyde. For these reactions, only a small excess of acetone was used compared to benzaldehyde (Equation 37, Table 5).

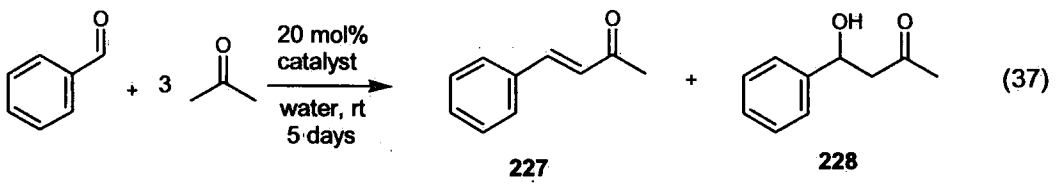

(37)

Table 5: Screening of catalysts **126, 127, 136** and **129** for aldol reaction.

Entry	Catalyst	Conversion[a]	Ratio 227:228[b]
1	**126**	< 5%	N.A.
2	**127**	< 5%	N.A.
3	**136**	< 5%	N.A.
4	**129**	> 99%	95:5

[a]Conversion based on disappearance of benzaldehyde in crude ^{1}H NMR spectrum.
[b]Based on crude ^{1}H NMR spectrum.

The screening of our bifunctional catalysts **126, 127, 136** and **129** revealed that only catalyst **129** (Table 5, entry 4) was active towards the aldol reaction, which was a starting point for our research founding this area. In the next screening reactions, only the active catalyst **129** was used under different circumstances and in that way, the best conditions could be applied on larger scale and with different substrates.

It was found that the active catalyst **129** could be generated in two different ways: as pure, dry compound; or *in situ*. When the synthesis pathway in Scheme 17 was followed, **129** precipitated out of DCM and could be isolated as a pure, dry solid. This could then be added to the different aldol reactions. An alternative way for the generation of catalyst **129** was *in situ*. In that case, the boroxine **136** was employed together with exactly three equivalents of aqueous NaOH. After 30 minutes, there was a clear difference in solubility and the mixture became more homogeneous which showed that catalyst **129** had been formed. Further evidence was given by ^{11}B NMR spectra which showed a shift of the boron peak from δ 18.0 ppm to lower δ 0.3 ppm, corresponding to a tetrahedral boron complex, i.e. the "ate"-complex **129**. The ketone and aldehyde could then be added to the reaction mixture to carry out the aldol reaction.

The following reactions were chosen to investigate the influence of the solvent upon the catalyst and the aldol reaction. Again, the reactions were carried out on a small scale and the same substrates and conditions were used as in Equation 37, apart from time and solvent (Table 6).

Table 6: Influence of solvent on aldol reaction with **129**.

Entry	Catalyst	Solvent (1:1:1 ratio)	Time (days)	Conversion[a]	Ratio 227:228[b]
1	**136**+3 eq.NaOH	H_2O	5	> 99%	95:5
2	**136**+3 eq.NaOH	THF+H_2O	5	> 99%	95:5
3	**136**+3 eq.NaOH	THF	9	> 97%	5:95
4	"dry" **129**	THF	10	> 99%	0:100
5	"dry" **129**	CH_3CN	9	> 95%	35:65
6	"dry" **129**	CH_3CN+THF	9	> 95%	25:75
7	"dry" **129**	CH_3CN+THF+H_2O	10	> 99%	25:75

[a]Conversion based on disappearance of benzaldehyde in crude ^{1}H NMR spectrum.
[b]Based on crude ^{1}H NMR spectrum.

It was immediately clear there was almost no difference in results between **129** which was formed *in situ* or when added as a pre-made solid complex. This can be observed by comparing Table 5, entry 4 with Table 6, entry 1 and Table 6, entries 3 and 4. Therefore, it was considered that in future for larger scale reactions it would be easier to generate **129** *in situ*, being practically simpler and less time consuming. A striking discovery was the difference in the results between the use of water and THF (Table 6, entries 1 and 3). When our catalyst was used in water (entry 1) only product **227**[180] was formed, but in THF (entry 3) it was the complete reverse and only the aldol product **228**[181] was obtained. Although the reaction in THF was much slower, it was interesting that the use of the same catalyst could produce selectively one product depending upon the solvent. Besides water and THF, MeCN was also introduced. It was clear that the presence of MeCN (Table 6, entries 5-7) gave a mixture of both aldol and condensation products. In entry 7, a mixture of the three solvents was applied since it was the only mixture wherein the "ate"-complex fully dissolved, and this resulted in a mixture of products, favouring the aldol product in a 3:1 ratio.

Because it was now possible to produce selectively the aldol product in THF, it was considered necessary to explore this reaction more deeply. The major drawback of this reaction was the long reaction time, so different modifications such as substrates and reaction temperature were made to improve the reaction rate. Again, the reactions were carried out on a small scale to investigate the outcome (Equation 38, Table 7).

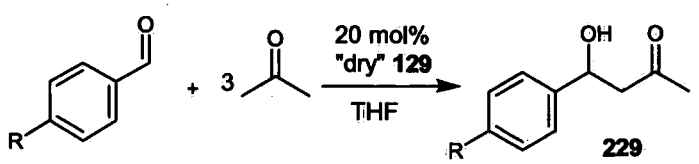

(38)

Table 7: Screening of **129** in THF.

Entry	R	Temp (°C)	Time (days)	Conversion[a]
1	NO_2	25	10	< 10%
2	MeO	25	13	< 3%
3	H	40	2	> 99%
4	NO_2	40	3	< 10%
5	NO_2	Reflux	3	< 10%

[a]Conversion based on disappearance of aldehyde in crude ^{1}H NMR spectrum.

It was surprising that with catalyst **129** and other substrates like *p*-anisaldehyde (Table 7, entry 1) and *p*-nitrobenzaldehyde (Table 7, entry 2) that there was almost no reaction. When the temperature was raised to 40 °C and to reflux, no significant improvement in conversion with *p*-nitrobenzaldehyde was observed (Table 7, entries 4 and 5). In contrast, an increase in temperature to 40 °C did accelerate the conversion of benzaldehyde from 10 to 2 days (Table 7, entry 3), but when this result was examined more closely, the crude ^{1}H NMR spectrum was seen to be messy and almost no aldol product was actually formed. Because of these disappointing results, it was better to keep with the old conditions using benzaldehyde at room temperature.

Some of these reactions were repeated on larger scale in order to obtain isolated yields for the different products (Equation 39, Table 8).

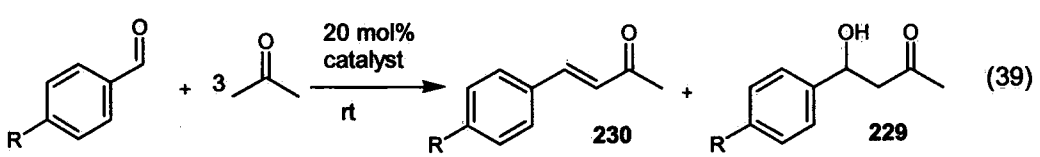

(39)

Table 8: Aldol reactions with **129** on large scale.

Entry	R	Catalyst	Solvent	Time (d)	Conv.[a] (%)	Ratio[b] **230**:**229**	Isolated **230**	Isolated **229**
1	H	**136**+3 eq. NaOH	THF	7	> 90	5:95	7%	19%
2	H	**136**+3 eq. NaOH	H_2O	3	> 99	97:3	66%	N.A.
3	NO_2	**136**+3 eq. NaOH	THF	10	< 10	0:100	0%	8%
4	H	NaOH	THF	4	> 95	95:5	28%	N.A.

[a]Conversion based on disappearance of benzaldehyde in crude ^{1}H NMR spectrum.
[b]Based on crude ^{1}H NMR spectrum.

Generally, it was observed that the isolated yield of the products was lower than expected upon examination of the crude ^{1}H NMR spectrum. This could be explained by the presence of many side products which made it hard to isolate pure products, especially in THF. In some cases the

product was present in the crude ^{1}H NMR spectrum, but it was not possible to isolate it due to the interference of another side product or due to the low mass recovery from the reaction. This was the reason why our catalyst **129** in THF only yielded 19% of aldol product **228** (Table 8, entry 1). However, as expected, the aldol product was the major compound in THF. The presence of product **227** in entry 1 could be to the result of the small amount of water which was used in the 40% NaOH solution. In contrast, in water our catalyst gave mostly product **227** (Table 8, entry 2). Also, the reaction with *p*-nitrobenzaldehyde (Table 8, entry 3) was repeated on larger scale, but after 10 days still a large amount of starting material (58% isolated) was present. After column chromatography, only 8% of aldol product **231**[181] could be isolated but no condensation product was present. The reaction was also repeated with pure NaOH in THF but this appeared to give a messy reaction (Table 8, entry 4). Only 28% of product **227** could be isolated but almost no aldol product was present. This indicated that NaOH and our catalyst followed a different mechanism and that the NaOH forming the "ate"-complex in our catalyst **129** could not be responsible for the catalysis.

3.3.4.Screening of "ate"-complex **129** with 2-butanone

Besides acetone, an asymmetric ketone, namely 2-butanone, was screened on larger scale. In this way, it was possible to investigate if our catalyst **129** produced the kinetic or thermodynamic product. The danger in this reaction was the possibility of a mixture of different products, because not only were there the kinetic and thermodynamic aldol products, but also the kinetic and thermodynamic condensation products. The two most interesting solvents (water and THF) were applied together with benzaldehyde since this gave the best results in previous screenings. Also, the number of equivalents of 2-butanone was increased to five to avoid possible side products and screenings were carried out at room temperature over several days (Equation 40, Table 9).

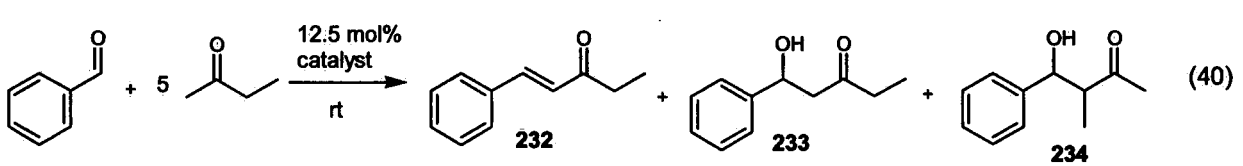

(40)

Table 9: Screening of aldol reaction with 2-butanone.

Entry	Cat.	Solvent	Time (d)	Conv.[a]	Ratio[b] 232:233:234	Isolated 232	Isolated 233	Isolated 234
1	"dry" **129**	THF	10	> 95%	0:73:27	0%	19%	7%
2	"dry" **129**	H_2O	1	> 95%	79:18:3	18%	N.A.	N.A.
3	"dry" **129**	THF+H_2O+ MeCN	10	> 99%	44:30:26	22%	15%	13%
4	NaOH	THF	2	> 95%	N.A.	N.A.	N.A.	N.A.
5	NaOH	H_2O	2	> 95%	92:4:4	24%	N.A.	N.A.

[a]Conversion based on disappearance of benzaldehyde in crude ^{1}H NMR spectrum.
[b]Based on crude ^{1}H NMR spectrum.

The first screenings (Table 9, entries 1-3) were done with the pre-made "ate"-complex **129** under different solvents. As expected, catalyst **129** delivered only the aldol product in THF (entry 1). Although the isolated yields were low due to purification problems, it was interesting to note that the kinetic aldol product **233**[182] was the major compound.[183] No condensation product was formed, probably because the pure catalyst **129** was added and no water was present. When the reaction was run in water (entry 2), it appeared to give a messy reaction and only the kinetic condensation product **232**[180] could be isolated. Using a mixture of different solvents (entry 3) improved the yield modestly which could be explained by the fact that the "ate"-complex **129** was now completely soluble in this mixture. As expected from previous experiments, a mixture of products was gained this time. Besides the "ate"-complex **129**, NaOH was also used as catalyst to compare with the boron-based system (Table 9, entries 4 and 5). Both in THF and in water, the reaction was a mess and only kinetic condensation product **232** could be isolated. An interesting observation was that all reactions (both with "ate"-complex **129** and NaOH) delivered only the kinetic condensation product **232**, and the corresponding thermodynamic product was never witnessed.

3.3.5.Screening of "ate"-complex 129 with acetone

Previous experiments showed us that most reactions with the "ate"-catalyst **129** gave a mixture of several side products, especially in THF. This resulted in difficult isolation and subsequently low yield. It was therefore important to find the right conditions for our catalyst which gave a clean reaction and high yield. Several modifications were made to improve the yield. One was to use only water as solvent since this gave mostly condensation product (Table 5, entry 4) and less

side reactions. Another was to increase the amount of acetone to ten equivalents relative to the aldehyde. In that way, the concentration of acetone could be considered as constant and catalyst **129** and the aldehyde would be soluble in the solvent mixture. Under these new conditions the reaction was rerun with acetone but now with different aldehydes. In all cases, the "ate"-complex **129** was formed *in situ* and was added after the other reagents (Equation 41, Table 10).

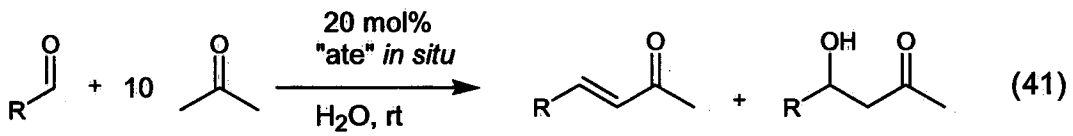

(41)

235 **236**

Table 10: Screening of "ate"-complex **129** with acetone for aldol reaction.

Entry	Aldehyde (R)	Time (h)	Conv.[a]	**235**[b] (product)	**236**[b] (product)	S.M.[b]
1	C_6H_5	7	>99%	77% (**227**)	19% (**228**)	N.A.
2	*p*-$NO_2C_6H_4$	7	>99%	64% (**237**)	N.A.	N.A
3	*p*-$MeOC_6H_4$	9	>90%	81% (**238**)	10% (**240**)	8%
4	C_6H_5CHCH	7	>85%	75% (**239**)	10% (**241**)	12%

[a] Based on crude ^1H NMR.
[b] Isolated product.

The first significant improvement from these modifications was an increase in the rate of reaction. While in previous attempts the reaction took several days, under these new conditions reactions took only several hours. Another advantage was the purity of the reaction product, with only three fractions being produced, it was possible to recover almost every fraction as a pure compound. In all cases (Table 10, entries 1-4), the condensation products **227**, **237**,[184] **238**,[185] and **239**[186] were the major components as expected, however, in entries 3, 4 and especially in 1, there was a significant amount of the aldol products **228**, **240**[181] and **241**.[187] With *p*-nitrobenzaldehyde (entry 2), the recovery of product **237** was lower, which could be due to the higher reactivity of the aldehyde leading to more side products. In contrast, with *p*-anisaldehyde (entry 3), the reaction took longer since it is less reactive. Also, this result showed that the elimination reaction of the alcohol was faster than the aldol under these reaction conditions. This could be observed from entries 3 and 4 which had mainly condensation products **238** and **239** with some starting material still left. Besides aromatic aldehydes, the use of aliphatic aldehydes was also tried. These were more problematic. Not only were complete mixtures produced, but the high volatility of the product compounds made it impossible to isolate anything. With propionaldehyde the TLC showed 8 spots. After purification by silica gel column chromatography a fraction with the

alcohol (11%) and one with the condensation product (11%) was obtained, though still impure. This reaction was also repeated with trimethylacetaldehyde and in this case, the reaction gave only 3 spots by TLC. However, the reaction was too slow, probably due to the steric hindrance of the aldehyde. Because of these problems, it was suggested that it would be easier to follow this reaction, and perhaps other reactions also, by gas chromotography. After making different standards of the trimethylacetaldehyde-derived products (condensation and aldol product) with NaOH, the reaction was repeated, however, because of the slow nature of the reaction and overlapping GC peaks this method of monitoring was abandoned.

Because of the high loading of catalyst **129** (20 mol%), it was considered necessary to repeat the benzaldehyde reaction with only 5 mol% "ate"-complex. Due to the low conversion, the reaction was quenched after nine days and after purification, only benzoic acid could be isolated; no other products being present. Because of the small amount of catalyst, the reaction did not proceed and the benzaldehyde started to oxidize under the reaction conditions. It was clear that a 20 mol% loading was the best set of conditions to use the "ate"-complex, so for the next screenings, these conditions were applied.

3.3.6.Screening of "ate"-complex **129** with hydroxyacetone

Since our active catalyst **129** consisted of a boron atom, it was considered interesting to also screen it with hydroxyacetone.[190] In this way, it was hoped that the hydroxyl group of the ketone would complex with the boron which would accelerate the reaction significantly. The same conditions as the previous screening with acetone were applied (10 equiv. of ketone in water at room temperature) together with different aldehydes (Equation 42, Table 11).

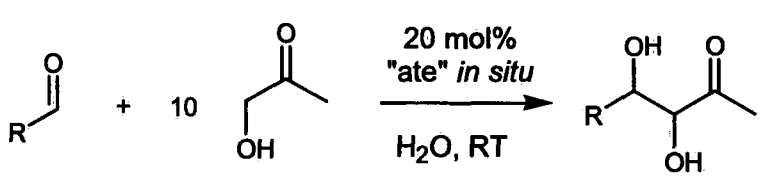

(42)

242

Table 11: Screening of catalyst **129** with hydroxyacetone.

Entry	Product **242**	Time (h)	Conv.[a]	d.e.[a] (syn:anti)	Yield[b]
1	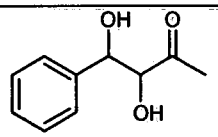 **243**[188]	7	>99%	11:4	97%
2	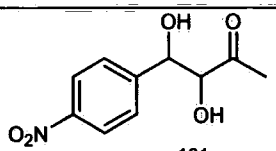 **244**[181]	7	>99%	11:2	76%
3	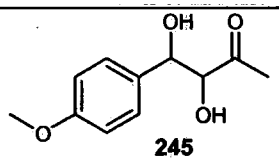 **245**	9	~70%	11:5	46%
4	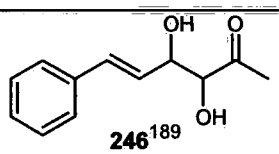 **246**[189]	7	>99%	4:3	64%
5	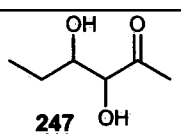 **247**	7	>99%	2:1	68%
6	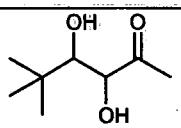 **248**	7	>99%	1:0	62%

[a] Based on crude ^{1}H NMR.
[b] Isolated product.

Again, a significant acceleration was observed and most of the reactions were already finished within several hours. Even more surprising was the formation of the corresponding alcohol instead of the condensation product. To our delight, the reaction appeared to be clean, with almost no side products and in all cases, the major product was the thermodynamic diol **242**. This high regioselectivity was rather unexpected since hydroxyacetone is an asymmetric ketone, hence, a mixture of both kinetic and thermodynamic aldol products was possible. As mentioned before, all the reactions were finished within 7 hours except for *p*-anisaldehyde (Table 11, entry 3). In this reaction there was still starting material after 9 hours, which can be explained by the

methoxy group, being an electron donating group and thus making the aldehyde less reactive. The broadness of this process was also interesting. Not only was catalyst **129** effective for aromatic aldehydes (Table 11, entries 1-4), but also aliphatic (propionaldehyde, entry 5) and bulky aldehydes (trimethylacetaldehyde, entry 6) delivered clean diols of type **242**. Since catalyst **129** was achiral, there were four diols produced; the two *syn*-enantiomers (*S,R* and *R,S)*; and the two *anti*-enantiomers (*R,R* and *S,S)*. These two diastereomers were observed by TLC which showed two spots close together. Only in the reaction with cinnamaldehyde (entry 4) was a single diastereomer isolated.

Two important characteristics of the diastereomers were observed:

1) Firstly, the regioselectivity of the deprotonation of the hydroxyacetone giving, in all cases, only the vicinal diol **242**.

2) Secondly, the formation of mainly the *syn*-diol. This was confirmed by the coupling between the two protons attached on the carbons with the hydroxyl groups attached. These gave small couplings, corresponding to the *syn*-adduct.[188] Further evidence was provided by the HPLC analysis and the crystal structures obtained from compounds **244** (Figure 2, see appendix for crystallography data) and **248** (Figure 3, see appendix for crystallography data) which supported this observation. Even in the case of trimethylacetaldehyde, only the *syn*-product was formed; there was no other diastereomer. This indicated that the bulky *t*-butyl group must play a key role in the conformation of the transition state (see below).

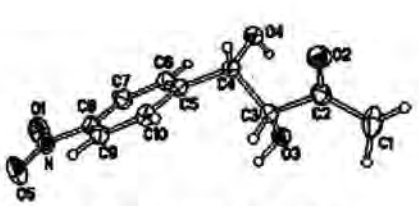

Figure 2. crystal of **244**.

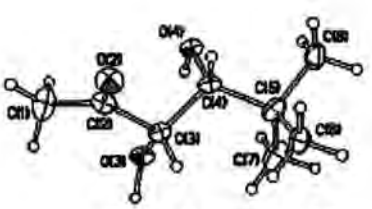

Figure 3. crystal of **248**.

3.3.7.Screening of the blank reactions

To be sure it was the "ate"-catalyst **129** which was responsible for the reactions observed above instead of NaOH, it was needed to do the same reactions under the same conditions but with different catalysts. For convenience, benzaldehyde was chosen as the substrate aldehyde (Equation 43, Table 12).

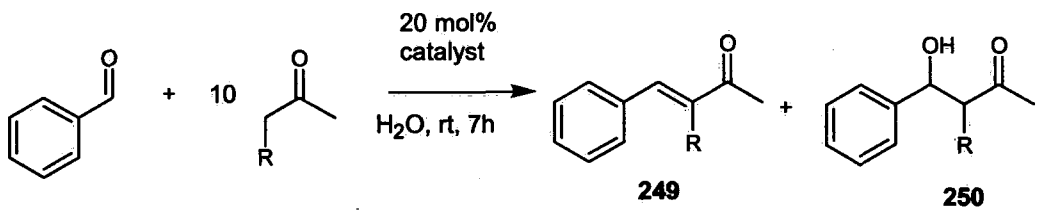

(43)

Table 12: Screening of the blank reactions.

Entry	Catalyst	R	Conv.[a]	**249**[b]	**250**[b]
1	NaOH	H	>99%	99%	N.A.
2	NaOH	OH	>99%	N.A.	49%
3	$PhB(OH)_2$	OH	<2%	N.A.	N.A.
4	Boroxine **136**	OH	<2%	N.A.	N.A.
5	NaOH + $PhB(OH)_2$	OH	<2%	N.A.	N.A.
6	NaOH + $PhB(OH)_2$ + 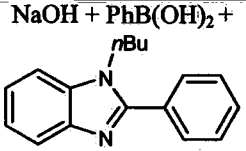	OH	<2%	N.A.	N.A.

[a] based on crude ^{1}H NMR.
[b] isolated product.

With NaOH, full conversion of the starting material was observed (Table 12, entries 1 and 2). The same conversion was observed in the identical reactions with "ate"-catalyst **129** (Table 10, entry 1 and Table 11, entry 1). The difference, however, was in the products, i.e. when Table 12, entry 1 is compared to Table 10, entry 1, it is clear that NaOH only gives product **227**, but the "ate"-complex **129** gives a mixture of mainly condensation product with 19% alcohol. Also, between Table 11, entry 1 and Table 12, entry 2 there is a difference; although the major product in both cases is the diol **243**, the reaction with "ate"-catalyst **129** gives exclusively the diol while the reaction with NaOH gives a mixture of several products, as determined by the crude ^{1}H NMR spectrum and TLC. Both these cases show that the presence of the boron in the "ate"-complex **129** tends to soften the basicity of NaOH. In Table 12, entries 3-6, no conversion was observed.

It is interesting that $PhB(OH)_2$ totally neutralises the NaOH, presumably to form $PhB(OH)_3^-$, from which only starting material could be isolated.

3.3.8.Kinetic data on aldol reaction with "ate"-complex 129

To gain extra information about the novelty of this new type of catalysis, a comparison on the basis of kinetic data[191] between catalyst **129** and NaOH was considered. This data would not only dismiss any assumption that NaOH was responsible for the catalysis in the "ate"-complex **129**, but would also give a deeper insight in the mechanistics of this new type of catalyst. In previous work on this topic it was already shown by Blatch and Grosjean that there was a significant difference in rate between the claimed to be "ate"-complex **129**, and NaOH. The different rate constants for the aldol condensation between benzaldehyde and acetone catalysed by NaOH and the "ate"-complex **129** were compared by following the consumption of the aldehyde and the formation of condensation product by ^1H NMR spectroscopy (see Figure 4 and Figure 5) over time.

Figure 4. Phenylboronate benzimidazole **129** (0.094 M) catalysed aldol reaction of benzaldehyde (0.624 M) with acetone (7.84 M), product formation and benzaldehyde consumption.

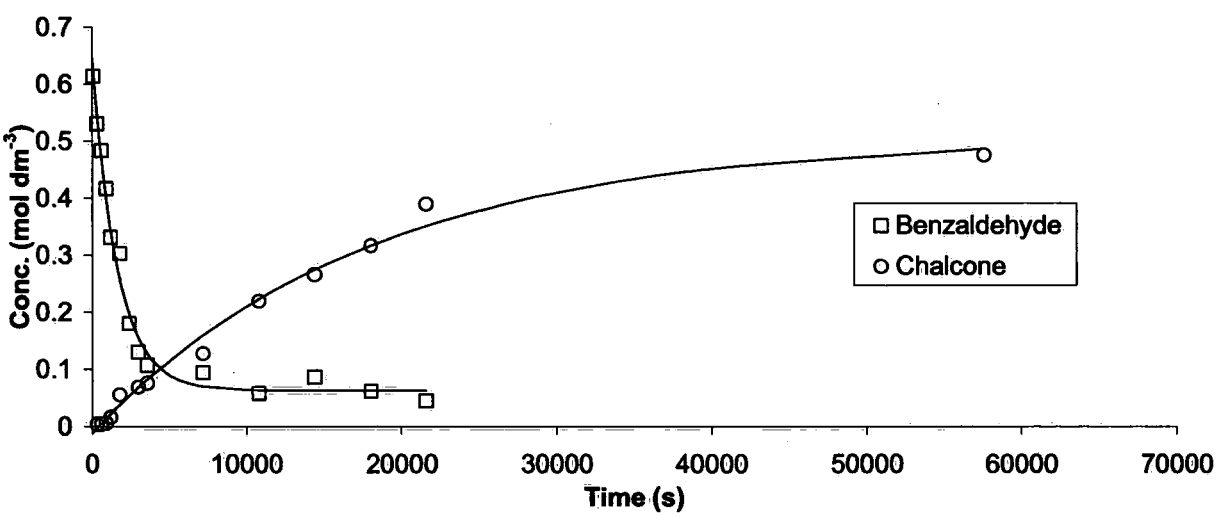

Note: the rate of consumption of benzaldehyde is higher than that of formation of the condensation product ($k_{benzaldehyde} = 6.10 \pm 0.42 \times 10^{-4}\ s^{-1}$ and $k_{chalcone} = 5.54 \pm 0.53 \times 10^{-5}\ s^{-1}$).

Figure 5. Sodium hydroxide (0.094 M) catalysed aldol reaction of benzaldehyde (0.624 M) with acetone (7.84 M), chalcone formation and benzaldehyde consumption.

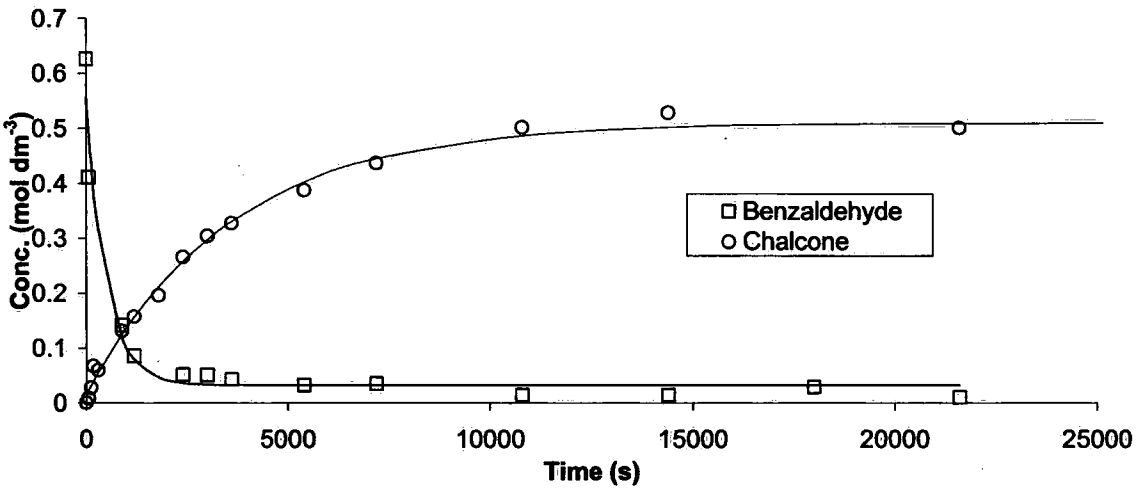

Note: the rate of consumption of the aldehyde is significantly faster than that of formation of the chalcone, and the data can be fitted to first order kinetics although the error recorded on fitting is probably indicative of more complex kinetics ($k_{benzaldehyde} = 1.99 \pm 0.44 \times 10^{-3}$ s^{-1} and $k_{chalcone} = 2.81 \pm 0.16 \times 10^{-4}$ s^{-1}). Further experiments are required to calculate the individual rate constants.

The following data were obtained for the "ate"-complex **129**: $k_{benzaldehyde} = 6.10 \pm 0.42 \times 10^{-4}$ s^{-1} and $k_{chalcone} = 5.54 \pm 0.53 \times 10^{-5}$ s^{-1}; and for NaOH: $k_{benzaldehyde} = 1.99 \pm 0.44 \times 10^{-3}$ s^{-1} and $k_{chalcone} = 2.81 \pm 0.16 \times 10^{-4}$ s^{-1} which showed unambiguously that there was a different catalytic pathway between the "ate"-complex **129** and NaOH since the reaction with NaOH was faster. In both cases, it was also clear that benzaldehyde consumption was faster than the formation of the chalcone and that the data was best fitted to first order kinetics. This implied that concentration of acetone could be considered as constant due to its excess and that the rate was only dependent upon the concentration of benzaldehyde. Because there was a rate difference in benzaldehyde consumption and chalcone formation, the mechanism had to involve the presence of at least one intermediate, most likely the aldol product. In accordance with the kinetic data, two concurrent pathways were proposed where the "ate"-complex **129** could either react to form the aldol adduct (Scheme 30) or catalyse the dehydration of the latter (Scheme 31).

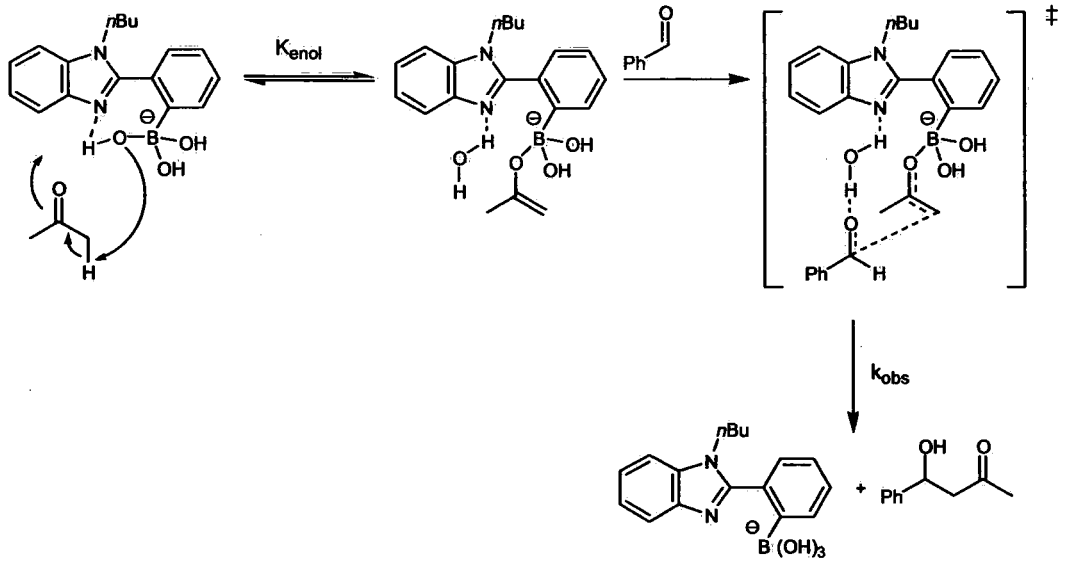

Scheme 30. Proposed catalytic mechanism for **129** with acetone to aldol product.

Since the kinetic data for the reaction was first order in the benzaldehyde, the k_{obs}, corresponding to the rate of benzaldehyde consumption, had to be the addition step on the aldehyde of the enolate giving the aldol product (Scheme 30). This implied that the enolate formation with acetone had to be an equilibrium.

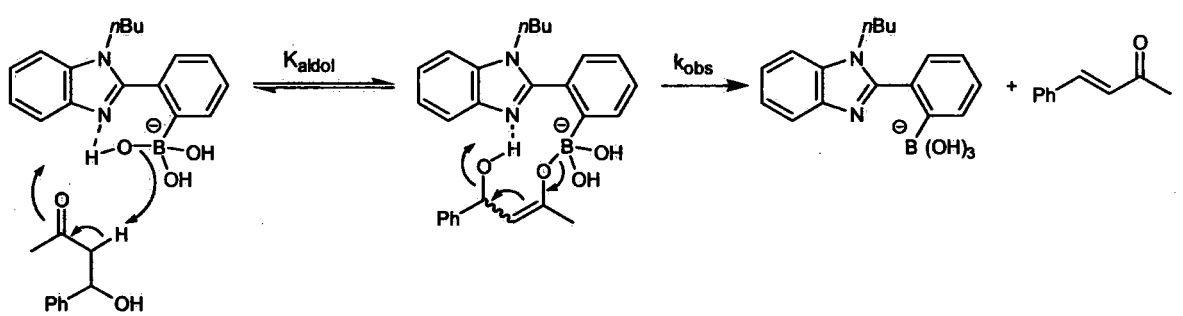

Scheme 31. Proposed catalytic mechanism for **129** with acetone to chalcone.

In the second pathway (Scheme 31), the k_{obs} corresponds to the rate of the chalcone formation and this rate is only dependent upon the concentration of the aldol product.

These mechanistic speculations were supported by the absence of catalytic activity from the phenylboronic acid-hydroxide complex both in the presence and absence of *N*-butylphenyl-

benzimidazole. This implied the need for two functional groups on the same molecule in order to achieve catalysis, and hence, behave as bifunctional catalysts.

No kinetic data was yet available for the reaction with hydroxyacetone. Therefore, in the first attempt, this reaction with benzaldehyde was catalysed by "ate"-complex **129** and NaOH, and the reactions were followed by gas chromatography. Unfortunately, the diol was not stable on GC so the analysis had to be continued using HPLC and in fact, chiral HPLC since this produced the best separation. By using 1,4-dimethoxybenzene as internal standard, the increase in the product could be accurately followed over time, giving four peaks corresponding with the four diol stereoisomers. Because of the overlap of the benzaldehyde peak with the solvent peak, the consumption of the benzaldehyde could not be followed accurately, so only the increase in the diol product was considered. In collaboration with Grosjean, the kinetic data was processed and fitted, and a mechanistic pathway was proposed (Figure 6 and Figure 7).

Figure 6. Conversion *versus* time plot for the complex **129** (0.112 M) catalysed reaction of benzaldehyde (0.554 M) with hydroxyacetone (5.53 M), product formation.

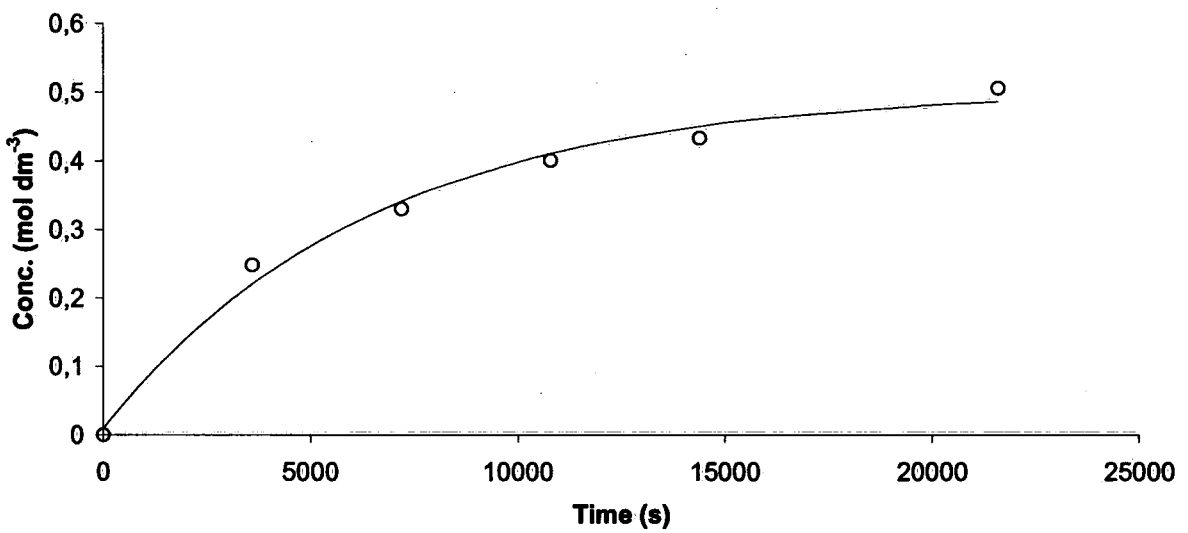

Note: the data was fitted to first order kinetics and the observed rate constant for formation of the aldol adduct k_{obs} was found to be $k_{obs} = 1.54 \pm 0.27 \times 10^{-4}$ s^{-1}.

Figure 7. Conversion *versus* time plot for the NaOH (0.112 M) catalysed reaction of benzaldehyde (0.554 M) with hydroxyacetone (5.53 M), product formation.

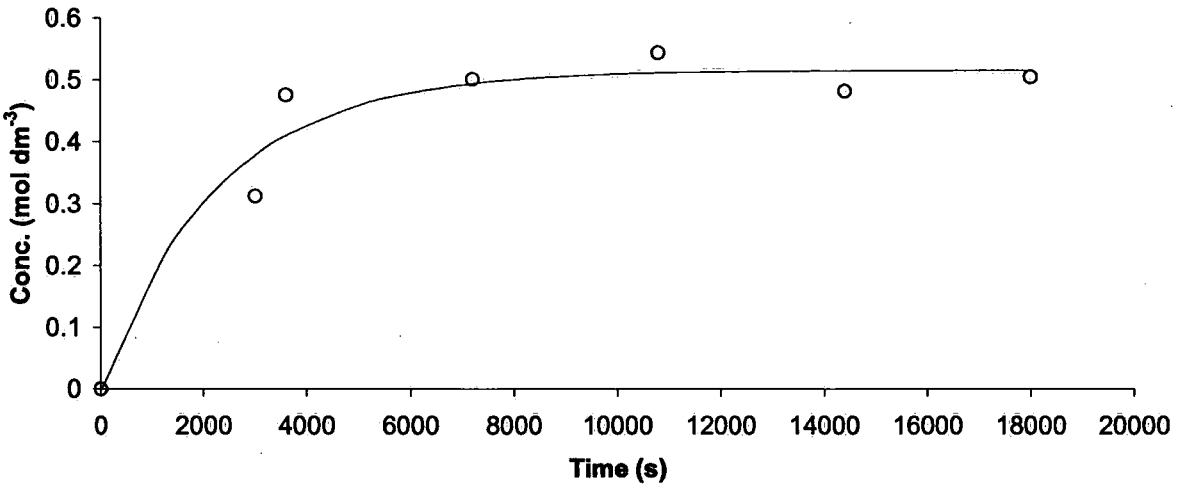

Note: the data was fitted to first order kinetics and the observed rate constant for formation of the aldol adduct k_{obs} was found to be $k_{obs} = 4.41 \pm 1.18\times10^{-4}$ s^{-1}.

In both cases, the data was best fitted to a first order reaction, implying that the concentration of hydroxyacetone could be considered as constant. The following rate constants were obtained: for "ate"-complex **129**: $k_{obs} = 1.54 \pm 0.27\times10^{-4}$ s^{-1}; and for NaOH: $k_{obs} = 4.41 \pm 1.18\times10^{-4}$ s^{-1}. This showed again that the reaction with NaOH was actually proceeding faster. Surprisingly, the isolated yield after 7 hours of the product with NaOH was lower than with "ate-complex **129** (Table 12, entry 2 and Table 11, entry 1). This could only be explained by overreaction of the product. It was thought that in the reaction catalysed by NaOH, the diol was formed early on in the reaction, but since NaOH was so reactive, the product was consumed leading to more side products. This was verified by HPLC analysis and ^1H NMR over time. In the case of the "ate"-complex **129**, the product was formed much slower but because this catalyst is less reactive, it did not consume the product. Using this kinetic data, a model was proposed as outlined in Scheme 32.

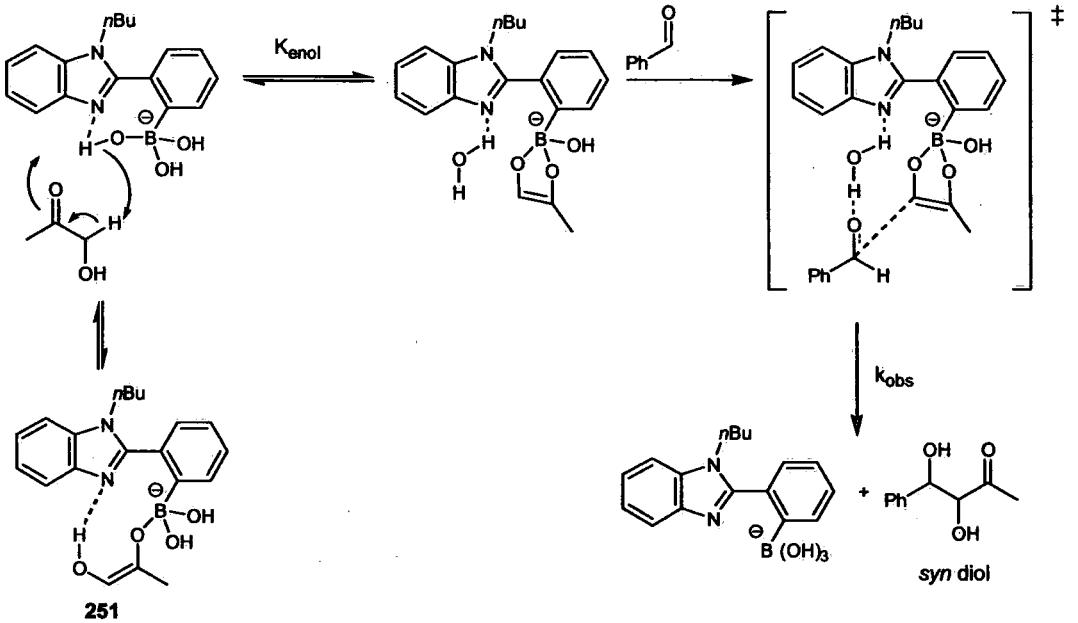

Scheme 32. Proposed catalytic mechanism for **129** with hydroxyacetone.

The kinetic data revealed that the reaction was first order in the aldehyde. In this case, the k_{obs}, corresponding to rate of the diol formation, had to be also the addition step of the hydroxyacetone enolate onto the aldehyde giving the diol product (Scheme 32).

Again, this model was supported by the information gained from the blank reactions (Table 12, entries 3-6) which implied the presence of two functional groups. Another interesting observation was the difference in the reaction rate between the consumption of benzaldehyde (recorded in the condensation with acetone) and the aldol reaction with hydroxyacetone both catalysed by the "ate"-complex **129**. It was clear that the consumption of benzaldehyde ($k_{benzaldehyde} = 6.10 \pm 0.42 \times 10^{-4}\ s^{-1}$) was much faster than the hydroxyacetone reaction ($k_{obs} = 1.54 \pm 0.27 \times 10^{-4}\ s^{-1}$). This could perhaps be explained by the presence of an intermediate **251** which could be stabilised by H-bonding between the hydroxyl group and the nitrogen. In that way, the nitrogen is not available anymore to complex with a water molecule which is hydrogen bonded to the aldehyde, and hence, ordering the developing transition state.

3.3.9.A close mechanistic view on the "ate" catalysed aldol reaction

Since now the kinetic data was available for the both aldol reactions with acetone and hydroxyacetone, a deeper mechanistic look was possible and also a catalytic cycle could be proposed. When the catalytic cycle was created, it was important to consider the fact that both reactions were first order to the aldehyde and that the catalytic mechanism had to include the two functional groups working cooperatively. For the reaction with acetone in water, Scheme 33 was developed by combining two concurrent pathways (Scheme 30 and Scheme 31). It was important to notice that the reaction was done in water, so water molecules play a part in the catalysis. In the first step, the "ate"-complex does a deprotonation of the acetone leading to a boron enolate intermediate **252**. The water molecule, coordinated by the nitrogen, will then position the aldehyde to the enolate which will attack the previous. It is important to focus on the R group of the aldehyde, which is orientated away from the enol due to steric hindrance. This attack will eventually give the corresponding aldol product **236**. This aldol product can then react further on leading again to a boron enolate **253** which can be stabilized by an intramolecular H-bonding between the hydroxyl group and the nitrogen. An elimination step will eventually remove the hydroxyl group and result in the corresponding chalcone **235**.

When the reaction is done in THF, a very similar pathway is considered, but this time, the catalyst **254** possesses a sodium cation instead of a water molecule. This cation will also position the aldehyde to the enolate giving the aldol product **236**. Although at this moment it is not clear why in THF the aldol product does not react further, but it is thought that the sodium cation prohibits the formation of the intramolecular H-bond between the hydroxyl group and the nitrogen. In that way, the second boron enolate **253** will be less stabilized and so it will be more difficult for it to be formed.

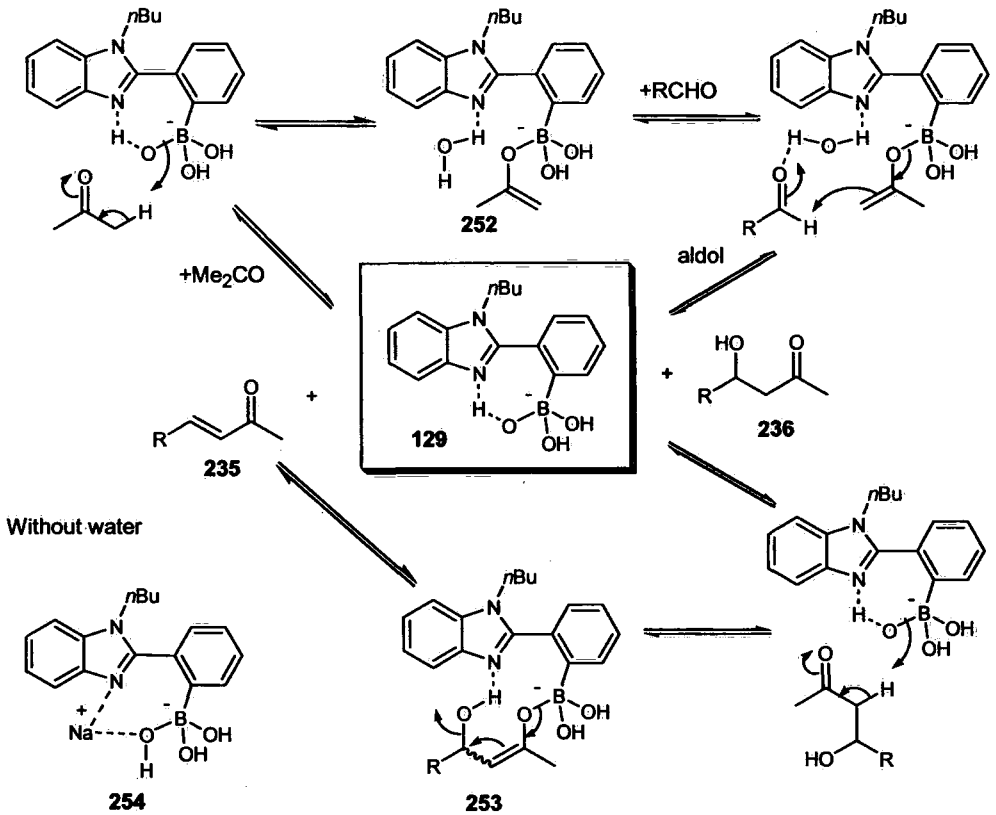

Scheme 33. Proposed mechanism for **129** with acetone in water.

A very similar pathway was considered for the reaction with hydroxyacetone, but this time it was important to incorporate the stereochemistry, since the "ate"-catalyst **129** produced mainly the *syn*-diol **242**. Since the reaction was run in water, water would also play a role in the catalysis. Again, the cycle will start off with the deprotonation of the hydroxyacetone, but this time, the boron first complexes with the hydroxyl group, so bringing the proton next to the hydroxyl group close to the "ate"-complex for deprotonation. This explains the regioselective deprotonation of hydroxyacetone. The newly formed boron enolate **255** is now stabilised by two oxygen-boron bonds. It is important to notice that the methyl group of the boron enolate will be positioned away from the water molecule due to steric hindrance. In the next step, the aldehyde will be introduced by the water molecule, again with the R group away from the boron enolate due to steric hindrance. It is this conformation **256**, with the methyl group and the R-group pointed away from each other which is responsible for the *syn*-diol (Scheme 34).

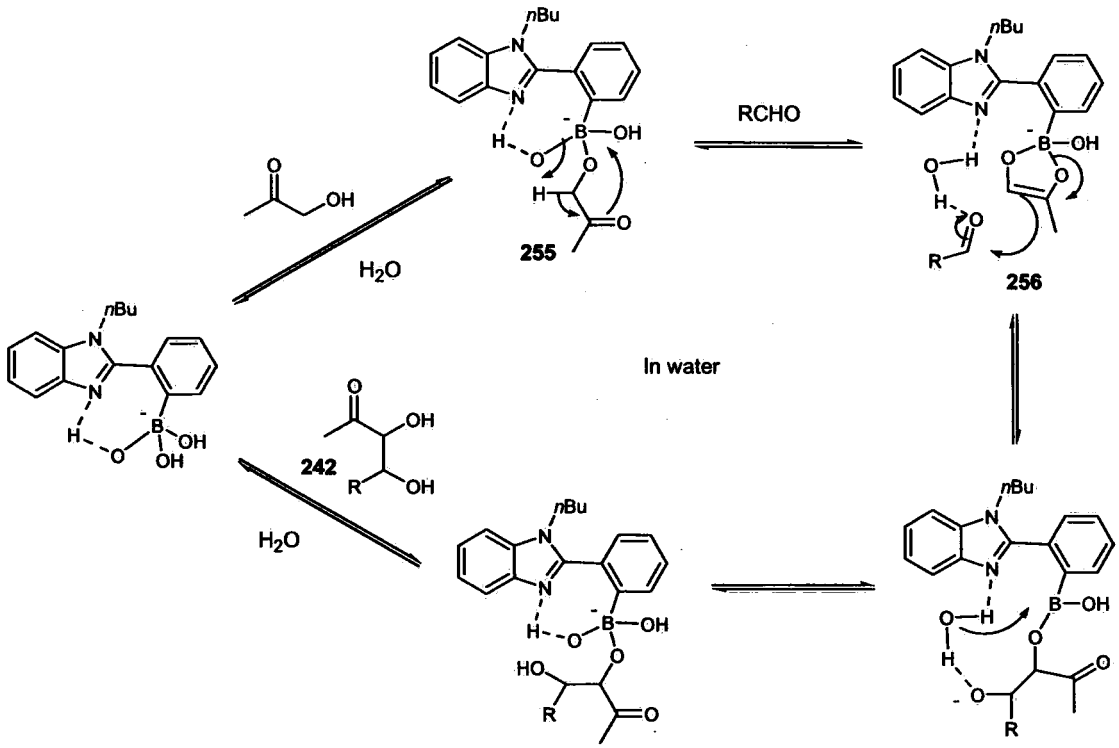

Scheme 34. Proposed mechanism for **129** with hydroxyacetone in water.

The boron enolate will eventually attack the aldehyde and depending on which *face* is attacked, the corresponding enantiomer will be formed. At the end, the diol will be liberated through hydrolysis giving **242**.

Because both mechanisms are based on the presence of a boron enolate intermediate, it is important to have evidence of this. Therefore, an NMR experiment was considered in which it was hoped to trap the formation of the enolate, and observe it by the shifts in the ^{1}H NMR spectrum. So, the boroxine **136** was dissolved in a CD_3CN/D_2O (1:1) mixture, and exactly 3 equivalents of NaOD were added. After intensive shaking, it was noticed the "ate"-complex **129** was formed by the shift of the boron peak to lower ppm (from 18.0 ppm to 0.3 ppm). Then dry acetone/hydroxyacetone was added and the tube was shaken again. After 5 minutes, a new boron peak could be observed next to the previous one at 6.5 ppm. Also, on the ^{1}H NMR spectrum new peaks appeared. In the case of acetone, peaks appeared at 6.92 (d, *J* 8.8) and 6.82 (t, *J* 6.8) ppm and for hydroxyacetone new peaks appeared at 7.06 (d, *J* 9.6) and 6.95 (t, *J* 7.6) ppm. Because

the peaks were very small it is not sure if they could be assigned to the corresponding enol or rather to artefacts.

3.3.10.A recapitulation

It was now clear that a reaction was found in which our bifunctional system **129** behaved as a catalyst. By optimising the conditions, good yields were gained for the aldol reaction with acetone and hydroxyacetone. Also, a peculiarity was found by using our catalyst **129** in water and THF which produced selectively the condensation and aldol product. To verify the activity of catalyst **129**, different tests were done as blank reactions and kinetic data. Also, a mechanistic view was proposed to support our findings. Since catalyst **129** was achiral, the next step was to create a chiral version and look for its ability to induce asymmetric product formation.

3.4.Synthesis of new chiral bifunctional catalyst

In the previous chapter it was shown that our bifunctional catalysts were active for the aldol reaction, especially catalyst **129**. Because catalyst **129** is achiral, it was considered useful to create a chiral version. Important in this version was to maintain the active catalytic centres. This implied that the new catalyst should also have an imidazole group and the boronic acid placed at approximately the same distance apart as in **129**. In that way, these functional groups would have the same cooperative effect for catalysis. Keeping these conditions in mind, it was possible to create a closed ring system with the benzimidazole attached to the phenyl ring through this alkyl tail. In that way, the phenyl ring would not be able to rotate freely, and therefore, would create a certain angle between the benzimidazole and the phenyl ring which induced the chirality (mimicking BINOL for example). Because the aim was to induce the highest degree of chirality, it was important to have a wide angle between the two groups and a high rotational barrier to atropisomer interconversion. Using the modelling program Spartan,[192] it was proposed that a seven-membered ring delivered the best of the desired angle properties (Figure 8).

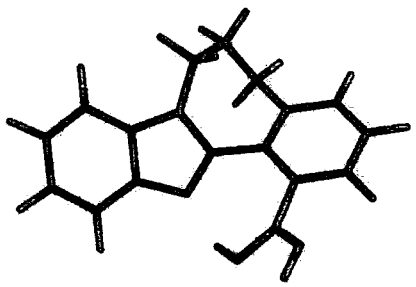

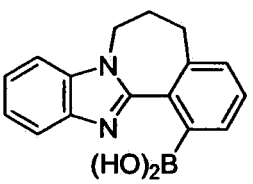

257

Figure 8. Model structure of **257** by "spartan".

Important on this model structure **257** is the presence of the hydrogen bond between the nitrogen of the imidazole and the hydroxyl group of the boronic acid. This bond will be responsible for the stabilization of the angle between the two aromatic groups and potentially, catalysis. By creating this seven-membered ring it was hoped this angle would sustain and no atropisomer inversion would be allowed. Therefore, it would also be wise in the future to do the screenings at the lowest temperature possible in order to induce the highest e.e. Since it was now clear how our chiral catalyst might look, it was time to consider a synthetic pathway.

3.4.1.Retrosynthetic pathway of **257**

The retrosynthetic analysis consisted of two possible pathways which would create the scaffold **258** with the seven-membered ring, and the final step would then include the introduction of the boron atom. This introduction of the boron atom was based on the direct lithiation reaction which was previous done on the corresponding 2-phenylbenzimidazole compound **135**. It was hoped that the sp^2 nitrogen of the imidazole would control the lithiation to the *ortho*-position, as before. The only difference now would be the rigid structure of the phenyl group.

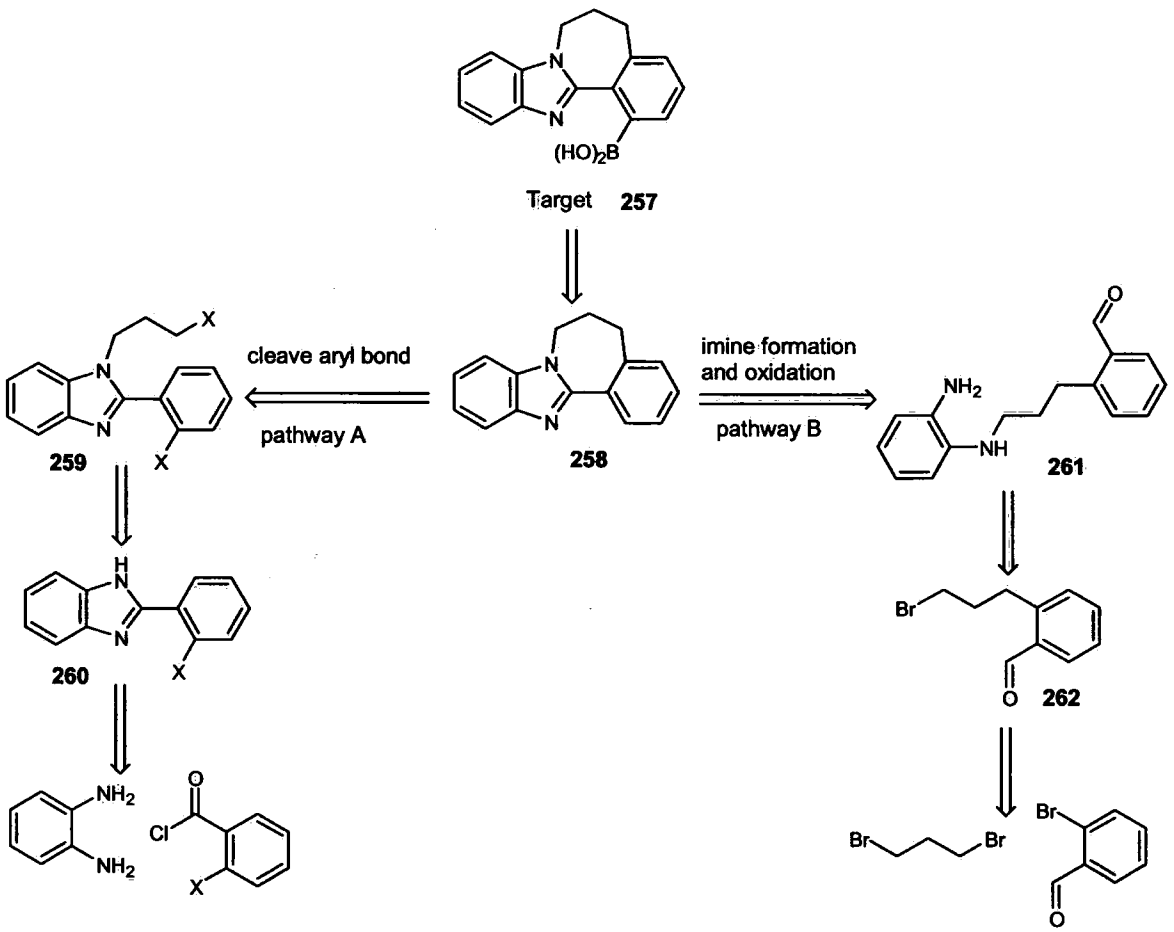

Scheme 35. Retrosynthetic pathway to **257**.

The synthesis of scaffold **258** was based on two pathways:

1) Pathway A included first the making of the 2-phenylbenzimidazole molecule **260** to which an alkyl tail would be added. The final step would then be a intramolecular C-C coupling in **259** between the sp^3 carbon and the aryl group. To make this coupling possible the introduction of different functional groups (=X) was needed. These groups could be halogens or double bonds depending on the used reaction.

2) Pathway B on the other hand, would first start off with the C-C coupling between the phenyl group and the alkyl to create this tail on **262**. To this tail, the diamine was connected to give **261** which would finalize in a cyclisation with an oxidation to result in this benzimidazole **258**.

It was clear that both pathways had their advantages and drawbacks, but for convenience, pathway A was tried first.

3.4.2.Pathway A: Cyclisation by direct lithiation

In a first attempt to create scaffold **258** it was thought to follow pathway A through a direct lithiation. In this way only two reactions would be needed and the final intramolecular cyclisation reaction would make use of a regioselective direct lithiation controlled by the nitrogen, as before (Scheme 36).

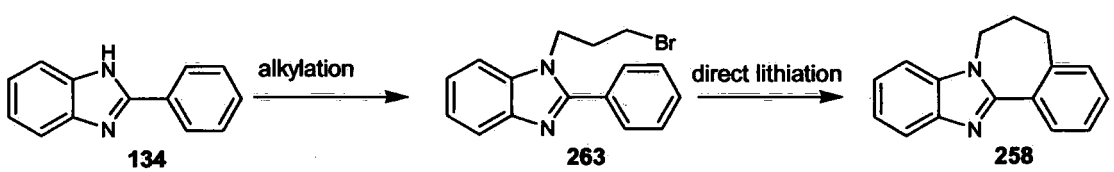

Scheme 36. Synthetic pathway to **258** by direct lithiation.

The first step was the alkylation of the 2-phenylbenzimidazole **134**.[193] It became clear that there was competition between the wanted alkylation product **263** and corresponding elimination product **264**. Probably, the imidazole **134** preferred to act as a base for the elimination of 1,3-dibromopropane rather than forming the alkylation product **263**. This allyl bromide reacted easily with another imidazole to form **264**. This also explained why there was always a significant amount of starting material present in crude mixture. The reaction was repeated under different conditions to improve the yield (Equation 44, Table 13).

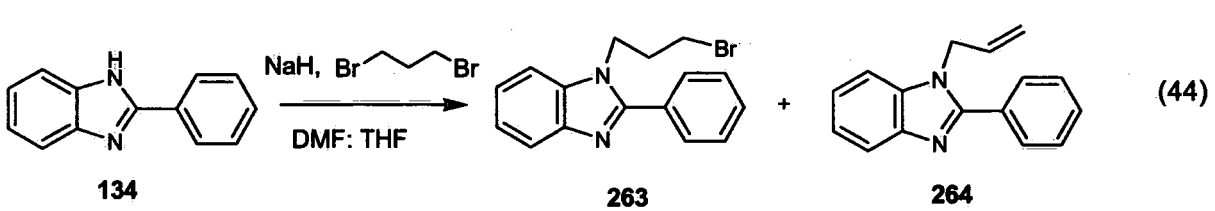

(44)

Table 13: Screening of alkylation of **134** with 1,3-dibromopropane.

Entry	Solvent	Time	Eq.of Br⌒⌒Br	Temp. (°C)	**263**[a] %	**264**[a] %
1	DMF	18h	1.1	reflux	2	12
2	DMF	1h	3	100	5	32
3	DMF	1h	7	25	6	21*
4	DMF	1h	10	-10	37*	13*
5	DMF	1h	10	-61	17	10
6	THF	1h	10	-78	16*	5*
7	DMF:THF 4:1	30 min	10	-78	33	10

[a] isolated yield except * which is based on conversion on crude ^{1}H NMR.

The first test reaction (Table 13, entry 1) was done under the same conditions as the *n*-butyl alkylation of 2-phenylbenzimidazole **134** (Scheme 17). Unfortunately, only very low yields of **263** were recovered. Therefore, it seemed more reasonable to follow the reaction firstly by ^{1}H NMR spectroscopy. It became clear the reaction was fast because after only 1 hour, product **263** and **264** were already observed. After 2 hours the amount of product **263** started to decrease and different side products appeared. Therefore, it was important to keep the reaction time as short as possible. To reduce the amount of side products, the imidazole anion was added dropwise to the electrophile and a large excess of electrophile was used. It was clear that lowering the temperature inhibited product **264**, probably due to entropic reasons disfavouring the elimination step. Due to the low melting point of DMF (-61 °C), another solvent was needed to reach -78 °C. In THF (Table 13, entry 6), the imidazole anion did not dissolve very well and therefore, gave a lower yield of **263**. The best result was gained with a mixture of DMF and THF (Table 13, entry 7) at –78 °C; the purification of product **263** was difficult since starting material, **263** and **264** have almost the same Rf value (this also explains the low yields). Two columns were needed; the first one with Al_2O_3 to remove starting material, and 2nd on silica gel to separate **263** and **264**, in a corresponding yield of 33% and 10%. Instead of NaH, a weaker base Cs_2CO_3, was tried in an attempt to reduce the amount of elimination product.[194] Unfortunately, no difference was noticed.

Since it was now possible to form **263** in a reasonable yield, several attempts were made to induce the cyclisation by direct lithiation (Equation 45, Table 14). Because the reactions were messy, only the most significant products (**265** and **266**) could be isolated. Unfortunately, these were not the desired product **258**. One of the side products was the debrominated derivative

265.[195] This was expected since it is known that lithium-halogen exchange is kinetically faster than direct lithiation. A rather unexpected product was **266**. Presumably it originates from the debrominated product which does an intramolecular addition onto the imidazole ring (Scheme 37), forming a chiral aminal (this was observed on the ^{1}H NMR spectrum by the geminal protons).

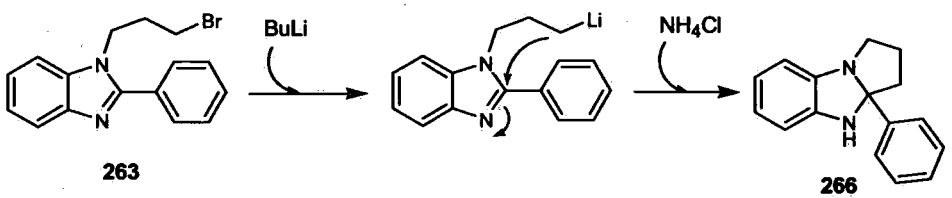

Scheme 37. Intramolecular addition by lithium halogen exchange on **263**.

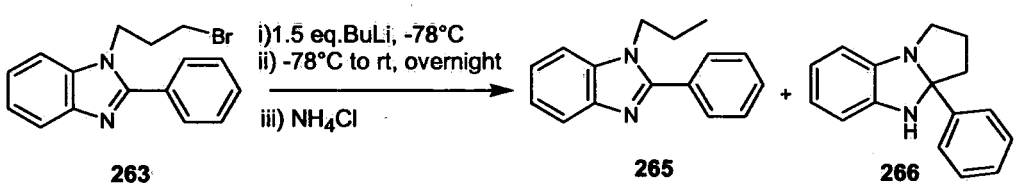

(45)

***Table 14*:** Direct lithiation on **263**.

Entry	Type of BuLi	Solvent	**265**[a]	**266**[a]
1	*t*-BuLi	THF	19%	6%
2	*n*-BuLi	Et_2O	18%	38%

[a] Isolated yield.

It was clear that under milder conditions, such as using *n*-BuLi (Table 14, entry 2) instead of *t*-BuLi (Table 14, entry 1), the reaction gave less side products. Interestingly, in none of the crude ^{1}H NMR spectra was any starting material observed. However, since these lithiation reactions were too messy and none of them gave the desired product, a different route was examined.

3.4.3.Pathway A: Cyclisation by Heck reaction

A different way to cyclise the molecule was by making use of the Heck reaction. The Heck reaction is known to be clean and efficient to form intramolecular ring systems.[196] To be able to do a Heck reaction, an alkene and a halogen on the substrate were needed. Therefore, it was proposed to place an allyl tail on the nitrogen, followed by using a direct lithiation to put a

bromide onto the phenyl ring. This would mean making molecule **267** which could then be used for the actual Heck cyclisation (Scheme 38).

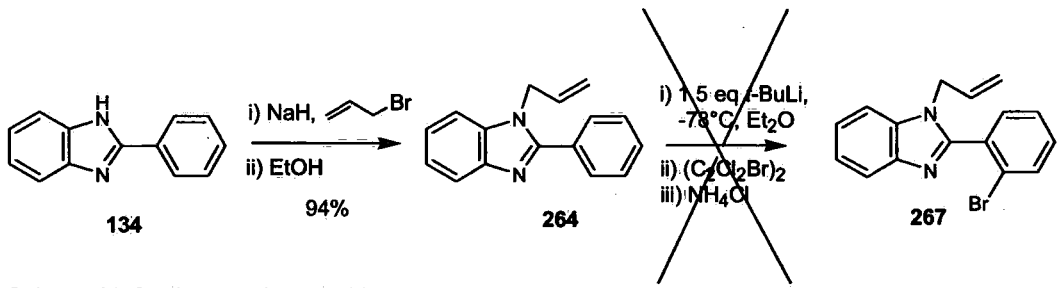

Scheme 38. Synthesis pathway to **267**.

The allylation on the imidazole **134** was a clean reaction giving **264** in a good yield of 94%.[197] The next step, which was the direct lithiation, was more complicated resulting in a mixture of products. After purification using silica gel column chromatography, a fraction containing **267** could be isolated. Unfortunately, this fraction consisted still of a mixture of **264** and **267**. Because of the low mass recovery and difficult separation, the reverse approach was chosen, employing first the bromine addition, and then, the allylation. Hence, 2-phenylbenzimidazole **134** was submitted to a direct lithiation using 2.5 equivalents of *n*-BuLi (1 equivalent extra to neutralize the acidic proton) and 2 equivalents of dibromotetrachloroethane at -25 °C. Also, in this case, a mixture of products was obtained. Therefore, it seemed more useful to create the corresponding imidazole **268** by condensation reaction (Equation 46, Table 15).

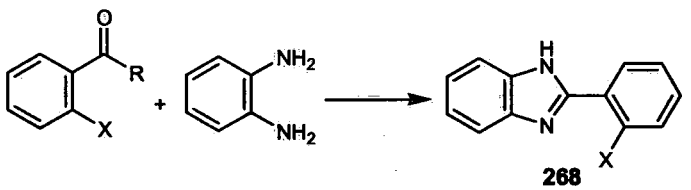

(46)

Table 15. Synthesis of **268** by condensation reaction.

Entry	R	X	Conditions	**268**[a] (%)
1	H	Br	K_2CO_3, KI/I_2, H_2O, 90 °C, 3h	32
2	Cl	Br	Dry sieves, dioxane, reflux, 18h	6
3	Cl	Br	Dry sieves, pyridine, dioxane, reflux, 3d	7
4	Cl	Br	Dean Stark, toluene, reflux, 43h	19
5	Cl	Br	Dean Stark, *p*-xylene, reflux, 42h	34
6	Cl	I	Dean Stark, *o*-xylene, reflux, 28h	30
7	Cl	Br	Dry sieves, 4N HCl, MeOH:dioxane (1:1), reflux, 27h	9
8	Cl	I	Dry sieves, 4N HCl, MeOH:dioxane (1:1), reflux, 22h	28
9	Cl	Br	CH_3COOH (0.2M), THF, reflux, 23h	22
10	Cl	Br	Dean Stark, *p*-TsOH (1.8 eq.), *o*-xylene, reflux, 40h	64
11	Cl	Br	Dean Stark, *p*-TsOH (2 eq.), *o*-xylene, reflux, 42h	86
12	Cl	I	Dean Stark, *p*-TsOH (2 eq.), *o*-xylene, reflux, 42h	71

[a] Isolated yield.

In the first attempt (Table 15, entry 1), the corresponding aldehyde was used to form the cyclised diamine which was further oxidised with I_2 to get the imidazole.[198] Although the yield was reasonable, the purification gave a lot of problems due to the identical Rf value of **268** and the cyclised diamine. Therefore, two columns were needed (on silica gel and Al_2O_3) to obtain the pure product **268**. Because of these purification problems, another way was followed using the corresponding acid chloride. In this case, a simple condensation was needed by removing the water and the purification would be much easier since only starting material and mono-acylated product[199] would be present in the mixture. Although several dehydrating methods were tried, such as dry sieves[200] (Table 15, entries 2, 3, 7 and 8) and Dean Stark conditions (Table 15, entries 4-6),[201] no yield higher than 34% was obtained. This indicated an extra catalyst was needed. By trial and error, it became clear there were two important factors, firstly the temperature, and secondly the catalyst. At higher temperatures, the most thermodynamically stable compound should be formed, hence, the more imidazole **268** should be obtained. Therefore, *o*-xylene (b.p. 141 °C) gave the best results (entries 5 and 6). The other important factor was the catalyst. It was known that acid catalysis[202] improves this reaction, but it was important to use the right acid. Because *o*-xylene was used as solvent, the best results were gained with *p*-TsOH (Table 15, entries 10-12), giving yields between 64 and 86%.[203] This was not only because of its high acidity but was also due to its toluene group which made it reasonably soluble under the solvent conditions used. With both the bromine and iodine derivatives, good yields were obtained under these conditions (Table 15, entries 10-12).

Next, imidazole **268** was used for the allylation and then the Heck reaction (Scheme 39).

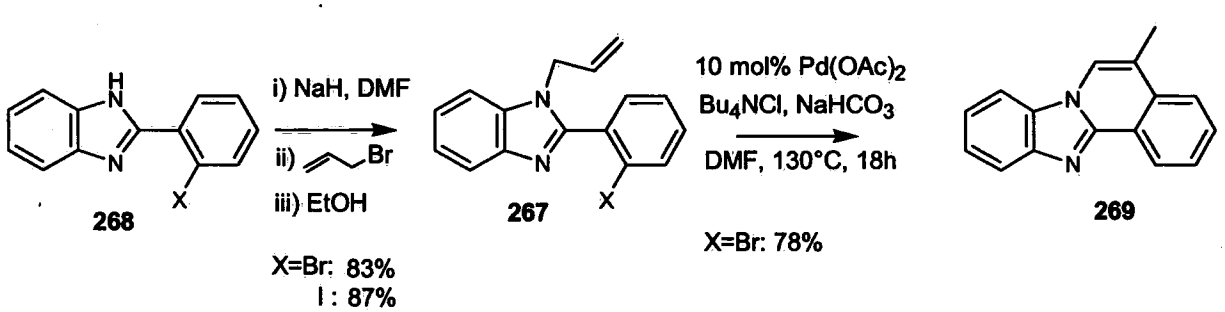

Scheme 39. The cyclisation by Heck reaction.

The allylation of **268** was straightforward giving **267** in a good yield (83 and 87%) for both halogen derivatives. The next step was the most important one. Although it was known that the Heck coupling was more favourable for an *exo*ring closure when 5, 6 and 7-membered rings are formed, our target molecule had a 7-membered ring, so it should be possible.[196] Not unexpectedly, the competing 6-membered ring formation occurred to give compound **269** with a good yield (78%). Interestingly, there was also a shift of the alkene to the inside of the ring in product **269**. The shift of the double bond was probably due to the reaction conditions which favour the thermodynamic product leading to aromatic compound **269**. Although, this molecule was not our target molecule, it possessed some interesting characteristics such as the methyl group on the 6-membered ring. If it was possible to reduce **269** to **270**; the methyl group would favour an equatorial position and would provide the six-membered ring with some conformational stability and a new chiral centre. This could be useful to control the angle between the benzimidazole and the phenyl group and hence, for chiral induction. Out of molecule **270** a corresponding bifunctional catalyst would then be possible be placing the boron group through a direct lithiation approach. Therefore, several attempts were made to reduce **269** (Equation 47, Table 16).

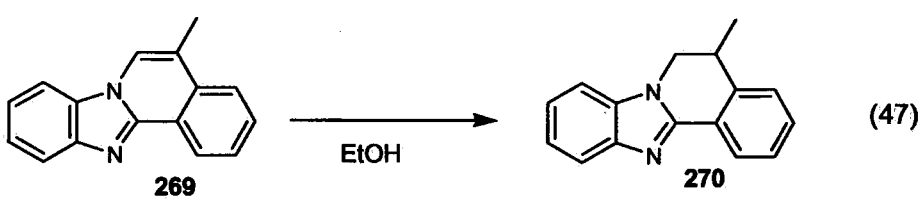

269 **270** (47)

Table 16 : Reduction of **269**.

Entry	Reducing agent (Eq.)	Time	Temp. (°C)	H_2 pressure	Yield **270**
1	Pd/H_2 (10%)	20 min.	30	50 bar	S.M.
2	Pd/H_2 (10%)	1.5h	50	80 bar	S.M.
3	$NaBH_4$ (10 eq.)	29h	reflux	N.A.	S.M.

The first attempts at reduction of **269** (Table 16, entries 1 and 2) involved hydrogenation and Pd under high pressure. In both cases, only starting material was obtained. The aromaticity of the molecule **269** made it hard to reduce even under extreme conditions. Also, an alternative method of using $NaBH_4$ (Table 16, entry 3) (since some papers[204] used this on similar molecules)

produced only starting material. Because of these problems to reduce **269**, the focus was again on our target molecule **257**.

3.4.4.Pathway A: Radical cyclisation

Since now molecule **267** was created, it was considered useful to try also a radical reaction on it. In the literature, there are several papers reporting the synthesis of seven-membered rings by radical reaction using these functional groups (a halogen on phenyl group and a double bond), since it was known that a radical was more stable on a secondary carbon than on a primary one. So, it was expected in our case that the formed radical on the phenyl would attack the alkene at the terminal carbon giving a 7-membered ring. Therefore, several attempts were made to generate **258** (Equation 48, Table 17).[205]

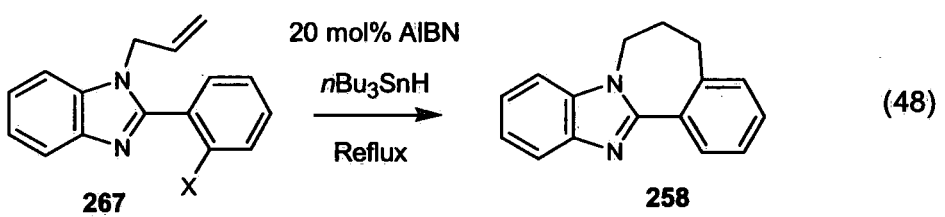

267 **258** (48)

Table 17: Radical cyclisation on **267**.

Entry	X	Solvent	Temp. (°C)	Time (h)	Yield
1	Br	benzene	80	24	Only S.M.
2	Br	toluene	110	23	Only S.M.
3	Br	*o*-xylene	141	23	Only S.M.
4	I	*o*-xylene	141	48	Only S.M.

* Based on crude ^{1}H NMR.

Unfortunately, in none of the cases was a significant amount of product **258** formed and only starting material was recovered, even under the most severe conditions at 141 °C for 2 days (Table 17, entry 4). Strangely, not even the dehalogenated product **264** was observed. This indicated that the initial debromination/deiodination step was not proceeding, implying that the halogen-carbon bond was too strong. It was concluded that this type of molecule was unreactive towards radicals, and therefore, only resulted in starting material. So another reaction had to be considered.

3.4.5.Pathway A: Parham cyclisation

Another option to create the scaffold **258** was found in the Parham cyclisation. This type of cyclisation was first introduced by Parham *et al.* in 1975[206] and it was based on a selective lithium-halogen exchange followed by an intramolecular S_N2 cyclisation (general Equation 49). The lithium-halogen exchange was triggered by *n*-BuLi which would selectively exchange with the bromide on the phenyl group. This high selectivity was based on the higher stability of the formed anion on a sp^2 carbon than on a sp^3 carbon. Through this mechanism this group had managed to create different rings with sizes between 4 to 7 members.

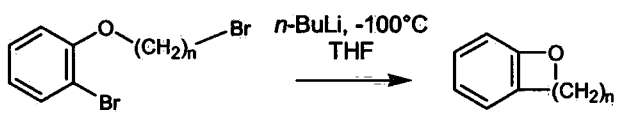

(49)

n: 1,2,3,4

n: 1 68%
2 78%
3 80%
4 73%

Since it was reported that also 7-membered rings were created in high yield, this reaction seemed interesting to try. Therefore, it was first necessary to attach a 3-bromopropyl group onto molecule **268**. Knowing from previous experiments (Equation 44) how difficult it was to avoid the elimination side reaction on this type of molecules, several attempts were made. By gradually increasing the temperature, it was found that at 0 °C, the best results were obtained for the alkylation onto **268**. Under these conditions the elimination product was negligible and still a considerable amount of product **271** was formed. Although the yields were rather poor (especially for the iodine derivative), it was considered appropriate to continue and to optimize the reaction afterwards, if the outcome was positive for the cyclisation (Equation 50).

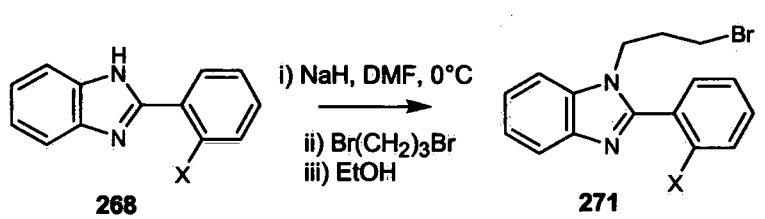

268 **271**

(50)

X= Br: 50%
I: 24%

The next step was now to examine the Parham cyclisation on molecule **271**. Because the bromine derivative of molecule **271** was more available, it was examined for the test reaction (Equation 51, Table 18).

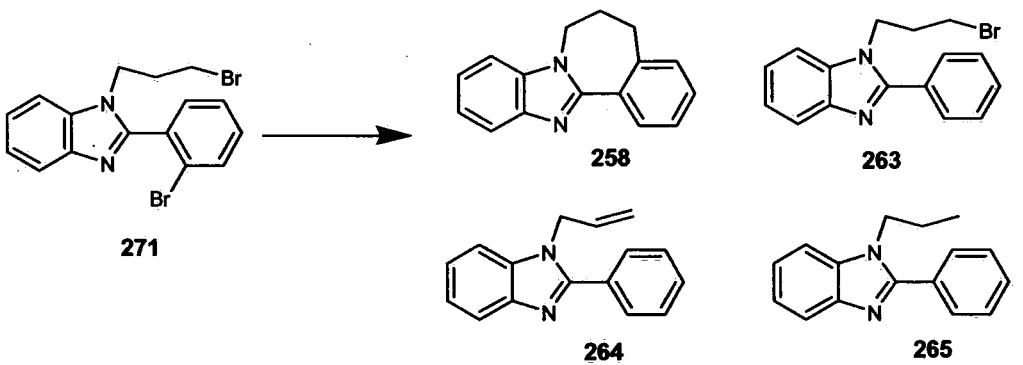

(51)

***Table 18*: Parham cyclisation on 271.**

Entry	BuLi (Equiv.)	Solvent	Conditions	258[a]	263[a]	264[a]	265[a]
1	*t*-Buli (1.25)	Et_2O	1.5h at -78 °C, from -78 °C to rt overnight	0%	29%*	0%	17%
2	*n*-BuLi (1.1)	THF	2h at -78 °C, from -78 °C to rt overnight	18%	45%	11%	0%
3	*n*-BuLi (1.25)	Et_2O	2h at -78 °C, from -78 °C to rt overnight	7%	26%*	6%	0%
4	*n*-BuLi (1.4)	THF	2h at -42 °C, from -42 °C to rt overnight	4%	22%	4%	0%
5	*n*-BuLi (1.4)	THF	1.5h at –42 °C, from -42 °C to 0 °C, 6h at 0 °C, from 0 °C to rt overnight	17%	18%	7%	0%
6	*n*-BuLi (1.25)	*t*-BuME	2h at -78 °C, TMEDA used, from -78 °C to 0 °C, 3h at 0 °C, from 0 °C to rt overnight	0%	15%*	6%	0%
7	*n*-BuLi (1.4)	*t*-BuME	1h at -78 °C, Li_2CuCl_4 used, from -78 °C to rt overnight	0%	17%	15%	0%
8	*n*-BuLi (1.3)	THF	1.5h at -78 °C, Me_2S-CuBr used, From -78 °C to rt overnight	0%	26%	3%	0%

[a] Isolated yield, * Small fractions of S.M. present.

In the first attempt (Table 18, entry 1), *t*-BuLi was used and it became clear that these conditions were too reactive since the reaction mixture was messy. Out of the different products, only **263** and **265** could be recovered and no product **258** was present. The presence of **265** showed that *t*BuLi was too reactive, and it even exchanged with the bromine on the sp^3 carbon. Therefore, it was decided to follow the same conditions as Parham *et al.* by using *n*-BuLi (entry 2) instead. Under these conditions, the desired product **258** was formed but rather in low yield of 18%. The high presence of **263** showed that lithium-halogen exchange was good in selectivity and conversion, but the cyclisation was slow (this is typical for 7-membered rings). Another interesting side product was **264**, which indicated that there was also an elimination reaction

competing which could be either intermolecular or intramolecular. The presence of these side products made it hard to isolate the desired product **258** since all three compounds had almost the same Rf value. In an attempt to increase the amount of **258**, the original procedure was repeated, but this time in diethyl ether (entry 3). This solvent was chosen since it was known that the anion remained longer in Et_2O than in THF (at 25 °C the $t_{1/2}$ for *n*-BuLi in THF is 10 min, in Et_2O 6 days). In that way, more product **258** could be generated instead of being neutralized to **263**. Unfortunately, only 7% of **258** could be isolated. Presumably, the Et_2O is not polar enough to enhance the S_N2 reaction. In other attempts (Table 18, entries 4 and 5) to convert **271** into **258**, the temperature was increased to –42 °C and the reaction time was extended. These modifications should normally help the cyclisation, but again in vain. To check if any anions were still present on the next day, entry 5 was quenched with TMSCl instead of normal water. After isolation and analysis no product with the TMS group attached was spotted, indicating all anions were already neutralised by the solvent. With this information the reaction was repeated but now with *t*-butyl methyl ether (entry 6). This solvent is even more resistant towards strong bases (at 25 °C the $t_{1/2}$ for *n*-BuLi in *t*-BuME is 14 days) than Et_2O. Also TMEDA[207] was added in the hope of breaking a possible nitrogen-lithium-anion chelation (see below) and to give the anion more freedom, but again, no improvement was noticed. In the last attempts, copper catalysts were added (Table 18, entries 7 and 8) to soften the anion. These catalysts would reduce the elimination side reaction, and they are known to improve the C-C coupling reaction. In entry 7, Kochi's catalyst (Li_2CuCl_4)[208] was tried and in entry 8 Me_2S-CuBr was used,[209] unfortunately, in both cases no improvement in the yield of product **258** was observed.

These results showed that system **271** was not really suitable for the Parham cyclisation. Although product **258** was formed, the yield was too low and there were too many side products. Especially product **263** was significant, not only did it complicate the isolation of **258** but it also showed that the problem was the actual cyclisation step. One of concerns was the use of BuLi. By using BuLi, the reaction could only be run at low temperature for a relatively short time, otherwise the solvent would neutralize the anion. These are just the conditions which inhibit the ring formation. Due to these limitations, it was thought to change the metal lithium to magnesium and to use a Grignard reaction.

3.4.6.Pathway A: Cyclisation by Grignard reaction

From previous experiments, knowledge was obtained that our product **258** could be created through organometallic reactions. The problem was not the selectivity for the anion position, which was only present on the sp^2 carbon, but rather the actual cyclisation itself. Because the Parham reaction only was possible at reasonably low temperatures, it was decided to repeat the reaction this time with magnesium. The advantage of the Grignard reaction was the possibility to increase the temperature to reflux for a considerable amount of time without the anion being neutralized by the solvent due to the less ionic magnesium carbon bond. These conditions would favour the cyclisation, especially for difficult 7-membered rings. To improve the formation of **258**, Kochi's catalyst (Li_2CuCl_4) was added.[208] Kochi's catalyst is well known to accelerate C-C coupling reaction, especially the couplings with alkyl halides under Grignard conditions. For this screening, both derivatives of molecule **271** were tried (Equation 52, Table 19).

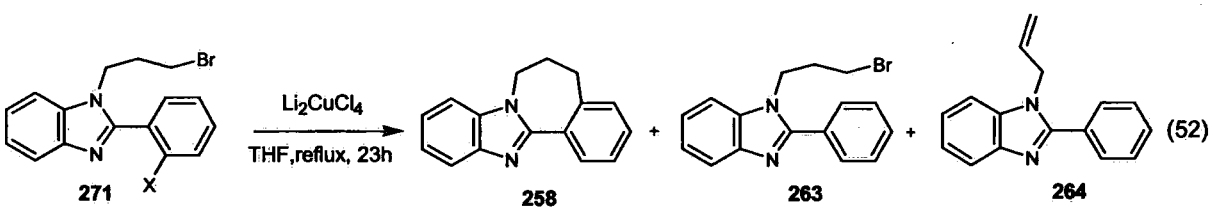

(52)

Table 19: Grignard reaction on **271**.

Entry	X	Grignard	258	263	264
1	Br	^{i}PrMgCl	Only S.M.		
2	Br	Mg	Only S.M.		
3	I	^{i}PrMgCl	N.A.	traces	N.A.
4	I	Mg	25%	17%	11%

[a] Isolated yield.

In the first reactions (Table 19, entries 1 and 2) the bromine derivative **271** was initiated under two different conditions; by the conventional Grignard reaction and by the halogen-magnesium exchange. The latter was well known from the chemistry of Knochel who introduced this type of Grignard derivative.[210] Because the conventional Grignard reaction can be sluggish and hard to initiate, this ^{i}PrMgCl type of halogen magnesium derivative could be a good alternative. Unfortunately, under both conditions, only starting material was obtained. By replacing the bromine with an iodine it was hoped to be more successful since the iodine derivatives are more reactive. Although the halogen-magnesium exchange was not very fruitful (entry 3), the conventional conditions (entry 4) were more effective for our iodine derivative **271**. Although

our wanted product **258** was formed (25%), there was only a small improvement in yield compared to the Parham cyclisation and still the two side products **263** and **264** were present.

These disappointing results indicated that **271** was not really suitable for organometallic reactions, more precisely for the Parham and Grignard cyclisations. The low yields could be due to two major reasons:

1) The rigid structure of **271**. When looking back at the example of the Parham cyclisation (Equation 49), the alkyl chain is flexible and should help the cyclisation. In our molecule **271**, this alkyl chain only consists of three carbons which are attached to the less flexible benzimidazole section. It is this benzimidazole that presumably inhibits the ring formation, especially for 7-membered rings which are already hard to make.
2) Nitrogen-metal chelation. Since the metal-halogen exchange will occur on the phenyl group at the *ortho*-position, this metal will not only be chelated to the corresponding anion, but also to the sp^2 nitrogen of the benzimidazole group (see **272**). This chelated conformation will inhibit the free rotation of the phenyl group, and since the alkyl group is situated at the other site of the molecule, it may also prevent cyclisation.

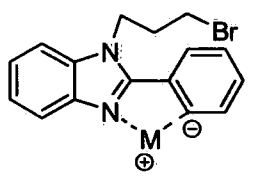

272

Since the various efforts to make **258** through pathway A were not satisfactory (the synthesis of product **258** was possible but the yields were too low and too many side products interfered with the isolation), a new synthetic path had to be found.

3.4.7.Pathway B: C-C Coupling

In the new pathway B it was thought necessary to start off with this the problematic C-C coupling by attaching the alkyl chain to the phenyl ring creating **274**. This chain would eventually become the backbone of the 7-membered ring. In that way, any problematic side product could be removed in future steps and the final scaffold **258** would be easier to obtain pure. Compound **274** was already known in the literature,[211] but it took four complicated steps to be made. Because of time constraints it was better to synthesise **274** in one step using a new

method. Therefore, 2-bromobenzaldehyde was protected at the carbonyl group with ethylene glycol using a standard Dean Stark method which gave **273** in a good yield (84%).[212] The next step was the coupling of **273** with the 1,3-dibromopropane. In order to have a good yield, several attempts were made (Equation 53, Table 20).

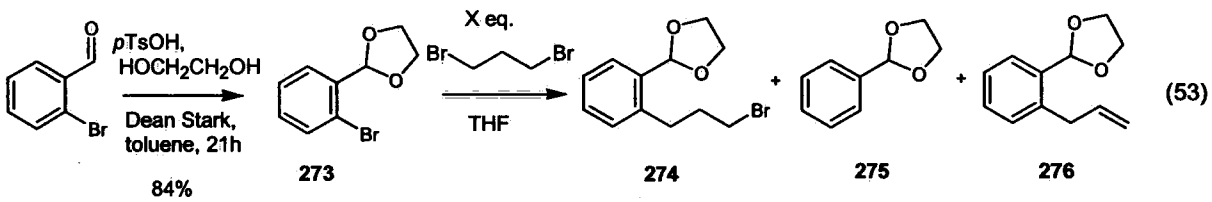

(53)

Table 20 : The C-C coupling of **273** with 1,3-dibromopropane.

Entry	Metal (eq.)	Catalyst (eq.)	X (eq.)	Conditions	**274**[b]	**275**[b]	**276**[a]	S.M.[a]
1	*s*-BuLi (1.3)	None	5	-78 °C, -78 °C to rt, over 16.5h	7%	26%	0%	28%
2	Mg (1.2)	Li_2CuCl_4 (0.02)	5	0 °C (2h), 0 °C to rt over 16.5h	8%	48%	0%	0%
3	^{i}PrMgCl (1.2)	Li_2CuCl_4 (0.02)	10	Reflux, 24h	0%	0%	0%	100%
4	Mg (1.2)	CuBr (0.05), HMPA	5	Reflux, 18h	20%	38%	0%	0%
5	Mg (1.2)	CuBr (0.1), HMPA	7.5	Reflux, 67h	43%	17%	17%	0%

[a] Isolated yield.
[b] **274** and **275** isolated in same fraction, yield on basis of recovered mass and ratio ^{1}H NMR.

In the first approach a standard lithium-halogen exchange was tried with *s*-BuLi (Table 20, entry 1).[213] Unfortunately, only 7% of **274** was obtained and the reaction was mainly a mixture of starting material and debrominated compound **275**. To push the reaction further, a Grignard reaction was suggested. In that way, the reaction could be run at higher temperature (improving the yield of **274**) but also the conversion of starting material would be complete (this is typical for Grignard reactions when it initiates). To improve the coupling, Kochi's catalyst was also added (entry 2).[208] Although all starting material was consumed, the yield was still low (only 8%). The reaction was repeated with Knochel's Grignard derivative (entry 3),[210] but in this case, no exchange was observed. Besides Li_2CuCl_4, another coupling reagent (CuBr) was tested (entries 4 and 5).[214] To improve the solubility of the copper metal, HMPA was added. This time a significant improvement in yield of **274** was observed. Because there was still a lot of **275**, which indicated that not all the Grignard derivative had reacted, the amount of CuBr was

increased, as was the time. These adaptations led to a moderate yield (43%) of **274**. Although there was still **275** present, it could be concluded that the reaction was finished since it was thought that **275** acted as a base for the elimination side reaction. This explained why there was exactly the same amount of elimination product **276** present. It appeared that when the Grignard method was followed, the order of addition was very important. Only when the Grignard derivative was added to the 1,3-dibromopropane, CuBr and the HMPA mixture, was product **274** formed. When the reverse was done (adding the electrophile to the Grignard), only side products were obtained. Also, it was found that both **274** and **275** had the same Rf values, so only mixed fractions of **274** were isolated. In an attempt to purify **274** by distillation, it was found that the boiling points of **274** and **275** were too close to be separated.

Since this coupling reaction was to be the most difficult step of the pathway, the moderate yield of 43% was considered sufficient at this stage. The mixed fraction of **274** did not cause a problem either, because the next step was an S_N2 reaction of the 1,2-benzenediamine. Since this diamine could only target **274**, the presence of **275** in this fraction would not cause any side reactions. So pathway B was further continued.

3.4.8.Pathway B: Synthesis of scaffold **258**

Since the coupling reaction was now achieved in moderate yield, pathway B was continued. The next steps should be easier so only a small amount of optimization was needed. The rest of the pathway B is shown in Scheme 40.

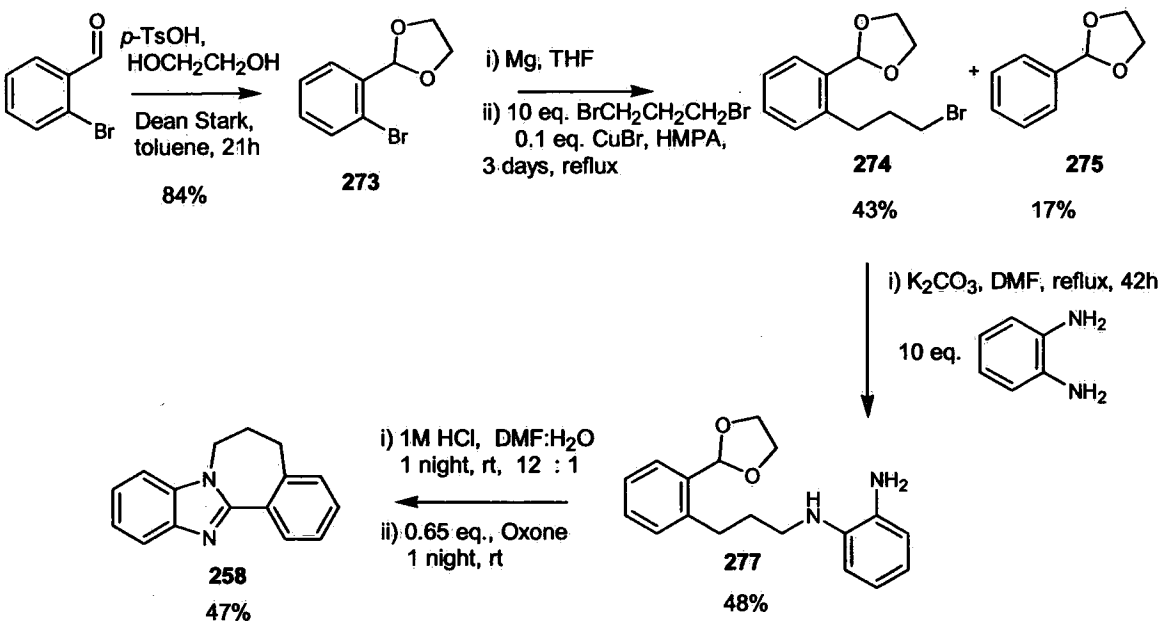

Scheme 40. Pathway B for synthesis of **258**.

After the protection of the aldehyde to **273** and the addition of the alkyl chain to give **274**, the mixture of **274** and **275** was slowly added to an excess of the 1,2-benzenediamine.[215] This excess was needed to avoid any double alkylation on the same diamine. The reaction was clean giving only three spots by TLC corresponding to the excess of diamine, product **277** and debrominated **275**. Through this reaction it was now possible to remove the side product **275** and to obtain **277** as pure compound through silica gel column chromatography. Although the reaction was straightforward, it was noticed that product **277** was unstable. This explained the moderate yield and also inhibited obtaining a full characterisation of **277**. So, after the purification and drying on high vacuum, **277** was immediately used in the next step. This next step was a 2-step, one-pot synthesis consisting of a deprotection and an oxidation. This was more convenient and less time consuming. In the first part, the protecting group of the aldehyde was removed by a HCl/water mixture overnight.[212] It was thought that after the deprotection the molecule would automatically cyclise by an attack of the nitrogens on the aldehyde forming an imidazolidine. Therefore, it was important to dilute the mixture sufficiently so that only intramolecular cyclisation would occur. The following day, the mixture was neutralised and Oxone® was added to form the corresponding benzimidazole group.[216] By using a 20% NaOH solution in the work up, all side products and starting material were removed and almost pure product **258** was obtained in

reasonable yield (47%). Unfortunately, the ^{1}H NMR spectrum showed that **258** was not atropisomeric stable, not even at 0 and -30 °C. This indicates that the rotational barrier is too low to prevent interconversion. It was hoped by replacing the proton on the *ortho*-position by a more bulky group the rotational barrier would increase and prevent this inversion.

It was clear pathway B was the best way to synthesise scaffold **258**. Not only was the purification much easier but also the overall yield was much higher compared to pathway A. Now the pure **258** had been isolated, and the final step was possible.

3.4.9.Direct lithiation on scaffold **258**

The final step to form our target molecule **257** consisted of a direct lithiation on scaffold **258**. It was hoped that the same regioselectivity was possible with **258** as previously mentioned with molecule **135** (Scheme 17). In this way, the same sp^2 nitrogen in the benzimidazole group would control the *ortho*-deprotonation. Due to time limitations only two test reactions were possible on our new scaffold **258** (Scheme 41).

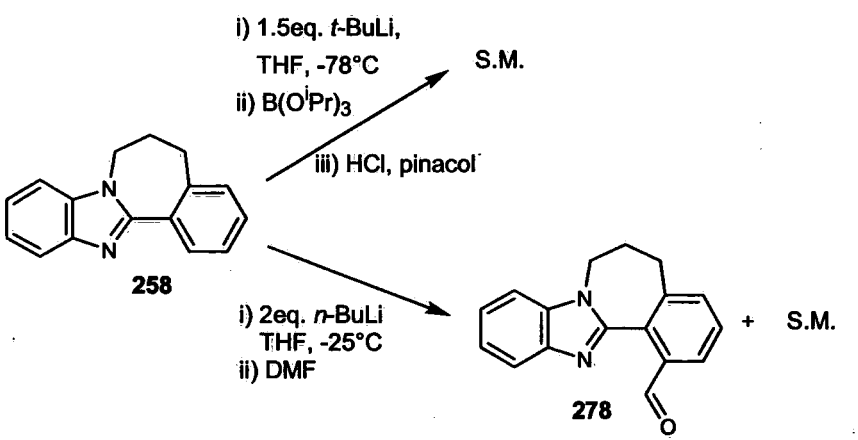

Scheme 41. Direct lithiation on scaffold **258**.

It was decided first to apply the same conditions as with the synthesis of boroxine **136**. So again, *t*-BuLi was used at -78 °C with $B(O^iPr)_3$ as electrophile. Pinacol was also added at the end to make the corresponding boronic ester which would facilitate the isolation. Unfortunately, only starting material was isolated. Because of the absence of any product, it was proposed to increase

the reactivity by rerunning the reaction at -25 °C using *n*-BuLi. Now, DMF was added as electrophile so the corresponding aldehyde **278** would be formed. This time, there was product **278** formation albeit in low yield (29%). Although these were reactive conditions, still starting material was present. However, it was pleasing to observe only aldehyde **278** was formed which implied that even on scaffold **258** the regioselectivity for the direct lithiation was still high. Interestingly, the last reaction conditions used were the same conditions as used with the *n*-butyl 2-phenylbenzimidazole **135** (Equation 22), but in that case, a yield of 87% was isolated. Since with scaffold **258** starting material was still present, it indicated that the direct lithiation of **258** was more difficult. This could be caused by the extra ring which limited the flexibility of the phenyl group. So it was harder to obtain the right angle between the nitrogen-lithium-phenyl anion chelation **272**. For future reactions it will be necessary to increase the temperature to 0 °C, as long as the regioselectivity is sustained. Also different electrophiles can influence on the direct lithiation, which needs to be taken into account.

3.4.10.Summary

Our final objective was to create this new chiral bifunctional catalyst **257**, which was not reached due to time shortage but it was clear that the synthesis almost was finished. Although pathway A did not lead to the desired product **258**, it gave some interesting information about different reactions and also different side products like **266** and **269** were obtained. On the other hand, pathway B was very successful. Not only was it possible now to access **274** in one step, but it was also a new way to synthesise the seven-membered ring **258**. Further, it was shown by product **278** that still regioselectivity could be obtained in the direct lithiation of new scaffold **258**. In the future, the bifunctional catalyst **257** may be prepared by changing the electrophile to $B(O^iPr)_3$.

4.Conclusions and future work

It is clear this PhD work has revealed some interesting information both on synthetic chemistry as in the catalytic field. It is now possible to optimize the synthetic pathway of some old catalysts like **127**, **136** and **129**, and to make their syntheses reliable. During the making of these catalysts some interesting side effects were observed like the formation of **132**. Also the regioselective direct lithiation on **135** was investigated and optimised for the different electrophiles. Unfortunately, some of the planned catalysts, like **143** and **150**, were unable to be completed to different reasons (purification problems or instability etc.). Although the screening of these catalysts **126**, **127** and **136** showed they were inactive towards both the Morita-Baylis-Hillman reaction and the aza-Morita-Baylis-Hillman reaction, some deeper insight was gathered from the standard runs and the new imine synthesis of **164**.

The screening on the aldol reaction was more successful especially with **129**. Not only was it possible to select which product would be formed by only changing the solvent (see THF for aldol product, water for condensation product), but also information was gained on the regioselectivity using 2-butanone. The biggest scoop was the use of hydroxyacetone; with catalyst **129** some good yields were gained between 46 to 97 %, not only on aromatic aldehydes, but also on aliphatic and sterically hindered aldehydes like trimethylacetaldehyde. The high regioselectivity and the *syn*-diastereomeric excess with hydroxyacetone were remarkable. From the blank reactions and the kinetic data it was proven that catalyst **129** was the actual catalyst. This kinetic data revealed that both the reactions with acetone and hydroxyacetone were first order and a mechanistic view could be proposed.

In the final stage of this PhD, a corresponding chiral derivative **257** was introduced. Two different pathways were considered: pathway A and pathway B. Pathway A was shown to be unsuccessful due to low yield and difficult purification, still some interesting side products like **266** and **269** were isolated. Pathway B was much better, leading us to the seven-membered scaffold using some new chemistry to create **274** (by C-C coupling through Grignard) and scaffold **258** (by a one-pot intramolecular cyclisation and oxidation). Unfortunately, the final

catalyst **257** was not produced but the corresponding aldehyde **278** using DMF was. This showed that the direct lithiation on scaffold **258** was regioselective giving the *ortho*-product **278**. In the future, it must now be possible to create chiral catalyst **257** using the same chemistry but changing the electrophile to a boron derivative.

5.Experimental work

5.1.General Experimental

All starting materials were obtained commercially from Aldrich, Lancaster or Fluka and were used as received or prepared by known methods, unless otherwise stated. Solvents were also used as received or dried by known methods, unless otherwise stated. In the case of DCM and toluene this involved refluxing over $CaCO_3$ under argon and in the case of ether and THF involved refluxing over sodium and benzophenone under argon. Purification by column chromatography was performed using Lancaster silica gel with pore size 60 Å, 40 Å or Florisil®. TLC was carried out using Merck aluminium-backed or plastic-backed pre-coated plates. TLC plates were analysed by UV at 254 and 365 nm, and visualisation was performed using standard solutions of 4-anisaldehyde, vanillin or PMA. NMR spectra were recorded at 200, 300 or 400 MHz using a Varian Mercury 200 MHz spectrometer, Varian Unity 300 MHz spectrometer or a Brucker 400 MHz spectrometer, respectively, otherwise stated. Electrospray (ES) mass spectra were recorded using a Micromass LCT spectrometer. Infra red spectra were obtained using FT1600 series spectrometer. Ultra-violet spectra were measured using a Unicam UV-VIS UV2 spectrometer. Melting points were measured with an Electrothermal apparatus and were uncorrected. Evaporations were carried out at 20 mmHg using a Büchi rotary evaporator and water bath, followed by evaporation to dryness under vacuum (<2 mmHg). Chloroform used in the preparation of the phosphoryl compounds was Aldrich HPLC grade 99.9% stabilised with amylases. Elemental analysis was performed at the Chemistry department of the University of Durham by technical staff.

5.2.Synthesis of catalysts

Synthesis of morpholinobenzylamine-2-boronic acid **127**

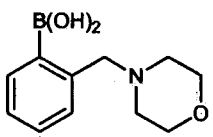

127

To a stirred suspension of 3Å molecular sieve pellets (13 g) in dry THF (45 ml) was added 2-formylbenzeneboronic acid **130** (6.0 mmol, 0.897 g) and morpholine **131** (6.6 mmol, 0.575 ml). under argon. The reaction was stirred for one day at room temperature, then sodium triacetoxy-borohydride (24.0 mmol, 5.1 g) was added. After one day, the reaction was quenched with DCM (50 ml), filtered through Celite, extracted with DCM (2 x 50 ml) and the combined organic extracts evaporated. The crude mixture was redissolved in DCM (50 ml) and washed with brine (3 x 20 ml) and water (15 ml). Both phases were evaporated and this was repeated for 2 more times. The crude product was again diluted in DCM, dried ($MgSO_4$) and evaporate to give product **127** as a white powder (0.68 g, 51% yield). Mp: 199-201 °C. IR (neat): ν_{max}/cm^{-1} 3389w (OH), 2865br (Ph-H), 1445, 1343 (N-Ar), 1119 (NR_3). δ_H (400 MHz; $CDCl_3$; D_2O) 2.45 (4H, br s, $(CH_2)_2N$), 3.56 (2H, s, $ArCH_2$), 3.65 (4H, br s, $(CH_2)_2O$), 7.04-7.10 (1H, m, Ph), 7.22-7.28 (2H, m, Ph) and 7.88 (1H, t, *J* 5.2, Ph) ppm; δ_H (500 MHz; DMSO; 70 °C) 2.43 (4H, t, *J* 2.5, $(CH_2)_2N$), 3.10 (2H, s, $ArCH_2$), 3.58 (4H, t, *J* 2.0, $(CH_2)_2O$), 7.20 (1H, d, *J* 7, Ph), 7.25 (1H, t, *J* 7, Ph), 7.29 (1H, t, *J* 7, Ph) and 7.69 (1H, d, *J* 7, Ph) ppm. δ_C (100 MHz; $CDCl_3$; D_2O) 52.4 (2C), 64.5, 66.4 (2C), 127.7, 130.2, 130.8, 136.5 and 140.3 (carbon next to boron not seen) ppm; δ_B (128 MHz; $CDCl_3$; D_2O) 29.2 ppm. *m/z* EI (+) 222.1295 (M^+, 100%) $C_{11}H_{17}O_3NB$ requires 222.1296. Found: C, 59.55; H, 7.30; N, 6.03. $C_{11}H_{16}O_3NB$ requires C, 59.71; H, 7.23; N, 6.33%.

Synthesis of **132**

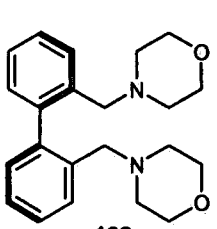

132

Morpholinobenzylamine-2-boronic acid **127** (0.40 g, 1.81 mmol) was added to water (3 ml) and was heated until it completely dissolved. After approximately 12 months in a sealed flask with a needle hole allowing slow evaporation, crystallisation occurred. The colourless crystals (51 mg, 16%) were collected by filtration and analysed corresponding to **132**. Mp: 251-253 °C. IR

(neat):ν_{max}/cm^{-1} 2925 (br, Ar), 2874 (br, CH), 1454 (s), 1314 (m) and 1086 cm^{-1}. δ_H (400 MHz, $CDCl_3$) 2.20 (8H, t, *J* 4.4, ($PhCH_2N(CH_2CH_2)_2O)_2$), 3.06 (2H, d, *J* 13.4, ($PhCH_2N(CH_2CH_2)_2O)_2$), 3.16 (2H, d, *J* 13.4, ($PhCH_2N(CH_2CH_2)_2O)_2$), 3.55 (8H, t, *J* 4.8, ($PhCH_2N(CH_2CH_2)_2O)_2$), 7.06 (2H, dd, J_1 7.4, J_2 1.6, Ar), 7.19 (2H, td, J_1 6.8, J_2 1.2, Ar), 7.26 (2H, td, J_1 7.4, J_2 1.2, Ar) and 7.46 (2H, d, *J* 7.2, Ar) ppm. δ_C (100 MHz, $CDCl_3$) 53.5 (4C), 60.3 (2C), 67.1 (4C), 126.3 (2C), 127.1 (2C), 129.0 (2C), 130 (2C), 136.0 (2C) and 141.2 (2C) ppm. Found C, 74.92; H, 8.06; N, 7.93. $C_{22}H_{28}N_2O_2$ requires C, 74.97; H, 8.01; N, 7.95%

Synthesis of *N*-benzylmorpholine **133**

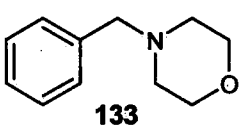

133

Morpholine **127** (100 mg, 0.45 mmol) was dissolved in water (13 ml) and the solution was slightly heated until everything was dissolved. $Pd(OAc)_2$ (7 mg, 0.03 mmol) was added and the mixture was left stirring for 4 days at rt with air bubbling through. After 4 days, the reaction was extracted with DCM (3 x 30 ml), the combined organic phases were dried ($MgSO_4$) and evaporated to give a brown crude oil (89.3 mg) which was purified by silica gel column chromatography (hexane: ethyl acetate, gradient elution) to provide **133** (64 mg, 0.361 mmol) in 80% yield as an orange oil. IR (neat):ν_{max}/cm^{-1} 3468 (br, OH), 2954 (br, Ar), 2865 (s, CH), 1445 (s), 1343 (BenzN) and 1119 (NR_3) (m) cm^{-1}. δ_H (400 MHz, $CDCl_3$) 2.35 (4H, t, *J* 4.2, $PhCH_2N(CH_2CH_2)_2O$), 3.41 (2H, s, $PhCH_2N(CH_2CH_2)_2O$), 3.62 (4H, t, *J* 4.2, $PhCH_2N(CH_2CH_2)_2O$) and 7.14-7.35 (5H, m, Ar) ppm. δ_C (100 MHz, $CDCl_3$) 52.6 (2C), 62.4, 66.0 (2C), 126.1, 127.2 (2C), 128.2 (2C) and 136.8 ppm. m/z EI(+) 178.1228 ($M+H^+$, 100%), $C_{11}H_{15}ON$ requires 178.1226 ($M+H^+$).

Synthesis of 2-phenyl-*N*-*n*-butylbenzimidazole **135**

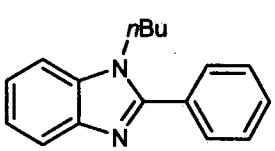

135

NaH (300 mg of 60% oil suspension, 7.5 mmol) was washed with dry hexane (3 x 10 ml) and suspended under argon in anhydrous DMF (25 ml). **134** (971 mg, 5.0 mmol) was added with stirring, and after 10 min., *n*-BuBr (0.54 ml, 5.0 mmol) was added dropwise over 15 min. The mixture was heated to 140 °C and allowed to cool after 6 h. The reaction was quenched with EtOH (0.5 ml) and evaporated after 10 min. The mixture was diluted with ether (20 ml), washed

with 20% aqueous NaOH (3 x 10 ml). The organic phase was dried ($MgSO_4$), and evaporated to give **135** (1.10 g, 4.39 mmol) as a dark yellow oil in 88% yield. All spectroscopic and analytical details were identical to those reported by Blatch.[145] IR (neat):ν_{max}/cm^{-1} 3157 (br, amine) 2978 (br, Ar), 2905 (s, CH), 1453 (s), and 1314 (m) cm^{-1}. δ_H (400 MHz, $CDCl_3$) 0.69 (3H, t, *J* 7.2, $NCH_2CH_2CH_2\mathit{CH_3}$), 1.09 (2H, hextet, *J* 7.6, $NCH_2CH_2\mathit{CH_2}CH_3$), 1.62 (2H, quintet, *J* 7.4, $NCH_2\mathit{CH_2}CH_2CH_3$), 4.04 (2H, t, *J* 7.4, $N\mathit{CH_2}CH_2CH_2CH_3$), 7.14-7.16 (2H, m, Ar), 7.24-7.26 (1H, m,Ar), 7.34-7.36 (3H, m, Ar), 7.55-7.57 (2H, m, Ar) and 7.70-7.73 (1H, m, Ar) ppm. δ_C (100 MHz, $CDCl_3$) 12.4, 18.7, 30.7, 43.4, 109.1, 118.6, 121.2, 121.6, 127.7 (2C), 128.2 (2C), 128.6, 129.8, 134.6, 142.1 and 152.6 ppm. *m/z* EI (+) 251.1542 ($M+H^+$, 100%) $C_{17}H_{19}N_2$ requires 251.1543.

Synthesis of 2-(*N*-*n*-butyl-benzimidazole)phenyl boroxine **136**

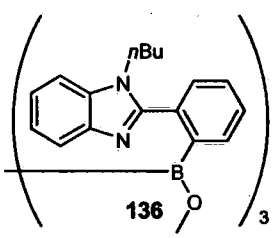

After drying 2-phenyl-*N*-*n*-butylbenzimidazole **135** (338 mg, 1.35 mmol) on P_2O_5 overnight, it was dissolved in dry THF (14 ml) under argon and cooled to -78 °C. *t*-BuLi (1.35 ml, 1.5 M in pentane, 2.02 mmol) was added dropwise over 40 min. After stirring for 2 h at -78 °C, $B(^iOPr)_3$ (0.65 ml, 2.69 mmol) was added. After stirring for 1 h at -78 °C, the mixture was allowed to warm slowly to rt over 12 h. The reaction was quenched with 10% NaOH (8 ml), after 10 mins. it was neutralised with 10% aqueous HCl (8.5 ml) evaporated. A white precipitate formed which was collected by filtration to give a crude solid which was purified with alumina chromatography (ethyl acetate to 15% MeOH/CH_3CN, gradient elution), giving the product **136** (246 mg, 0.297 mmol) as a white powder in 66% yield. Mp: 238-239 °C. IR (neat): ν_{max}/cm^{-1} 3055, 2957, 2931, 2869, 1459, 1433, 1397, 1358, 1297 and 737 cm^{-1}. δ_H (400 MHz, $CDCl_3$) 0.77 (9H, t, *J* 7.2, $NCH_2CH_2CH_2\mathit{CH_3}$), 1.21 (6H, hextet, *J* 8, $NCH_2CH_2\mathit{CH_2}CH_3$), 1.60 (6H, quintet, *J* 7.6, $NCH_2\mathit{CH_2}CH_2CH_3$), 3.96 (6H, t, *J* 7.2, $N\mathit{CH_2}CH_2CH_2CH_3$), 7.02 (3H, d, *J* 8, Ar), 7.09-7.19 (12H, m, Ar), 7.27-7.30 (3H, m, Ar) and 7.53-7.55 (6H, m, Ar) ppm. δ_c (100 MHz, $CDCl_3$) 13.6 (3), 20.1 (3C), 31.5 (3C), 44.5 (3C), 109.7 (3C), 117.3 (3C), 122.3 (3C), 122.9 (3C), 124.5 (3C), 127.6 (3C), 130.1 (3C), 132.2 (3C), 132.4 (3C), 135.6 (3C), 136.6 (3C),149.1 (br, 3C, carbon next to boron) and 155.2 (3C) ppm. δ_B (128 MHz, $CDCl_3$) 18.0 ppm.

m/z EI (+) 829.4375 ($M+H^+$, 100%) $C_{51}H_{51}N_6O_3B_3$ requires 829.4364. Found C, 72.26; H, 6.10; N, 9.86. $C_{51}H_{51}N_6O_3B_3$ requires C, 73.94; H, 6.21; N, 10.14%.

Synthesis of "ate"-complex **129**

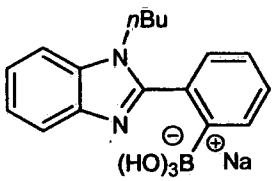

129

Boroxine **136** (209 mg, 0.252 mmol) was dissolved in DCM (4 ml) and treated with 40 % aqueous NaOH (45.4 µl, 0.756 mmol, 3 equivalents). After 17 h at rt, a white precipitate was observed. After filtration, the white solid was left to dry under high vacuum, giving the "ate"-complex **129** (125.3 mg, 0.375 mmol) in 50% yield as a white solid. Mp: 147-149 °C. IR (neat):ν_{max}/cm^{-1} 3049, 2874, 1455, 1393, 1277 and 745 cm^{-1}. δ_H (400 MHz, CD_3CN:D_2O (1:1)) 1.36 (3H, t, *J* 7.2, $NCH_2CH_2CH_2\mathit{CH_3}$), 1.80 (2H, hextet, *J* 7.2, $NCH_2CH_2\mathit{CH_2}CH_3$), 2.28 (2H, quintet, *J* 7.2, $NCH_2\mathit{CH_2}CH_2CH_3$), 4.56 (2H, m, $N\mathit{CH_2}CH_2CH_2CH_3$), 7.81-7.89 (4H, m, Ar), 7.94-7.98 (1H, m, Ar), 8.09-8.11 (1H, m, Ar), 8.24 (1H, d, *J* 7.2, Ar) and 8.30 (1H, d, *J* 7.2, Ar) ppm. δ_c (100 MHz, CD_3CN:D_2O (1:1)) 13.5, 20.2, 31.8, 44.9, 111.4 (2C), 118.7, 123.1 (2C), 125.6, 129.4, 132.2, 133.1 (2C), 135.4 and 161.3 ppm. δ_B (128 MHz, CD_3CN:D_2O (1:1)) 0.3 ppm. *m/z* EI (+) 667.1 (100%), 345.3 (91%). Found: C, 60.71; H, 5.94; N, 8.05. $C_{17}H_{20}O_3BN_2Na$ requires C, 61.10; H, 6.03; N, 8.38%.

Synthesis of 2-(*N*-*n*-butylbenzimidazole)benzaldehyde **137**

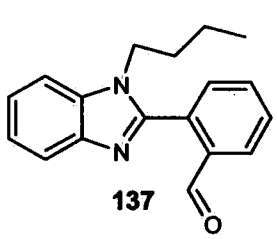

137

After drying 2-phenyl-N-*n*-butylbenzimidazole **135** (186 mg, 0.74 mmol) on P_2O_5 overnight, it was dissolved in dry THF (7 ml) under argon and cooled down to -25 °C. *n*-BuLi (0.93 ml, 1.6 M in hexane, 1.48 mmol) was added dropwise over 20 min. After stirring for 3 h at -25 °C, anhydrous DMF (0.46 ml, 5.93 mmol) was added dropwise and the mixture stirred for 1 h at -25 °C and allowed to warm to rt overnight. The reaction quenched was with aqueous NH_4Cl (10 ml), extracted with ether (3 x 7 ml), the combined organic phases were dried ($MgSO_4$) and evaporated to give a yellow crude oil (0.224 g). Purification by silica gel column chromatography (hexane: ethyl acetate, gradient elution) gave **137** (179 mg, 0.64

mmol) in 87% yield as a yellow thick oil. IR (neat):ν_{max}/cm^{-1} 3059, 2957, 2930, 2870, 1693, 1453, 1385, 1329 and 743 cm^{-1}. δ_H (400 MHz, $CDCl_3$) 0.69 (3H, t, *J* 7.6, $NCH_2CH_2CH_2CH_3$), 1.08 (2H, hextet, *J* 7.2, $NCH_2CH_2CH_2CH_3$), 1.61 (2H, quintet, *J* 7.6, $NCH_2CH_2CH_2CH_3$), 4.01 (2H, t, *J* 7.6, $NCH_2CH_2CH_2CH_3$), 7.24-7.31 (2H, m, Ar), 7.37-7.40 (1H, m, Ar), 7.53 (1H, d, *J* 7.6, Ar), 7.60 (1H, t, *J* 7.6, Ar), 7.67 (1H, t, *J* 7.6, Ar), 7.76 (1H, dd, J_1 6.6, J_2 2, Ar), 8.04 (1H, d, *J* 7.6, Ar) and 9.88 (1H, s, OC*H*) ppm. δ_c (100 MHz, $CDCl_3$) 12.4, 18.8, 30.6, 43.4, 109.2, 119.2, 121.6, 122.2, 127.6, 129.3, 130.0, 132.3, 132.5, 134.0, 134.6, 142.1, 149.0 and 189.9 ppm. *m/z* EI (+) 279.1494 ($M+H^+$, 100%) $C_{18}H_{19}ON_2$ requires 279.1492.

Synthesis of 2-(2-trimethylsilanylphenyl)-*N*-*n*-butylbenzimidazole **139**:

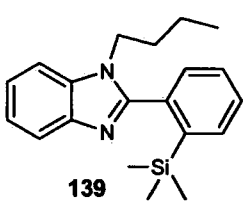

139

After drying 2-phenyl-*N*-*n*-butylbenzimidazole **135** (393 mg, 1.57 mmol) on P_2O_5 overnight, it was dissolved in dry THF (13 ml) under argon and cooled to -42 °C. *n*-BuLi (1.96 ml, 1.6 M in hexane, 3.14 mmol) was added dropwise over 30 min. After stirring for 2 h at -42 °C, anhydrous TMSCl (0.397 ml, 3.14 mmol) was added dropwise and the mixture stirred for 1 h at -42 °C and was allowed to warm to rt overnight. The reaction was quenched with aqueous NH_4Cl (10 ml), extracted with ether (3 x 10 ml), the combined organic phases were dried ($MgSO_4$), and evaporated to give a yellow crude oil (0.545 g). Purification by silica gel column chromatography (hexane: ethyl acetate, gradient elution) gave **139** (438.0 mg, 1.36 mmol) in 87% yield as a yellow thick oil. IR (neat):ν_{max}/cm^{-1} 3051, 2955, 2896, 2872, 1454, 1385, 1328, 835 and 750 cm^{-1}. δ_H (400 MHz, $CDCl_3$) 0.00 (9H, s, $Si(CH_3)_3$), 0.85 (3H, t, *J* 7.6, $NCH_2CH_2CH_2CH_3$), 1.28 (2H, hextet, *J* 8, $NCH_2CH_2CH_2CH_3$), 1.72 (2H, quintet, *J* 7.2, $NCH_2CH_2CH_2CH_3$), 3.94 (2H, t, *J* 7.6, $NCH_2CH_2CH_2CH_3$), 7.26-7.32 (2H, m, Ar), 7.37-7.49 (4H, m, Ar), 7.69-7.72 (1H, m, Ar) and 7.78-7.82 (1H, m, Ar) ppm. δ_c (100 MHz, $CDCl_3$) 0.00 (3C), 13.6, 20.5, 32.2, 44.7, 110.3, 120.4, 122.4, 122.9, 128.7, 129.1, 130.1, 135.0, 135.4, 136.5, 141.9, 143.2 and 154.8 ppm. *m/z* EI (+) 323.1940 ($M+H^+$, 100%) $C_{20}H_{27}SiN_2$ requires 323.1938.

Synthesis of 2-(2-bromophenyl)-*N*-*n*-butylbenzimidazole **138**:

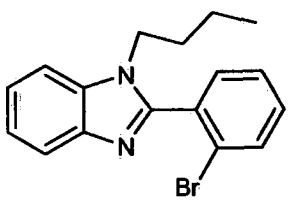

138

After drying 2-phenyl-*N*-*n*-butylbenzimidazole **135** (307 mg, 1.23 mmol) on P_2O_5 overnight, it was dissolved in dry THF (10 ml) under argon and cooled to -25 °C. *n*-BuLi (1.54 ml, 1.6 M in hexane, 2.46 mmol) was added dropwise over 20 min. After stirring for 3 h at -25 °C, a solution of 1,2-dibromotetrachloroethane (0.800, 2.46 mmol) in dry THF (1.5 ml) was added dropwise and the mixture was stirred for 1 h at -25 °C and allowed to warm to rt overnight. The reaction was quenched with aqueous NH_4Cl (10 ml), extracted with ether (3 x 7 ml), the combined organic phases dried ($MgSO_4$) and evaporated to give a dark brown crude oil (0.535 g). Purification by silica gel column chromatography (hexane: ethyl acetate, gradient elution) gave **138** (20 mg, 0.061 mmol) in a yield of 5% yield as a red thick oil. IR (neat): ν_{max}/cm^{-1} 3049, 2956, 2930, 2871, 1444, 1393, 1281, 1025, 743 and 726 cm^{-1}. δ_H (400 MHz, $CDCl_3$) 0.71 (3H, t, *J* 7.6, $NCH_2CH_2CH_2\mathit{CH_3}$), 1.10 (2H, hextet, *J* 8, $NCH_2CH_2\mathit{CH_2}CH_3$), 1.62 (2H, quintet, *J* 7.2, $NCH_2\mathit{CH_2}CH_2CH_3$), 3.99 (2H, t, *J* 7.2, $N\mathit{CH_2}CH_2CH_2CH_3$), 7.25-7.47 (6H, m, Ar), 7.66 (1H, dd, J_1 8, J_2 0.8, Ar) and 7.81 (1H, dd, J_1 6.2, J_2 3.2, Ar) ppm. δ_c (100 MHz, $CDCl_3$) 12.4, 18.8, 30.4, 43.6, 104.4, 118.7, 122.1, 122.5, 122.8, 126.6, 130.1, 130.8, 131.4, 132.1, 133.0, 141.1 and 150.4 ppm. *m/z* EI (+) 329.0646 and 331.0627 ($M+H^+$, 100%) $C_{17}H_{19}ON_2Br$ requires 329.0648 and 331.0627.

Synthesis of 1-(2-bromo-benzyl)-1,3,4,6,7,8-hexahydro-2H-pyrimido[1,2-α]pyrimidine **142**

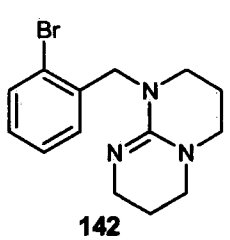

142

NaH (350 mg of 60% oil suspension, 8.78 mmol) was washed with dry hexane (3 x 8 ml) and dissolved in dry THF (15 ml) and stirred under argon. **140** (1.09 g, 7.80 mmol) was added and stirred for 10 min. at rt. After cooling to 0 °C, **141** (0.93 ml, 6.00 mmol) was added dropwise over 15 min. After 1 h, the reaction was quenched with EtOH (0.45 ml) and stirred for 10 min. at rt. After evaporation and dilution with water (15 ml), the mixture was extracted with DCM (3 x 15 ml), and the combined organic phases were dried ($MgSO_4$), and evaporated to give **142** (1.84 g, 5.97

mmol) was obtained as a light yellow powder, 100%. Mp: 79-81 °C. IR (neat): ν_{max}/cm^{-1} 2865 (br, Ph-H), 1595 (s, C=N), 1301 (m, Ar-NR_2), and 1107 (m, R_3N) cm^{-1}. δ_H (400 MHz, $CDCl_3$) 1.79 (2H, quint, *J* 6, $NCH_2CH_2CH_2N$), 1.89 (2H, quint, *J* 6.4, $NCH_2CH_2CH_2N$), 3.02 (2H, t, *J* 6, CH_2CH_2N), 3.12 (2H, t, *J* 6.4, CH_2CH_2N), 3.15 (2H, t, *J* 6.4, CH_2CH_2N), 3.32 (2H, t, *J* 6, CH_2CH_2N), 4.64 (2H, s, $ArCH_2N$), 7.03 (1H, t, *J* 6.6, Ph-H), 7.19-7.27 (2H, m, Ph-H) and 7.44 (1H, d, *J* 7.8, Ph-H) ppm. δ_C (100 MHz; $CDCl_3$) 22.8 (2C), 42.9, 45.1, 48.4, 48.6, 51.9, 123.8, 127.5, 128.3, 129.2, 132.7, 137.4 and 151.1 ppm. *m/z* EI (+) 308.0753 (M^+, 100%) $C_{14}H_{19}N_3{}^{79}Br$ requires 308.0757. Found: C, 50.58; H, 5.52; N, 12.48. $C_{14}H_{19}N_3Br$ requires C, 54.56; H, 5.89; N, 13.63%.

5.3.Synthesis of MBH and aza-MBH products

Synthesis of 3-phenyl-3-hydroxy-2-methylenepropanoic acid methyl ester **154**

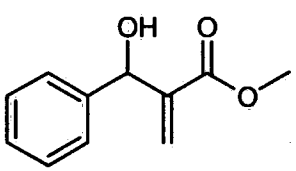

154

To a mixture of methyl acrylate (1.10 ml, 12.2 mmol) and DABCO (137 mg, 1.22 mmol) was added benzaldehyde (0.95 ml, 9.42 mmol). After stirring it at room temperature for 8 days, the reaction was diluted with DCM (20 ml), washed with dilute aqueous hydrochloric acid (10%, 3 x 10ml), followed by water (3 x 10 ml). After drying ($MgSO_4$), the solvent was evaporated to give a yellow oil (1.54 g). Purification by silica gel column chromatography (EtOAc:hexane, 2:8, as eluent) gave the product **154** (1.36 g, 75%) as a colourless oil. All spectroscopic and analytical details were identical to those reported in the literature.[16] IR (neat): 3481 (w), 3088- 2903 (s), 1722 (m), 1631 (s), 1604 (m); 1494 (m) and 1441 (w) cm^{-1}. δ_H (400 MHz; $CDCl_3$) 2.93 (1H, s, OH), 3.65 (3H, s, OCH_3), 5.49 (1H, s, $ArCHOH$), 5.79 (1H, s, $CR_2=CH_2$), 6.21 (1H, s, $CR_2=CH_2$) and 7.19-7.38 (5H, m, Ph) ppm. δ_C (100 MHz; $CDCl_3$) 51.9, 73.4, 126.1, 126.6 (2C), 127.8, 128.4 (2C), 141.3, 142.0 and 166.8 ppm.

Synthesis of 3-phenyl-3-hydroxy-2-methylenepropanoic acid butyl ester **155**

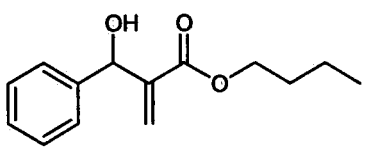

155

To a mixture of *n*-butyl acrylate (1.76 ml, 12.2 mmol) and DABCO (137 mg, 1.22 mmol,) was added benzaldehyde (0.95 ml, 9.42 mmol). After stirring at room temperature for 5 days, the reaction was quenched by diluting with DCM (20 ml) and the organic extract was washed with diluted aqueous hydrochloric acid (10%, 3 x 10 ml), followed by water (3 x 10 ml), drying ($MgSO_4$), and evaporation to give a yellow oil (0.94 g). Purification by silica gel column chromatography (EtOAc:hexane, 2:8, as solvent) gave the product **155** (0.70 g, 32%) as a yellow oil. All spectroscopic and analytical details were identical to those reported in the literature.[16] IR (neat): 3468 (w), 3088-2875 (s), 1717 (m), 1633 (s), 1600 (m), 1493 (m) and 1455 (w) cm^{-1}. δ_H (400 MHz; $CDCl_3$) 0.83 (3H, t, *J* 7.6, $O(CH_2)_3CH_3$), 1.25 (2H, hextet, *J* 7.6, $O(CH_2)_2CH_2CH_3$), 1.52 (2H, quint, *J* 7.6, $OCH_2CH_2(C_2H_5)$), 2.91 (1H, s, OH), 4.05 (2H, t, *J* 6.4, $OCH_2(C_3H_7)$), 5.47 (1H, s, $ArCHOH$), 5.74 (1H, s, $CR_2=CH_2$), 6.28 (1H, s, $CR_2=CH_2$) and 7.21-7.31 (5H, m, Ph) ppm. δ_C (100 MHz; $CDCl_3$) 13.6, 19.1, 30.5, 64.8, 75.8, 125.9, 126.6 (2C), 127.8, 128.4 (2C), 141.4, 142.2 and 166.4 ppm.

Synthesis of methyl 3-hydroxy-2-methylenepentanoate **156**

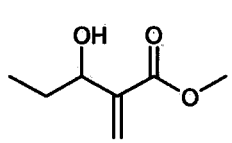

156

To a mixture of methyl acrylate (0.93 ml, 10.3 mmol) and DABCO (50 mg, 0.45 mmol) was added propionaldehyde (1.24 ml, 17.2 mmol). After stirring at room temperature for 11 days, the reaction was quenched by diluting with DCM (20 ml), the organic extract was washed with dilute aqueous hydrochloric acid (10%, 3 x 10 ml), followed by water (3 x 10 ml), drying ($MgSO_4$), and evaporation to give a yellow oil (0.113 g). Purification by silica gel column chromatography (EtOAc:hexane, 2:8, as solvent) give the product **156** (0.104 g, 7%) as a colourless oil. All spectroscopic and analytical details were identical to those reported in the literature.[93] IR (neat): 3440 (w), 3005-2867 (s), 1720 (m) and 1130 (w) cm^{-1}. δ_H (400 MHz; $CDCl_3$) 0.88 (3H, t, *J* 7.6, CH_2CH_3), 1.55-1.71 (2H, m, CH_2CH_3), 2.46 (1H, s, OH), 3.71 (3H, s, OCH_3), 4.26 (1H, t, *J* 6.4, $CHOH$), 5.73 (1H, s, CR2=CH_2) and 6.17 (1H, s, CR2=CH_2) ppm. δ_C (100 MHz; $CDCl_3$) 10.1, 29.1, 51.8, 73.2, 125.1, 142.2 and 167.0 ppm.

Synthesis of 3-[hydroxy-(4-nitrophenyl)-methyl]-but-3-en-2-one **157**

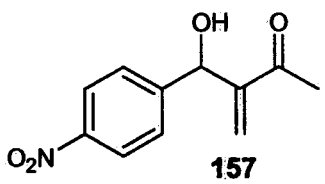

157

To a mixture of 4-nitrobenzaldehyde (151 mg, 1.0 mmol) and DABCO (56 mg, 0.5 mmol) in sulfolane (2 ml) under argon was added methyl vinyl ketone (0.243 ml, 3 mmol). After stirring at room temperature for 24 h, the reaction was quenched by diluting it with water (20 ml) and the product was extracted with ether (3 x 20 ml). After drying ($MgSO_4$), the solvent was evaporated to give a yellow oil. Purification by silica gel column chromatography (EtOAc:hexane, gradient elution) gave the product **157** (31.4 mg, 14%) as a yellow oil. All spectroscopic and analytical details were identical to those reported in the literature.[58] δ_H (400 MHz, $CDCl_3$) 2.29 (3H, s, CH_3),. 3.30 (1H, br, OH), 5.61 (1H, s, ArCH), 5.98 (1H, s, C=CH_2), 6.18 (1H, s, C=CH_2), 7.48 (2H, d, *J* 7.6, Ph) and 8.13 (2H, d, *J* 7.6, Ph) ppm. δ_C (100 MHz; $CDCl_3$) 25.3, 71.1, 122.7 (2C), 126.3 (2C), 126.7, 146.4, 148.1, 148.7 and 199.0 ppm.

Synthesis of 3-(4-nitrophenyl)-3-hydroxy-2-methylenepropanoate methyl ester **158**

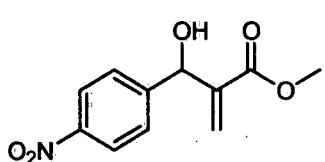

158

To a mixture of 4-nitrobenzaldehyde (151 mg, 1.0 mmol) and DABCO (56 mg, 0.5 mmol) in DCM (2 ml) under argon was added methyl acrylate (0.09 ml, 1 mmol). After stirring at room temperature for 3 days, the reaction was quenched by diluting with dichloromethane (20 ml), washed with dilute aqueous hydrochloric acid (10%, 3 x 10 ml), followed by water (3 x 10 ml), drying ($MgSO_4$) and evaporation to give a yellow oil. Purification by silica gel column chromatography (EtOAc:hexane, 3:7 as eluent) gave the product **158** (0.11 g, 47%) as a yellow oil. All spectroscopic and analytical details were identical to those reported in the literature.[35] IR (neat): ν_{max}/cm^{-1} 3512 (w, OH), 1699 (m, C=O) and 1628 (s) cm^{-1}. δ_H (400 MHz, $CDCl_3$) 3.19 (1H, br, OH), 3.57 (3H, s, OCH_3), 5.55 (1H, s, ArCH), 5.82 (1H, s, C=CH_2), 6.32 (1H, s, C=CH_2), 7.49 (2H, d, *J* 8.6, Ph) and 8.11 (2H, d, *J* 8.6, Ph) ppm. δ_C (100 MHz; $CDCl_3$) 52.2, 72.6, 123.6 (2C), 127.2, 127.4 (2C), 141.1, 147.5, 148.7 and 166.4 ppm.

Synthesis of 3-(4-phenyl)-3-hydroxy-2-methylenepropanoate 2-hydroxyethyl ester **161**

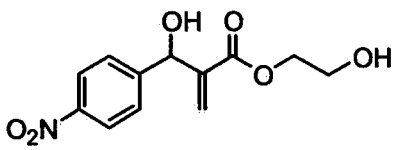

161

To a mixture of 4-nitrobenzaldehyde (151 mg, 1.0 mmol) and DABCO (56 mg, 0.5 mmol) in DCM (2 ml) under argon was added 2-hydroxyethyl acrylate (0.115 ml, 1.0 mmol). After stirring at room temperature for 3 days, the reaction was quenched by diluting with DCM (20 ml).and washed with dilute aqueous hydrochloric acid (10%, 3 x 10 ml), followed by water (3 x 10 ml), drying ($MgSO_4$), and evaporation to give a yellow oil. Purification by silica gel column chromatography (EtOAc:hexane, gradient elution) give the product **161** (0.1598 g, 60%) as a yellow oil. All spectroscopic and analytical details were identical to those reported in the literature.[21] IR (neat): ν_{max}/cm^{-1} 3417 (w), 1719 (m) and 1615 (s) cm^{-1}. δ_H (400 MHz, $CDCl_3$) 2.61 (2H, m, OH),. 3.72 (2H, s, CH_2OH), 4.16 (2H, s, OCH_2CH_2OH), 5.58 (1H, s, ArCH), 5.78 (1H, s, $C=CH_2$), 6.35 (1H, s, $C=CH_2$), 7.48 (2H, d, *J* 8.8, Ph,) and 8.09 (2H, d, *J* 8.8, Ph) ppm. δ_C (100 MHz; $CDCl_3$) 59.3, 65.5, 71.3, 122.6 (2C), 126.4 (2C), 126.8, 140.3, 146.4, 147.7 and 165.0 ppm.

Synthesis of *N*-(*p*-nitrobenzylidene)toluene-*p*-sulfonamide **164**

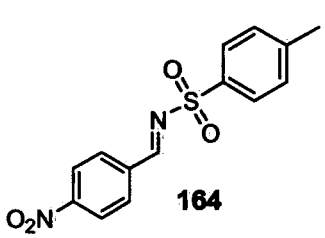

164

To a stirred solution of 4-nitrobenzaldehyde (0.756 g, 5 mmol) and *p*-toluenesulfonamide (0.856 g, 5 mmol) in DCM (20 ml) under argon was added trifluoroacetic anhydride (1.05 ml, 7.5 mmol). The mixture was heated at 65 °C for 4 days. The reaction was evaporatorated and dried under high vacuum to remove TFA and TFAA. After several hours, the mixture was diluted with DCM (20 ml), dried ($MgSO_4$), evaporated and crystallised from ethyl acetate to give the product **164** (0.98 g, 65%) as yellow needles. The filtrate was used again for crystallisation (0.39 g, 26%) to give a total yield of product **164** of 91%. All spectroscopic and analytical details were identical to those reported in the literature.[164] IR (neat): ν_{max}/cm^{-1} 3854sm (N=CH), 1615m, 1595s, 1523s, 1348s and 1160s (Tos). δ_H (400 MHz, $CDCl_3$) 2.39 (3H, s, $ArCH_3$), 7.31 (2H, d, *J* 8.00, Ph), 7.84 (2H, d, *J* 8.00, Ph), 8.04 (2H, d, *J* 8.8, Ph), 8.25 (2H, d, *J* 8.8, Ph) and 9.04 (1H, s, N=CR*H*) ppm. δ_C (100 MHz;

$CDCl_3$) 21.7, 124.2 (2C), 128.4 (2C), 130.0 (2C), 131.8 (2C), 134.2, 137.5, 145.3, 151.2, and 167.3 ppm.

Synthesis of 2-[(4-nitrophenyl) (toluene-4-sulfonylamino)methylene acrylic acid] methyl ester **166**

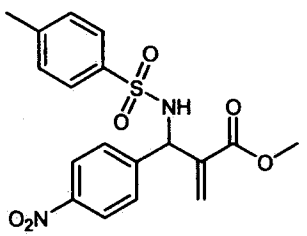

166

To a mixture of **164** (304 mg, 1.0 mmol) and DABCO (56 mg, 0.5 mmol) in DCM (2 ml) under argon was added methyl acrylate (0.09 ml, 1 mmol). After stirring at room temperature for 3 days, the reaction was quenched with DCM (20 ml), washed with dilute aqueous hydrochloric acid (10%, 3 x 10 ml), followed by water (3 x 10 ml), drying ($MgSO_4$) and evaporation to give a yellow oil. Purification by silica gel column chromatography (EtOAc:hexane, 3:7, as eluent) gave the product **166** (223 mg, 57%) as a yellow oil. All spectroscopic and analytical details were identical to these reported in the literature.[12] δ_H (400 MHz, $CDCl_3$) 2.34 (3H, s, $ArCH_3$), 3.41 (1H, br, NH), 3.55 (3H, s, OCH_3), 5.30 (1H, s, ArCH), 5.75 (1H, s, $C=CH_2$), 6.17 (1H, s, $C=CH_2$), 7.17 (2H, d, *J* 8.2, Ph), 7.32 (2H, d, *J* 8.8, Ph), 7.59 (2H, d, *J* 8.2, Ph) and 8.01 (2H, d, *J* 8.8, Ph) ppm. δ_C (100 MHz; $CDCl_3$) 20.3, 47.9, 51.1, 121.4, 122.6 (2C), 125.7 (2C), 128.0 (2C), 130.1 (2C), 136.5, 139.8, 141.7, 145.2, 148.7 and 165.8 ppm.

5.4.The aldol reactions

General aldol procedure with "ate"-complex **129** formed *in situ.*

Boroxine **136** (110.4 mg, 0.13 mmol) was dissolved in corresponding solvent (2 ml). To this mixture, 40% aqueous NaOH solution (24 µl, 3 equivalents) was added. This solution was added to a mixture of the aldehyde and ketone and the mixture was left stirring at room temperature for corresponding time. Then the mixture was diluted with 5% HCl solution (3 ml) and the product was extracted with DCM (3 x 10 ml) and ethyl acetate (3 x 10 ml). The combined organic phases were dried ($MgSO_4$) and evaporated to give the crude oil. Purification by silica gel column chromatography (hexane: ethyl acetate, gradient elution) gave the corresponding products:

General aldol procedure with "ate"-complex **129** added directly as dry solid.

The corresponding aldehyde and ketone were dissolved in the appropriate solvent (2 ml). To this mixture "ate"-complex **129** was added and left stirring on room temperature for corresponding time. Then the mixture was diluted with 5% HCl solution (3 ml) and the product was extracted with DCM (3 x 10 ml) and ethyl acetate (3 x 10 ml). The combined organic phases were dried ($MgSO_4$) and evaporated to give the crude oil. Purification by silica gel column chromatography (hexane: ethyl acetate, gradient elution) gave the corresponding products:

4-Hydroxy-4-phenylbutan-2-one **228**[181]

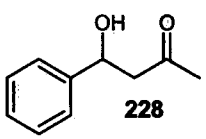

228

δ_H (400 MHz, $CDCl_3$) 2.10 (3H, s, PhCHOHCH$_2$COC*H*$_3$), 2.69-2.84 (2H, m; PhCHOHC*H*$_2$COCH$_3$), 3.36 (1H, b, PhCH*OH*CH$_2$COCH$_3$), 5.06 (1H, dd, J_1 9, J_2 3.2, PhC*H*OHCH$_2$COCH$_3$) and 7.17-7.27 (5H, m, *Ph*CHOHCH$_2$COCH$_3$) ppm. δ_C (100 MHz, $CDCl_3$) 29.8, 51.0, 68.9, 124.7 (2C), 126.8, 127.5 (2C), 141.8 and 208 (CO) ppm.

4-Phenylbut-3-en-2-one **227**[180]

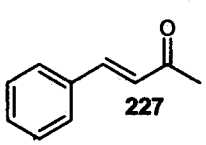

227

δ_H (400 MHz, $CDCl_3$) 2.22 (3H, s, PhCHCHCOC*H*$_3$), 6.57 (1H, d, *J* 16, PhCHC*H*COCH$_3$), 7.24-7.27 (2H, m, Ar + 1H, m) and 7.35-7.40 (3H, m, Ar) ppm. δ_C (100 MHz, $CDCl_3$) 27.7, 126.8, 127.4 (2C), 127.9 (2C), 134.3, 139.0, 143.5 and 197.3 (CO) ppm.

1-Phenylpent-1-en-3-one **232**[180]

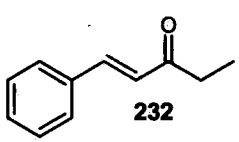

232

δ_H (400 MHz, $CDCl_3$) 1.10 (3H, t, *J* 7.4, PhCHCHCOCH$_2$C*H*$_3$), 2.63 (2H, q, *J* 7.4, PhCHCHCOC*H*$_2$CH$_3$), 6.67 (1H, d, *J* 16.4, PhCHC*H*COCH$_2$CH$_3$), 7.30-7.33 (2H, m, Ar + 1H, m) and 7.46-7.51 (3H, m, Ar) ppm. δ_C (100 MHz, $CDCl_3$) 8.2, 34.0, 126.0, 128.2 (2C), 128.9 (2C), 130.3, 134.6, 142.2 and 200.9 (CO) ppm.

1-Hydroxy-1-phenylpentan-3-one **233**[182]

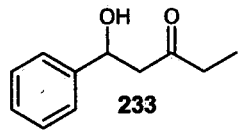

233

δ_H (400 MHz, $CDCl_3$) 0.99 (3H, t, *J* 7.2, PhCHOHCH$_2$COCH$_2$C*H*$_3$), 2.39 (2H, q, *J* 7.2, PhCHOHCH$_2$COC*H*$_2$CH$_3$), 2.74-2.78 (2H, m, PhCHOHC*H*$_2$COCH$_2$CH$_3$), 3.38 (1H, b, PhCH*OH*CH$_2$COCH$_2$CH$_3$), 5.09 (1H, dd, J_1 9, J_2 3.2, PhC*H*OHCH$_2$COCH$_2$CH$_3$) and 7.17-7.30 (5H, m, Ar) ppm. δ_C (100 MHz, $CDCl_3$) 6.5, 35.9, 49.7, 69.0, 124.6 (2C), 126.6, 127.5 (2C), 141.9 and 210.8 (CO) ppm.

4-Hydroxy-3-methyl-4-phenylbutan-2-one **234**[183]

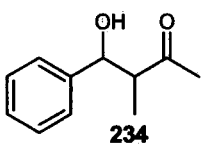

234

δ_H (400 MHz, $CDCl_3$) 0.86 (3H, d, *J* 7.6, PhCHOHCH(C*H*$_3$)COCH$_3$), 2.15 (3H, s, PhCHOHCH(CH$_3$)COC*H*$_3$), 2.82-2.89 (1H, m, PhCHOHC*H*(CH$_3$)COCH$_3$), 3.21 (1H, b, PhCH*OH*CH(CH$_3$)COCH$_3$), 4.66 (1H, d, *J* 8.4, PhC*H*OHCH(CH$_3$)COCH$_3$) and 7.20-7.29 (5H, m, Ar) ppm. δ_C (100 MHz, $CDCl_3$) 13.1, 29.9, 52.7, 75.6, 125.6 (2C), 127.0, 127.5 (2C), 141.0, and 205.9 (CO) ppm.

4-Hydroxy-4-(4-nitrophenyl)butan-2-one **231**[181]

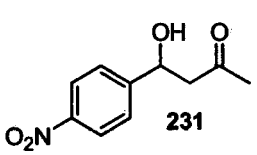

231

δ_H (400 MHz, $CDCl_3$) 2.16 (3H, s, RCHOHCH$_2$COC*H*$_3$), 2.78-2.80 (2H, m, RCHOHC*H*$_2$COCH$_3$), 3.53 (1H, b, RCH*OH*CH$_2$COCH$_3$), 5.20 (1H, dd, J_1 7.8, J_2 4.4, RC*H*OHCH$_2$COCH$_3$), 7.46-7.48 (2H, m, Ar) and 8.13-8.15 (2H, m, Ar) ppm. δ_C (100 MHz, $CDCl_3$) 29.7, 50.5, 67.9, 122.8 (2C), 125.4 (2C), 148.9, 166.3 and 207.4 (CO) ppm.

4-(4-Nitrophenyl)but-3-en-2-one **237**[184]

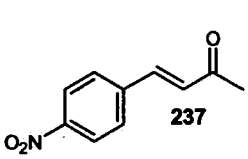

237

δ_H (400 MHz, $CDCl_3$) 2.34 (3H, s, RCHCHCOC*H*$_3$), 6.75 (1H, d, *J* 16.4, RCHC*H*COCH$_3$), 7.47 (1H, d, *J* 16.4, RC*H*CHCOCH$_3$), 7.63 (2H, d, *J* 8.8, Ar) and 8.16 (2H, d, *J* 8.8, Ar) ppm. δ_C (100 MHz, $CDCl_3$) 28.0, 124.4 (2C), 129.0 (2C), 130.4, 140.4, 140.7, 148.6 and 197.5 (CO) ppm.

4-(4-Methoxyphenyl)but-3-en-2-one **238**[185]

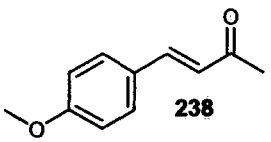

238

δ_H (400 MHz, $CDCl_3$) 2.24 (3H, s, MeOPhCHCHCOC*H*$_3$), 3.72 (3H, s, *Me*OPhCHCHCOCH$_3$), 6.49 (1H, dd, J_1 16.2 J_2 1.6, RCHC*H*COCH$_3$), 6.81 (2H, dd, J_1 8.4 J_2 1.6, RC*H*CHCOCH$_3$ + Ar) and 7.34-7.39 (3H, m, Ar) ppm. δ_C (100 MHz, $CDCl_3$) 27.3, 55.3, 114.4 (2C), 125.0, 127.6, 129.9 (2C), 143.2, 161.6 and 206.7 (CO) ppm.

4-Hydroxy-4-(4-methoxyphenyl)butan-2-one **240**[181]

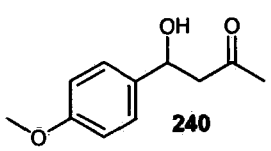

240

δ_H (400 MHz, $CDCl_3$) 2.11 (3H, s, MeOPhCHOHCH$_2$COC*H*$_3$), 2.68-2.85 (2H, m, MeOPhCHOHC*H*$_2$COC*H*$_3$), 3.17 (1H, b, MeOPhCHO*H*CH$_2$COCH$_3$), 3.72 (3H, s, *Me*OPhCHOHCH$_2$COCH$_3$), 5.03 (1H, dd, J_1 9.2 J_2 3.2, MeOPhC*H*OHCH$_2$COCH$_3$), 6.81 (2H, d, J 8.2, Ar) and 7.20 (2H, d, J 8.2, Ar) ppm. δ_C (100 MHz, $CDCl_3$) 30.8, 52.0, 55.3, 70.0, 113.9 (2C), 126.9 (2C), 135.0, 159.2 and 209.0 (CO) ppm.

6-Phenylhexa-3,5-dien-2-one **239**[186]

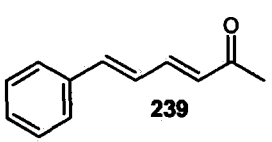

239

δ_H (400 MHz, $CDCl_3$) 2.22 (3H, s, PhCHCHCHCHCOC*H*$_3$), 6.57 (1H, d, J 15.6, PhCHCHCHC*H*COCH$_3$), 6.74-6.89 (2H, m, PhCHC*H*C*H*CHCOCH$_3$), 7.16-7.30 (1H, m, PhC*H*CHCHCHCOCH$_3$ + 3H, m, Ar) and 7.36-7.39 (2H, m, Ar) ppm. δ_C (100 MHz, $CDCl_3$) 27.4, 126.7, 127.3 (2C), 129.1 (2C), 129.1, 130.5, 135.0, 141.3, 143.0 and 197.3 (CO) ppm.

4-Hydroxy-6-phenylhex-5-en-2-one **241**[187]

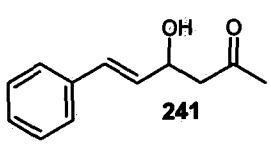

241

δ_H (400 MHz, $CDCl_3$) 2.14 (3H, s, PhCHCHCHOHCH$_2$COC*H*$_3$), 2.69 (2H, d, J 6.4, PhCHCHCHOHC*H*$_2$COCH$_3$), 3.03 (1H, b, PhCHCHCHO*H*CH$_2$COCH$_3$), 4.69 (1H, d, J 6.4,

PhCHCHC*H*OHCH$_2$COCH$_3$), 6.13 (1H, dd, J_1 16.2 J_2 6.4, PhCHC*H*CHOHCH$_2$COCH$_3$), 6.57 (1H, d, *J* 15.8, PhC*H*CHCHOHCH$_2$COCH$_3$) and 7.16-7.31 (5H, m, *Ph*CHOHCH$_2$COCH$_3$) ppm. δ_C (100 MHz, $CDCl_3$) 29.8, 50.0, 67.5, 125.5 (2C), 126.8, 127.6 (2C), 129.1, 129.5, 135.5 and 207.9 (CO) ppm.

3,4-Dihydroxy-4-phenylbutan-2-one **243**[188]

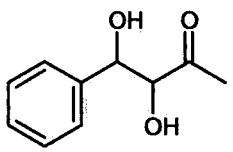

243

δ_H (400 MHz, $CDCl_3$) 1.75 (3H, s, PhCHOHCHOHCOC*H*$_3$), 2.02 (3H, s, PhCHOHCHOHCOC*H*$_3$), 3.56 (1H, b, PhCHOHCHO*H*COCH$_3$), 3.82 (1H, b, PhCHO*H*CHOHCOCH$_3$), 4.14 (1H, d, *J* 2.6, PhCHOHC*H*OHCOCH$_3$), 4.26 (1H, d, *J* 4.6, PhCHOHC*H*OHCOCH$_3$), 4.79 (1H, d, *J* 4.6, PhC*H*OHCHOHCOCH$_3$), 4.81 (1H, d, *J* 2.6, PhC*H*OHCHOHCOCH$_3$) and 7.17-7.24 (5H, m, Ar) ppm. δ_C (100 MHz, $CDCl_3$) 26.6, 27.8, 74.0, 74.9, 80.8, 81.1, 126.3 (2C), 128.0, 129.0 (2C), 139.3, 140.1 and 208.7 (CO) ppm.

3,4-Dihydroxy-4-(4-nitrophenyl)butan-2-one **244**[181]

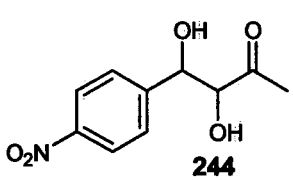

244

δ_H (400 MHz, $CDCl_3$) 1.96 (3H, s, 4-NO$_2$PhCHOHCHOHCOC*H*$_3$), 2.29 (3H, s, 4-NO$_2$PhCHOHCHOHCOC*H*$_3$), 2.70 (1H, d, *J* 6.4, 4-NO$_2$PhCHOHCHO*H*COCH$_3$), 2.87 (1H, b, 4-NO$_2$PhCHOHCHO*H*COCH$_3$), 3.61 (1H, d, *J* 4.8, 4-NO$_2$PhCHO*H*CHOHCOCH$_3$), 3.67 (1H, d, *J* 4.4, 4-NO$_2$PhCHO*H*CHOHCOCH$_3$), 4.35 (1H, t, *J* 2.8, 4-NO$_2$PhCHOHC*H*OHCOCH$_3$), 4.41 (1H, t, *J* 4.4, 4-NO$_2$PhCHOHC*H*OHCOCH$_3$), 5.01-5.04 (1H, m, 4-NO$_2$PhC*H*OHCHOHCOCH$_3$), 5.11-5.18 (1H, m, 4-NO$_2$PhC*H*OHCHOHCOCH$_3$), 7.54 (2H, d, *J* 8.6, Ar) and 8.18 (2H, d, *J* 8.6, Ar) ppm. δ_C (100 MHz, $CDCl_3$) 25.9, 27.7, 72.9, 74.4, 80.0, 80.6, 123.7 (2C), 127.1 (2C), 147.3, 147.7 and 206.6 (CO) ppm. Crystals (Figure 2) were obtained from chloroform. Mp: 154-156 °C.

3,4-Dihydroxy-4-(4-methoxy)butan-2-one **245**

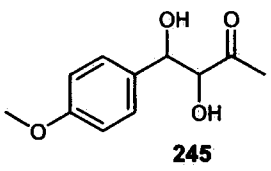

245

IR (neat): ν_{max}/cm^{-1} 3437, 2938,1714, 1603, 1514, 1251 and 835. δ_H (400 MHz, $CDCl_3$) 1.92 (3H, s, 4-MeOPhCHOHCHOHCOC*H*$_3$), 2.09 (3H, s, 4-MeOPhCHOHCHOHCOC*H*$_3$), 2.93 (1H, b, 4-MeOPhCHOHCHO*H*COCH$_3$), 3.05 (1H, b, 4-MeOPhCHOHCHO*H*COCH$_3$), 3.59 (1H, b, 4-MeOPhCHO*H*CHOHCOCH$_3$), 3.66 (1H, b, 4-MeOPhCHO*H*CHOHCOCH$_3$), 3.73 (3H, s, 4-*Me*OPhCHOHCHOHCOCH$_3$), 3.82 (3H, s, 4-*Me*OPhCHOHCHOHCOCH$_3$), 4.25 (1H, b, 4-MeOPhCHOHC*H*OHCOCH$_3$), 4.34 (1H, d, *J* 3.2, 4-MeOPhCHOHC*H*OHCOCH$_3$), 4.83 (1H, b, MeOPhC*H*OHCHOHCOCH$_3$), 6.78-6.84 (2H, m, Ar) and 7.2-7.27 (2H, m, Ar) ppm. δ_C (100 MHz, $CDCl_3$) 25.5, 26.6, 54.3, 54.6, 72.9, 73.6, 79.8, 80.0, 113.0 (2C), 113.3 (2C), 126.7 (2C), 127.0 (2C), 130.3, 131.1, 158.5, 207.1 (CO) and 207.5 (CO) ppm. *m/z* EI (+) 228.1230 ($M+NH_4^+$, 100%) $C_{11}H_{18}O_4N$ requires 228.1230.

(*syn*)-3,4-Dihydroxy-6-phenylhex-5-en-2-one **246**[189]

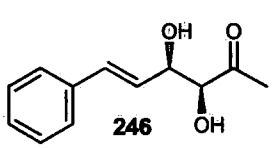

246

IR (neat): ν_{max}/cm^{-1} 3418, 3062, 3032, 2927, 2539, 1717, 1459, 1451, 1113 and 699. δ_H (400 MHz, $CDCl_3$) 2.25 (3H, s, PhCHCHCHOHCHOHCOC*H*$_3$), 2.46 (1H, b, PhCHCHCHOHCHO*H*COCH$_3$), 3.73 (1H, b, PhCHCHCHO*H*CHOHCOCH$_3$), 4.17 (1H, b, PhCHCHCHOHC*H*OHCOCH$_3$), 4.60 (1H, b, PhCHCHC*H*OHCHOHCOCH$_3$), 6.27 (1H, dd, J_1 16, J_2 6.4, PhCHC*H*CHOHCHOHCOCH$_3$), 6.63 (1H, d, *J* 16, PhC*H*CHCHOHCHOHCOCH$_3$), 7.19 (1H, d, *J* 6.8, Ar), 7.24 (2H, t, *J* 7.2, Ar) and 7.32 (2H, d, *J* 7.6, Ar) ppm. δ_C (100 MHz, $CDCl_3$) 26.0, 73.0, 79.9, 127.0 (2C), 127.6, 128.1, 128.5 (2C), 132.5, 136.1, and 207.6 (CO) ppm. MS (MALDI): $C_{12}H_{14}O_3$ *m/z* calcd 206.24, found 245 ($M+K^+$, 100%) and 229 ($M+Na^+$, 48%).

3,4-Dihydroxyhexan-2-one **247**

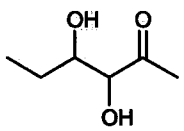

247

IR (neat): ν_{max}/cm^{-1} 3418, 2969, 2938, 2880, 1715, 1462, 1359, 1132, 1076 and 976. δ_H (400 MHz, $CDCl_3$) 0.94 (3H, t, *J* 7.4, $CH_3CH_2CHOHCHOHCOCH_3$), 1.59 (2H, q, *J* 7.4, $CH_3CH_2CHOHCHOHCOCH_3$), 2.20 (3H, s, $CH_3CH_2CHOHCHOHCOCH_3$), 2.69 (1H, b, $CH_3CH_2CHOHCHOHCOCH_3$), 3.82 (1H, t, *J* 6.4, $CH_3CH_2CHOHCHOHCOCH_3$), 3.86 (1H, b, $CH_3CH_2CHOHCHOHCOCH_3$), 4.04 (1H, s, $CH_3CH_2CHOHCHOHCOCH_3$) and 4.18 (1H, s, $CH_3CH_2CHOHCHOHCOCH_3$) ppm. δ_C (100 MHz, $CDCl_3$) 10.1, 10.2, 24.8, 25.2, 25.4, 27.1, 73.3, 74.2, 79.0, 80.4, 207.5 (CO) and 208.9 (CO) ppm. *m/z* EI (+)150.1125 ($M+NH_4^+$, 100%), $C_6H_{16}O_3N$ requires 150.1125.

3,4-Dihydroxy-5,5-dimethylhexan-2-one **248**

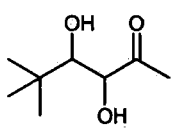

248

IR (neat): ν_{max}/cm^{-1} 3307, 2959, 2871, 1711, 1413, 1361, 1107 and 1057. δ_H (400 MHz, $CDCl_3$) 0.97 (9H, s, $(CH_3)_3CCHOHCHOHCOCH_3$), 2.21 (3H, s, $(CH_3)_3CCHOHCHOHCOCH_3$), 3.51 (1H, b, $(CH_3)_3CCHOHCHOHCOCH_3$), 3.72 (1H, d, *J* 4.0, $(CH_3)_3CCHOHCHOHCOCH_3$), and 4.24 (1H, d, J 2.8, $(CH_3)_3CCHOHCHOHCOCH_3$) ppm. δ_C (100 MHz, $CDCl_3$) 23.9, 25.3 (3C), 34.7, 76.6, 77.5 and 207.8 (CO) ppm. Anal. Calcd for $C_8H_{16}O_3$: C, 59.97; H, 10.07. Found C,59.92; H, 10.12. Crystals (Figure 3) were obtained from cyclohexane. Mp: 57-59 °C.

General procedure for the kinetic studies of the aldol reaction with acetone.

A stirred solution of benzaldehyde (75 µl, 0.733 mmol) in a mixture of D_2O and acetone (1:1, 1.1 ml), was treated with catalyst **129** or NaOH (0.11 mmol). The mixture was shaken periodically over a period of 72 hours at room temperature during which the reaction was analysed by ^1H NMR. This study was done by Dr. Alexandra Blatch. The fitting of the kinetical data was done using Scientist version 2.01, Mirco-Math Research, Saint Louis, Missouri, USA by Dr. C. Grosjean. Both linear and non-linear least square regression analysis were attempted and the latter was chosen to obtain the first order rate constans. For Figure 4 the correlation coefficient was 0.995 and R^2 was 0.739. For Figure 5 the correlation coefficient was 0.982 and R^2 was 0.641. Because of the relatively poor correlation coefficients, a first order process cannot be

confirmed on the basis of the data. The observed deviation from linearity in both cases for a Ln [reactant] vs time fit also disputes a first order process. A higher order fitting was not attempted.

General procedure for the kinetic studies of the aldol reaction with hydroxyacetone.
Benzaldehyde (40 µl, 0.394 mmol), hydroxyacetone (271 µl, 3.93 mmol) and an aqueous solution of catalyst (400 µl, 0.2 M cat. in water) were mixed and stirred vigorouly for the appropriate time. The reaction was quenched at a specific time with 5 % aqueous HCl (80 µl), extracted with EtOAc (3 x 4 ml), evaporated and to the crude product redissolved in DCM (4 ml) containing 1,4-dimethoxyphenyl as internal standard (6.76 mM) and analyzed by HPLC: (Chiracel OJ, Hexane:EtOH:MeOH = 90:6.6:3.3, flow rate 1.0 ml/min, λ = 210 nm) t_R = 19.89 (*anti*), 22.42 (*anti*), 24.85 (*syn*) and 29.40 (*syn*) min. t_R Internal standard = 8.78 min. The fitting of the kinetical data was done using Scientist version 2.01, Mirco-Math Research, Saint Louis, Missouri, USA by Dr. C. Grosjean. Both linear and non-linear least square regression analysis were attempted and the latter was chosen to obtain the first order rate constans. For Figure 7 the correlation coefficient was 0.975 and R^2 was 0.474. Because of the relatively poor correlation coefficients, a first order process cannot be confirmed on the basis of the data. The observed deviation from linearity in both cases for a Ln [reactant] vs time fit also disputes a first order process. A higher order fitting was not attempted.

5.5.Synthesis of new chiral catalyst

Synthesis of 1-(3-bromopropyl)-2-phenylbenzimidazole **263**

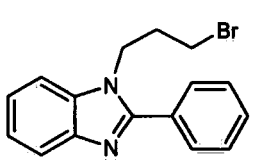

263

To a solution of 2-phenylbenzimidazole **134** (348.5 mg, 2 mmol) in anhydrous DMF (3 ml) was added NaH (80 mg, 2 mmol) and the mixture left stirring at rt for 30 min. This solution was added to a mixture of 1,3-dibromopropane (2.03 ml, 20 mmol) dissolved in anhydrous DMF (8 ml) and THF (2 ml) and cooled to -78 °C dropwise. After 30 min. the reaction was quenched with 200 µl water and allowed to warm to rt. After evaporation, the mixture was diluted with DCM

(25 ml), the organic phase was washed with water (3 x 10 ml), dried ($MgSO_4$) and evaporated to give 542.2 mg of crude material. The crude product was purified by neutral alumina column chromatography, then using silica gel column chromatography (hexane/ethyl acetate, gradient elution) to give the product **263** (211 mg, 0.67 mmol, 33%) as white solid. Mp: 121-123 °C IR (neat): ν_{max}/cm^{-1} 3023, 2957, 1508, 1443, 1391, 1263, 1026, 751 and 702. δ_H (400 MHz, $CDCl_3$) 2.21-2.29 (2H, m, $NCH_2CH_2CH_2Br$), 3.22 (2H, t, *J* 6, $NCH_2CH_2CH_2Br$), 4.38 (2H, t, *J* 7.2, $NCH_2CH_2CH_2Br$), 7.22-7.29 (2H, m, Ar), 7.39-7.42 (1H, m, Ar), 7.43-7.49 (3H, m, Ar), 7.63-7.66 (2H, m, Ar) and 7.74-7.78 (1H, m, Ar) ppm. δ_C (100 MHz, $CDCl_3$) 29.6, 32.4, 43.1, 109.9, 120.1, 122.7, 123.0, 128.9 (2C), 129.3 (2C), 130.0, 130.2, 135.5, 143.0 and 153.6 ppm. *m/z* EI (+) 315.0493 ($M+H^+$, 100%) $C_{16}H_{17}N_2{}^{79}Br$ requires 315.0491.

Synthesis of 3a-phenyl-2,3,3a,4-tetrahydrobenzopyrroloimidazole **266**

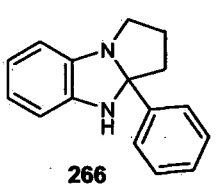

266

After drying **263** (211 mg, 0.67 mmol) over P_2O_5 overnight, it was dissolved in dry Et_2O (10 ml) under argon and cooled to -78 °C. *n*-BuLi (0.4 ml, 2.5 M in hexane, 1.0 mmol) was added dropwise over 15 min. After stirring for 2 h at -78 °C, the reaction was allowed to warm to rt during overnight, quenched with aqueous NH_4Cl (10 ml), extracted with ether (3 x 10 ml) and the combined organic phases dried ($MgSO_4$) and evaported to give a yellow crude oil (0.183 g). Purification by silica gel column chromatography (hexane: ethyl acetate, gradient elution) gave **266** (59.8 mg, 0.25 mmol) in 38% as a yellow thick oil and **265** (28.1 mg, 0.12 mmol) in a yield of 18% also as a yellow thick oil. IR (neat): ν_{max}/cm^{-1} 3353, 2926, 1491, 1263, 1016, 736 and 701. δ_H (400 MHz, $CDCl_3$) 1.56-167 (1H, m, $NCH_aH_bCH_aH_bCH_aH_bCPh$), 1.74-1.85 (1H, m, $NCH_aH_bCH_aH_bCH_aH_bCPh$), 2.13-2.21 (1H, m, $NCH_aH_bCH_aH_bCH_aH_bCPh$), 2.25-2.32 (1H, m, $NCH_aH_bCH_aH_bCH_aH_bCPh$), 3.23-3.30 (1H, m, $NCH_aH_bCH_aH_bCH_aH_bCPh$), 3.40-3.46 (1H, m, $NCH_aH_bCH_aH_bCH_aH_bCPh$), 4.15 (1H, b, N*H*), 6.45-6.49 (1H, m, Ar), 6.58-6.65 (2H, m, Ar), 6.67-6.73 (1H, m, Ar), 7.17-7.22 (1H, m, Ph), 7.26-7.31 (2H, m, Ph) and 7.46-7.50 (2H, m, Ph) ppm. δ_C (100 MHz, $CDCl_3$) 22.9, 38.9, 53.0, 91.3, 109.3, 110.2, 119.9, 120.0, 124.2 (2C), 126.4, 127.6 (2C), 139.5, 144.2 and 144.9 ppm. MS (ESI+): $C_{16}H_{17}N_2$ *m/z* calcd 237 ($M+H^+$), found 237 (100%).

2-Phenyl-1-propylbenzimidazole **265**[195]

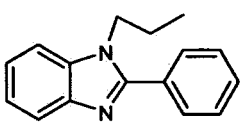

265

δ_H (400 MHz, $CDCl_3$) 0.79 (3H, t, *J* 7.2, $NCH_2CH_2CH_3$), 1.77 (2H, hextet, *J* 7.6, $NCH_2CH_2CH_3$), 4.12 (2H, t, J 7.6, $NCH_2CH_2CH_3$), 7.19-7.25 (2H, m, Ar), 7.32-7.36 (1H, m, Ar), 7.42-7.47 (3H, m, Ar), 7.61-7.65 (2H, m, Ar) and 7.72-7.77 (1H, m, Ar) ppm. δ_C (100 MHz, $CDCl_3$) 10.2, 22.1, 45.3, 109.1, 119.0, 121.3, 121.6, 127.7 (2C), 128.2 (2C), 128.3, 129.8, 134.7, 142.1 and 152.8 ppm.

Synthesis of 1-allyl-2-phenylbenzimidazole **264**

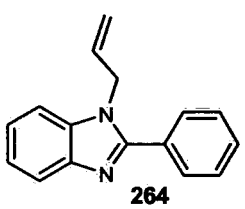

264

To a solution of 2-phenylbenzimidazole **134** (348.5 mg, 2 mmol) in anhydrous DMF (10 ml) was added NaH (96 mg, 2.4 mmol) and left stirring at rt for 15 min. Allyl bromide (0.21 ml, 2.4 mmol) was added and the mixture left stirring for 1 h at rt. The reaction was quenched with EtOH (200 µl), evaporated and diluted with ether (25 ml). The organic phase was washed with water (3 x 10 ml) and dried ($MgSO_4$) and evaporated to give 0.497 g of crude product which was purified with silica gel column chromatography (hexane/ethyl acetate, gradient elution) to give the product **264** (443 mg, 1.89 mmol, 94%) as white solid. All spectroscopic and analytical details were identical to those reported in the literature.[197] δ_H (400 MHz, $CDCl_3$) 4.71-4.74 (2H, m, $NCH_2CHCH_aH_b$), 5.00 (1H, d, *J* 17.2, $NCH_2CHCH_aH_b$), 5.23 (1H, d, J 10.4, $NCH_2CHCH_aH_b$), 5.92-6.05 (1H, m, $NCH_2CHCH_aH_b$), 7.17-7.29 (3H, m, Ar), 7.39-7.44 (3H, m, Ar), 7.65-7.71 (2H, m, Ar) and 7.74-7.78 (1H, m, Ar) ppm. δ_C (100 MHz, $CDCl_3$) 46.1, 109.3, 116.4, 118.9, 121.5, 121.8, 127.7 (2C), 128.2 (2C), 128.8, 129.2, 131.4, 135.0, 142.1 and 152.8 ppm. *m/z* EI (+) 235.1228 ($M+H^+$, 100%) $C_{16}H_{15}N_2$ requires 235.1230.

Synthesis of 2-(2-bromophenyl)benzimidazole **268a**

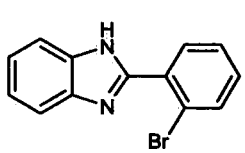

268a

To a solution of 1,2-phenylenediamine (1.08 g, 10 mmol) in anhydrous *o*-xylene (80 ml) was added 2-bromobenzoyl chloride (1.58 ml, 12 mmol) dropwise. The mixture was left stirring at rt for 1 h and then *p*TsOH

monohydrate (3.8 g, 20 mmol) was added. The mixture was refluxed using a Dean Stark procedure for 42 h and then cooled to rt and quenched with 5% aqueous NaOH (20 ml). After evaporation, ethyl acetate (60 ml) and THF (10 ml) was added, the organic phase was washed with 10% aqueous NaOH (3 x 20 ml), dried ($MgSO_4$) and evaporated to give 3.30 g crude product which was purified by silica gel column chromatography (hexane/THF, gradient elution) to give **268a** (2.36 g, 86%) as light brown solid and 2-aminophenyl-2-bromobenzamide (320 mg, 11%) as dark brown solid. All spectroscopic and analytical details were identical to those reported in the literature.[200] δ_H (400 MHz, $CDCl_3$) 7.21-7.28 (3H, m, Ar), 7.38 (1H, td, J_1 8, J_2 1.2, Ar), 7.62 (3H, dd, J_1 7.8, J_2 0.8, Ar), 8.20 (1H, dd, J_1 7.8, J_2 1.6, Ar) and 10.29 (1H, b, N*H*) ppm. δ_C (100 MHz, $CDCl_3$) 110.8, 120.6, 123.3, 128.3 (2C), 130.8, 131.4 (2C), 133.0 (2C), 134.2 (2C) and 150.0 ppm. .

2-Aminophenyl-2-bromobenzamide[199]

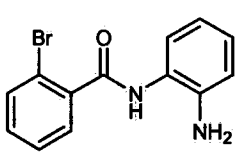

δ_H (400 MHz, $CDCl_3$) 3.89 (2H, b, N*H*$_2$), 6.75-6.81 (2H, m, Ar), 7.01-7.07 (1H, m, Ar), 7.24-7.30 (1H, m, Ar), 7.31-7.38 (2H, m,Ar) and 7.52-7.63 (3H, m, 2H Ar +CON*H*) ppm. δ_C (100 MHz, $CDCl_3$) 118.3, 119.5, 119.8, 123.8, 125.7, 127.9, 128.0, 130.2, 132.0, 133.7, 137.8, 141.2 and 166.3 (CO) ppm.

Synthesis of 2-(2-iodophenyl)benzimidazole **268b**

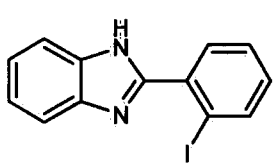

268b

To a solution of 1,2-phenylenediamine (649 mg, 6.0 mmol) in anhydrous *o*-xylene (48 ml) was added 2-iodobenzoyl chloride (1.92 g, 7.2 mmol) slowly. The mixture was left stirring at rt for 1 h and then *p*TsOH monohydrate (2.05 g, 10.8 mmol) was added. The mixture was then left refluxing using a Dean Stark procedure for 42 h and then cooled to rt and quenched with 5% aqueous NaOH (10 ml). After evaporation, ethyl acetate (50 ml) and THF (10 ml) was added, the organic phase was washed with 10% aqueous NaOH (3 x 20 ml), dried ($MgSO_4$) and evaporated to give 1.623 g of crude product which was purified by silica gel column chromatography

(hexane/THF, gradient elution) to give **268b** (1.36 g, 71%) as light brown solid. All spectroscopic and analytical details were identical to those reported in the literature.[202] δ_H (400 MHz, DMSO-d^6) 7.21-7.31 (3H, m, Ar), 7.51-7.58 (2H, m, Ar), 7.62 (1H, dd, J_1 7.6, J_2 2, Ar), 7.67-7.72 (1H, m, Ar), 8.06 (1H, d, J 7.6, Ar) and 12.67 (1H, b, N*H*) ppm. δ_C (100 MHz, DMSO-d^6) 98.1, 112.2, 119.8, 122.2, 123.3, 128.8, 131.9, 132.1, 135.1, 137.3, 140.3, 143.9 and 153.3 ppm.

Synthesis of 1-allyl-2-(2-bromophenyl)benzimidazole **267a**

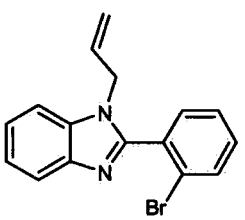

267a

To a solution of 2-(2-bromophenyl)benzimidazole **268a** (181.2 mg, 0.663 mmol) in anhydrous DMF (5 ml) was added NaH (32 mg, 0.796 mmol) and left stirring at rt for 10 min. Allyl bromide (0.068 ml, 0.796 mmol) was added and the mixture left stirring for another 30 min at rt. The reaction was quenched with EtOH (100 µl), evaporated, diluted with ether (20 ml) and the organic phase washed with water (3 x 7 ml), dried ($MgSO_4$) and evaporated to give 0.220 g of crude product. The crude material was purified by silica gel column chromatography (hexane/ethyl acetate, gradient elution) to give the product **267a** (0.172 mg, 0.55 mmol, 83%) as yellow oil. IR (neat): ν_{max}/cm^{-1} : 3059, 2923, 1614, 1455, 1389, 1329, 1027 and 749. δ_H (400 MHz, $CDCl_3$) 4.55 (2H, d, J 5.2, NC*H*$_2$CHCH$_a$H$_b$), 5.90 (1H, dd, J_1 17.2, J_2 0.8, NCH$_2$CHC*H*$_a$H$_b$), 5.08 (1H, dd, J_1 2.4, J_2 0.8, NCH$_2$CHCH$_a$*H*$_b$), 5.71-5.82 (1H, m, NCH$_2$C*H*CH$_a$H$_b$), 7.21-7.42 (6H, m, Ar), 7.63 (H, J_1 8.2, J_2 1.6, Ar), and 7.75-7.81 (1H, m, Ar) ppm. δ_C (100 MHz, $CDCl_3$) 47.3, 110.8, 118.1, 120.5, 122.7, 123.3, 124.1, 127.6, 131.7, 132.2, 132.3, 132.5, 133.1, 134.9, 143.2 and 152.4 ppm. *m/z* EI (+) 313.0335 and 315.0314 (M+H$^+$, 100%) $C_{16}H_{14}N_2Br$ requires 313.0335 and 315.0314.

Synthesis of 1-allyl-2-(2-iodophenyl)benzimidazole **267b**

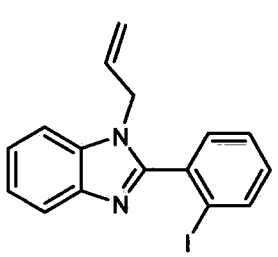

267b

To a solution of 2-(2-iodophenyl)benzimidazole **268b** (343.1 mg, 1.07 mmol) in anhydrous DMF (13 ml) was added NaH (31 mg, 1.29 mmol) and left stirring at rt for 10 min. Allyl bromide (0.11 ml, 1.286 mmol)

was added and the mixture stirred for another 60 min. The reaction was quenched with EtOH (200 µl) and the mixture was evaporated, diluted with ether (30 ml), the organic phase washed with water (3 x 10 ml), dried ($MgSO_4$) and evaporated to give 0.395 g of crude product. The crude material was purified with silica gel column chromatography (hexane/ethylacetate, gradient elution) to give the product **267b** (0.336 mg, 0.934 mmol, 87%) as yellow oil. IR (neat): ν_{max}/cm^{-1} : 3411, 2983, 2931, 1644, 1455, 1387, 1330, 1283, 1015 and 745. δ_H (400 MHz, $CDCl_3$) 4.53 (2H, d, *J* 4.8, $NCH_2CHCH_aH_b$), 4.91 (1H, d, *J* 17.2, $NCH_2CHCH_aH_b$), 5.08 (1H, d, *J* 10.4, $NCH_2CHCH_aH_b$), 5.72-5.82 (1H, m, $NCH_2CHCH_aH_b$), 7.10-7.15 (1H, m, Ar), 7.22-7.28 (2H, m, Ar), 7.31-7.40 (3H, m, Ar), 7.77-7.81 (1H, m, Ar), and 7.89 (1H, d, *J* 8, Ar) ppm. δ_C (100 MHz, $CDCl_3$) 47.1, 98.6, 110.5, 117.9, 120.4, 122.5, 123.1, 128.0, 131.3, 131.5, 132.0, 134.6, 136.3, 139.2, 142.9 and 154.1 ppm. *m/z* EI (+) 361.0192 ($M+H^+$, 100%) $C_{16}H_{14}N_2I$ requires 361.0196.

Synthesis of 5-methylbenzimidazo[2,1]isoquinoline **269**

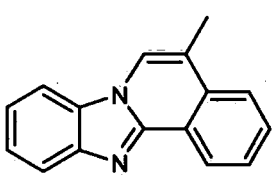

269

To a dried Schlenk tube under argon was added $Pd(OAc)_2$ (25 mg, 0.11 mmol), tetrabutylammonium chloride (309 mg, 1.11 mmol) and $NaHCO_3$ (233mg, 2.78 mmol). A solution of **267a** (348 mg, 1.11 mmol) in anhydrous DMF (22 ml) was added to the Schlenk tube and the mixture degassed using the freeze-pump-thaw method (3 x) and heated to 130 °C for 18 h. The mixture was cooled to rt and evaporated, extracted with ether (25 ml), washed with water (3 x 10 ml) and dried ($MgSO_4$) to give 625 mg of crude product. The crude material was purified by silica gel column chromatography (EtOAc/hexane, gradient elution) to give **269** (200 mg, 78%) as yellow oil. IR (neat): ν_{max}/cm^{-1} : 3373, 3055, 1645, 1518, 1450, 1369, 1251 and 756. δ_H (400 MHz, $CDCl_3$) 2.41 (3H, s, $ArCH_3$), 7.27 (1H, t, *J* 7.6, Ar), 7.39 (1H, t, *J* 7.6, Ar), 7.59 (2H, m, Ar), 7.67 (2H, m, Ar), 7.81 (1H,m, Ar),7.90 (1H, d, *J* 8.4, Ar) and 8.75 (1H, d, *J* 6, NCH) ppm. δ_C (100 MHz, $CDCl_3$) 16.6, 110.0, 117.7, 119.4, 119.9, 121.8, 123.5, 124.2, 124.6, 125.4, 128.1, 130.1 (2C), 132.4, 143.8 and 147.2 ppm. *m/z* EI (+) 233.1072 ($M+H^+$, 100%) $C_{16}H_{13}N_2$ requires 233.1073.

Synthesis of 2-(2-bromophenyl)-1-(3-bromopropyl)-1*H*-benzimidazole **271a**

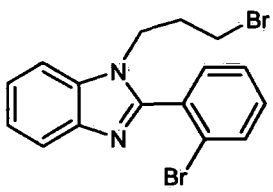

271a

To a solution of 2-(2-bromophenyl)benzimidazole **268a** (1.057 g, 3.87 mmol) in anhydrous DMF (12 ml), NaH (97 mg, 4.06 mmol) was added and left stirring at rt for 30 min. This solution was added to a mixture of 1,3-dibromopropane (3.93 ml, 38.7 mmol) dissolved in anhydrous DMF (20 ml) pre-cooled to 0 °C dropwise over 30 min. After 1 h at 0 °C, the reaction was quenched with water (1 ml) and allowed to warm to rt. After evaporation, 10% aqueous NaOH (20 ml) was added and the product was extracted with DCM (3 x 30 ml). The combined organic phases were dried ($MgSO_4$) to give 1.79 g of crude product which was purified by silica gel column chromatography (hexane/ethyl acetate, gradient elution) to give the product **271a** (0.762 mg, 1.94 mmol, 50%) as viscous yellow oil. IR (neat): ν_{max}/cm^{-1} 3054, 2957, 1613, 1508, 1449, 1395, 1256, 1026 and 747. δ_H (400 MHz, $CDCl_3$) 2.15 (2H, quintet, *J* 6.8, $NCH_2CH_2CH_2Br$), 3.16 (2H, t, *J* 5.6, $NCH_2CH_2CH_2Br$), 4.17 (2H, t, *J* 6.8, $NCH_2CH_2CH_2Br$), 7.24-7.46 (6H, m, Ar), 7.63 (1H, d, *J* 8, Ar) and 7.75 (1H, J_1 6.6, J_2 1.6, Ar) ppm. δ_C (100 MHz, $CDCl_3$) 28.6, 31.3, 41.7, 109.1, 119.2, 121.7, 122.4, 122.8, 126.7, 130.7, 130.8, 131.1, 132.1, 133.5, 141.6 and 150.9 ppm. HRMS (ESI+): $C_{16}H_{15}N_2Br_2$ *m/z* calcd 392.9597, 394.9576 and 396.9556 ($M+H^+$), found 392.9594, 394.9572 and 396.9555.

Synthesis of 2-(2-iodophenyl)-1-(3-bromopropyl)-1*H*-benzimidazole **271b**

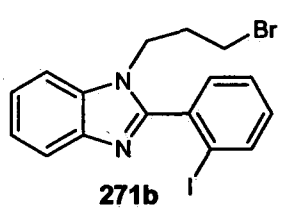

271b

To a solution of 2-(2-iodophenyl)benzimidazole **268b** (1.358 g, 4.24 mmol) in anhydrous DMF (10 ml) was added NaH (204 mg, 5.09 mmol). After 30 min., this solution was added to a mixture of 1,3 dibromopropane (4.3 ml, 42.4 mmol) in anhydrous DMF (20 ml) pre-cooled to 0 °C over a period of 30 min. After 2 h at 0 °C, the reaction was quenched with water (2 ml) and allowed to warm to rt. After evaporation, 10% aqueous NaOH (20 ml) was added and the product was extracted with DCM (3 x 30 ml), the combined organic phases were dried ($MgSO_4$ and evaporated to give 2.64 g of crude product. Purification by silica gel column chromatography (hexane/ethyl acetate, gradient elution) gave the product **271b** (0.426 mg, 0.967 mmol, 23%) as viscous yellow oil. IR (neat): ν_{max}/cm^{-1} 3053, 2929, 2348,

1723, 1444, 1392, 1256, 1014 and 746. δ_H (400 MHz, $CDCl_3$) 2.17 (2H, quintet, *J* 6.4, $NCH_2CH_2CH_2Br$), 3.19 (2H, t, *J* 6.4, $NCH_2CH_2CH_2Br$), 4.11-4.27 (2H, m, $NCH_2CH_2CH_2Br$), 7.14-7.19 (1H, m, Ar), 7.23-7.31 (2H, m, Ar), 7.39-7.46 (3H, m, Ar), 7.77-7.81 (1H, m, Ar) and 7.91-7.94 (1H, m, Ar) ppm. δ_C (100 MHz, $CDCl_3$) 29.7, 32.5, 42.8, 97.7, 109.9, 120.5, 122.6, 123.3, 128.3, 131.4, 131.5, 132.6, 133.4, 139.4, 142.1 and 152.8 ppm. HRMS (ESI+): $C_{16}H_{15}N_2{}^{79}Br^{127}I$ *m/z* calcd 440.9458 ($M+H^+$), found 440.9458.

Parham cyclisation: synthesis of 6,7-dihydro-5*H*-7a,12-diazadibenzo[a,e] azulene **258**

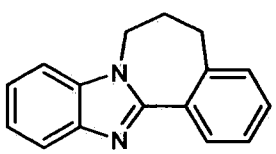

258

Compound **271a** (128 mg, 0.324 mmol) was dissolved in anhydrous THF (13 ml) and anhydrous ether (5 ml) and cooled to -78 °C. *n*-BuLi (143 µl, 0.357 mmol) was added dropwise over a period of 10 min. and the mixture was left stirring at -78 °C for 2 h and allowed to warm to rt overnight (16 h). The mixture was quenched with aqueous NH_4Cl (7 ml) and extracted with ether (3 x 13 ml). The combined organic phases were dried ($MgSO_4$) and evaporated to give 113 mg of crude material which was purified by silica gel column chromatography (hexane/ethyl acetate, gradient elution) to give **258** (14 mg, 0.06 mmol) in 18% as light brown viscous oil. IR (neat): ν_{max}/cm^{-1}.3061, 2948, 2862, 1453, 1397, 1277, 1026 and 754. δ_H (400 MHz, $CDCl_3$) 2.33 (2H, quint., *J* 6.8, $NCH_2CH_2CH_2Ar$), 2.71 (2H, t, *J* 7.2, $NCH_2CH_2CH_2Ar$), 4.04 (2H, t, *J* 6.8, NCH_2CHCH_2Ar), 7.20-7.27 (3H, m, Ar), 7.29-7.36 (3H, m, Ar), 7.76-7.80 (1H, m, Ar), and 7.89-7.92 (1H, m, Ar) ppm. δ_C (100 MHz, $CDCl_3$) 30.6, 30.9, 41.3, 108.9, 120.0, 122.1, 122.5, 127.3, 129.4, 129.5, 130.2, 130.9, 135.5, 138.9, 143.3 and 154.5 ppm. HRMS (ESI+): $C_{16}H_{15}N_2$ *m/z* calcd 235.1229 ($M+H^+$), found 235.1230.

Grignard cyclisation: synthesis of 6,7-dihydro-5*H*-7a,12-diazadibenzo[a,e] azulene **258**

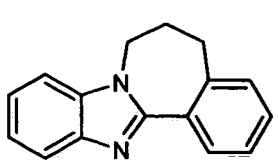

258

To a solution of **271b** (199 mg, 0.453 mmol) in anhydrous THF (3 ml) were added Mg turnings (12.1 mg, 0.498 mmol) and a crystal of iodine.

The mixture was heated to reflux until the Grignard reaction initiated. After leaving the mixture refluxing for 2 h, Li_2CuCl_4 (91 µl, 9.1 µmol) was added and the mixture was left refluxing overnight (16 h). The mixture was quenched with 20% aqueous NaOH (15 ml) and the product was extracted with DCM (3 x 20 ml). The combined organic phases were dried ($MgSO_4$) and evaporated to give 109 mg of crude material which was purified by silica gel column chromatography (hexane/ethyl acetate, gradient elution) to give **258** (26.2 mg, 0.11 mmol) in 25% as light brown viscous oil. All spectroscopic and analytical properties were identical to these reported in the previous experiment.

Synthesis of 2-(2-bromophenyl)-[1,3]dioxolane **273**

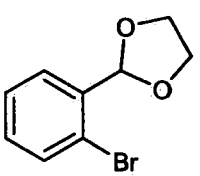

273

To a mixture of 2-bromobenzaldehyde (1.168 ml, 10 mmol) and diglyme (696 µl, 12.5 mmol) in toluene (10 ml) was added *p*TsOH (19 mg, 0.1 mmol). The mixture was heated at reflux using a Dean Stark procedure for 21 h and cooled to rt. After evaporation, ether (30 ml) was added and the organic phase was washed with saturated aqueous $NaHCO_3$ solution (3 x 10 ml) and dried ($MgSO_4$) to give 2.29 g of crude material which was purified by silica gel column chromatography (hexane/THF, gradient elution) to give **273** (1.93 g, 8.42 mmol) of 84% as colourless oil. All spectroscopic and analytical properties were identical to those reported in the literature.[212] δ_H (400 MHz, $CDCl_3$) 4.05-4.11 (2H, m, OCH_2CH_2O), 4.13-4.17 (2H, m, OCH_2CH_2O), 6.10 (1H, s, Bz), 7.17-7.39 (1H, m, Ar), 7.29-7.39 (1H, m, Ar) and 7.53-7.64 (2H, m, Ar) ppm. δ_C (100 MHz, $CDCl_3$) 70.8 (2C), 105.3, 123.5, 127.3, 128.3, 129.1, 131.4 and 140.5 ppm

Synthesis of 2-[2-(3-bromopropyl)phenyl]-[1,3]dioxolane **274**

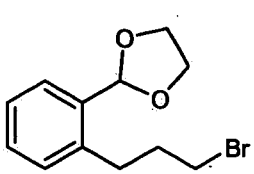

274

To a solution of **273** (1.0 ml, 6.7 mmol) in anhydrous THF (8 ml) were added Mg turnings (195 mg, 8.0 mmol) and a crystal of iodine. The mixture was heated to reflux until the Grignard reaction initiated and left refluxing for 2 h. In another flask, 1,3-dibromopropane (5.075 ml, 50 mmol), CuBr (93.24 mg, 0.65 mmol) and dry HMPA (1.5 ml) was dissolved in anhydrous THF (8 ml) and heated to reflux. The solution of **273** was added

dropwise over a period of 30 min. to the solution of 1,3-dibromopropane. This mixture was left refluxing for 69 h, quenched with saturated aqueous NH_4Cl solution (15 ml) and the product extracted with DCM (3 x 30 ml). The combined organic phases were dried ($MgSO_4$) and evaporated to give 3.44 g of crude product. The crude material was purified by silica gel column chromatography (hexane/ethyl acetate, gradient elution) to give **274** and **275** in the same fraction (943 mg) in 43% (2.85 mmol) and 17% (1.14 mmol) as a light yellow oil. All spectroscopic and analytical details were identical to those reported in the literature.[211] δ_H (400 MHz, $CDCl_3$) 2.01-2.08 (2H, m, $PhCH_2CH_2CH_2Br$), 2.76 (2H, t, *J* 7.6, $PhCH_2CH_2CH_2Br$), 3.30 (2H, t, *J* 5.2, $PhCH_2CH_2CH_2Br$), 3.87-4.03 (4H, m, OCH_2CH_2O), 5.84 (1H, s, Bz), 7.09-7.14 (1H, m, Ar), 7.22-7.24 (1H, m, Ar), 7.31-7.35 (1H, m, Ar) and 7.42 (1H, dd, J_1 7.4, J_2 1.2, Ar) ppm. ^{13}C-NMR could not be fully analysed due to the interference of peaks of side product **275**.

Synthesis of *N*-[3-(2-[1,3]dioxolan-2-ylphenyl)propyl]benzene-1,2-diamine **277**

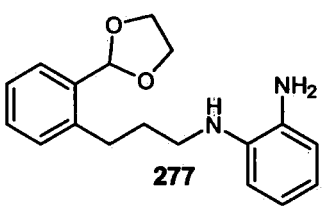

277

To a solution of 1,2-benzenediamine (3.08 g, 28.5 mmol) in anhydrous DMF (40 ml) was added K_2CO_3 (3.93 g, 28.5 mmol). This mixture was heated to reflux for 30 min. The sample of **274** and **275** prepare from the previous experiment (943 mg, 2.85 mmol and 1.14 mmol) was dissolved in anhydrous DMF (5 ml) and added to the 1,2-benzenediamine solution. This mixture was left refluxing for 42 h and quenched with EtOH (2 ml). After removing all sovents, the crude mixture was diluted in brine (20 ml, pH 8-9) and the product was extracted with DCM (3 x 30 ml). The combined organic phases were dried ($MgSO_4$) and evaporated to give 1.28 g of crude product. The crude material was further purified silica gel column chromatography (hexane/ethyl acetate, gradient elution) to give **277** (410.3 mg, 1.375 mmol) in 48% as a dark brown oil. Due to the instability of this product, no further analysis was possible and the product was used immediately for the next step. Rf value: 0.24 in hexane: ethyl acetate (6:4)

Pathway B: synthesis of 6,7-dihydro-5*H*-7a,12-diazadibenzo[a,e]azulene **258**

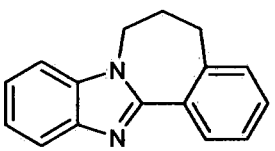

258

277 (410.3 mg, 1.375 mmol) was dissolved in DMF (5.0 ml) and 1 M HCl (2.2 ml). This mixture was left stirring for 16 h at rt and then neutralised to pH 6-7. To this solution further DMF was added (20 ml) together with the Oxone® (0.550 g, 0.894 mmol). The solution was again left stirring for another 23 h at rt and quenched with 20% aqueous NaOH (6.0 ml). After removing all solvents, 20% NaOH solution (20 ml) was added and the product was extracted with DCM (3 x 30 ml). The combined organic phases were dried ($MgSO_4$) and evaporated to give 316 mg of crude product. The crude material was further purified by silica gel column chromatography (hexane/ethyl acetate, gradient elution) to give **258** (151 mg, 0.644 mmol) 47% as light brown viscous oil. All spectroscopic and analytical data were identical to those reported above.

Synthesis of 6,7-dihydro-5*H*-7a,12-diazadibenzo[*a,e*]azulene-1-carbaldehyde **278**

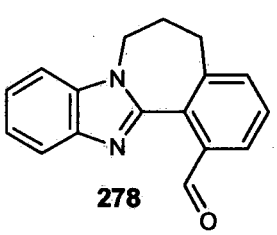

278

After drying **258** (143 mg, 0.609 mmol) over P_2O_5 overnight, it was dissolved in dry THF (5 ml) under argon and cooled to -25 °C. *n*-BuLi (0.508 ml, 2.5 M in hexane, 1.27 mmol) was added dropwise over 15 min. After 2 h at -25 °C, anhydrous DMF (0.395 ml, 5.09 mmol) was added dropwise and the mixture continued to stir for 1 h at -25 °C and was allowed to warm to rt overnight. The reaction was quenched by adding saturated aqueous NH_4Cl (7 ml) and extracted with ether (3 x 10 ml). The combined organic phases were dried ($MgSO_4$) and the solvent was evaporated to give a yellow crude oil (0.177 g). Purification by silica gel column chromatography (hexane: ethyl acetate, gradient elution) provided **278** (46.5 mg, 0.177 mmol) in a yield of 29% as a yellow thick oil. IR (neat): ν_{max}/cm^{-1} 3055, 2941, 2857, 1685, 1593, 1453, 1380, 1248 and 743. δ_H (400 MHz, $CDCl_3$) 2.33 (2H, quint., *J* 7.2, $NCH_2CH_2CH_2Ar$), 2.65 (2H, t, *J* 7.2, $NCH_2CH_2CH_2Ar$), 4.13 (2H, t, *J* 6.8, $NCH_2CH_2CH_2Ar$), 7.20-7.31 (2H, m, Ar), 7.35-7.39 (H, m, Ar), 7.47-7.50 (2H, m, Ar), 7.78-7.83 (1H, m, Ar), 7.94-7.98 (1H, m, Ar) and 10.46 (1H, s, OC*H*) ppm. δ_C (100 MHz, $CDCl_3$) 29.5, 29.6, 39.7, 108.0,

119.4, 121.4, 122.3, 125.4, 129.2, 132.1, 133.3, 133.8, 134.6, 139.0, 142.3, 148.6 and 191.6 ppm. HRMS (ESI+): $C_{17}H_{15}ON_2$ *m/z* calcd 263.1179 ($M+H^+$), found 263.1176.

6.References

1. Breslow, R.; Dong, S. D. *Tetrahedron Lett.* **1998**, *39*, 9343.

2. Imbriglia, J. E.; Vasbinder, M. M.; Miller, S. J. *Org. Lett.* **2003**, *20*, 3741-3743.

3. Rowlands, G. J. *Tetrahedron* **2001**, *57*, 1865-1882.

4. Shibasaki, M.; Sasai, H.; Arai, T. *Angew. Chem. Int. Ed.* **1997**, *36*, 1237-1256.

5. Corey, E. J.; Bakshi, R. K.; Shibata, S. *J. Am. Chem. Soc.* **1987**, *109*, 5551-5553.

6. Morita, K.; Suzuki, Z.; Hirose, H. *Bull. Chem. Soc. Jpn.* **1968**, *41*, 2815.

7. Baylis, A. B.; Hillman, M. E. D. German patent 2155113; *Chem. Abstr.* **1972**, *77*, 34174q.

8. Drewes, S. E.; Emalie, N. D. *J. Chem. Soc., Perkin. Trans. 1* **1982**, 2079-2083.

9. Hoffmann, H. M. R.; Rabe, J. *Angew. Chem. Int. Ed.* **1983**, *22*, 795-796.

10. Shi, M.; Li, C.-K.; Jiang, J.-K. *Chem. Commun.* **2001**, 833-834.

11. Basavaiah, D.; Gowriswari, V. V. L. *Tetrahedron Lett.* **1986**, *27*, 2031-2032.

12. Shi, M.; Xu, Y.-M. *Eur. J. Org. Chem.* **2002**, 696-701. Kawahara, S.; Nakano, A.; Esumi, T.; Iwabuchi, Y.; Hatakeyama, S. *Org. Lett.* **2003**, *17*, 3103-3105. Balan, D.; Adolfsson, H. *Tetrahedron Lett.* **2003**, *44*, 2521-2524.

13. Shi, M.; Xu, Y.-M.; Zhao, G.-L.; Wu, X.-F. *Eur. J, Org. Chem.* **2002**, 3666-3679.

14. Santos, L. S.; Pavam, C. H.; Almeido, W. P.; Coelho, F.; Eberlin, M. N. *Angew. Chem. Int. Ed.* **2004**, *43*, 4330-4333.

15. Bodé, M. L.; Kaye, P. T. *Tetrahedron Lett.* **1991**, *32*, 5611-5614.

16. Fort, Y.; Berthe, M. C.; Caubere, P. *Tetrahedron* **1992**, *48*, 6371-6384.

17. Aggarwal, V. K.; Fulford, S. Y.; Lloyd-Jones, G. C. *Angew. Chem. Int. Ed.* **2005**, *44*, 1706-1708.

18. Buskens, P.; klankermayer, J.; Leitner, W. *J. Am. Chem. Soc.* **2005**, *127*, 16762-16763.

19. Price, K. E.; Broadwater, S. J.; Jung, H. M.; McQuade, D. T. *Org. Lett.* **2005**, *7*, 147-150.

20. Masson, G.; Housseman, C.; Zhu, J. *Angew. Chem. Int. Ed.* **2007**, *46*, 4614-4628.

21. Basavaiah, D.; Sorma, P. K. S. *Synth. Commun.* **1990**, *20*, 1611-1615.

22. Lee, W.-D.; Yang, K.-S.; Chen, K. *Chem. Commun.* **2001**, 1612-1613.

23. Kundu, M. K.; Mukherjee, S. B.; Balu, N.; Padmakumar, R.; Bhat, S. V. *Synlett* **1994**, 444.

24. Ciganek, E., *Organic Reactions*; Paquette, L.A., Ed.; John Wiley& Sons: New York, **1997**; Vol. 51, p 201.

25. Hill, J. S.; Isaacs, N. S. *Tetrahedron Lett.* **1986**, *27*, 5007. Schuurman, R. J. W.; Van der Linden, A.; Grimbergen, R. P. F.; Nolte, R. J. M.; Scheeren, H. W. *Tetrahedron* **1996**, *52*, 8307.

26. Rafel, S.; Leahy, J. W. *J. Org. Chem.* **1997**, *62*, 1521-1522.

27. Mack, J.; Shumba, M. *Green Chem.* **2007**, *9*, 328-330.

28. Rose, P. M.; Clifford, A. A.; Rayner, C. M. *Chem. Commun.* **2002**, 968-969.

29. Cai, J.; Zhou, Z.; Zhao, G.; Tang, C. *Org. Lett.* **2002**, *26*,4723-4725.

30. Aggarwal, V. K.; Dean, D. K., Mereu, A.; Williams, R. *J. Org. Chem.* **2002**, *67*, 510-514.

31. Krishna, P. R.; Manjuvani, A.; Kannan, V.; Sharma, G. V. M. *Tetrahedron Lett.* **2004**, *45*, 1183-1185.

32. Davies, H. J.; Ruda, A. M.; Tomkinson, N. C. O. *Tetrahedron Lett.* **2007**, *48*, 1461-1464.

33. Yu, C.; Liu, B.; Hu, L. *J. Org. Chem.* **2001**, *66*, 5413-5418.

34. Augé, J.; Lubin, N.; Lubineau, A. *Tetrahedon Lett.* **1994**, *43*, 7947-7948.

35. Basavaiah, D.; Krishnamachoryulu, M.; Rao, A. J. *Synth. Commun.* **2000**, *30*, 2061-2069.

36. Caumul, P.; Hailes, H. C. *Tetrahedron Lett.* **2005**, *46*, 8125-8127.

37. Luo, S.; Wang, P. G.; Cheng, J.-P. *J. Org. Chem.* **2004**, *69*, 555-558.

38. Rosa, J. N.; Afonso, C. A. M.; Santos, A. G. *Tetrahedron* **2001**, *57*, 4189-4193.

39. Kim, E. J.; Ko, S. Y. *Helv. Chim. Acta* **2003**, *86*, 894-899.

40. Kumar, A.; Pawar, S. S. *J. Mol. Catal. A: Chem.* **2004**, *211*, 43-47.

41. Santos, L. S.; Neto, B. A. D.; Consorti, C. S.; Pavam, C. H.; Almeida, W. P.; Coelho, F.; Dupont, J.; Eberlin, M. N. *J. Phys. Org. Chem.* **2006**, *19*, 731-736.

42. Afonso, C. A. M.; Branco, L. C.; Candeias, N. R.; Gois, P. M. P.; Lourenço, N. M. T.; Mateus, N. M. M.; Rosa, J. N. *Chem. Commun.* **2007**, 2669-2679.

43. Aggarwal, V. K.; Emme, I.; Mereu, A. *Chem. Commun.* **2002**, 1612-1613.

44. Gong, H.; Cai, C.; Yang, N.; Yang, L.; Zhang, J.; Fan, Q. *J. Mol. Catal. A: Chem.* **2006**, *249*, 236-239.

45. Zhao, S.-H.; Zhang, H.-R.; Feng, L.-H.; Chen, Z.-B. *J. Mol. Catal. A: Chem.* **2006**, *258*, 251-256.

46. Hsu, J.-C.; Yen, Y.-H.; Chu, Y.-H. *Tetrahedron Lett.* **2004**, *45*, 4673-4676.

47. Mi, X.; Luo, S.; Cheng, J.-P. *J. Org. Chem.* **2005**, *70*, 2338-2341.

48. Mi, X.; Luo, S.; Xu, H.; Zhang, L.; Cheng, J.-P. *Tetrahedron* **2006**, *62*, 2537-2544.

49. Lin, Y.-S.; Lin, C.-Y.; Liu, C.-W.; Tsai, T. Y. R. *Tetrahedron* **2006**, *62*, 872-877.

50. Kawamura, M.; Kobayashi, S. *Tetrahedron Lett.* **1999**, *40*, 1539-1542.

51. Kumar, A.; Pawor, S. S. *Tetrahedron* **2003**, *59*, 5019-5026.

52. Ameer, F.; Drewes, S. E.; Freese, S. D.; Kaye, P. T. *Synth. Commun.* **1988**, *18*, 495-500.

53. Drewes, S. E.; Freese, S. D.; Emslie, N. D.; Roos, G. H. P. *Synth. Commun.* **1988**, *18*, 1565-1572.

54. Aggarwal, V. K.; Emme, I.; Fulford, S.Y. *J. Org. Chem.* **2003**, *68*, 692-700.

55. Shi, M.; Xu, Y.-M. *Eur. J. Org. Chem.* **2002**, 696-701.

56. Shi, M.; Liu, Y.-H. *Org. Biomol. Chem.* **2006**, 4, 1468-1470.

57. He, Z.; Tang, X.; Chen, Y.; He, Z. *Adv. Synth. Catal.* **2006**, *348*, 413-417.

58. Tang, X.; Zhang, B.; He, Z.; Gao, R.; He, Z. *Adv. Synth. Catal.* **2007**, *349*, 2007-2017.

59. De Souza, R.; Meireles, B. A.; Aguiar, L.; Vasconcellos, M. *Synthesis* **2004**, 1595-1600.

60. Roth, F.; Gygax, P.; Frater, G. *Tetrahedron Lett.* **1992**, *33*, 1045-1048.

61. Luo, S.; Mi, X.; Xu, H.; Wang, P. G.; Cheng, J.-P. *J. Org. Chem.* **2004**, *69*, 8413-8422.

62. He, L.; Jian, T.-Y.; Ye, S. *J. Org. Chem.* **2007**, *72*, 7466-7468.

63. Pei, W.; Wei, H.-X.; Li, G. *Chem. Commun.* **2002**, 2412-2413.

64. Li, G.; Wei, H.-X.; Gao, J. J.; Caputo, T. D. *Tetrahedron Lett.* **2000**, *41*, 1-5.

65. Aggarwal, V. K.; Mereu, A. *Chem. Commun.* **1999**, 2311-2312.

66. Leadbeater, N. E.; Van der Pol, C. *J. Chem. Soc., Perkin Trans. 1* **2001**, 2831-2835.

67. Luo, S.; Zhang, B.; He, J.; Janczuk, A.; Wang, P. G.; Cheng, J.-P. *Tetrahedron Lett.* **2002**, *43*, 7369-7371.

68. Luo, S.; Mi, X.; Wang, P. G.; Cheng, J.-P. *Tetrahedron Lett.* **2004**, *45*, 5171-5174.

69. Richter, H.; Jung, G. *Tetrahedron Lett.* **1998**, *39*, 2729-2730.

70. Corma, A.; Garcia, H.; Leyva, A. *Chem. Commun.* **2003**, 2806-2807.

71. Zhao, L.-J.; He, H. S.; Shi, M.; Toy, P. H. *J. Comb. Chem.* **2004**, *6*, 680-683.

72. Zhao, L.-J.; Kwong, C. K.-W.; Shi, M.; Toy, P. H. *Tetrahedron* **2005**, *61*, 12026-12032.

73. Kwong, C. K.-W.; Huang, R.; Zhang, M.; Shi, M.; Toy, P. H. *Chem. Eur. J.* **2007**, *13*, 2369-2376.

74. Maher, D. J.; Connon, S. J. *Tetrahedron Lett.* **2004**, *45*, 1301-1305.

75. Aggarwal, V. K.; Tarver, G. J.; McCague, R. *Chem. Commun.* **1996**, 2713-2714.

76. Kataoka, T.; Iwama, T.; Tsujiyama, S.-I. *Chem. Commun.* **1998**, 197-198.

77. You, J.; Xu, J.; Verkade, J. G. *Angew. Chem. Int. Ed.* **2003**, *42*, 5054-5056.

78. Walsh, L. M.; Winn, C. L.; Goodman, J. M. *Tetrahedron Lett.* **2002**, *43*, 8219-8222.

79. Yi, W.-B.; Cai, C.; Wang, X. *J. Fluorine Chem.* **2007**, *128*, 919-924.

80. Kündig, E. P.; Xu, L.-H.; Romanes, P.; Bernardinelli, G. *Tetrahedron Lett.* **1993**, *34*, 7049-7052.

81. Kündig, E. P.; Xu, L.-H.; Schnell, B. *Synlett* **1994**, 413-414.

82. Gilbert, A.; Heritage, T. W.; Isaacs, N. S. *Tetrahedron Asymmetry* **1991**, *10*, 969-972.

83. Basavaiah, D.; Gowriswari, V. V. L.; Sarma, P. K. S.; Rao, P. D. *Tetrahedron Lett.* **1990**, *11*, 1621-1624.

84. Bauer, T.; Tarasiuk, J. *Tetrahedron Asymmetry* **2001**, *12*, 1741-1745.

85. Aggarwal, V. K.; Castro, A. M. M.; Mereu, A.; Adams, H. *Tetrahedron Lett.* **2002**, *43*, 1577-1581.

86. Davis, F. A.; Szewczyk, J. M.; Reddy, R. E. *J. Org. Chem.* **1996**, *61*, 2222.

87. Shi, M.; Xu, Y.-M. *Tetrahedron Asymmetry* **2002**, *13*, 1195-1200.

88. Krishna, P. R.; Kannan, V.; Sharma, G. V. M.; Ramana Rao, M. H. V. *Synlett* **2003**, *6*, 888-890.

89. Krishna, P. R.; Manjuvani, A.; Kannan, V. *Tetrahedron Asymmetry* **2005**, *16*, 2691-2703.

90. Krishna, P. R.; Kannan, V.; Ilangovan, A.; Sharma, G. V. M. *Tetrahedron Asymmetry* **2001**, *12*, 829-837.

91. Krishna, P. R.; Sachwani, R.; Kannan, V. *Chem. Commun.* **2004**, 2580-2581.

92. Brzezinski, L. J.; Rafel, S.; Leahy, J. W. *J. Am. Chem. Soc.* **1997**, *119*, 4317-4318.

93. Brezinski, L. J.; Rafel, S.; Leahy, J. W. *Tetrahedron* **1997**, *48*, 16423-16434.

94. Yang, K.-S.; Chen, K. *Org. Lett.* **2000**, *6*, 729-731.

95. Oishi, T.; Oguri, H.; Hirama, M. *Tetrahedron Asymmetry* **1995**, *6*, 1241-1244

96. Marko, I. E.; Giles, P. R.; Hindley, N. J. *Tetrahedron* **1997**, *3*, 1015-1024.

97. Iwabuchi, Y.; Nakatani, M.; Yokoyama, N.; Hatakeyama, S. *J. Am. Chem. Soc.* **1999**, *121*, 10219-10220.

98. Nakano, A.; Kawahara, S.; Akamatsu, S.; Morokuma, K.; Nakatani, M.; Iwabuchi, Y.; Takahashi, K.; Ishihara, B.; Hatakeyama, S. *Tetrahedron* **2006**, *62*, 381-189.

99. Nakano, A.; Ushiyama, M.; Iwabuchi, Y.; Hatakeyama, S. *Adv. Synth. Catal.* **2005**, *347*, 1790-1796.

100. Shi, M.; Jiang, J.-K. *Tetrahedron Asymmetry* **2002**, *13*, 1941-1947.

101. Shi, M.; Xu, Y.-M. *Angew. Chem. Int. Ed.* **2002**, *41*, 4507-4510.

102. Kawahara, S.; Nakano, A.; Esumi, T.; Iwabuchi, Y.; Hatakeyama, S. *Org. Lett.* **2003**, *17*, 3103-3105.

103. Balan, D.; Adolfsson, H. *Tetrahedron Lett.* **2003**, *44*, 2521-2524.

104. Shi, M.; Jiang, J.-K.; Li, C.-Q. *Tetrahedron Lett.* **2002**, *43*, 127-130.

105. Vasbinder, M. M.; Imbriglio, J. E.; Miller, S.J. *Tetrahedron* **2006**, *62*, 11450-11459.

106. Reetz, M. T.; Mondière, R.; Carballeira, J.D. *Tetrahedron Lett.* **2007**, *48*, 1679-1681.

107. Tang, H.; Gao, P.; Zhao, G.; Zhou, Z.; He, L.; Tang, C. *Catal. Commun.* **2007**, *8*, 1811-1814.

108. Tang, H.; Zhao, G.; Zhou, Z.; Zhou, Q.; Tang, C. *Tetrahedron Lett.* **2006**, *47*, 5717-5721.

109. Utsumi, N.; Zhang, H.; Tanaka, F.; Barbas, C.F. *Angew. Chem. Int. Ed.* **2007**, *46*, 1878-1880.

110. Vesely, J.; Dziedzic, P.; Cordova, A. *Tetrahedron Lett.* **2007**, *48*, 6900-6904.

111. Barrett, A. G. M.; Cook, A. S.; Kamimura, A. *Chem. Commun.* **1998**, 2533-2534.

112. Barrett, A. G. M.; Dozzo, P.; White, A. J. P.; Williams, D. J. *Tetrahedron* **2002**, *58*, 7303-7313.

113. Krishna, P. R.; Kannan, V.; Reddy, P. V. N. *Adv. Synth. Catal.* **2004**, *346*, 603-606.

114. Hayashi, Y.; Tamura, T.; Shoji, M. *Adv. Synth. Catal.* **2004**, *346*, 1106-1110.

115. Xu, J.; Guan, Y.; Yang, S.; Ng, Y.; Peh, G.; Tan, C.-H. *Chem. Asian J.* **2006**, *1*, 724-729.

116. Pereira, S. I.; Adrio, J.; Silva, A. M. S.; Carretero, J. C. *J. Org. Chem.* **2005**, *70*, 10175-10177.

117. Li, W.; Zhang, Z.; Xiao, D.; Zhang, X. *J. Org. Chem.* **2000**, *65*, 3489-3496.

118. Sohtome, Y.; Tanatani, A.; Hashimoto, Y.; Nagasawa, K. *Tetrahedron Lett.* **2004**, *45*, 5589-5592.

119. Berkessel, A.; Roland, K.; Neudörf, J. M. *Org. Lett.* **2006**, *19*, 4195-4198.

120. Wang, J.; Li, H.; Yu, X.; Zu, L.; Wang, W. *Org. Lett.* **2005**, *19*, 4293-4296.

121. Raheem, I. T.; Jacobsen, E. N. *Adv. Synth. Catal.* **2005**, *347*, 1701-1708.

122. Hayase, T.; Shibata, T.; Soai, K.; Wakatsuki, Y. *Chem. Commun.* **1998**, 1271-1272.

123. Yamada, Y. M. A.; Ikegami, S. *Tetrahedron Lett.* **2000**, *41*, 2165-2169.

124. McDougal, N. T.; Trevellini, W. L.; Rodgen, S. A.; Kliman, L. T.; Schaus, S. E. *Adv. Synth. Catal.* **2004**, *346*, 1231-1240.

125. McDougal, N. T.; Schaus, S. E. *J. Am. Chem. Soc.* **2003**, *125*, 12094-12095.

126. Shi, M.; Chen, L.-H. *Chem. Commun.* **2003**, 1310-1311.

127. Shi, M.; Li, C.-Q. *Tetrahedron: Asymmetry* **2005**, *16*, 1385-1391.

128. Shi, M.; Chen, L.-H.; Li, C.-Q. *J. Am. Chem. Soc.* **2005**, *127*, 3790-3800.

129. Shi, M.; Chen, L.-H.; Teng, W.-D. *Adv. Synth. Catal.* **2005**, *347*, 1781-1789.

130. Matsui, K.; Takizawa, S.; Sasai, H. *Synlett* **2006**, *5*, 761-765.

131. Matsui, K.; Tanaka, K.; Horii, A.; Takizawa, S.; Sasai, H. *Tetrahedron: Asymmetry* **2006**, *17*, 578-583.

132. Matsui, K.; Takizawa, S.; Sasai, H. *J. Am. Chem. Soc.* **2005**, *127*, 3680-3681.

133. Liu, Y.-H.; Chen, L.-H.; Shi, M. *Adv. Synth. Catal.* **2006**, *348*, 973-979.

134. Ito, K.; Nishida, K.; Gotanda, T. *Tetrahedron Lett.* **2007**, *48*, 6147-6149.

135. Mocquet, C. M.; Warriner, S. L. *Synlett* **2004**, *2*, 356-358.

136. Aggarwal, V. K.; Mereu, A.; Tarver, G. J.; McCague, R. *J. Org. Chem.* **1998**, *63*, 7183-7189.

137. Matsui, K.; Takizawa, S.; Sasai, H. *Tetrahedron Lett.* **2005**, *46*, 1943-1946.

138. Yang, K.-S.; Lee, W.-D.; Pan, J.-F.; Chen, K. *J. Org. Chem.* **2003**, *68*, 915-919.

139. Pégot, B.; Vo-Thanh, G.; Gori, D.; Loupy, A. *Tetrahedron Lett.* **2004**, *45*, 6425-6428.

140. Gausepohl, R.; Buskens, P.; Kleinen, J.; Bruckmann, A.; Lehmann, C. W.; Klankermayer, J.; Leitner, W. *Angew. Chem. Int. Ed.* **2006**, *45*, 3689-3692.

141. Shibasaki, M.; Kanai, M.; Funabashi, K. *Chem. Commun.* **2002**, 1989-1999.

142. Letsinger, R.; Morrison, J. *J. Am. Chem. Soc.* **1963**, 2227-2229. Letsinger, R.; Wysocki, A. *J. Org. Chem.* **1963**, 3199-3201.

143. Coghlan, S. W.; Giles, R. L.; Howard, J. A. K.; Patrick, L. G. F.; Probert, M. R.; Smith, G. E.; Whiting, A. *J. Organomet. Chem.* **2005**, *690*, 4784-4793.

144. Arnold, K.; Davies, B.; Giles, R. L.; Grosjean, C.; Smith, E. S.; Whiting, A. *Adv. Synth. Catal.* **2006**, *348*, 813-820.

145. Blatch, A. J.; Chetina, O. V.; Howard, J. A. K.; Patrick, L. G. F.; Smethurst, C. A.; Whiting, A. *Org. Biomol. Chem.* **2006**, *4*, 3297-3302.

146. Abdel-Magid, A.-F.; Carson, K. G.; Harris, B. D.; Maryanoff, C. A.; Shah, R. D. *J. Org. Chem.* **1996**, *61*, 3849-3862.

147. Wolf, C.; Xu, H. *Tetrahedron Lett.* **2007**, *48*, 6886-6889. Parrish, J. P.; Jung, Y. C.; Floyd, R. J.; Jung, K. W. *Tetrahedron Lett.* **2002**, *43*, 7899-7902.

148. Wong, M. S.; Zhang, X. L. *Tetrahedron Lett.* **2001**, *42*, 4087-4089.

149. Stibrany, R. T.; Schulz, D. N.; Kacker, S.; Patil, A. O.; Baugh, L. S.; Rucker, S. P.; Zushma, S.; Berluche, E.; Sissano, J. A. *Macromolecules* **2003**, *36*, 8584-8586.

150. Pei, J.; Ni, J.; Zhou, X.-H.; Cao, X.-Y.; Lai, Y.-H. *J. Org. Chem.* **2002**, *67*, 4924-4936.

151. Hérault, D.; Aelvoet, K.; Blatch, A. J.; Al-Majid, A.; Smethurst, C. A.; Whiting, A. *J. Org. Chem.* **2007**, *72*, 71-75.

152. Alder, R. W.; Mowlam, R. W.; Vachon, D. J.; Weisman, G. R. *Chem. Commun.* **1992**, 507-508.

153. Genski, T.; MacDonald, G.; Wei, X.; Lewis, N.; Taylor, R. J. K. *ARKIVOC* **2000**, *4*, 445-451.

154. Ward, C. J.; Patel, P.; James, T. D. *J. Chem. Soc., Perkin. Trans. 1* **2002**, 462-470.

155. de Koning, C. B.; Michael, J. P.; Rousseau, A. L. *J. Chem. Soc., Perkin. Trans. 1* **2000**, 787-797.

156. Baudoin, O.; Guénard, D.; Guéritte, F. *J. Org. Chem.* **2000**, *65*, 9268-9271.

157. Murata, M.; Oyama, T.; Watanabe, S.; Masuda, Y. *J. Org. Chem.* **2000**, *65*, 164-168.

158. Pathak, R.; Vandayar, K.; van Otterlo, W. A. L.; Michael, J. P.; Fernandes, M. A.; de koning, C. B. *Org. Biomol. Chem.* **2004**, *2*, 3504-3509.

159. Liu, Y.; McWorther Jr., W. W. *J. Am. Chem. Soc.* **2003**, *125*, 4240-4252.

160. Slätt, J.; Bergman, J. *Tetrahedron* **2002**, *58*, 9187-9191.

161. Schütz, T.; Whiting, A. unpublished results.

162. McKay, W. R.; Practor, G. R. *J. Chem. Soc., Perkin. Trans. 1* **1981**, 2435-2442.

163. Lee, K. Y.; Gan, E.; Kim, S. N. *Tetrahedron Lett.* **2003**, *44*, 1231-1234.

164. Albrecht, R.; Kresze, G.; Mlokar, B. *Chem. Ber.* **1964**, *97*, 483.

165. Wurtz, C. A. *Bull. Soc. Chim. Fr.* **1872**, *17*, 436-442.

166. Zimmerman, H. E.; Traxler, M. D. *J. Am. Chem. Soc.* **1957**, *79*, 1920-1923

167. Masamune, S.; Choy, W. *Aldrichimica Acta* **1982**, *15*, 47.

168. Evans, D. A.; Takacs, J. M.; McGee, L. R.; Mathre, D. J.; Bartroli, J. *Pure Appl. Chem.* **1981**, *53*, 1109.

169. Walker, M. A.; Heathcock, C. H. *J. Org. Chem.* **1991**, *56*, 5747.

170. Evans, D. A.; Bender, S. L.; Morris, J. *J. Am. Chem. Soc.* **1988**, *110*, 2506-2526.

171. List, B.; Lerner, R. A.; Barbas 3th, C. F. *J. Am. Chem. Soc.* **2000**, *122*, 2395-2396.

172. Notz, W.; List, B. *J. Am. Chem. Soc.* **2000**, *122*, 7386-7387.

173. Northrup, A. B.; MacMillan, D. W. C. *J. Am. Chem. Soc.* **2002**, *124*, 6798-6799.

174. Ito, Y.; Sawamura, M.; Hayashi, T. *J. Am. Chem. Soc.* **1986**, *108*, 6406-6407.

175. Yoshikawa, N.; Yamada, Y. M. A.; Das, J.; Sasai, H.; Shibasaki, M. *J. Am. Chem. Soc.* **1999**, *121*, 4168-4178.

176. Yoshikawa, N.; Shibasaki, M. *Tetrahedron* **2001**, *57*, 2569-2579.

177. Shibasaki, M.; Matsunaga, S. *Chem. Soc. Rev.* **2006**, *35*, 269-279.

178. Calter, M. A.; Orr, R. K. *Tetrahedron Lett.* **2003**, *44*, 5699-5701.

179. Trost, B. M.; Ito, H. *J. Am. Chem. Soc.* **2000**, *122*, 12003-12004.

180. Tanaka, K.; Shoji, T. *Org. Lett.* **2005**, *7*, 3561-3563.

181. Fernandez-Lopez, R.; Kofoed, J.; Machuqueiro, M.; Darbre, T. *Eur. J. Org. Chem.* **2005**, 5268-5276.

182. Shibata, I.; Suwa, T.; Sakakibara, H.; Baba, A. *Org. Lett.* **2002**, *2*, 301-303.

183. Denmark, S. E.; Pham, S. M. *J. Org. Chem.* **2003**, *68*, 5045-5055.

184. Dambacher, J.; Zhao, W.; El-Batta, A.; Aness, R.; Jiang, C.; Bergdahl, M. *Tetrahedron Lett.* **2005**, *46*, 4473-4477.

185. Yi, W.-B.; Cai, C. *J. Fluorine Chem.* **2005**, *126*, 1553-1558.

186. Nongkhlaw, R. L.; Nongrum, R.; Myrboh, B. J. *Chem. Soc., Perkin. Trans. 1* **2001**, 1300-1303.

187. Fukuzawa, S.-I.; Tsuruta, T.; Fujinami, T.; Sakai, S. *J. Chem. Soc., Perkin. Trans. 1* **1987**, 1473-1477.

188. Calderon, F.; Fernandez, R.; Sanchez, F.; Fernandez-Mayoralas, A. *Adv. Synth. Catal.* **2005**, *347*, 1395-1403.

189. Zhang, Y.; O'Doherty, G. A. *Tetrahedron* **2005**, *61*, 6337-6351.

190. Aelvoet, K.; Batsanov, A. S.; Blatch, A. J.; Grosjean, C.; Patrick, L. G. F.; Smethurst, C. A.; Whiting, A. *Angew. Chem. Int. Ed.* **2008**, *47*, 768-770.

191. The kinetical data analysis was done using Scientist version 2.01, Mirco-Math Research, Saint Louis, Missouri, USA.

192. Modelling program Spartan®

193. Xiao, R.; Yu, H.; Gao, G.; Xie, R.-G. *J. Chem. Res. (S)* **2003**, 668-670.

194. He, H.; Zatorska, D.; Kim, J.; Aguirre, J.; Llauger, L.; She, Y.; Wu, N.; Immormino, R. M.; Gewirth, D. T.; Chiosis, G. *J. Med. Chem.* **2006**, *49*, 381-390.

195. Commercial available product

196. Gibson, S. E.; Guillo, N.; Middleton, R. J.; Thuilliez, A.; Tozer, M. J. *J. Chem. Soc., Perkin. Trans. 1* **1997**, 447-455. Kim, G.; Kim, J. H.; Kim, W.-J.; Kim, Y. A. *Tetrahedron Lett.* **2003**, *44*, 8207-8209.

197. Ramachary, D. B.; Reddy, G. B. *Org. Biomol. Chem.* **2006**, *4*, 4463-4468.

198. Gogoi, P.; Konwar, D. *Tetrahedron Lett.* **2006**, *47*, 79-82.

199. Yamakawa, K.; Kobayashi, H.; Ito, I. Jpn. Kokai Tokkyo Koho (1998), patent

200. Heravi, M. M.; Tajbakhsh, M.; Ahmadi, A. N.; Mohajerani, B. *Monatsh. Chem.* **2006**, *137*, 175-179.

201. Fonesca, T.; Gigante, B.; Gilchrist, T. L. *Tetrahedron* **2001**, *57*, 1793-1799.

202. Charton, J.; Girault-Mizzi, S.; Debreu-Fontaine, M.-A.; Foufelle, F.; Hainault, I.; Bizot-Espiard, J.-G.; Caignard, D.-H.; Sergheraert, C. *Bioorg. Med. Chem.* **2006**, *14*, 4490-4518. Charton, J.; Girault-Mizzi, S.; Sergheraert, C. *Chem. Pharm. Bull.* **2005**, *53*, 492-497.

203. DeLuca, M. R.; Kerwin, S. M. *Tetrahedron* **1997**, *53*, 457-464.

204. Deady, L. W.; Rodemann, T. *Aust. J. Chem.* **2001**, *54*, 529-534.

205. Ghosh, K.; Ghatak, U.R. *J. Indian Inst. Sci.* **2001**, *81*, 239-264. Singh, V.; Batra, S. *Tetrahedron Lett.* **2006**, *47*, 7043-7045.

206. Bradsher, C. K.; Reames, D. C. *J. Org. Chem.* **1981**, *46*, 1384-1388. Parham, W. E.; Jones, L. D.; Sayed, Y. *J. Org. Chem.* **1975**, *40*, 2394-2399.

207. Onuma, K.; Hashimoto, H. *Bull. Chem. Soc. Jpn.* **1972**, *45*, 2582-2586.

208. Tamura, M.; Kochi, J. *J. Am. Chem. Soc.* **1971**, *93*, 1487.

209. U.S. Pat. Appl. Publ., 2006089405, 17 Apr. 2006.

210. Hauk, D.; Lang, S.; Murso, A. *Org. Process Res. Dev.* **2006**, *10*, 733-738. Knochel, P.; Dohle, W.; Gommermann, N.; Kneisel, F. F.; Kopp, F.; Korn, T.; Sapountzis, I.; Vu, V. A. *Angew. Chem. Int. Ed.* **2003**, *42*, 4302-4320.

211. Zhang, H.-Y.; Blasko, A.; Yu, J.-Q.; Bruice, T. C. *J. Am. Chem. Soc.* **1992**, *114*, 6621-6630.

212. Peters, M. V.; Stoll, R. S.; Goddard, R.; Buth, G.; Hecht, S. *J. Org. Chem.* **2006**, *71*, 7840-7845.

213. Balczewski, P.; Koprowski, M.; Bodzioch, A.; Marciniak, B.; Rozycka-Sokolowska, E. *J. Org. Chem.* **2006**, *71*, 2899-2902.

214. Nishirma, J.; Yamada, N.; Horiuchi, Y.; Ueda, E.; Ohbayashi, A.; Oku, A. *Bull. Chem. Soc. Jpn.* **1986**, *59*, 2035-2037. Zhang, H.-Y.; Yu, J.-Q.; Bruice, T.C. *Tetrahedron* **1994**, *50*, 11339-11362.

215. Plater, M. J.; Greig, I.; Helfrich, M. H.; Ralston, S. H. *J. Chem. Soc., Perkin Trans. 1* **2001**, 2553-2559.

216. Beaulieu, P. L.; Haché, B.; von Moos, E. *Synthesis* **2003**, *11*, 1683-1692.

7.Appendix: Crystal Data

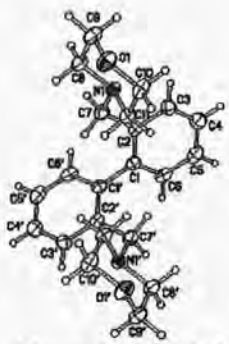

Figure 1. Crystal of **132**.

Table 21. Crystal data and structure refinement for 06srv158.

Identification code	KA28	
Empirical formula	C22 H28 N2 O2	
Formula weight	352.46	
Temperature	120(2) K	
Wavelength	0.71073 Å	
Crystal system	Orthorhombic	
Space group	$P2_12_12$ (No. 18)	
Unit cell dimensions	a = 53.649(4) Å	α= 90°
	b = 6.4069(5) Å	β= 90°
	c = 8.5441(7) Å	γ = 90°
Volume	2936.8(4) Å^3	
Z	6	
Density (calculated)	1.196 g/cm^3	
Absorption coefficient	0.077 mm^{-1}	
F(000)	1140	
Crystal size	0.45 × 0.28 × 0.08 mm^3	
θ range for data collection	0.76 to 27.30°.	
Index ranges	$-63 \leq h \leq 68$, $-8 \leq k \leq 7$, $-10 \leq l \leq 8$	
Reflections collected	17543	
Independent reflections	3677 [R(int) = 0.0439]	

Reflections with I>2σ(I)	3067
Completeness to θ = 25.00°	99.3 %
Absorption correction	None
Refinement method	Full-matrix least-squares on F^2
Data / restraints / parameters	3677 / 0 / 352
Largest final shift/e.s.d. ratio	0.000
Goodness-of-fit on F^2	1.088
Final R indices [I>2σ(I)]	R1 = 0.0495, wR2 = 0.0986
R indices (all data)	R1 = 0.0640, wR2 = 0.1029
Largest diff. peak and hole	0.221 and -0.210 e.Å^{-3}

Table 22. Atomic coordinates (×10^4) and equivalent isotropic displacement parameters (Å^2 ×10^4) for 06srv158. U(eq) is defined as one third of the trace of the orthogonalized Uij tensor.

	x	y	z	U(eq)
O(1)	493.5(4)	8537(3)	3111(2)	321(5)
N(1)	419.7(4)	7738(4)	-136(3)	229(5)
C(1)	131.6(5)	4605(4)	-3316(3)	229(6)
C(2)	319.9(5)	5635(4)	-2491(3)	236(6)
C(3)	562.1(5)	4847(5)	-2539(3)	297(7)
C(4)	617.4(5)	3049(5)	-3385(4)	337(7)
C(5)	431.5(6)	2019(5)	-4191(4)	340(7)
C(6)	189.6(5)	2797(5)	-4168(3)	279(7)
C(7)	268.6(5)	7605(4)	-1554(3)	272(7)
C(8)	418.6(5)	9868(4)	494(4)	285(7)
C(9)	582.5(5)	9942(5)	1935(4)	315(7)
C(10)	492.2(6)	6456(4)	2510(4)	312(7)
C(11)	330.2(5)	6294(4)	1062(3)	264(6)
O(2)	2111.4(4)	5148(3)	2977(2)	314(5)
O(3)	1138.4(4)	-2064(3)	3536(2)	319(5)
N(2)	2063.1(4)	4259(4)	6228(3)	229(5)
N(3)	1228.4(4)	-1311(4)	6785(3)	236(5)
C(12)	1829.9(5)	973(4)	9542(3)	212(6)
C(13)	1998.9(4)	2043(4)	8576(3)	204(6)
C(14)	2244.2(5)	1319(4)	8467(3)	255(6)

C(15)	2320.5(5)	-467(4)	9252(3)	264(6)
C(16)	2150.6(5)	-1545(4)	10182(3)	254(6)
C(17)	1909.2(5)	-827(4)	10320(3)	224(6)
C(18)	1922.0(5)	3992(4)	7692(3)	249(6)
C(19)	1980.3(5)	2783(5)	5032(3)	293(7)
C(20)	2133.4(6)	3062(5)	3561(3)	322(7)
C(21)	2190.4(6)	6601(5)	4143(4)	334(7)
C(22)	2038.0(5)	6378(4)	5621(3)	274(6)
C(23)	1569.1(5)	1755(4)	9767(3)	201(6)
C(24)	1363.0(5)	716(4)	9118(3)	236(6)
C(25)	1124.5(5)	1498(5)	9398(4)	319(7)
C(26)	1089.6(5)	3290(5)	10276(4)	357(8)
C(27)	1292.0(5)	4323(5)	10925(4)	317(7)
C(28)	1529.6(5)	3554(4)	10671(3)	273(6)
C(29)	1390.6(5)	-1263(4)	8168(4)	272(6)
C(30)	1214.1(5)	-3417(4)	6135(3)	276(6)
C(31)	1045.3(5)	-3429(5)	4716(4)	308(7)
C(32)	1154.4(6)	9(5)	4139(3)	316(7)
C(33)	1319.2(5)	113(5)	5560(3)	276(6)

Table 23. Bond lengths [Å] and angles [°] for 06srv158.

O(1)-C(10)	1.429(3)	C(4)-H(4)	0.9499
O(1)-C(9)	1.431(3)	C(5)-C(6)	1.390(4)
N(1)-C(7)	1.460(3)	C(5)-H(5)	0.9500
N(1)-C(11)	1.461(4)	C(6)-H(6)	0.9499
N(1)-C(8)	1.467(3)	C(7)-H(71)	0.9900
C(1)-C(2)	1.398(4)	C(7)-H(72)	0.9902
C(1)-C(6)	1.404(4)	C(8)-C(9)	1.514(4)
C(1)-C(1)#1	1.500(5)	C(8)-H(81)	0.9897
C(2)-C(3)	1.395(4)	C(8)-H(82)	0.9900
C(2)-C(7)	1.519(4)	C(9)-H(91)	0.9898
C(3)-C(4)	1.392(4)	C(9)-H(92)	0.9900
C(3)-H(3)	0.9498	C(10)-C(11)	1.515(4)
C(4)-C(5)	1.380(4)	C(10)-H(101)	0.9900

C(10)-H(102)	0.9902	C(20)-H(201)	0.9902
C(11)-H(111)	0.9900	C(20)-H(202)	0.9899
C(11)-H(112)	0.9898	C(21)-C(22)	1.511(4)
O(2)-C(21)	1.428(4)	C(21)-H(211)	0.9900
O(2)-C(20)	1.431(3)	C(21)-H(212)	0.9898
O(3)-C(31)	1.425(3)	C(22)-H(221)	0.9900
O(3)-C(32)	1.427(3)	C(22)-H(222)	0.9902
N(2)-C(22)	1.460(3)	C(23)-C(24)	1.405(4)
N(2)-C(19)	1.462(4)	C(23)-C(28)	1.404(4)
N(2)-C(18)	1.472(3)	C(24)-C(25)	1.395(4)
N(3)-C(30)	1.461(4)	C(24)-C(29)	1.512(4)
N(3)-C(29)	1.467(3)	C(25)-C(26)	1.384(4)
N(3)-C(33)	1.471(3)	C(25)-H(25)	0.9498
C(12)-C(17)	1.398(4)	C(26)-C(27)	1.387(4)
C(12)-C(13)	1.405(4)	C(26)-H(26)	0.9500
C(12)-C(23)	1.498(4)	C(27)-C(28)	1.384(4)
C(13)-C(14)	1.398(3)	C(27)-H(27)	0.9501
C(13)-C(18)	1.517(4)	C(28)-H(28)	0.9496
C(14)-C(15)	1.388(4)	C(29)-H(291)	0.9899
C(14)-H(14)	0.9502	C(29)-H(292)	0.9900
C(15)-C(16)	1.393(4)	C(30)-C(31)	1.513(4)
C(15)-H(15)	0.9502	C(30)-H(301)	0.9900
C(16)-C(17)	1.380(4)	C(30)-H(302)	0.9901
C(16)-H(16)	0.9501	C(31)-H(311)	0.9900
C(17)-H(17)	0.9501	C(31)-H(312)	0.9903
C(18)-H(181)	0.9901	C(32)-C(33)	1.504(4)
C(18)-H(182)	0.9900	C(32)-H(321)	0.9899
C(19)-C(20)	1.512(4)	C(32)-H(322)	0.9900
C(19)-H(191)	0.9901	C(33)-H(331)	0.9904
C(19)-H(192)	0.9899	C(33)-H(332)	0.9900

C(10)-O(1)-C(9)	109.7(2)	C(2)-C(1)-C(1)#1	121.4(3)
C(7)-N(1)-C(11)	111.2(2)	C(6)-C(1)-C(1)#1	119.2(3)
C(7)-N(1)-C(8)	110.9(2)	C(3)-C(2)-C(1)	119.2(3)
C(11)-N(1)-C(8)	109.3(2)	C(3)-C(2)-C(7)	119.0(2)
C(2)-C(1)-C(6)	119.4(2)	C(1)-C(2)-C(7)	121.8(2)

C(4)-C(3)-C(2)	120.9(3)	N(1)-C(11)-C(10)	109.9(2)
C(4)-C(3)-H(3)	119.6	N(1)-C(11)-H(111)	109.7
C(2)-C(3)-H(3)	119.5	C(10)-C(11)-H(111)	109.7
C(5)-C(4)-C(3)	120.1(3)	N(1)-C(11)-H(112)	109.7
C(5)-C(4)-H(4)	119.9	C(10)-C(11)-H(112)	109.6
C(3)-C(4)-H(4)	120.0	H(111)-C(11)-H(112)	108.2
C(4)-C(5)-C(6)	119.7(3)	C(21)-O(2)-C(20)	109.9(2)
C(4)-C(5)-H(5)	120.2	C(31)-O(3)-C(32)	109.7(2)
C(6)-C(5)-H(5)	120.1	C(22)-N(2)-C(19)	109.0(2)
C(5)-C(6)-C(1)	120.7(3)	C(22)-N(2)-C(18)	111.3(2)
C(5)-C(6)-H(6)	119.6	C(19)-N(2)-C(18)	111.3(2)
C(1)-C(6)-H(6)	119.7	C(30)-N(3)-C(29)	110.9(2)
N(1)-C(7)-C(2)	112.7(2)	C(30)-N(3)-C(33)	108.7(2)
N(1)-C(7)-H(71)	109.1	C(29)-N(3)-C(33)	111.3(2)
C(2)-C(7)-H(71)	109.1	C(17)-C(12)-C(13)	119.1(2)
N(1)-C(7)-H(72)	109.0	C(17)-C(12)-C(23)	119.9(2)
C(2)-C(7)-H(72)	109.1	C(13)-C(12)-C(23)	121.0(2)
H(71)-C(7)-H(72)	107.8	C(14)-C(13)-C(12)	119.0(2)
N(1)-C(8)-C(9)	109.0(2)	C(14)-C(13)-C(18)	119.8(2)
N(1)-C(8)-H(81)	109.8	C(12)-C(13)-C(18)	121.3(2)
C(9)-C(8)-H(81)	109.8	C(15)-C(14)-C(13)	121.3(3)
N(1)-C(8)-H(82)	110.0	C(15)-C(14)-H(14)	119.5
C(9)-C(8)-H(82)	110.0	C(13)-C(14)-H(14)	119.3
H(81)-C(8)-H(82)	108.3	C(14)-C(15)-C(16)	119.4(2)
O(1)-C(9)-C(8)	111.0(2)	C(14)-C(15)-H(15)	120.3
O(1)-C(9)-H(91)	109.4	C(16)-C(15)-H(15)	120.2
C(8)-C(9)-H(91)	109.3	C(17)-C(16)-C(15)	119.9(3)
O(1)-C(9)-H(92)	109.5	C(17)-C(16)-H(16)	120.0
C(8)-C(9)-H(92)	109.5	C(15)-C(16)-H(16)	120.1
H(91)-C(9)-H(92)	108.1	C(16)-C(17)-C(12)	121.3(3)
O(1)-C(10)-C(11)	111.1(2)	C(16)-C(17)-H(17)	119.4
O(1)-C(10)-H(101)	109.5	C(12)-C(17)-H(17)	119.3
C(11)-C(10)-H(101)	109.5	N(2)-C(18)-C(13)	112.2(2)
O(1)-C(10)-H(102)	109.4	N(2)-C(18)-H(181)	109.2
C(11)-C(10)-H(102)	109.3	C(13)-C(18)-H(181)	109.1
H(101)-C(10)-H(102)	108.0	N(2)-C(18)-H(182)	109.1

C(13)-C(18)-H(182)	109.2	C(25)-C(26)-H(26)	119.8
H(181)-C(18)-H(182)	107.9	C(27)-C(26)-H(26)	119.7
N(2)-C(19)-C(20)	109.9(2)	C(28)-C(27)-C(26)	119.2(3)
N(2)-C(19)-H(191)	109.8	C(28)-C(27)-H(27)	120.4
C(20)-C(19)-H(191)	109.7	C(26)-C(27)-H(27)	120.3
N(2)-C(19)-H(192)	109.7	C(27)-C(28)-C(23)	121.2(3)
C(20)-C(19)-H(192)	109.7	C(27)-C(28)-H(28)	119.4
H(191)-C(19)-H(192)	108.1	C(23)-C(28)-H(28)	119.4
O(2)-C(20)-C(19)	110.8(2)	N(3)-C(29)-C(24)	113.1(2)
O(2)-C(20)-H(201)	109.4	N(3)-C(29)-H(291)	108.8
C(19)-C(20)-H(201)	109.5	C(24)-C(29)-H(291)	108.9
O(2)-C(20)-H(202)	109.6	N(3)-C(29)-H(292)	109.1
C(19)-C(20)-H(202)	109.4	C(24)-C(29)-H(292)	109.0
H(201)-C(20)-H(202)	108.0	H(291)-C(29)-H(292)	107.8
O(2)-C(21)-C(22)	111.2(2)	N(3)-C(30)-C(31)	109.9(2)
O(2)-C(21)-H(211)	109.5	N(3)-C(30)-H(301)	109.8
C(22)-C(21)-H(211)	109.3	C(31)-C(30)-H(301)	109.8
O(2)-C(21)-H(212)	109.4	N(3)-C(30)-H(302)	109.6
C(22)-C(21)-H(212)	109.4	C(31)-C(30)-H(302)	109.5
H(211)-C(21)-H(212)	108.0	H(301)-C(30)-H(302)	108.2
N(2)-C(22)-C(21)	109.6(2)	O(3)-C(31)-C(30)	110.7(2)
N(2)-C(22)-H(221)	109.7	O(3)-C(31)-H(311)	109.7
C(21)-C(22)-H(221)	109.8	C(30)-C(31)-H(311)	109.6
N(2)-C(22)-H(222)	109.8	O(3)-C(31)-H(312)	109.4
C(21)-C(22)-H(222)	109.8	C(30)-C(31)-H(312)	109.3
H(221)-C(22)-H(222)	108.2	H(311)-C(31)-H(312)	108.1
C(24)-C(23)-C(28)	119.2(2)	O(3)-C(32)-C(33)	111.6(2)
C(24)-C(23)-C(12)	121.7(2)	O(3)-C(32)-H(321)	109.2
C(28)-C(23)-C(12)	119.1(2)	C(33)-C(32)-H(321)	109.3
C(25)-C(24)-C(23)	119.0(3)	O(3)-C(32)-H(322)	109.3
C(25)-C(24)-C(29)	118.9(2)	C(33)-C(32)-H(322)	109.3
C(23)-C(24)-C(29)	122.1(2)	H(321)-C(32)-H(322)	108.0
C(26)-C(25)-C(24)	121.0(3)	N(3)-C(33)-C(32)	110.6(2)
C(26)-C(25)-H(25)	119.5	N(3)-C(33)-H(331)	109.5
C(24)-C(25)-H(25)	119.5	C(32)-C(33)-H(331)	109.5
C(25)-C(26)-C(27)	120.5(3)	N(3)-C(33)-H(332)	109.6

C(32)-C(33)-H(332)	109.5	H(331)-C(33)-H(332)	108.1

Symmetry transformations used to generate equivalent atoms: #1 -x,-y+1,z

Table 24. Anisotropic displacement parameters ($Å^2 \times 10^4$) for 06srv158. The anisotropic displacement factor exponent takes the form: $-2\pi^2[h^2 a^{*2}U_{11} + ... + 2 h k a^* b^* U_{12}]$

	U_{11}	U_{22}	U_{33}	U_{23}	U_{13}	U_{12}
O(1)	486(12)	251(11)	225(10)	-37(10)	-31(9)	-20(9)
N(1)	275(12)	188(12)	224(12)	-21(11)	-35(10)	-19(10)
C(1)	287(13)	225(15)	174(14)	20(12)	39(11)	-40(11)
C(2)	325(14)	212(14)	170(14)	2(12)	30(12)	-14(12)
C(3)	285(14)	322(16)	284(16)	-8(15)	37(13)	-3(13)
C(4)	343(16)	339(17)	329(17)	-8(16)	111(14)	10(13)
C(5)	512(18)	247(15)	261(16)	-32(15)	195(15)	10(14)
C(6)	407(16)	258(15)	172(14)	-38(13)	57(13)	-101(13)
C(7)	320(15)	241(15)	253(16)	-50(13)	-75(12)	15(12)
C(8)	351(15)	205(14)	298(17)	-10(14)	-47(13)	-38(12)
C(9)	410(16)	232(14)	303(16)	-34(14)	-39(14)	-60(13)
C(10)	477(18)	208(15)	251(16)	2(14)	-32(14)	19(13)
C(11)	313(14)	206(14)	274(17)	-13(13)	-1(12)	-36(12)
O(2)	469(12)	271(11)	202(10)	46(9)	-10(9)	-13(10)
O(3)	463(12)	253(10)	243(11)	-37(9)	0(9)	8(9)
N(2)	296(12)	199(11)	192(12)	15(10)	22(10)	-23(10)
N(3)	255(11)	226(12)	228(12)	24(11)	-47(10)	-7(10)
C(12)	284(13)	187(13)	165(14)	-12(12)	-26(11)	-18(11)
C(13)	232(13)	210(13)	170(13)	-18(12)	0(11)	-25(11)
C(14)	252(13)	293(15)	221(15)	30(13)	-3(12)	-35(12)
C(15)	254(13)	310(16)	228(15)	15(14)	-16(12)	29(12)
C(16)	322(14)	241(14)	198(14)	38(13)	-64(12)	30(12)
C(17)	278(13)	230(14)	163(14)	9(12)	8(11)	-30(11)
C(18)	312(14)	208(14)	227(15)	34(12)	32(12)	-12(12)
C(19)	419(16)	200(14)	260(16)	8(13)	-44(13)	-26(13)
C(20)	502(18)	246(15)	217(15)	14(14)	-6(14)	40(14)
C(21)	480(17)	291(16)	230(15)	47(14)	50(13)	-124(14)

C(22)	401(16)	173(14)	248(16)	26(13)	29(13)	-36(12)
C(23)	274(13)	194(13)	134(13)	23(12)	12(10)	-13(11)
C(24)	281(14)	222(14)	204(14)	51(13)	15(12)	-3(11)
C(25)	311(15)	355(17)	292(17)	38(15)	14(13)	-5(13)
C(26)	333(15)	381(18)	356(18)	91(16)	104(14)	122(14)
C(27)	445(17)	267(15)	238(16)	20(14)	100(13)	60(13)
C(28)	383(15)	229(15)	207(15)	15(13)	29(12)	-14(12)
C(29)	262(13)	247(15)	309(16)	27(13)	-79(12)	-6(12)
C(30)	286(14)	226(14)	316(17)	4(13)	-28(12)	-19(12)
C(31)	340(15)	266(15)	318(17)	-25(14)	-42(13)	-55(13)
C(32)	416(16)	282(15)	248(15)	20(14)	35(14)	54(14)
C(33)	328(14)	209(14)	291(16)	19(13)	45(13)	-5(12)

Table 25. Hydrogen coordinates ($\times 10^4$) and isotropic displacement parameters ($Å^2 \times 10^3$) for 06srv158.

	x	y	z	U(iso)
H(3)	691	5547	-1987	36
H(4)	783	2530	-3409	40
H(5)	469	785	-4761	41
H(6)	62	2095	-4734	34
H(71)	303	8837	-2219	33
H(72)	90	7639	-1260	33
H(81)	246	10280	772	34
H(82)	482	10857	-304	34
H(91)	755	9558	1644	38
H(92)	585	11381	2357	38
H(101)	429	5490	3323	37
H(102)	665	6033	2246	37
H(111)	335	4849	654	32
H(112)	156	6633	1334	32
H(14)	2361	2064	7842	31
H(15)	2487	-952	9156	32
H(16)	2201	-2770	10724	30
H(17)	1794	-1571	10956	27

H(181)	1742	3910	7446	30
H(182)	1949	5228	8367	30
H(191)	1802	3020	4794	35
H(192)	1999	1338	5425	35
H(201)	2311	2756	3790	39
H(202)	2076	2064	2754	39
H(211)	2173	8040	3735	40
H(212)	2369	6362	4387	40
H(221)	2097	7390	6415	33
H(222)	1861	6679	5394	33
H(25)	984	789	8981	38
H(26)	926	3815	10437	43
H(27)	1268	5547	11533	38
H(28)	1668	4255	11119	33
H(291)	1566	-1393	7823	33
H(292)	1352	-2477	8841	33
H(301)	1149	-4392	6936	33
H(302)	1383	-3889	5829	33
H(311)	1033	-4866	4296	37
H(312)	876	-2976	5029	37
H(321)	985	504	4417	38
H(322)	1222	946	3319	38
H(331)	1492	-275	5267	33
H(332)	1322	1559	5968	33

Table 26. Torsion angles [°] for 06srv158.

C(11)-N(1)-C(7)-C(2)	-74.0(3)	C(9)-O(1)-C(10)-C(11)	-58.4(3)
C(8)-N(1)-C(7)-C(2)	164.1(2)	C(7)-N(1)-C(11)-C(10)	179.5(2)
C(3)-C(2)-C(7)-N(1)	-35.3(4)	C(8)-N(1)-C(11)-C(10)	-57.8(3)
C(1)-C(2)-C(7)-N(1)	145.3(3)	O(1)-C(10)-C(11)-N(1)	58.1(3)
C(7)-N(1)-C(8)-C(9)	-178.6(2)	C(17)-C(12)-C(13)-C(14)	-2.4(4)
C(11)-N(1)-C(8)-C(9)	58.4(3)	C(23)-C(12)-C(13)-C(14)	176.6(2)
C(10)-O(1)-C(9)-C(8)	59.6(3)	C(22)-N(2)-C(18)-C(13)	-164.4(2)
N(1)-C(8)-C(9)-O(1)	-59.9(3)	C(19)-N(2)-C(18)-C(13)	73.9(3)

C(14)-C(13)-C(18)-N(2)	30.9(3)
C(12)-C(13)-C(18)-N(2)	-150.9(2)
C(22)-N(2)-C(19)-C(20)	58.4(3)
C(18)-N(2)-C(19)-C(20)	-178.5(2)
C(21)-O(2)-C(20)-C(19)	58.2(3)
N(2)-C(19)-C(20)-O(2)	-58.8(3)
C(20)-O(2)-C(21)-C(22)	-58.5(3)
C(19)-N(2)-C(22)-C(21)	-58.3(3)
C(18)-N(2)-C(22)-C(21)	178.6(2)
O(2)-C(21)-C(22)-N(2)	59.1(3)
C(17)-C(12)-C(23)-C(24)	-72.1(3)
C(13)-C(12)-C(23)-C(24)	108.9(3)
C(17)-C(12)-C(23)-C(28)	106.8(3)
C(13)-C(12)-C(23)-C(28)	-72.1(3)
C(30)-N(3)-C(29)-C(24)	-165.7(2)
C(33)-N(3)-C(29)-C(24)	73.2(3)
C(25)-C(24)-C(29)-N(3)	43.2(3)
C(23)-C(24)-C(29)-N(3)	-138.8(3)
C(29)-N(3)-C(30)-C(31)	179.8(2)
C(33)-N(3)-C(30)-C(31)	-57.6(3)
C(32)-O(3)-C(31)-C(30)	-59.3(3)
N(3)-C(30)-C(31)-O(3)	60.2(3)
C(31)-O(3)-C(32)-C(33)	58.1(3)
C(30)-N(3)-C(33)-C(32)	56.4(3)
C(29)-N(3)-C(33)-C(32)	178.7(2)
O(3)-C(32)-C(33)-N(3)	-57.3(3)

Symmetry transformations used to generate equivalent atoms: #1 -x,-y+1,z

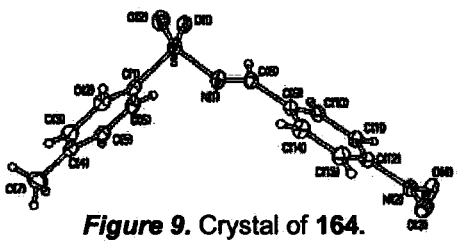

Figure 9. Crystal of **164.**

Table 27. Crystal data and structure refinement for 06srv324.

Identification code	ka prod 47	
Empirical formula	C14 H12 N2 O4 S	
Formula weight	304.32	
Temperature	120(2) K	
Wavelength	0.71073 Å	
Crystal system	Orthorhombic	
Space group	$P2_12_12_1$ (no. 19)	
Unit cell dimensions	a = 5.5768(7) Å	α= 90°
	b = 7.8860(9) Å	β= 90°
	c = 30.933(3) Å	γ = 90°
Volume	1360.4(3) Å^3	
Z	4	
Density (calculated)	1.486 g/cm^3	
Absorption coefficient	0.256 mm^{-1}	
F(000)	632	
Crystal size	0.50 × 0.34 × 0.09 mm^3	
θ range for data collection	2.6 to 29.0°.	
Index ranges	$-7 \leq h \leq 3$, $-9 \leq k \leq 10$, $-35 \leq l \leq 42$	
Reflections collected	8985	
Independent reflections	3592 [R(int) = 0.0269]	
Reflections with I>2σ(I)	3391	
Completeness to θ = 29.0°	99.2 %	
Absorption correction	Semi-empirical from equivalents	

Max. and min. transmission	1.0000 and 0.8854
Refinement method	Full-matrix least-squares on F^2
Data / restraints / parameters	3592 / 0 / 238
Largest final shift/e.s.d. ratio	0.002
Goodness-of-fit on F^2	1.070
Final R indices [I>2σ(I)]	R1 = 0.0341, wR2 = 0.0791
R indices (all data)	R1 = 0.0374, wR2 = 0.0804
Absolute structure parameter	-0.01(6)
Largest diff. peak and hole	0.350 and -0.244 e.Å^{-3}

Table 28. Atomic coordinates ($\times 10^4$) and equivalent isotropic displacement parameters (Å^2 $\times 10^4$) for 06srv324. U(eq) is defined as one third of the trace of the orthogonalized U_{ij} tensor.

	x	y	z	U(eq)
S	5737.6(7)	222.4(5)	6105.5(1)	199(1)
O(1)	4837(2)	-1231(2)	6334.5(4)	241(3)
O(2)	8270(2)	570(2)	6117.3(4)	279(3)
O(3)	-1507(3)	9044(2)	7106.2(4)	300(3)
O(4)	-4226(3)	7375(2)	7367.0(5)	348(3)
N(1)	4389(3)	2016(2)	6262.9(5)	221(3)
N(2)	-2362(3)	7632(2)	7168.3(5)	229(3)
C(1)	4832(3)	83(2)	5563.8(5)	192(3)
C(2)	6266(3)	784(2)	5241.7(6)	219(3)
C(3)	5557(3)	629(2)	4812.6(6)	243(3)
C(4)	3448(3)	-202(2)	4701.7(5)	225(3)
C(5)	2039(3)	-887(2)	5030.8(6)	233(3)
C(6)	2703(3)	-747(2)	5460.9(6)	225(3)
C(7)	2697(4)	-379(3)	4237.2(6)	336(4)
C(8)	2689(3)	1876(2)	6539.9(5)	198(3)
C(9)	1415(3)	3378(2)	6700.5(5)	182(3)
C(10)	-695(3)	3161(2)	6933.2(5)	192(3)
C(11)	-1960(3)	4549(2)	7085.7(5)	202(3)
C(12)	-1051(3)	6145(2)	7002.0(5)	188(3)
C(13)	1050(3)	6414(2)	6775.1(6)	230(4)
C(14)	2287(3)	5021(2)	6621.4(5)	230(3)

Table 29. Bond lengths [Å] and angles [°] for 06srv324.

S-O(1)	1.4379(13)	C(5)-H(5)	0.90(2)
S-O(2)	1.4391(13)	C(6)-H(6)	0.90(2)
S-N(1)	1.6740(15)	C(7)-H(71)	1.00(4)
S-C(1)	1.7537(16)	C(7)-H(73)	0.91(3)
O(3)-N(2)	1.2260(19)	C(7)-H(72)	0.87(3)
O(4)-N(2)	1.225(2)	C(8)-C(9)	1.468(2)
N(1)-C(8)	1.282(2)	C(8)-H(8)	1.012(18)
N(2)-C(12)	1.475(2)	C(9)-C(10)	1.390(2)
C(1)-C(2)	1.392(2)	C(9)-C(14)	1.406(2)
C(1)-C(6)	1.393(2)	C(10)-C(11)	1.385(2)
C(2)-C(3)	1.390(3)	C(10)-H(10)	0.87(2)
C(2)-H(2)	0.96(2)	C(11)-C(12)	1.381(2)
C(3)-C(4)	1.389(2)	C(11)-H(11)	0.94(2)
C(3)-H(3)	0.87(2)	C(12)-C(13)	1.382(2)
C(4)-C(5)	1.395(2)	C(13)-C(14)	1.381(2)
C(4)-C(7)	1.503(2)	C(13)-H(13)	0.98(2)
C(5)-C(6)	1.386(2)	C(14)-H(14)	0.93(2)
O(1)-S-O(2)	118.81(8)	C(3)-C(2)-H(2)	121.9(13)
O(1)-S-N(1)	111.90(7)	C(1)-C(2)-H(2)	119.1(13)
O(2)-S-N(1)	105.84(8)	C(4)-C(3)-C(2)	121.21(16)
O(1)-S-C(1)	108.66(8)	C(4)-C(3)-H(3)	121.1(14)
O(2)-S-C(1)	108.60(8)	C(2)-C(3)-H(3)	117.7(14)
N(1)-S-C(1)	101.63(8)	C(3)-C(4)-C(5)	118.63(16)
C(8)-N(1)-S	117.01(12)	C(3)-C(4)-C(7)	121.07(17)
O(4)-N(2)-O(3)	123.96(15)	C(5)-C(4)-C(7)	120.30(17)
O(4)-N(2)-C(12)	117.66(14)	C(6)-C(5)-C(4)	121.30(16)
O(3)-N(2)-C(12)	118.37(15)	C(6)-C(5)-H(5)	120.6(14)
C(2)-C(1)-C(6)	120.87(15)	C(4)-C(5)-H(5)	118.1(14)
C(2)-C(1)-S	119.57(13)	C(5)-C(6)-C(1)	118.98(16)
C(6)-C(1)-S	119.56(13)	C(5)-C(6)-H(6)	123.8(14)
C(3)-C(2)-C(1)	119.00(16)	C(1)-C(6)-H(6)	117.2(14)

C(4)-C(7)-H(71)	112.2(18)	C(9)-C(10)-H(10)	117.9(15)
C(4)-C(7)-H(73)	111.5(19)	C(12)-C(11)-C(10)	118.01(15)
H(71)-C(7)-H(73)	99(3)	C(12)-C(11)-H(11)	119.5(12)
C(4)-C(7)-H(72)	115.6(19)	C(10)-C(11)-H(11)	122.4(12)
H(71)-C(7)-H(72)	101(3)	C(11)-C(12)-C(13)	123.11(15)
H(73)-C(7)-H(72)	115(3)	C(11)-C(12)-N(2)	118.52(14)
N(1)-C(8)-C(9)	121.01(15)	C(13)-C(12)-N(2)	118.36(14)
N(1)-C(8)-H(8)	120.4(10)	C(14)-C(13)-C(12)	118.41(15)
C(9)-C(8)-H(8)	118.5(10)	C(14)-C(13)-H(13)	121.5(13)
C(10)-C(9)-C(14)	119.75(15)	C(12)-C(13)-H(13)	120.1(13)
C(10)-C(9)-C(8)	119.09(15)	C(13)-C(14)-C(9)	120.04(15)
C(14)-C(9)-C(8)	121.15(15)	C(13)-C(14)-H(14)	121.7(13)
C(11)-C(10)-C(9)	120.68(15)	C(9)-C(14)-H(14)	118.3(13)
C(11)-C(10)-H(10)	121.4(15)		

Table 30. Anisotropic displacement parameters ($Å^2 \times 10^4$) for 06srv324. The anisotropic displacement factor exponent takes the form: $-2\pi^2[h^2 a^{*2}U_{11} + ... + 2 h k a^* b^* U_{12}]$

	U_{11}	U_{22}	U_{33}	U_{23}	U_{13}	U_{12}
S	167(2)	216(2)	214(2)	-46(2)	20(2)	2(2)
O(1)	263(6)	221(6)	238(6)	-3(5)	35(5)	25(5)
O(2)	187(5)	377(7)	274(6)	-81(5)	7(5)	-5(5)
O(3)	415(8)	151(6)	335(7)	-28(5)	-33(6)	6(5)
O(4)	310(7)	290(7)	443(8)	-113(6)	110(7)	33(6)
N(1)	216(7)	205(7)	243(7)	-52(5)	40(6)	-12(6)
N(2)	285(8)	191(7)	212(7)	-40(5)	-22(6)	33(6)
C(1)	178(7)	167(8)	229(7)	-39(6)	15(6)	16(6)
C(2)	187(7)	184(7)	284(8)	-13(6)	20(7)	-19(6)
C(3)	253(8)	215(8)	262(8)	41(6)	49(7)	8(7)
C(4)	258(8)	175(7)	241(8)	-6(6)	-14(6)	69(6)
C(5)	171(7)	237(8)	290(9)	-42(7)	-25(7)	-2(7)
C(6)	176(7)	243(8)	257(8)	-17(6)	51(7)	-13(6)
C(7)	385(11)	364(11)	257(9)	9(8)	-74(8)	26(10)
C(8)	176(7)	215(8)	202(7)	-44(6)	-5(6)	-10(6)

C(9)	194(8)	182(7)	170(7)	-13(6)	9(6)	0(6)
C(10)	220(8)	164(7)	192(7)	-16(6)	15(7)	-34(7)
C(11)	201(7)	201(8)	206(7)	-9(6)	36(6)	-17(6)
C(12)	218(8)	167(7)	179(7)	-37(5)	-12(6)	13(6)
C(13)	264(9)	161(7)	267(8)	-1(6)	15(7)	-46(7)
C(14)	207(7)	220(8)	262(8)	-6(7)	43(6)	-49(7)

Table 31. Hydrogen coordinates ($\times 10^3$) and isotropic displacement parameters ($Å^2 \times 10^3$) for 06srv324.

	x	y	z	U(iso)
H(2)	772(4)	135(3)	532(1)	29(6)
H(3)	646(4)	109(3)	462(1)	24(5)
H(5)	68(4)	-143(3)	496(1)	30(6)
H(6)	183(4)	-117(3)	568(1)	29(6)
H(71)	101(6)	-81(4)	421(1)	81(11)
H(73)	348(6)	-125(4)	411(1)	66(9)
H(72)	263(6)	56(4)	409(1)	62(9)
H(8)	216(3)	72(2)	664(1)	10(4)
H(10)	-122(4)	213(3)	697(1)	31(6)
H(11)	-335(4)	444(2)	725(1)	22(5)
H(13)	161(4)	757(3)	672(1)	27(6)
H(14)	372(4)	514(3)	647(1)	25(5)

Table 32. Torsion angles [°] for 06srv324.

O(1)-S-N(1)-C(8)	-3.65(16)	S-N(1)-C(8)-C(9)	179.41(12)
O(2)-S-N(1)-C(8)	-134.49(14)	N(1)-C(8)-C(9)-C(10)	167.69(16)
C(1)-S-N(1)-C(8)	112.13(14)	N(1)-C(8)-C(9)-C(14)	-12.0(3)
O(1)-S-C(1)-C(2)	-149.79(13)	O(4)-N(2)-C(12)-C(11)	-1.3(2)
O(2)-S-C(1)-C(2)	-19.22(16)	O(3)-N(2)-C(12)-C(11)	177.55(15)
N(1)-S-C(1)-C(2)	92.08(14)	O(4)-N(2)-C(12)-C(13)	179.66(16)
O(1)-S-C(1)-C(6)	29.42(16)	O(3)-N(2)-C(12)-C(13)	-1.5(2)
O(2)-S-C(1)-C(6)	159.99(13)		
N(1)-S-C(1)-C(6)	-88.71(15)		

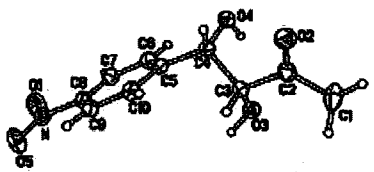

Figure 2. Crystal of **244.**

Table 33. Crystal data and structure refinement for 06srv325.

Identification code	KA prod 151 fr:12-19	
Empirical formula	C10 H11 N O5	
Formula weight	225.20	
Temperature	120(2) K	
Wavelength	0.71073 Å	
Crystal system	Orthorhombic	
Space group	$P2_12_12_1$ (no. 19)	
Unit cell dimensions	a = 4.6812(6) Å	α= 90°
	b = 9.2627(11) Å	β= 90°
	c = 23.407(3) Å	γ = 90°
Volume	1014.9(2) Å^3	
Z	4	
Density (calculated)	1.474 g/cm^3	
Absorption coefficient	0.120 mm^{-1}	
F(000)	472	
Crystal size	0.40 × 0.17 × 0.15 mm^3	
θ range for data collection	1.74 to 29.00°.	
Index ranges	$-6 \leq h \leq 6, -12 \leq k \leq 11, -31 \leq l \leq 31$	
Reflections collected	10539	
Independent reflections	1601 [R(int) = 0.0279]	
Reflections with I>2σ(I)	1470	
Completeness to θ = 29.00°	99.6 %	
Absorption correction	Semi-empirical from equivalents	
Max. and min. transmission	1.0000 and 0.8913	
Refinement method	Full-matrix least-squares on F^2	
Data / restraints / parameters	1601 / 0 / 190	

Largest final shift/e.s.d. ratio	0.000
Goodness-of-fit on F^2	1.100
Final R indices [I>2σ(I)]	R1 = 0.0386, wR2 = 0.1045
R indices (all data)	R1 = 0.0422, wR2 = 0.1068
Extinction coefficient	0.020(4)
Largest diff. peak and hole	0.233 and -0.216 e.Å^{-3}

Table 34. Atomic coordinates ($\times 10^4$) and equivalent isotropic displacement parameters (Å^2 $\times 10^4$) for 06srv325. U(eq) is defined as one third of the trace of the orthogonalized Uij tensor.

	x	y	z	U(eq)
O(1)	1507(4)	6166(2)	7960.5(6)	404(4)
O(2)	10914(3)	3727(2)	4682.1(6)	319(3)
O(3)	5566(3)	6254(2)	5039.2(5)	251(3)
O(4)	10660(3)	6249(1)	5653.0(5)	248(3)
O(5)	-107(4)	4062(2)	7725.5(6)	428(4)
N	1427(4)	5111(2)	7643.2(6)	280(3)
C(1)	8102(6)	5170(3)	4051.7(9)	410(6)
C(2)	8918(4)	4563(2)	4621.0(7)	259(4)
C(3)	7030(4)	4930(2)	5134.5(7)	212(3)
C(4)	8803(4)	5030(2)	5683.1(7)	212(3)
C(5)	6911(4)	5082(2)	6209.3(7)	216(3)
C(6)	6674(4)	6319(2)	6542.6(7)	252(4)
C(7)	4851(4)	6339(2)	7013.9(7)	261(4)
C(8)	3300(4)	5106(2)	7136.8(7)	241(4)
C(9)	3477(4)	3858(2)	6815.2(7)	247(4)
C(10)	5321(4)	3858(2)	6349.3(7)	251(4)

Table 35. Bond lengths [Å] and angles [°] for 06srv325.

O(1)-N	1.227(2)	C(3)-H(3)	0.97(3)
O(2)-C(2)	1.222(2)	C(4)-C(5)	1.518(2)
O(3)-C(3)	1.422(2)	C(4)-H(4)	1.01(3)
O(3)-H(03)	0.90(4)	C(5)-C(6)	1.390(2)
O(4)-C(4)	1.427(2)	C(5)-C(10)	1.396(2)
O(4)-H(04)	0.88(3)	C(6)-C(7)	1.395(2)
O(5)-N	1.224(2)	C(6)-H(6)	0.99(2)
N-C(8)	1.474(2)	C(7)-C(8)	1.383(3)
C(1)-C(2)	1.496(3)	C(7)-H(7)	0.94(3)
C(1)-H(11)	0.92(3)	C(8)-C(9)	1.382(2)
C(1)-H(12)	0.98(3)	C(9)-C(10)	1.391(2)
C(1)-H(13)	1.00(5)	C(9)-H(9)	0.97(3)
C(2)-C(3)	1.530(2)	C(10)-H(10)	0.99(3)
C(3)-C(4)	1.532(2)		

C(3)-O(3)-H(03)	106(2)	C(4)-C(3)-H(3)	109.4(13)
C(4)-O(4)-H(04)	109.8(17)	O(4)-C(4)-C(5)	111.72(14)
O(5)-N-O(1)	123.69(16)	O(4)-C(4)-C(3)	109.67(13)
O(5)-N-C(8)	118.23(15)	C(5)-C(4)-C(3)	111.47(14)
O(1)-N-C(8)	118.08(16)	O(4)-C(4)-H(4)	108.4(15)
C(2)-C(1)-H(11)	108.1(18)	C(5)-C(4)-H(4)	110.8(14)
C(2)-C(1)-H(12)	109.7(19)	C(3)-C(4)-H(4)	104.5(14)
H(11)-C(1)-H(12)	108(3)	C(6)-C(5)-C(10)	119.67(16)
C(2)-C(1)-H(13)	106(2)	C(6)-C(5)-C(4)	121.90(16)
H(11)-C(1)-H(13)	112(3)	C(10)-C(5)-C(4)	118.40(15)
H(12)-C(1)-H(13)	113(3)	C(5)-C(6)-C(7)	120.24(17)
O(2)-C(2)-C(1)	122.53(18)	C(5)-C(6)-H(6)	122.1(13)
O(2)-C(2)-C(3)	119.37(16)	C(7)-C(6)-H(6)	117.7(13)
C(1)-C(2)-C(3)	117.96(17)	C(8)-C(7)-C(6)	118.34(16)
O(3)-C(3)-C(2)	110.28(14)	C(8)-C(7)-H(7)	121.7(16)
O(3)-C(3)-C(4)	109.91(14)	C(6)-C(7)-H(7)	119.9(16)
C(2)-C(3)-C(4)	111.03(14)	C(9)-C(8)-C(7)	123.07(16)
O(3)-C(3)-H(3)	112.7(15)	C(9)-C(8)-N	118.43(16)
C(2)-C(3)-H(3)	103.4(14)	C(7)-C(8)-N	118.48(15)

C(8)-C(9)-C(10)	117.67(17)	C(9)-C(10)-C(5)	121.00(16)
C(8)-C(9)-H(9)	120.7(15)	C(9)-C(10)-H(10)	121.4(17)
C(10)-C(9)-H(9)	121.6(15)	C(5)-C(10)-H(10)	117.5(17)

Table 36. Anisotropic displacement parameters ($Å^2 \times 10^4$) for 06srv325. The anisotropic displacement factor exponent takes the form: $-2\pi^2[h^2 a^{*2}U_{11} + ... + 2 h k a^* b^* U_{12}]$

	U_{11}	U_{22}	U_{33}	U_{23}	U_{13}	U_{12}
O(1)	498(9)	396(8)	318(7)	-67(6)	130(7)	5(8)
O(2)	281(7)	363(7)	311(6)	-71(6)	-8(6)	59(7)
O(3)	217(6)	271(6)	265(6)	29(5)	14(5)	34(6)
O(4)	212(6)	270(6)	261(6)	4(5)	-9(5)	-14(6)
O(5)	480(9)	443(9)	360(7)	6(6)	169(7)	-97(8)
N	290(7)	319(8)	232(7)	25(6)	34(6)	31(7)
C(1)	564(15)	435(13)	233(9)	7(9)	77(9)	154(12)
C(2)	256(9)	283(9)	237(7)	-58(7)	33(7)	-5(7)
C(3)	200(7)	227(8)	208(7)	-2(6)	15(6)	4(7)
C(4)	191(7)	237(8)	208(7)	3(6)	-5(6)	15(7)
C(5)	204(7)	259(8)	186(7)	20(6)	-26(6)	17(7)
C(6)	255(8)	241(8)	258(8)	-3(6)	-2(7)	-6(8)
C(7)	286(8)	258(8)	240(7)	-32(7)	10(7)	11(8)
C(8)	233(7)	297(8)	194(7)	19(6)	3(6)	23(7)
C(9)	263(8)	255(8)	224(7)	21(6)	-9(6)	-20(8)
C(10)	304(9)	237(8)	213(7)	4(6)	-5(7)	-4(8)

Table 37. Hydrogen coordinates ($\times 10^3$) and isotropic displacement parameters ($Å^2 \times 10^3$) for 06srv325.

	x	y	z	U(iso)
H(03)	385(8)	615(4)	521(1)	62(10)
H(04)	976(6)	698(3)	549(1)	31(6)
H(11)	827(7)	615(3)	407(1)	47(8)
H(12)	942(8)	482(3)	376(1)	56(9)

H(13)	609(11)	486(4)	398(2)	88(13)
H(3)	575(6)	411(3)	516(1)	27(6)
H(4)	1001(6)	412(3)	568(1)	35(6)
H(6)	776(6)	721(2)	646(1)	23(5)
H(7)	470(6)	718(3)	724(1)	33(6)
H(9)	240(6)	300(3)	692(1)	36(6)
H(10)	564(7)	298(3)	612(1)	40(7)

Table 38. Torsion angles [°] for 06srv325.

O(2)-C(2)-C(3)-O(3)	158.99(16)
C(1)-C(2)-C(3)-O(3)	-25.3(2)
O(2)-C(2)-C(3)-C(4)	36.9(2)
C(1)-C(2)-C(3)-C(4)	-147.36(19)
O(3)-C(3)-C(4)-O(4)	-54.74(18)
C(2)-C(3)-C(4)-O(4)	67.55(18)
O(3)-C(3)-C(4)-C(5)	69.52(18)
C(2)-C(3)-C(4)-C(5)	-168.19(14)
O(4)-C(4)-C(5)-C(6)	12.0(2)
C(3)-C(4)-C(5)-C(6)	-111.05(19)
O(4)-C(4)-C(5)-C(10)	-169.57(15)
C(3)-C(4)-C(5)-C(10)	67.3(2)
O(5)-N-C(8)-C(9)	-7.2(3)
O(1)-N-C(8)-C(9)	172.44(18)
O(5)-N-C(8)-C(7)	174.41(18)
O(1)-N-C(8)-C(7)	-6.0(3)

Table 39. Hydrogen bonds for 06srv325 [Å and °].

D-H...A	d(D-H)	d(H...A)	d(D...A)	<(DHA)
O(3)-H(03)...O(4)#1	0.90(4)	1.82(4)	2.7090(18)	168(3)
O(4)-H(04)...O(3)#2	0.88(3)	2.09(2)	2.8243(19)	140(2)

Symmetry transformations used to generate equivalent atoms: #1 x-1,y,z #2 x+1/2,-y+3/2,-z+1

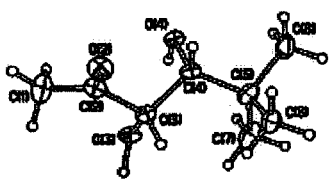

Figure 3. Crystal of **248.**

Table 40. Crystal data and structure refinement for 06srv326.

Identification code	KA prod 158 fr:4-7	
Empirical formula	C8 H16 O3	
Formula weight	160.21	
Temperature	120(2) K	
Wavelength	1.54178 Å	
Crystal system	Triclinic	
Space group	$P\bar{1}$ (No. 2)	
Unit cell dimensions	a = 9.4668(5) Å	α= 78.898(9)°
	b = 9.9480(5) Å	β= 83.568(9)°
	c = 10.0866(5) Å	γ = 87.511(9)°
Volume	926.04(8) Å^3	
Z	4	
Density (calculated)	1.149 g/cm^3	
Absorption coefficient	0.709 mm^{-1}	
F(000)	352	
Crystal size	0.28 × 0.12 × 0.07 mm^3	

θ range for data collection	4.49 to 60.36°.
Index ranges	$-10 \leq h \leq 10, -11 \leq k \leq 10, -10 \leq l \leq 10$
Reflections collected	4067
Independent reflections	2374 [R(int) = 0.0836]
Reflections with I>2σ(I)	1648
Completeness to θ = 50.00°	93.7 %
Absorption correction	None
Refinement method	Full-matrix least-squares on F^2
Data / restraints / parameters	2374 / 3 / 240
Largest final shift/e.s.d. ratio	0.000
Goodness-of-fit on F^2	0.952
Final R indices [I>2σ(I)]	R1 = 0.0673, wR2 = 0.1718
R indices (all data)	R1 = 0.0904, wR2 = 0.1902
Largest diff. peak and hole	0.309 and -0.288 e.Å^{-3}

Table 41. Atomic coordinates (×10^4) and equivalent isotropic displacement parameters (Å^2 ×10^4) for 06srv326. U(eq) is defined as one third of the trace of the orthogonalized Uij tensor.

	x	y	z	U(eq)
C(1)	2665(4)	1984(4)	5826(4)	567(12)
C(2)	4124(4)	1425(3)	5913(3)	341(8)
O(2)	4374(3)	297(2)	6555(2)	437(7)
C(3)	5355(4)	2272(3)	5086(3)	290(9)
O(3)	4853(3)	3521(2)	4306(2)	323(7)
O(4)	5815(2)	3677(2)	6662(2)	300(7)
C(4)	6398(4)	2568(3)	6039(3)	285(9)
C(5)	7931(6)	2802(5)	5402(8)	370(40)
C(6)	8571(4)	1469(4)	5016(4)	409(10)
C(7)	8064(5)	3946(4)	4143(5)	554(13)
C(8)	8783(4)	3174(5)	6478(5)	581(13)
C(3')	5250(30)	2300(30)	6350(40)	380(80)
O(3')	4670(20)	3514(18)	6770(20)	250(50)
O(4')	5770(20)	3800(20)	4070(20)	260(50)
C(4')	6250(30)	2620(30)	5020(30)	390(90)
C(5')	7990(20)	2840(20)	5240(20)	300(300)
C(6')	7930(40)	3920(30)	6090(30)	490(100)

C(7')	8480(30)	1480(30)	5950(40)	640(130)
C(8')	8700(30)	3290(40)	3840(30)	670(130)
C(11)	7673(4)	1677(4)	844(4)	461(10)
C(12)	6304(4)	1619(3)	268(3)	330(9)
O(12)	6209(3)	1076(2)	-704(3)	460(7)
C(13)	4967(3)	2219(3)	971(3)	284(8)
O(13)	5346(2)	3232(2)	1680(2)	343(6)
C(14)	3885(3)	2727(3)	-18(3)	301(8)
O(14)	4426(2)	3967(2)	-881(2)	325(6)
C(15)	2347(3)	2995(3)	575(3)	327(8)
C(16)	1790(4)	1717(3)	1547(4)	424(10)
C(17)	2226(4)	4197(3)	1326(4)	445(10)
C(18)	1433(4)	3335(4)	-606(4)	481(10)

Table 42. Bond lengths [Å] and angles [°] for 06srv326.

C(1)-C(2)	1.472(5)	C(5)-C(6)	1.534(6)
C(1)-H(10)	0.9604	C(6)-H(61)	0.9603
C(1)-H(11)	0.9603	C(6)-H(62)	0.9607
C(1)-H(12)	0.9603	C(6)-H(63)	0.9604
C(2)-O(2)	1.211(3)	C(7)-H(71)	0.9604
C(2)-C(3)	1.537(5)	C(7)-H(72)	0.9606
C(2)-C(3')	1.552(19)	C(7)-H(73)	0.9605
C(3)-O(3)	1.430(3)	C(8)-H(81)	0.9608
C(3)-C(4)	1.527(5)	C(8)-H(82)	0.9609
C(3)-H(3)	0.9600	C(8)-H(83)	0.9611
C(3)-H(4')	1.0143	C(3')-O(3')	1.426(19)
O(3)-H(03)	0.9521	C(3')-C(4')	1.53(5)
O(3)-H(04')	1.1658	C(3')-H(3')	1.0000
O(4)-C(4)	1.433(4)	O(3')-H(03')	0.8401
O(4)-H(04)	0.9221	O(4')-C(4')	1.455(18)
O(4)-H(03')	1.0135	O(4')-H(04')	0.8500
C(4)-C(5)	1.528(7)	C(4')-C(5')	1.7208
C(4)-H(4)	0.9600	C(4')-H(4')	0.9900
C(5)-C(8)	1.530(7)	C(5')-C(8')	1.4840
C(5)-C(7)	1.531(8)	C(5')-C(6')	1.4840

C(5')-C(7')	1.4854	C(13)-H(13)	0.9600
C(6')-H(6'1)	0.9800	O(13)-H(013)	0.91(4)
C(6')-H(6'2)	0.9800	C(14)-O(14)	1.443(3)
C(6')-H(6'3)	0.9800	C(14)-C(15)	1.543(4)
C(7')-H(7'1)	0.9800	C(14)-H(14)	0.9600
C(7')-H(7'2)	0.9800	O(14)-H(014)	0.77(4)
C(7')-H(7'3)	0.9800	C(15)-C(16)	1.523(4)
C(8')-H(8'1)	0.9800	C(15)-C(18)	1.528(5)
C(8')-H(8'2)	0.9800	C(15)-C(17)	1.528(5)
C(8')-H(8'3)	0.9800	C(16)-H(161)	0.9604
C(11)-C(12)	1.487(5)	C(16)-H(162)	0.9606
C(11)-H(111)	0.9610	C(16)-H(163)	0.9605
C(11)-H(112)	0.9608	C(17)-H(171)	0.9606
C(11)-H(113)	0.9609	C(17)-H(172)	0.9604
C(12)-O(12)	1.220(4)	C(17)-H(173)	0.9605
C(12)-C(13)	1.536(4)	C(18)-H(181)	0.9607
C(13)-O(13)	1.421(4)	C(18)-H(182)	0.9606
C(13)-C(14)	1.513(4)	C(18)-H(183)	0.9608

C(2)-C(1)-H(10)	110.3	C(4)-O(4)-H(04)	111.6
C(2)-C(1)-H(11)	109.2	O(4)-C(4)-C(3)	107.9(3)
H(10)-C(1)-H(11)	109.4	O(4)-C(4)-C(5)	112.9(3)
C(2)-C(1)-H(12)	109.0	C(3)-C(4)-C(5)	115.5(4)
H(10)-C(1)-H(12)	109.5	O(4)-C(4)-H(4)	107.1
H(11)-C(1)-H(12)	109.4	C(3)-C(4)-H(4)	106.6
O(2)-C(2)-C(1)	122.2(3)	C(5)-C(4)-H(4)	106.3
O(2)-C(2)-C(3)	119.3(3)	C(4)-C(5)-C(8)	107.7(5)
C(1)-C(2)-C(3)	118.4(3)	C(4)-C(5)-C(7)	113.2(3)
O(2)-C(2)-C(3')	101.8(12)	C(8)-C(5)-C(7)	109.1(4)
C(1)-C(2)-C(3')	118.6(9)	C(4)-C(5)-C(6)	109.5(4)
O(3)-C(3)-C(4)	110.5(3)	C(8)-C(5)-C(6)	108.0(4)
O(3)-C(3)-C(2)	111.6(3)	C(7)-C(5)-C(6)	109.1(5)
C(4)-C(3)-C(2)	109.7(3)	C(5)-C(6)-H(61)	109.4
O(3)-C(3)-H(3)	108.4	C(5)-C(6)-H(62)	110.6
C(4)-C(3)-H(3)	108.2	H(61)-C(6)-H(62)	109.4
C(2)-C(3)-H(3)	108.3	C(5)-C(6)-H(63)	108.4
C(3)-O(3)-H(03)	107.6	H(61)-C(6)-H(63)	109.5

H(62)-C(6)-H(63)	109.4	C(5')-C(6')-H(6'3)	103.8
C(5)-C(7)-H(71)	109.1	H(6'1)-C(6')-H(6'3)	109.5
C(5)-C(7)-H(72)	109.9	H(6'2)-C(6')-H(6'3)	109.5
H(71)-C(7)-H(72)	109.4	C(5')-C(7')-H(7'1)	114.9
C(5)-C(7)-H(73)	109.6	C(5')-C(7')-H(7'2)	105.2
H(71)-C(7)-H(73)	109.4	H(7'1)-C(7')-H(7'2)	109.5
H(72)-C(7)-H(73)	109.4	C(5')-C(7')-H(7'3)	107.0
C(5)-C(8)-H(81)	109.5	H(7'1)-C(7')-H(7'3)	109.5
C(5)-C(8)-H(82)	109.0	H(7'2)-C(7')-H(7'3)	109.5
H(81)-C(8)-H(82)	109.4	C(5')-C(8')-H(8'1)	112.8
C(5)-C(8)-H(83)	110.2	C(5')-C(8')-H(8'2)	108.4
H(81)-C(8)-H(83)	109.4	H(8'1)-C(8')-H(8'2)	109.5
H(82)-C(8)-H(83)	109.4	C(5')-C(8')-H(8'3)	107.1
H(6'1)-C(8)-H(6'3)	87.2	H(8'1)-C(8')-H(8'3)	109.5
O(3')-C(3')-C(4')	112(2)	H(8'2)-C(8')-H(8'3)	109.5
O(3')-C(3')-C(2)	113.9(18)	C(12)-C(11)-H(111)	108.8
C(4')-C(3')-C(2)	100.9(19)	C(12)-C(11)-H(112)	109.8
O(3')-C(3')-H(3')	111.8	H(111)-C(11)-H(112)	109.4
C(4')-C(3')-H(3')	105.2	C(12)-C(11)-H(113)	110.0
C(2)-C(3')-H(3')	112.3	H(111)-C(11)-H(113)	109.4
C(3')-O(3')-H(03')	109.7	H(112)-C(11)-H(113)	109.4
C(4')-O(4')-H(04')	110.3	O(12)-C(12)-C(11)	122.2(3)
O(4')-C(4')-C(3')	113(2)	O(12)-C(12)-C(13)	119.8(3)
O(4')-C(4')-C(5')	109.0(17)	C(11)-C(12)-C(13)	117.9(3)
C(3')-C(4')-C(5')	114.9(17)	O(13)-C(13)-C(14)	113.4(2)
O(4')-C(4')-H(4')	109.3	O(13)-C(13)-C(12)	110.2(3)
C(3')-C(4')-H(4')	101.4	C(14)-C(13)-C(12)	111.5(3)
C(5')-C(4')-H(4')	108.9	O(13)-C(13)-H(13)	106.9
C(8')-C(5')-C(6')	113.9	C(14)-C(13)-H(13)	107.4
C(8')-C(5')-C(7')	114.5	C(12)-C(13)-H(13)	107.1
C(6')-C(5')-C(7')	113.7	C(13)-O(13)-H(013)	109(2)
C(8')-C(5')-C(4')	104.5	O(14)-C(14)-C(13)	107.2(3)
C(6')-C(5')-C(4')	104.2	O(14)-C(14)-C(15)	109.3(2)
C(7')-C(5')-C(4')	104.4	C(13)-C(14)-C(15)	117.7(3)
C(5')-C(6')-H(6'1)	109.3	O(14)-C(14)-H(14)	107.7
C(5')-C(6')-H(6'2)	115.1	C(13)-C(14)-H(14)	107.4
H(6'1)-C(6')-H(6'2)	109.5	C(15)-C(14)-H(14)	107.2

C(14)-O(14)-H(014)	106(3)	C(15)-C(17)-H(171)	109.5
C(16)-C(15)-C(18)	109.4(3)	C(15)-C(17)-H(172)	109.4
C(16)-C(15)-C(17)	108.9(3)	H(171)-C(17)-H(172)	109.5
C(18)-C(15)-C(17)	108.2(3)	C(15)-C(17)-H(173)	109.6
C(16)-C(15)-C(14)	109.9(2)	H(171)-C(17)-H(173)	109.4
C(18)-C(15)-C(14)	107.8(3)	H(172)-C(17)-H(173)	109.4
C(17)-C(15)-C(14)	112.6(3)	C(15)-C(18)-H(181)	109.9
C(15)-C(16)-H(161)	109.6	C(15)-C(18)-H(182)	108.6
C(15)-C(16)-H(162)	109.3	H(181)-C(18)-H(182)	109.4
H(161)-C(16)-H(162)	109.4	C(15)-C(18)-H(183)	110.0
C(15)-C(16)-H(163)	109.6	H(181)-C(18)-H(183)	109.4
H(161)-C(16)-H(163)	109.4	H(182)-C(18)-H(183)	109.4
H(162)-C(16)-H(163)	109.4		

Table 43. Anisotropic displacement parameters ($Å^2 \times 10^4$) for 06srv326. The anisotropic displacement factor exponent takes the form: $-2\pi^2[h^2 a^{*2}U_{11} + ... + 2 h k a^* b^* U_{12}]$

	U_{11}	U_{22}	U_{33}	U_{23}	U_{13}	U_{12}
C(1)	420(20)	390(20)	820(30)	28(19)	0(20)	26(18)
C(2)	450(20)	236(17)	350(20)	-52(14)	-90(16)	26(15)
O(2)	558(16)	291(13)	419(15)	73(10)	-99(12)	-24(11)
C(3)	390(20)	187(17)	250(20)	15(14)	-10(17)	54(17)
O(3)	509(17)	208(12)	223(14)	25(9)	-62(12)	72(12)
O(4)	420(15)	192(12)	268(14)	-19(9)	-10(11)	55(11)
C(4)	440(20)	171(17)	220(20)	10(13)	-13(17)	41(16)
C(5)	390(40)	290(40)	420(40)	-59(17)	80(20)	-27(17)
C(6)	340(20)	380(20)	490(30)	-100(18)	-9(19)	49(18)
C(7)	490(30)	360(20)	690(30)	70(20)	180(20)	-40(20)
C(8)	320(20)	810(30)	710(30)	-400(30)	0(20)	-100(20)
C(11)	350(20)	480(20)	500(20)	-28(17)	-4(18)	71(17)
C(12)	390(20)	260(17)	280(20)	43(14)	0(16)	43(15)
O(12)	490(16)	462(15)	437(16)	-143(12)	-43(12)	136(12)
C(13)	339(19)	222(16)	263(19)	4(13)	-5(15)	30(14)
O(13)	465(14)	249(12)	287(14)	6(10)	-34(11)	34(11)
C(14)	398(19)	192(15)	263(18)	50(12)	12(15)	22(14)

O(14)	432(14)	216(12)	275(15)	30(9)	44(12)	32(10)
C(15)	337(18)	257(17)	350(20)	6(13)	-4(16)	26(14)
C(16)	370(20)	344(19)	500(20)	-3(16)	81(17)	28(16)
C(17)	380(20)	370(20)	550(30)	-79(17)	87(18)	47(16)
C(18)	370(20)	560(20)	470(20)	3(18)	-54(18)	73(18)

Table 44. Hydrogen coordinates ($\times 10^4$) and isotropic displacement parameters ($Å^2 \times 10^3$) for 06srv326.

	x	y	z	U(iso)
H(10)	1997	1355	6375	81(8)
H(11)	2588	2839	6140	81(8)
H(12)	2463	2135	4896	81(8)
H(3)	5848	1739	4473	35
H(03)	4785	3368	3412	48
H(04)	5638	4444	6023	45
H(4)	6426	1772	6746	34
H(61)	8042	1209	4350	61
H(62)	9550	1586	4654	61
H(63)	8508	766	5818	61
H(71)	7559	3696	3455	83
H(72)	7666	4787	4371	83
H(73)	9049	4068	3806	83
H(81)	8453	4047	6678	87
H(82)	8647	2485	7289	87
H(83)	9777	3219	6153	87
H(3')	5837	1747	7025	46
H(03')	4993	4207	6227	38
H(04')	5642	3563	3325	39
H(4')	6182	1774	4646	47
H(6'1)	7497	3536	7009	74
H(6'2)	7415	4762	5733	74
H(6'3)	8925	4114	6120	74
H(7'1)	8022	1183	6872	96
H(7'2)	9502	1555	5966	96
H(7'3)	8306	803	5393	96

H(8'1)	8688	2586	3284	100
H(8'2)	9684	3512	3906	100
H(8'3)	8188	4112	3432	100
H(111)	8395	1198	356	81(8)
H(112)	7938	2614	753	81(8)
H(113)	7582	1250	1788	81(8)
H(13)	4542	1488	1642	34
H(013)	5380(40)	4060(40)	1110(40)	52(11)
H(14)	3847	2053	-577	36
H(014)	4850(40)	3740(40)	-1500(40)	59(15)
H(161)	2351	1510	2301	52(6)
H(162)	817	1877	1875	52(6)
H(163)	1847	958	1081	52(6)
H(171)	2729	3971	2118	51(6)
H(172)	2632	4994	737	51(6)
H(173)	1243	4383	1595	51(6)
H(181)	1454	2576	-1071	55(6)
H(182)	472	3509	-251	55(6)
H(183)	1782	4135	-1232	55(6)

Table 45. Torsion angles [°] for 06srv326.

O(2)-C(2)-C(3)-O(3)	175.1(3)	O(2)-C(2)-C(3')-O(3')	-130(2)
C(1)-C(2)-C(3)-O(3)	-1.2(5)	C(1)-C(2)-C(3')-O(3')	7(3)
O(2)-C(2)-C(3)-C(4)	-62.0(4)	O(2)-C(2)-C(3')-C(4')	109.9(15)
C(1)-C(2)-C(3)-C(4)	121.7(3)	C(1)-C(2)-C(3')-C(4')	-112.9(13)
O(3)-C(3)-C(4)-O(4)	44.4(4)	O(3')-C(3')-C(4')-O(4')	-38(3)
C(2)-C(3)-C(4)-O(4)	-79.1(3)	C(2)-C(3')-C(4')-O(4')	84(2)
O(3)-C(3)-C(4)-C(5)	-83.0(4)	O(3')-C(3')-C(4')-C(5')	88(2)
C(2)-C(3)-C(4)-C(5)	153.5(3)	C(2)-C(3')-C(4')-C(5')	-150.3(15)
O(4)-C(4)-C(5)-C(8)	51.5(4)	O(4')-C(4')-C(5')-C(8')	-46(2)
C(3)-C(4)-C(5)-C(8)	176.3(3)	C(3')-C(4')-C(5')-C(8')	-174(2)
O(4)-C(4)-C(5)-C(7)	-69.3(5)	O(4')-C(4')-C(5')-C(6')	74(2)
C(3)-C(4)-C(5)-C(7)	55.6(5)	C(3')-C(4')-C(5')-C(6')	-54(2)
O(4)-C(4)-C(5)-C(6)	168.7(4)	O(4')-C(4')-C(5')-C(7')	-167(2)
C(3)-C(4)-C(5)-C(6)	-66.4(5)	C(3')-C(4')-C(5')-C(7')	65(2)

O(12)-C(12)-C(13)-O(13)	-157.2(3)
C(11)-C(12)-C(13)-O(13)	25.2(3)
O(12)-C(12)-C(13)-C(14)	-30.4(4)
C(11)-C(12)-C(13)-C(14)	152.0(3)
O(13)-C(13)-C(14)-O(14)	52.5(3)
C(12)-C(13)-C(14)-O(14)	-72.6(3)
O(13)-C(13)-C(14)-C(15)	-71.0(4)
C(12)-C(13)-C(14)-C(15)	163.9(3)
O(14)-C(14)-C(15)-C(16)	-177.0(3)
C(13)-C(14)-C(15)-C(16)	-54.5(4)
O(14)-C(14)-C(15)-C(18)	63.9(4)
C(13)-C(14)-C(15)-C(18)	-173.6(3)
O(14)-C(14)-C(15)-C(17)	-55.4(3)
C(13)-C(14)-C(15)-C(17)	67.1(3)

Table 46. Hydrogen bonds for 06srv326 [Å and °].

D-H...A	d(D-H)	d(H...A)	d(D...A)	<(DHA)
O(3)-H(03)...O(13)	0.95	1.80	2.706(3)	158.5
O(4)-H(04)...O(3)#1	0.92	2.03	2.840(3)	145.8
O(13)-H(013)...O(14)#2	0.91(4)	1.95(4)	2.759(3)	148(3)
O(14)-H(014)...O(4)#3	0.77(4)	1.98(4)	2.733(3)	164(4)
O(3')-H(03')...O(3)#1	0.84	2.23	2.976(18)	148.4
O(3')-H(03')...O(4')#1	0.84	2.06	2.67(2)	129.6
O(4')-H(04')...O(13)	0.85	1.81	2.65(2)	174.6

Symmetry transformations used to generate equivalent atoms: #1 -x+1,-y+1,-z+1 #2 -x+1,-y+1,-z #3 x,y,z-1

Appendix

Attended international conferences with poster

International Symposium on Organocatalysis in organic synthesis

5-7 July 2006

University of Glasgow

UK

International Symposium: Synthesis in organic chemistry

16-19 July 2007

Cambridge

UK